



## **Terms and Conditions of Use of Digitised Theses from Trinity College Library Dublin**

### **Copyright statement**

All material supplied by Trinity College Library is protected by copyright (under the Copyright and Related Rights Act, 2000 as amended) and other relevant Intellectual Property Rights. By accessing and using a Digitised Thesis from Trinity College Library you acknowledge that all Intellectual Property Rights in any Works supplied are the sole and exclusive property of the copyright and/or other IPR holder. Specific copyright holders may not be explicitly identified. Use of materials from other sources within a thesis should not be construed as a claim over them.

A non-exclusive, non-transferable licence is hereby granted to those using or reproducing, in whole or in part, the material for valid purposes, providing the copyright owners are acknowledged using the normal conventions. Where specific permission to use material is required, this is identified and such permission must be sought from the copyright holder or agency cited.

### **Liability statement**

By using a Digitised Thesis, I accept that Trinity College Dublin bears no legal responsibility for the accuracy, legality or comprehensiveness of materials contained within the thesis, and that Trinity College Dublin accepts no liability for indirect, consequential, or incidental, damages or losses arising from use of the thesis for whatever reason. Information located in a thesis may be subject to specific use constraints, details of which may not be explicitly described. It is the responsibility of potential and actual users to be aware of such constraints and to abide by them. By making use of material from a digitised thesis, you accept these copyright and disclaimer provisions. Where it is brought to the attention of Trinity College Library that there may be a breach of copyright or other restraint, it is the policy to withdraw or take down access to a thesis while the issue is being resolved.

### **Access Agreement**

By using a Digitised Thesis from Trinity College Library you are bound by the following Terms & Conditions. Please read them carefully.

I have read and I understand the following statement: All material supplied via a Digitised Thesis from Trinity College Library is protected by copyright and other intellectual property rights, and duplication or sale of all or part of any of a thesis is not permitted, except that material may be duplicated by you for your research use or for educational purposes in electronic or print form providing the copyright owners are acknowledged using the normal conventions. You must obtain permission for any other use. Electronic or print copies may not be offered, whether for sale or otherwise to anyone. This copy has been supplied on the understanding that it is copyright material and that no quotation from the thesis may be published without proper acknowledgement.

**Molecular Analysis of the Interaction Between Protein A of  
*Staphylococcus aureus* and von Willebrand Factor**

**A thesis submitted for the degree of Doctor in Philosophy**

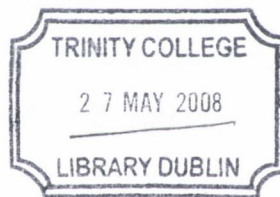
**by**

**Maghnus N. O Seaghdha**

**Moyne Institute of Preventive Medicine  
Department of Microbiology  
Trinity College Dublin**

**March 2007**



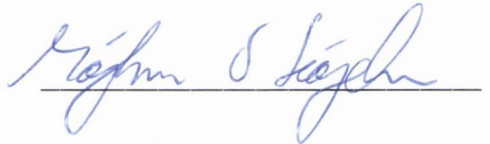


THESIS  
8435

## Declaration

I hereby declare that this thesis has not previously been submitted for a degree at this or any other university and that it is my own work except where it is duly acknowledged in the text.

I agree that this thesis may be lent or copied at the discretion of the Librarian, Trinity College Dublin.

A handwritten signature in blue ink, reading "Magnus N. O Seaghdha", is written over a horizontal line.

**Magnus N. O Seaghdha**

## Acknowledgements

Firstly, I would like to thank Prof. Tim Foster for giving me the opportunity to work in his laboratory, and for his constant help, advice and enthusiasm. For financial support during this project, my thanks to the Health Research Board. Thanks a million to everyone from the TJF group past and present for help and advice throughout the project. Thanks also to Drs. Dermot Cox, Steve Kerrigan and Marian Brennan from the Royal College of Surgeons for their advice and input on the platelet work. I am grateful to Dr. Peter Lenting and his group in UMC, Utrecht for giving me the opportunity (twice) to visit their lab for the early work on vWF, especially Carina, Ronan and Eric. Ronan, sorry for stealing a day of your life! Thanks also to my other collaborators Dr. Jonas Emsley and Elizabeth Hooley for structural work on vWF A1.

I would also like to thank everyone in the West bunker lab for making each day in work such a good laugh...Brian, thank you for the music (not!) and Enda, thanks for spotting any spills in the lab! Thanks also to everyone who has kicked a football in the name of microbiology (or genetics)...you gave me a reason to look forward to Thursdays (in addition to lab meetings, of course)! Thanks also to the North bunker...my second home for coffee and lunch!

Thanks to my parents for all their support during my education – I hope it was worth it! Finally and most importantly, thanks to Kirsty, for all your support during this project. I really couldn't have done it without you.

## Summary

*Staphylococcus aureus* continues to be a major cause of infection in normal as well as immunocompromised hosts, and the increasing prevalence of highly virulent community-acquired methicillin-resistant strains is a public health concern. Protein A (Spa) is a surface-associated protein of *S. aureus* best known for its ability to bind to the Fc region of IgG. This interaction is of importance in resistance of *S. aureus* to phagocytosis. Spa also binds strongly to the Fab region of the immunoglobulins bearing V<sub>H3</sub> heavy chains and more recently has been shown to bind von Willebrand factor (vWF) and tumour necrosis factor receptor-1 (TNFR1). Each Spa domain is organized into a three helix bundle and binding sites for Fc and V<sub>H3</sub> Fab have been identified. The site for Fc binding comprises of residues from helices 1 and 2 whereas contacts for V<sub>H3</sub> Fab binding are located on a distinct region made up of residues from helices 2 and 3. Binding to TNFR1 by Spa activates of tumor necrosis factor alpha (TNF-alpha) receptor 1 (TNFR1) signaling, inducing both chemokine expression and TNF-converting enzyme-dependent soluble TNFR1 (sTNFR1) shedding which has anti-inflammatory consequences, particularly in the lung. Previous studies have suggested that the protein A-vWF interaction is important in *S. aureus* adherence to platelets under conditions of shear stress. This thesis investigates the Spa-vWF interaction in greater detail. Spa expression is shown to be sufficient for adherence of bacteria to immobilized vWF under low fluid shear. The role of Spa in platelet aggregation is unclear and was also investigated in this study. In this work, it is demonstrated that Spa does not induce platelet aggregation but can adhere to resting platelets. This novel interaction occurs through the platelet glycoprotein,  $\alpha_{IIb}\beta_3$  and is distinct from the known interaction between Spa and the platelet receptor  $\text{gC1qR/p33}$ .

The full length recombinant Ig-binding region of protein A, Spa-EDABC, fused to glutathione-S-transferase (GST), bound recombinant vWF in a dose-dependent and saturable fashion with half maximal binding of about 30 nM in immunosorbent assays. Full length-Spa did not bind recombinant vWF A3 domain but displayed binding to recombinant vWF domains A1 and D'-D3 (half maximal binding at 100 nM and 250 nM, respectively). Each recombinant protein A Ig-binding domain bound to the A1 domain in a similar manner to the full length-Spa molecule. Amino acid substitutions were introduced in the GST-SpaD protein at sites including those known to be involved in IgG Fc or in V<sub>H3</sub> Fab binding. Mutants altered in residues that recognized IgG Fc but not those that recognized V<sub>H3</sub> Fab had reduced



binding to vWF A1 and D'-D3. This indicated that both vWF regions recognized a region on helices 1 and 2 that overlapped the IgG Fc binding site. The protein A binding site within vWF A1 may overlap the collagen and/or ristocetin binding site(s) as determined from inhibition studies. A model is proposed that Spa promotes adherence of *S. aureus* to platelets under conditions of high shear (where vWF is in an active conformation for platelet binding) or promotes adherence of *S. aureus* to sites of endothelial damage in blood vessels, when vWF binds to exposed sub-endothelial collagen.

The collection of GST-Spa variants was also used to identify the binding site on Spa for TNFR1. Spa variants were identified which were able to induce TNFR1 signaling but not shedding. This suggested that Spa had another ligand in the airway epithelium which has recently been identified to be the epidermal growth factor receptor (EGFR). The cellular location and ligand binding properties of a recently identified *S. aureus* Ig-binding protein with homology to the Ig-binding regions of Spa, Sbi, was also investigated in this work.

In summary, this study has identified the site on Spa for vWF binding. This is a similar site to the Fc and TNFR binding sites. This opens up the possibility for the design of peptides or humanised monoclonal antibodies that could provide passive immunization by blocking binding by Spa to many of its ligands. Blocking this site on Spa could prevent many diverse and important interactions in different niches within the host by this multifunctional virulence factor.

## Publications

Gomez, M.I., O'Seaghda, M., Magargee, M., Foster, T.J., and Prince, A.S. (2006) *Staphylococcus aureus* protein A activates TNFR1 signaling through conserved IgG binding domains. *J Biol Chem* **281**: 20190-20196.

O'Seaghda, M., van Schooten, C.J., Kerrigan, S.W., Emsley, J., Silverman, G.J., Cox, D., Lenting, P.J., and Foster, T.J. (2006) *Staphylococcus aureus* protein A binding to von Willebrand Factor A1 domain is mediated by conserved IgG binding regions. *FEBS J* **273**:4831-4841.

Gomez, M.I., O'Seaghda, M., and Prince, A.S. (2007) *Staphylococcus aureus* protein A activates TACE through EGFR-dependent signaling. *EMBO J* **26**:701-9.

## Contents

<b>Declaration</b> .....	ii
<b>Acknowledgements</b> .....	iii
<b>Summary</b> .....	iv
<b>Publications</b> .....	vi
<b>List of tables</b> .....	xiii
<b>List of figures</b> .....	xiv
<b>Key to abbreviations</b> .....	xviii

### Chapter 1 Introduction

1.1	The biology of <i>Staphylococcus aureus</i> .....	1
1.1.1	Classification and identification .....	1
1.1.2	Colonization and stress resistance.....	1
1.2	Sortase-mediated anchoring of cell-wall associated proteins.....	2
1.3	Immune evasion by <i>S. aureus</i> .....	3
1.3.1	Host defences against infection.....	3
1.3.2	Resistance to phagocytosis.....	4
1.3.2.1	Protein A.....	4
1.3.2.2	ClfA.....	5
1.3.2.3	Capsule.....	6
1.3.3	Complement evasion.....	6
1.3.4	Inhibition of neutrophil chemotaxis.....	8
1.3.5	Resistance to antimicrobial peptides.....	9
1.3.6	Immunomodulation.....	10
1.3.6.1	Protein A.....	10
1.3.6.2	Toxin superantigens.....	11
1.3.6.3	Major histocompatibility complex class II-analog protein.....	12
1.4	Mechanism of ligand binding by <i>S.aureus</i> surface proteins.....	12
1.4.1	The dock, lock and latch model for fibrinogen binding.....	12

1.4.2	The tandem beta-zipper mechanism for fibronectin binding.....	13
1.4.3	The ‘collagen hug’ mechanism .....	14
1.5	Other <i>S. aureus</i> surface proteins.....	15
1.5.1	Iron-regulated surface proteins.....	15
1.5.2	Serine-aspartate repeat (Sdr) and novel <i>S. aureus</i> surface (Sas) proteins.....	17
1.6	Regulation of virulence determinants of <i>S. aureus</i> .....	18
1.6.1	Regulation of the <i>spa</i> promoter.....	18
1.7	von Willebrand Factor.....	20
1.7.1	The von Willebrand Factor multimer.....	20
1.7.2	The von Willebrand Factor monomer.....	21
1.7.3	Structural studies on the A1 domain of von Willebrand Factor.....	21
1.8	Structural studies on protein A.....	23
1.9	Bacteria, platelets and cardiovascular disease.....	25
1.9.1	Platelets.....	26
1.9.2	The interaction of bacteria and platelets.....	28
1.9.2.1	<i>S. aureus</i> -platelet interactions.....	29
1.10	<i>S. aureus</i> pathogenesis of the airway epithelium.....	32
1.11	Rationale for this study.....	33
1.11.1	Aims and objectives.....	34

## **Chapter 2    Materials and methods**

2.1	Bacterial strains and growth conditions.....	35
2.2	Plasmids.....	35
2.3	DNA manipulations.....	35
2.4	Transformation of bacterial cells with plasmid DNA.....	35
2.4.1	Screening of transformants.....	36
2.5	PCR.....	36
2.6	DNA constructions.....	36
2.7	Site-directed mutagenesis.....	37
2.7.1	Mutagenesis of a single <i>spa</i> domain.....	37
2.7.2	Mutagenesis of the <i>vwfA1</i> domain.....	38
2.8	DNA purification.....	38



2.9	Electrophoresis.....	38
2.9.1	Agarose gel electrophoresis.....	38
2.9.2	SDS-PAGE.....	38
2.10	Protein detection.....	39
2.10.1	Protein labeling and antibodies.....	39
2.10.1.1	Protein labeling.....	39
2.10.1.2	Antibodies.....	39
2.10.2	Protein staining.....	39
2.10.3	Western immunoblotting.....	40
2.10.4	Western ligand affinity blotting.....	40
2.10.5	Dot immunoblotting.....	40
2.11	Protein expression and purification.....	41
2.11.1	Small-scale protein induction.....	41
2.11.2	Large-scale protein production.....	41
2.11.2.1	Expression and purification of recombinant Spa.....	41
2.11.2.2	Expression and purification of recombinant untagged Sbi-II and Spa.....	42
2.11.2.3	Expression and purification of recombinant vWF A1.....	42
2.11.2.4	Expression and purification of recombinant V <sub>H</sub> 3-Fab.....	42
2.12	Determination of protein concentration.....	43
2.13	Antibody fragmentation.....	43
2.14	Solid-phase binding assays.....	43
2.14.1	Protein:protein binding assays.....	43
2.14.1.1	Inhibition studies.....	43
2.14.2	Bacterial:protein binding assay.....	44
2.14.3	Platelet adherence assay.....	44
2.15	Preparation of human platelets.....	45
2.16	Platelet aggregation .....	45
2.17	Bacterial perfusion studies.....	46
2.17.1	Preparation of flow chamber slides.....	46
2.17.2	Videomicroscopy.....	46
2.18	Isolation of <i>S. aureus</i> cell wall and cell envelope components.....	46
2.18.1	Preparation of staphylococcal whole cell lysates.....	46
2.18.2	Preparation of the staphylococcal cell wall.....	47

2.18.3	Preparation of the staphylococcal protoplast and cytoplasm.....	47
2.18.4	Preparation of the extracellular proteins of <i>S. aureus</i> .....	47
2.19	Proteomics tools for the prediction of membrane topology.....	48

### **Chapter 3 Analysis of the Interaction Between Protein A and von Willebrand Factor using Recombinant Protein Truncates**

3.1	Introduction.....	49
3.2	Results.....	52
3.2.1	Surface expression of Spa on <i>Lactococcus lactis</i> .....	52
3.2.2	Surface expression of Spa on <i>Lactococcus lactis</i> is sufficient for bacterial adhesion to von Willebrand Factor-coated surfaces under flow.....	52
3.2.3	Recombinant GST-Spa truncates.....	53
3.2.4	Functional analysis of recombinant GST-Spa truncates.....	54
3.2.5	Interaction of GST-SpaEDABC with von Willebrand Factor.....	55
3.2.6	GST-SpaEDABC binds the vWF D'-D3 and A1-domains.....	56
3.2.7	Interaction of GST-Spa truncates with vWF D'-D3 and A1.....	57
3.2.7.1	Purification of recombinant vWF A1 in <i>Escherichia coli</i> .....	57
3.2.7.2	Interaction of GST-Spa truncates with D'-D3 and A1.....	58
3.3	Discussion.....	61

### **Chapter 4 Mapping the Protein A-vWF Binding Site**

4.1	Introduction.....	65
4.2	Results.....	67
4.2.1	The binding site on protein A for von Willebrand Factor.....	67
4.2.1.1	The protein A-vWF interaction is blocked by IgG and V <sub>H</sub> 3-IgM.....	67
4.2.1.2	Fc $\gamma$ but not V <sub>H</sub> 3-Fab specifically blocks protein A-vWF binding.....	67
4.2.2	Variants of the D domain of Spa.....	68
4.2.2.1	Interaction of GST-SpaD variants with Fc $\gamma$ of IgG and V <sub>H</sub> 3-Fab.....	69
4.2.2.2	Interaction of GST-SpaD variants with vWF.....	71
4.2.3	The protein A binding site on vWF A1.....	72

4.2.3.1	Inhibition studies.....	72
4.2.3.1.1	Anti-vWF A1 monoclonal antibodies.....	72
4.2.3.1.2	Ligands of vWF A1.....	73
4.2.3.2	vWF A1 variants.....	74
4.2.3.2.1	Functional analysis of vWF A1 variants.....	75
4.2.3.3	Interaction of vWF A1 variants with SpaD.....	76
4.2.4	Structural studies on the Spa-vWF A1 complex.....	76
4.2.5	The interaction of protein A and platelets.....	78
4.2.5.1	Role of protein A in platelet aggregation.....	78
4.2.5.2	Protein A binds directly to resting platelets.....	79
4.2.6	Studies on the interaction between protein A and TNFR1.....	80
4.3	Discussion.....	82

**Chapter 5 Studies on Sbi, a Second Immunoglobulin Binding Protein of *S. aureus***

5.1	Introduction.....	87
5.2	Results.....	88
5.2.1	Cellular location of Sbi.....	88
5.2.2	<i>In silico</i> analysis of Sbi.....	90
5.2.3	Construction of recombinant Sbi-II.....	91
5.2.4	Interaction of Sbi with IgG, IgM and von Willebrand Factor.....	92
5.3	Discussion.....	94

**Chapter 6 Discussion**

6.1	Discussion.....	96
-----	-----------------	----

<b>References.....</b>	<b>101</b>
------------------------	------------

## List of Tables

	Following page
2.1 Bacterial strains .....	35
2.2 List of plasmids .....	35
2.3 Oligonucleotides used for <i>spa</i> and <i>sbi</i> truncates.....	37
2.4 Oligonucleotides used for <i>spaD</i> and <i>vwfA1</i> variants.....	37
2.5 Antibodies and antibody fragments.....	39
4.1 Properties of vWF A1 ligands used in this study.....	73



## List of Figures

		Following page
1.1	Staphylococcal surface proteins .....	2
1.2	Surface protein anchoring in <i>Staphylococcus aureus</i> .....	3
1.3	Apo structures of domains N23 of ClfA, ClfB and SdrG and SdrG-peptide complex .....	12
1.4	Structure of the <i>Strep. dysgalactiae</i> B3 peptide in complex with <sup>1</sup> F1 <sup>2</sup> F1 type I fibronectin modules .....	14
1.5	The 'Collagen Hug' hypothesis model shown in a cartoon representation.....	15
1.6	Schematic overview of the regulation of <i>spa</i> .....	19
1.7	Biosynthesis of von Willebrand Factor.....	20
1.8	Schematic representation of the von Willebrand factor monomer.....	21
1.9	Ribbon representation of the crystal structure of vWF A1.....	22
1.10	The Ig-binding domains of protein A.....	23
1.11	Composite figure of a single Spa domain interacting simultaneously with Fc and a V <sub>H</sub> 3-Fab.....	24
3.1	Surface expression of Spa on <i>L. lactis</i> .....	52
3.2	Perfusion of <i>L. lactis</i> expressing Spa over vWF-coated slides.....	52
3.3	Plasmid pGEX-KG and recombinant GST-Spa truncates.....	53
3.4	Procedure for amplification of <i>spa</i> fragments.....	53
3.5	Purification of GST-Spa fusion proteins .....	54
3.6	SDS-PAGE analysis of GST-Spa truncates.....	54
3.7	Relative protein concentrations of GST-Spa truncates.....	54
3.8	IgG binding by GST-Spa truncates.....	55
3.9	Interaction of GST-SpaEDABC with rabbit and chicken immunoglobulin.....	55
3.10	Interaction of full-length vWF with GST-SpaEDABC.....	56
3.11	Inhibition of GST-SpaEDABC binding to vWF .....	56
3.12	Recombinant vWF constructs.....	57
3.13	Interaction of SpaEDABC with recombinant vWF truncates.....	57
3.14	Inhibition of platelet aggregation by the vWF A1 domain.....	58
3.15	Interaction of GST-SpaEDABC with vWF D'-D3, A1 and A3.....	58

3.16	Comparative binding of <i>P. pastoris</i> and <i>E. coli</i> -produced rvWF A1 to GST-SpaEDABC. ....	58
3.17	Inhibition studies using vWF A1 and D'-D3.....	58
3.18	Interaction of GST-Spa truncates with vWF A1.....	59
3.19	Interaction of single GST-Spa domains with vWF A1.....	59
4.1	Architecture of a Spa domain.....	65
4.2	Inhibition of Spa binding to vWF A1 by IgG and IgM.....	67
4.3	The pComb3:JMSPA3-08 soluble Fab-producing phagemid vector.....	68
4.4	Purification of V <sub>H</sub> 3-Fab.....	68
4.5	Binding of GST-SpaD to Fc $\gamma$ and V <sub>H</sub> 3-Fab.....	68
4.6	Inhibition of Spa binding to vWF A1 by Fc and V <sub>H</sub> 3-Fab.....	68
4.7	SpaD variants used in this study.....	69
4.8	Recombinant GST-SpaD variants.....	69
4.9	Binding of IgG to GST-SpaD variants.....	70
4.10	The Fc $\gamma$ -binding region on Spa determined by mutagenesis of SpaD.....	70
4.11	Binding of V <sub>H</sub> 3-IgM to GST-SpaD variants.....	71
4.12	The V <sub>H</sub> 3-Fab binding region on Spa determined by mutagenesis of SpaD.....	71
4.13	Binding of vWF A1 to GST-SpaD variants.....	71
4.14	The vWF-binding region on Spa.....	71
4.15	Binding of Spa to vWF D'-D3 and A1 domains.....	72
4.16	Effect of anti-vWF A1 monoclonal antibodies on the binding of Spa to vWF A1.	73
4.17	The binding regions on vWF A1 for botrocetin, ristocetin and collagen.....	73
4.18	Inhibition studies on the Spa-vWF A1 interaction using vWF ligands.....	74
4.19	vWF A1 variants used in this study.....	75
4.20	Effect of vWF A1 variants on ristocetin-induced platelet aggregation.....	75
4.21	Interaction of vWF A1 variants with GST-SpaD.....	76
4.22	Proposed Spa binding region on vWF A1.....	76
4.23	Gel filtraion analysis of SpaEDABC and SpaDAB.....	77
4.24	Gel filtraion analysis of SpaDA and SpaB.....	77
4.25	Gel filtraion analysis of vWF A1 and SpaEDABC/vWF A1.....	77
4.26	The effect of Spa expression on platelet aggregation.....	78
4.27	The effect of Spa on ristocetin-induced platelet aggregation.....	79

4.28	Inhibition of platelet aggregation by Spa.....	79
4.29	Adherence of platelets to bacteria expressing Spa.....	80
4.30	Interaction of Spa truncates with TNFR1-expressing airway epithelial cells.....	80
4.31	The TNFR1 binding region on Spa.....	81
5.1	Schematic diagram of the structural organisation of Sbi.....	87
5.2	Alignment of Spa and Sbi IgG-binding domains.....	87
5.3	Fractionation of the <i>S. aureus</i> cell envelope.....	88
5.4	Analysis of cell envelope fractions of <i>S. aureus</i> 8325-4 <i>spa</i> for Sbi.....	88
5.5	Analysis of cell envelope fractions of <i>S. aureus</i> Newman <i>spa</i> for Sbi.....	88
5.6	Analysis of cell envelope fractions of <i>S. aureus</i> SH1000 <i>spa</i> for Sbi.....	88
5.7	Analysis of cell envelope fractions of <i>S. aureus</i> 8325-4 <i>spa</i> for ClfA and EbpS...	89
5.8	Analysis of cell envelope fractions of <i>S. aureus</i> Newman and Newman <i>spa</i> for IgG binding.....	89
5.9	Kyte-Doolittle hydropathy plotting for putative transmembrane regions of Sbi. ...	90
5.10	Prediction of transmembrane $\alpha$ -helices on Sbi using the TMHMM program. ....	90
5.11	Prediction of possible transmembrane regions of a given peptide sequence is the dense alignment surface (DAS) method.....	91
5.12	Recombinant Sbi proteins used in this study.....	91
5.13	Interaction of Sbi and Spa truncates with rabbit immunoglobulin.....	92
5.14	Interaction of Sbi and Spa truncates with V <sub>H</sub> 3-Fab.....	92
5.15	Interaction of Sbi and Spa truncates with vWF A1.....	93
6.1	Model for the role of protein A binding vWF in the vascular endothelium.....	98
6.2	Model for inflammation of the airway epithelium caused by protein A.....	99

---

## Key to abbreviations

---

### Single letter amino acid code

A	Alanine
C	Cysteine
D	Aspartic acid
E	Glutamic acid
F	Phenylalanine
G	Glycine
H	Histidine
I	Isoleucine
K	Lysine
L	Leucine
M	Methionine
N	Asparagine
P	Proline
Q	Glutamine
R	Arginine
S	Serine
T	Threonine
V	Valine
W	Tryptophan
Y	Tyrosine

### Nucleotides

A	Adenine
T	Thymine
C	Cytosine
G	Guanine

---



---

### Key to abbreviations

---

Ap	Ampicillin
Erm	Erythromycin
Tet	Tetracycline
Kan	Kanamycin
aa	amino acid
bp	base pair(s)
BSA	bovine serum albumin
DNA	deoxyribonucleic acid
dNTP	deoxy nucleoside triphosphate
EDTA	ethylenediaminetetraacetic acid
ELISA	enzyme linked immunosorbent assay
Fg	fibrinogen
Fn	fibronectin
GFP	gel filtered platelets
h	hour(s)
Ig	immunoglobulin
V <sub>H</sub>	variable immunoglobulin heavy chain
kb	kilobase pair
kDa	kilodalton
min	minute(s)
nt	nucleotides
OD	optical density
PBS	phosphate buffered saline
PCR	polymerase chain reaction
PRP	platelet rich plasma
PPP	platelet poor plasma
GFPs	gel-filtered platelets
rpm	revolutions per minute
SDS	sodium dodecyl sulfate

---

---

**Key to abbreviations**

---

SDS-PAGE	sodium dodecyl sulfate polyacrylamide gel electrophoresis
Tris	trishydroxymethylaminomethane
TSA	trypticase soy agar
TSB	trypticase soy broth
BHI	brain-heart infusion medium
v/v	volume per volume
w/v	weight per volume
wt	wild-type

---

## **Chapter 1**

### **Introduction**

## **1.1 The biology of *Staphylococcus aureus***

### **1.1.1 Classification and identification**

*Staphylococcus aureus* is a Gram-positive, non-motile, non-spore-forming coccus that characteristically divides in more than one plane to form grape-like clusters. It forms smooth, entire, raised colonies that often contain a golden pigment. Taxonomic studies have placed the genus *Staphylococcus* in the *Bacillus-Lactobacillus-Streptococcus* cluster of the *Micrococccacea* (Ludwig *et al.*, 1985; Stackebrandt and Teuber, 1988). Staphylococci are most closely related to *Enterococcus*, *Bacillus* or *Listeria*. The staphylococci can be differentiated by their halotolerance (growth up to 3.5 M NaCl) and are resistant to desiccation. Their genomes contain DNA of a low G + C content (approximately 36 %). The *S. aureus* cell wall is composed of peptidoglycan which comprises lysine as the diamino acid, a pentaglycine cross-bridge and N-acetyl glucosamine-substituted ribitol teichoic acid. *S. aureus* is distinguished from other staphylococci by its ability to ferment mannitol, the secretion of coagulase and a thermostable DNase. Indeed, coagulase production is a marker for separation of *S. aureus* from other so-called coagulase-negative staphylococci (CoNS). CoNS are generally less virulent than coagulase-positive staphylococci (Phonimdaeng *et al.*, 1990). Commercially available agglutination tests which contain fibrinogen- and IgG-coated particles are used to test for the presence of coagulase, ClfA (fibrinogen-binding proteins) and protein A (an immunoglobulin-binding protein) and thereby identify *S. aureus*.

### **1.1.2 Colonisation and stress-resistance**

The primary habitat of *S. aureus* in humans is the moist squamous epithelium of the anterior nares. *S. aureus* persistently colonises approximately 20 % of healthy adults and another 60 % are intermittent carriers. The remaining 20 % of the population never carry *S. aureus* in the nasopharynx (Lowy, 1998; Peacock *et al.*, 2001). *S. aureus* can initiate infection after a breach of the skin or mucosal barrier which allows the organism to access neighbouring tissues or the bloodstream. The most common *S. aureus* infections are superficial skin lesions such as boils, abscesses and impetigo. The organism can cause bacteraemia if it enters the bloodstream, where it can infect internal tissues resulting in serious invasive diseases such as osteomyelitis (bone), septic arthritis (joints), pneumonia (lungs), and endocarditis (heart

valves). The interplay between *S. aureus* virulence factors and host defence mechanisms determines whether an infection is contained or spreads in the host (Lowy, 1998).

A number of mechanisms exist enabling *S. aureus* to respond to environmental stresses. Staphylococci are halotolerant and resistant to desiccation. In conditions of high salt, the organism shortens the interpeptide bridges of its cell wall peptidoglycan conferring mechanical strength to the cell wall. In addition, osmoprotectant solutes such as glycine, proline and betaine are accumulated (Townsend and Wilkinson, 1992; Vijaranakul *et al.*, 1995). Several genes have been identified as important for survival in the nutrient limited environment of the skin. A subpopulation of *S. aureus* can survive for several months on the skin which have increased resistance to acid and oxidative stress (Watson *et al.*, 1998).

A number of genes involved in stress resistance by Gram-positive bacteria, including *S. aureus*, are under the control of the alternative sigma factor,  $\sigma^B$ . Transcriptional analysis and phenotypic studies of deletion mutants of *sigB* have identified roles in acid and oxidative stress resistance and in the regulation of resistance determinants to the antibiotics methicillin and vancomycin (Chan *et al.*, 1998; Kullik *et al.*, 1998; Sieradzki and Tomasz, 1998; Singh *et al.*, 2003).  $\sigma^B$  is also involved in the regulation of virulence determinants, and deletion of *sigB* results in a marked attenuation of *S. aureus* in a murine model for septic arthritis (Jonsson *et al.*, 2004).

## 1.2 Sortase-mediated anchoring of cell-wall associated proteins

Many *S. aureus* surface proteins contain common motifs for targeted attachment to the cell wall, where they subsequently become covalently linked to the peptidoglycan layer, more specifically to the pentaglycine cross-bridges in a process referred to as 'sorting'. Proteins anchored by this mechanism include the immunoglobulin-binding protein A (Spa), the fibrinogen-binding proteins ClfA and ClfB and the collagen-binding protein, Cna (Fig. 1.1). Mutants defective in sortase are attenuated in animal models of septic arthritis and endocarditis (Jonsson *et al.*, 2002; Jonsson *et al.*, 2003; Weiss *et al.*, 2004). Table 1.1 contains a list of *S. aureus* proteins that are anchored by sortase.

Proteins destined for sortase-mediated anchoring to the cell wall have an N-terminal signal sequence of about 40 amino acids that terminates with motif AXA that directs the



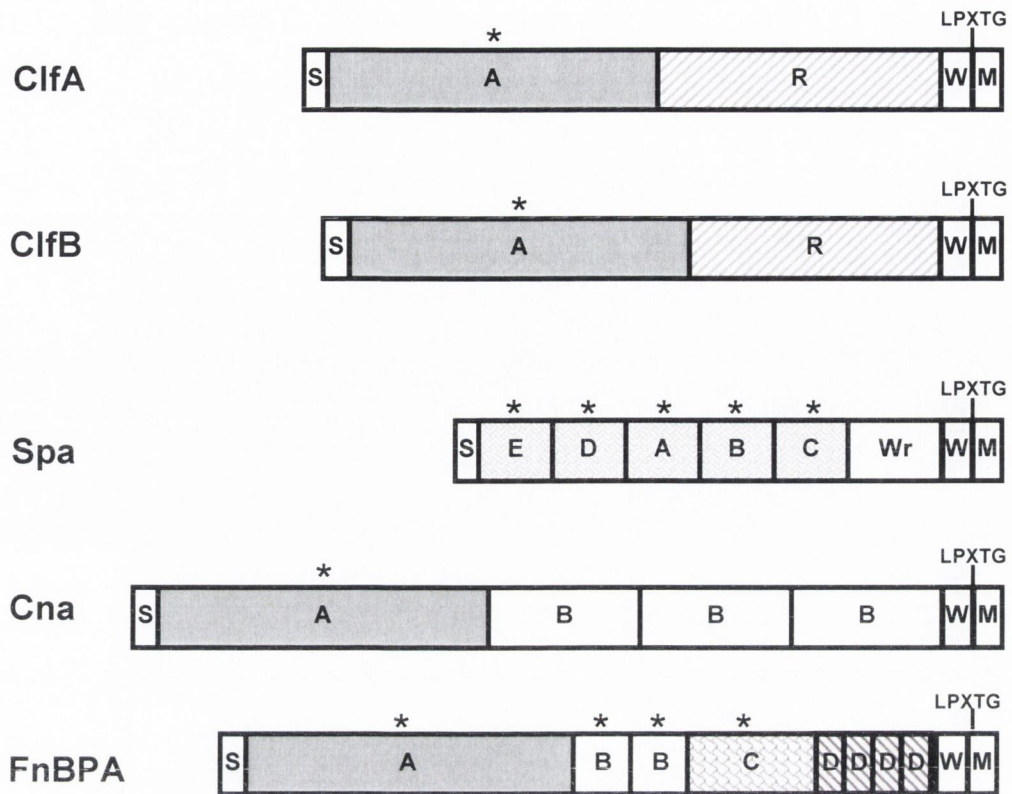


**Figure 1.1 Staphylococcal surface proteins.** Schematic representation demonstrating the common motif organisation found in surface proteins from *S. aureus* (Clumping factor A and B, ClfA, ClfB; protein A, Spa; collagen binding adhesin, Cna and fibronectin binding protein A, FnBPA). Ligand binding domains are denoted by an asterisk. The relative sizes of the signal sequence (S), A domain (A), B-repeat region (B), SD-repeat region (R), and wall/membrane spanning regions (WM) are shown. Sortase A recognition motifs (LPXTG) are indicated. Spa domains E, D, A, B and C are homologous ligand-binding repeats.

protein into the secretory (Sec) pathway. This motif is recognised and cleaved by the membrane-anchored signal peptidase enzymes SpsA and SpsB during translocation across the cytoplasmic membrane (Cregg *et al.*, 1996; Mazmanian *et al.*, 2001). The cleaved peptide is anchored to the cell wall via a C-terminal domain and the protein is subsequently covalently attached by the enzyme sortase. Sortase A is encoded by the *srtA* gene and recognises the motif LPXTG. In contrast, SrtB can recognise the NPQTN motif of IsdC, an iron-regulated surface protein (Mazmanian *et al.*, 2001; Mazmanian *et al.*, 2002; Pallen, 2002). Sortase cleaves the LPXTG motif between the threonine and glycine residues and covalently attaches the mature protein to the pentaglycine bridge via threonine (Ton-That *et al.*, 2000). The portion of the protein C-terminal of the LPXTG motif is released and degraded. Recognition of LPXTG is highly stringent and amino acid substitutions are not tolerated at positions 1, 2, 4 or 5 *in vitro* (Kruger *et al.*, 2004). The high resolution X-ray structure of sortase in complex with an LPETG peptide has provided more detailed information of the nature of the interaction and the LPXTG binding surface has been identified NMR analysis of the <sup>1</sup>H-<sup>15</sup>N chemical shifts of sortase in the presence or absence of ligand (Liew *et al.*, 2004; Zong *et al.*, 2004). Sortase-mediated anchoring of surface proteins is outlined in Fig. 1.2.

### **1.3 Immune evasion by *S. aureus***

#### **1.3.1 Host defences against infection**

When *S. aureus* breaches the outer physical barriers of the body comprising the skin and mucous surfaces, it encounters the innate and induced responses of the host's immune system. Infection of the skin by *S. aureus* stimulates a strong inflammatory response causing neutrophil and macrophage migration to the site of infection. The function of these cells is to engulf and dispose of the invading organisms in co-ordination with antibodies and complement present in the host's serum. The complement system comprises proteins and their proteolytic derivatives which function in both innate and acquired immunity to destroy foreign cells or induce other effectors involved in the immune response (Rus *et al.*, 2005). The primary role of complement fixation on *S. aureus* is opsonisation ie, to promote phagocytosis by professional phagocytes (neutrophils and macrophages). Formylated peptides released by growing bacteria and chemoattractant molecules released during complement activation (C3a

and C5a) attract phagocytes to the site of infection. The efficiency of phagocytosis is enhanced by expression of specific receptors on the phagocytes for complement fragments and formylated peptides. Neutrophils also carry specific receptors that can recognize the Fc $\gamma$  region of IgG and complement proteins bound to the bacterial surface that facilitate efficient uptake and killing.

*S. aureus* uptake by macrophages initially stimulates the acquired immune response. B cells in the lymph nodes differentiate and secrete antibodies to neutralise toxins and recognise bacterial surface molecules thereby promoting more efficient phagocytosis of bacterial cells. However, *S. aureus* has evolved to overcome the host's immune response. Antibody titres to *S. aureus* antigens already present in all humans rise following infection (Dryla *et al.*, 2005; Roche *et al.*, 2003). However, antibody production and immunological memory appear to be inadequate in the prevention of subsequent infections. *S. aureus* has evolved numerous strategies to thwart the host immune response to facilitate its survival and pathogenesis in superficial and invasive disease conditions. Selected examples of such mechanisms are discussed below.

### **1.3.2 Resistance to phagocytosis**

Phagocytosis results from Fc $\gamma$  receptors and complement receptors (CR1, CR3 and CR4) located on the neutrophil binding to IgG- and complement-coated particles, respectively (Celli and Finlay, 2002). The expression of surface-associated anti-opsonic proteins and a polysaccharide capsule by *S. aureus* can interfere with the deposition of antibodies and complement formation or restrict access by neutrophils to complement receptors and Fc $\gamma$  receptors.

#### **1.3.2.1 Protein A**

Protein A (Spa) is an immunoglobulin-binding protein that is expressed on the surface of over 95% of *S. aureus* strains (Forsgren and Nordstrom, 1974). The surface-expressed portion of the mature protein comprises four or five homologous 56-61 amino acid repeat domains designated E, D, A, B and C (Fig. 1.1). Each domain is capable of binding the Fc $\gamma$  region of IgG (Inganas *et al.*, 1981). However, the full-length Spa molecule can bind to two



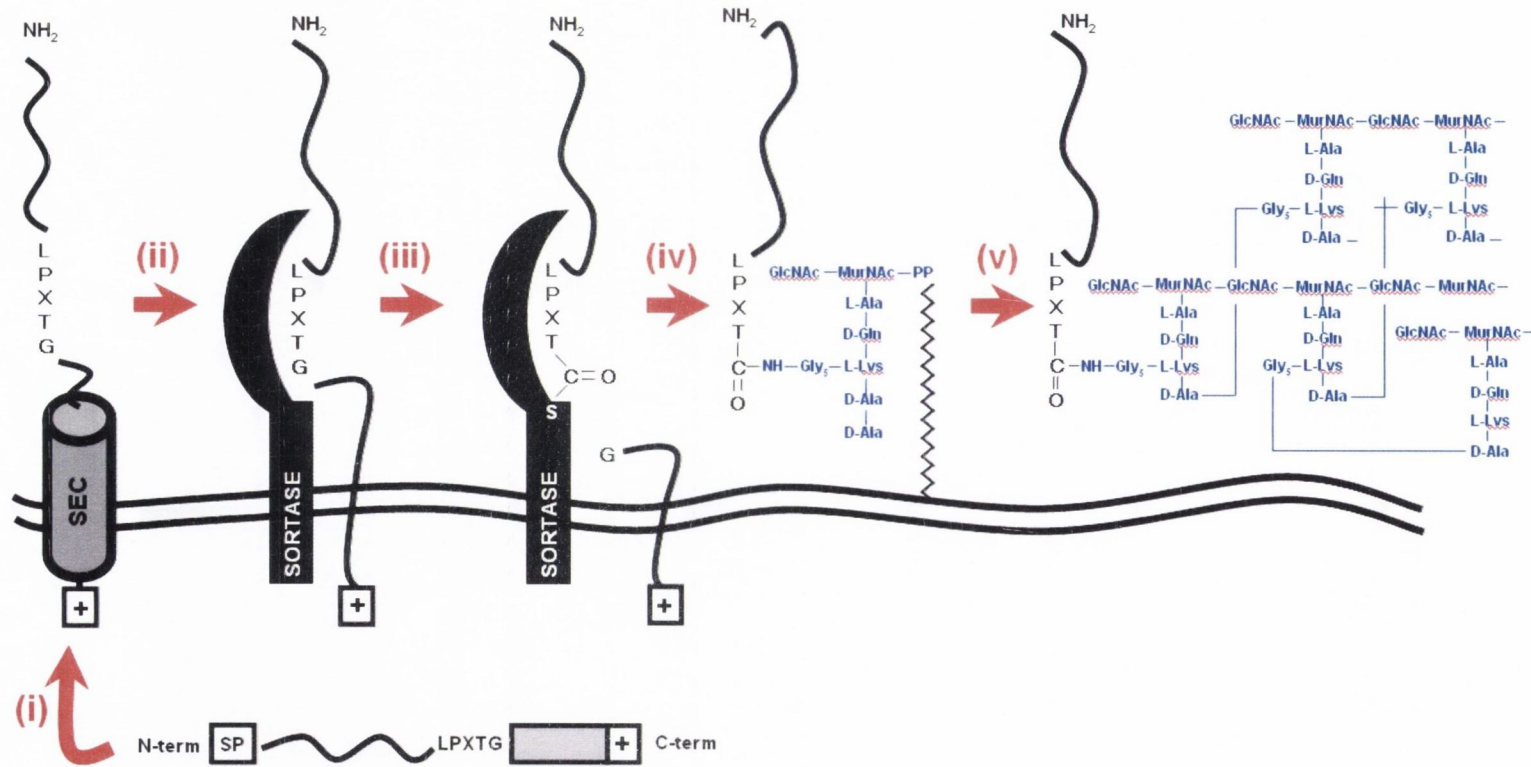


**Figure 1.2. Surface protein anchoring in *Staphylococcus aureus*.** (i) Export. Precursor proteins with an N-terminal signal peptide (SP) are initiated into the secretory (Sec) pathway and the signal peptide is removed. (ii) Retention. The C-terminal sorting signal retains polypeptides within the secretory pathway. (iii) Cleavage. Sortase cleaves between the threonine and the glycine of the LPXTG motif, resulting in the formation of a thioester enzyme intermediate. (iv) Linkage. Nucleophilic attack of the free amino group of lipid II by the thioester bond resolves the acyl-enzyme intermediate, synthesizing the amide bond between surface proteins and the pentaglycine cross-bridge and regenerating the active-site sulphhydryl. (v) Cell wall incorporation. Lipid-linked surface protein is first incorporated into the cell wall via the transglycosylation reaction. The murein pentapeptide subunit with attached surface protein is then cross-linked to other cell wall peptides, generating the mature murein tetrapeptide.

IgG molecules (Cedergren *et al.*, 1993; Jendeberg *et al.*, 1997; Yang *et al.*, 2003). Binding of the Fc $\gamma$ -region of IgG to staphylococcal protein A results in the coating of bacteria with IgG molecules in the incorrect orientation to be recognised by neutrophil Fc $\gamma$ -receptors. This inhibits opsono-phagocytosis by prevention of interactions between IgG and Fc $\gamma$  receptors on the polymorphonuclear leukocytes (PMNL) surface (Gemmell, 1991). The abundance of protein A on the *S. aureus* cell surface leads to coating of the cells with IgG which may protect the cells from recognition by other opsonins (Massey *et al.*, 2002). This explains why *S. aureus spa* mutants are phagocytosed more efficiently *in vitro* and exhibit decreased virulence in several animal infection models (Gemmell, 1991; Palmqvist *et al.*, 2002; Patel *et al.*, 1987).

### 1.3.2.2 Clumping factor A

Clumping factor A (ClfA) is the dominant *S. aureus* fibrinogen-binding surface protein on cells from the stationary phase of growth (Bischoff *et al.*, 2004; O'Brien *et al.*, 2002). ClfA binds to the  $\gamma$ -chain of fibrinogen via its N-terminal A-domain (Fig. 1.1). (McDevitt *et al.*, 1997). When dense suspensions of *S. aureus* cells are mixed with plasma the  $\gamma$ -chain C-termini of fibrinogen, which are located at either end of the bivalent molecule, can bind simultaneously to two ClfA molecules (on different cells). This results in cell clumping and is the basis of the clumping assay used for the rapid identification of *S. aureus*. However, *in vivo* the cell density is too low for clumping to occur. Instead, bacterial cells are coated with fibrinogen molecules.

*S. aureus clfA* mutants are significantly attenuated in a murine model for sepsis and arthritis (Josefsson *et al.*, 2001). This is supported by the observation that ClfA protects *S. aureus* from phagocytosis by murine macrophages and by human neutrophils and that protection is at least partly dependent on fibrinogen (Palmqvist *et al.*, 2004). In addition, bacteria expressing a non-fibrinogen binding ClfA mutant were phagocytosed more efficiently *in vitro* than bacteria expressing the wild-type protein (Higgins *et al.*, 2006). The coating of bacteria with fibrinogen may inhibit deposition of or access to opsonins. This opens up the possibility that other fibrinogen-binding surface proteins (ClfB, FnBPA and FnBPB) may also exhibit anti-phagocytic properties in a similar way during the exponential phase of growth, when these proteins are expressed in greater abundance than ClfA.



### 1.3.2.3 Capsule

The majority of clinical isolates of *S. aureus* produce serotype 5 or serotype 8 capsular polysaccharide (O'Riordan and Lee, 2004; Roghmann *et al.*, 2005). It is not known whether the small proportion of untypable strains express other types of capsule or are non-capsulated. Capsular polysaccharide expression in endocardial vegetations has been shown *in vivo* (Lee *et al.*, 1993). Expression of type 5 and type 8 capsule is associated with increased virulence in animal infection models (Baddour *et al.*, 1992; Lee *et al.*, 1997; Luong and Lee, 2002; Nilsson *et al.*, 1997; Thakker *et al.*, 1998). Capsular polysaccharide has been demonstrated to have antiphagocytic properties due to inhibition of binding of opsonising antibodies that recognise proteins, teichoic acids and peptidoglycan on the cell surface (Thakker *et al.*, 1998). However, high levels of specific anti-capsular polysaccharide antibodies promote opsonophagocytosis and protect against infection (Lee *et al.*, 1997; O'Riordan and Lee, 2004). Reduced O-acetylation of the capsular polysaccharide decreases its antiphagocytic activity, presumably due to increased antibody penetration and cell surface recognition (Bhasin *et al.*, 1998). The inhibition of opsonophagocytosis by capsular polysaccharide contributes to virulence by preventing bacterial clearance by PMNL in the bloodstream, liver and spleen (Bhasin *et al.*, 1998; Luong and Lee, 2002).

### 1.3.3 Complement evasion

A family of small, secreted proteins that counter various components of the complement system have been recently identified. These include proteins that block IgG recognition by C1q (staphylokinase), complement C3 activation (SCIN and homologues), C3b deposition (Efb), C5 activation (SSL7), C5a receptor activation (CHIPS). Current knowledge on these secreted proteins is summarised in this section.

A prerequisite for complement activation is the assembly of C3 convertases on the bacterial surface. This is performed by C4bC2a (classical and lectin pathways) and C3bBb (alternative pathway) by cleavage of C3 resulting in the release of soluble C3a and covalent attachment of C3b to the bacterium. C4bC2a and C3bBb are structurally and functionally similar. *Staphylococcus* complement inhibitor (SCIN), a 9.8-kDa protein secreted by *S.*

*aureus*, binds to and stabilizes both C4bC2a and C3bBb and inhibits C3b formation (Rooijackers *et al.*, 2005a). In doing this, SCIN inhibits amplification of C2 and factor B in the complement cascade and blocks further C3b deposition by all three complement pathways resulting in a substantial reduction in *S. aureus* killing by neutrophils. It is notable that SCIN is highly human specific and is not shown to inhibit complement in any other animal (Rooijackers *et al.*, 2005a).

The extracellular fibrinogen-binding protein Efb, is a 15.6 kDa excreted protein first identified for its ability to bind fibrinogen. Efb was recently shown to bind to complement factor C3 through the C3d region thereby blocking opsonisation via the classical pathway (Lee *et al.*, 2002; Lee *et al.*, 2004a; Lee *et al.*, 2004b). Component C3 is the common link of all three complement activation pathways. Blockage of C3 deposition by Efb therefore inhibits all pathways of complement activation and deposition. The binding site for C3b on Efb is distinct from the fibrinogen-binding site and Efb can bind both molecules simultaneously (Lee *et al.*, 2004b).

Staphylokinase is a 15.5 kDa protein that belongs to a family of plasminogen activators which bind plasminogen, activating it to plasmin. Staphylokinase inactivates C3b and IgG molecules bound to opsonised bacterial cells. Staphylokinase-mediated conversion of plasminogen to plasmin at the staphylococcal surface degrades extra-cellular matrix proteins surrounding the bacterium. Plasmin removes the entire Fc fragment by cleavage of IgG at position Lys 222, including the glycosylation site (Asn 297) essential for recognition by C1q. This cleavage inhibits the activation of the classical pathway of complement fixation and inhibits opsonophagocytosis of *S. aureus* (Rooijackers *et al.*, 2005b).

A number of staphylococcal superantigen-like proteins (SSLs) have been identified. These proteins are closely related to the superantigens but have different biological functions. SSL7 is a 23 kDa secreted protein that binds avidly to the complement protein C5, preventing its activation and thereby preventing complement-mediated cell lysis (Langley *et al.*, 2005). Another small, secreted protein with a remarkably similar structure to SSL7 is the chemotaxis inhibitory protein of staphylococci (CHIPS). CHIPS binds the C5a receptor and the formyl peptide receptor at distinct regions to inhibit the chemotaxis of neutrophils (de Haas *et al.*, 2004). This is discussed in the following section (1.3.4).

Capsular polysaccharide also plays an important role in the inhibition of complement fixation because it prevents access of complement proteins to the *S. aureus* cell surface (Cunnion *et al.*, 2003). Some complement factors can assemble on the cell-wall surface



underneath the polysaccharide, but these are presumably inaccessible to complement receptors on the surface of neutrophils.

#### **1.3.4 Inhibition of neutrophil chemotaxis**

N-formylated peptides secreted by *S. aureus* as a by-product of bacterial translation serve as chemoattractants for leukocyte migration to a site of infection. Chemoattractants are also secreted as a result of complement activation (the peptide fragments C3a and C5a) or by the activation of leukocytes (Schiffmann *et al.*, 1975). These secreted peptides are recognised avidly by specific transmembrane G-protein-coupled receptors on the neutrophil surface, resulting in migration of neutrophils from the blood to the site of inflammation. The chemotaxis inhibitory protein of staphylococci (CHIPS) is a 14.1-kD secreted protein that has binding sites for both the formyl peptide receptor (FPR) and the C5a receptor (C5aR) (de Haas *et al.*, 2004). CHIPS is secreted by about 60% of clinical isolates of *S. aureus* (de Haas *et al.*, 2004; Veldkamp *et al.*, 2000). Two separate active sites on CHIPS are involved in binding to the receptors for complement fragment C5a and the formylated peptide receptors on neutrophils and monocytes. The affinity of CHIPS for the C5a receptor is similar to that of C5a itself (apparent K<sub>d</sub> value of 1.1 nM) which explains why CHIPS can block ligand binding very effectively and is capable of reducing neutrophil recruitment to C5a in a murine peritonitis model of infection, despite having a much greater affinity for human cells (de Haas *et al.*, 2004). CHIPS is hypothesised to play a major role early in infection and is likely to be an important virulence factor.

FPR has two homologues, FPR-like 1 (FPRL1) and FPR-like 2 (FPRL2), which are differentially expressed on the surface of human phagocytes. Monocytes and basophils express FPR, FPRL1, and FPRL2 whereas only FPR and FPRL1 are expressed on the surface of neutrophils (Christophe *et al.*, 2001; Le *et al.*, 2001; Le *et al.*, 2002; Yang *et al.*, 2001). Mature dendritic cells express FPRL2 and FPR (in low amounts), but not FPRL1 (Yang *et al.*, 2001). A homology search of the *S. aureus* genome identified a putative open reading frame with 49% homology with the gene for CHIPS (*chp*) with a leader peptide and a peptidase cleavage site (amino acid sequence AXA). Cloning and expression of the ORF produced a 12 kDa protein with 28% homology with CHIPS (Prat *et al.*, 2006). The recombinant protein was termed the FPRL1 inhibitory protein (FLIPr) because it inhibited FPRL1 and the leukocyte

response to agonists of this receptor. Indeed, FLIPr inhibited neutrophil activation (through FPR) by the high affinity formylated peptide fMLP (Prat *et al.*, 2006). Inhibition was weaker than that of CHIPS, presumably because CHIPS binds FPR which is a higher affinity receptor for fMLP. It is likely that CHIPS and FLIPr function together in protecting *S. aureus* from early detection by the innate immune system.

The *S. aureus* extracellular adherence protein, Eap (also called the MHCII analogous protein, Map), is an anti-inflammatory factor that inhibits neutrophil recruitment. Eap also shows a high structural similarity to CHIPS (Haas *et al.*, 2005). It is predominantly present in the culture supernatant, but some molecules bind to the bacterial surface following secretion (Hussain *et al.*, 2002). Eap binds the intercellular adhesion molecule-1 (ICAM-1) on the surface of endothelial cells and disrupts receptor-mediated leukocyte adhesion to endothelial cells (Chavakis *et al.*, 2002). This process is essential for recruitment of inflammatory cells to the site of infection. This explains why expression of Eap by *S. aureus* reduced neutrophil recruitment to the peritoneal cavity of infected mice (Chavakis *et al.*, 2002). The inhibitory activities of CHIPS and Eap give *S. aureus* novel mechanisms to inhibit leukocyte migration and may potentially be exploited as anti-inflammatory therapeutic compounds.

### 1.3.5 Resistance to antimicrobial peptides

*S. aureus* has developed mechanisms to inhibit bacterial killing by defensins and other antimicrobial peptides once it becomes phagocytosed, in addition to resisting the process of opsonophagocytosis. Antimicrobial peptides form an important part of the innate immune response. They include small anionic peptides (e.g. dermicidin), small cationic peptides (e.g. cathelicidin LL-37, platelet microbicidal proteins), anionic and cationic peptides that form disulphide bonds (e.g.  $\alpha$ -defensins and  $\beta$ -defensins) and some small peptides derived from larger proteins (e.g. lactoferricin from lactoferrin) (Brogden, 2005). Antimicrobial activity is typically due to disruption of the integrity of lipid bilayers, but in some cases more specific inhibitory modes of action may occur (Brogden, 2005).

A significant fraction of engulfed *S. aureus* cells survive killing in *in vitro* neutrophil phagocytosis assays (Fedtke *et al.*, 2004; Peschel, 2002). The *S. aureus* *dlt* operon (*dltABCD*) is associated with the addition of D-alanine moieties to cell surface structures such as wall teichoic acids and lipoteichoic acids (Peschel *et al.*, 1999). These serve to partially neutralise



the negative charge of the cell surface that attracts cationic molecules. The MprF protein of *S. aureus* is involved in modification of membrane phosphatidylglycerol with L-lysine residues (Peschel *et al.*, 2001). This modification also lowers the overall negative charge of the cell surface to reduce binding by a broad range of cationic antimicrobial peptides. *S. aureus* mutants defective in Dlt or MprF are killed more efficiently by cationic antimicrobial proteins and neutrophils *in vitro*, and have markedly reduced virulence in several animal infection models.

*S. aureus* also secretes proteins which neutralize cationic peptides. The extracellular metalloprotease aureolysin cleaves and inactivates the human defensin peptide cathelicidin LL-37 and contributes significantly to resistance to the peptide *in vitro* (Sieprawska-Lupa *et al.*, 2004). Staphylokinase has potent defensin peptide binding activity and induces the release of defensins from leukocyte granules, effectively neutralising them. One molecule of staphylokinase can bind up to 6 defensin peptides (Jin *et al.*, 2004). Interestingly, the genes encoding staphylokinase, CHIPS, SCIN and the superantigen enterotoxin A are found on a pathogenicity island (SaPI5) carried by lysogenic bacteriophages (Rooijackers *et al.*, 2005a). The activities of each protein appear to be specific to the human immune response.

### **1.3.6 Immunomodulation**

#### **1.3.6.1 Protein A**

In addition to the anti-opsonic function of staphylococcal protein A (Spa) through binding the Fc $\gamma$  region of IgG (see section 1.3.2.1), Spa is also a potent suppressor of the immune response. The immunomodulatory function of Spa is attributed to its ability to bind to immunoglobulin bearing heavy chains of the V<sub>H</sub>3 subgroup via the constant portion of the Fab region (Sasso *et al.*, 1989, 1991). Approximately 30-50 % of human IgM bears V<sub>H</sub>3 heavy chains (Silverman *et al.*, 1993). Spa bound to B-cells bearing V<sub>H</sub>3 IgM stimulates their proliferation and apoptosis, leading to depletion of a significant proportion of the repertoire of potential antibody-secreting B cells in the spleen and bone marrow (Goodyear and Silverman, 2004). It has been demonstrated in murine models that recombinant Spa can stimulate and then delete B cells expressing the murine equivalent of human V<sub>H</sub>3 surface immunoglobulin (Silverman *et al.*, 2000). This targeted and specific B-cell apoptotic deletion occurred through



an activation-associated intrinsic pathway (Goodyear and Silverman, 2003). This allows Spa to be characterised as a B-cell superantigen with an immunomodulatory activity.

Studies on the B cell superantigens Spa and *Peptostreptococcus magnus* protein L (PpL) have provided much of our current understanding of structure-function relationships of superantigens. Crystal complexes of Spa and PpL have recently been characterised with their respective human immunoglobulin Fab fragment ligand (Graille *et al.*, 2000; Graille *et al.*, 2001). Both complexes demonstrate how a B cell superantigen can interact with conserved sites in the variable regions of either heavy ( $V_H$ ) or light ( $V_L$ ) chains of an immunoglobulin, distinct from the conventional binding regions for antigen-recognition. Spa and PpL interact with B-cell receptor contact sites comprised of conserved residues in the framework regions of the  $V_H$  and  $V_K$  gene segments, respectively. PpL is a 76–106-kDa protein that comprises 4–6 homologous domains that have both  $\alpha$ -helical and  $\beta$ -pleated sheet portions. Much like Spa, each domain can bind immunoglobulin, in this case with products of the human  $V_{K1}$ ,  $V_{K3}$  and  $V_{K4}$  gene families (Akerstrom and Bjorck, 1989; Bjorck, 1988). Indeed, PpL induces apoptotic death of  $V_K$ -susceptible B cells *in vivo* in a similar manner to that of Spa (Goodyear *et al.*, 2004).

#### 1.3.6.2 Toxin superantigens

Most *S. aureus* strains secrete several superantigen toxins that are associated with food poisoning and toxic shock syndrome (Fraser *et al.*, 2000; Michie and Cohen, 1998). Superantigens bind directly to invariant regions of MHC class II molecules on antigen-presenting cells and to T cell receptors. When expressed at high levels, superantigen toxins cause the unrestricted expansion of T-cells and massive release of cytokines from macrophages and T cells. This cytokine release mediates toxic shock, causing tissue damage and multi-organ dysfunction (Marrack and Kappler, 1990). Superantigen-mediated T cell activation is antigen-independent and the resultant inflammation does not serve to fight staphylococcal infection, but rather overwhelms the host immune system leading to toxic shock, multiple organ system failure and death. Low-level expression of superantigen toxins can cause immune suppression by the local depletion of T cells.

### **1.3.6.3 Major histocompatibility complex class II-analog protein**

The Major histocompatibility complex class II-analog protein (Map/Eap) comprises 6 repeated domains, each containing a 31-amino acid motif with strong homology to the MHC class II  $\beta$ -chain (Jonsson *et al.*, 1995). This motif allows Map to bind to T cell receptors, inhibiting antigen presentation and resulting in the alteration of T cell function. It reduces T cell proliferation causing a reduction in the delayed-type hypersensitivity (cell-mediated, Th1) response (Lee *et al.*, 2002). Map has been shown to inhibit clearance of bacteria from abscesses in internal organs in chronically infected mice (Lee *et al.*, 2002). It is hypothesised that Map may decrease phagocytic uptake of bacteria and enhance the intracellular survival of *S. aureus* by directing the immune system towards a Th2-type response (Harraghy *et al.*, 2003).

## **1.4 Mechanisms of ligand binding by *S. aureus* surface proteins**

### **1.4.1 The dock, lock and latch model for fibrinogen binding**

The *Staphylococcus epidermidis* surface protein SdrG is a member of the Sdr-Clf protein family characterized by a repeat region (R) made up of SD dipeptides (Hartford *et al.*, 2001b; McCrea *et al.*, 2000). The A domain of SdrG binds to the N terminus of the fibrinogen  $\beta$ -chain (Davis *et al.*, 2001). SdrG shares only 24 % and 23 % homology with the A domains of ClfA and ClfB, respectively. However the crystal structure of the SdrG N23 A domain truncate bears striking resemblance to that of the ClfA A domain N23 structure (Figure 1.3; (Davis *et al.*, 2001; Deivanayagam *et al.*, 2002)) and the ClfB A domain N23 structure (Figure 1.3; M. Höök, unpublished data). Each sub-domain has an IgG-like fold, named the DE-variant-IgG fold (DEv-IgG fold) with a cleft of approximately 3 nm separating the two folded domains (Ponnuraj *et al.*, 2003). The crystal structure of the SdrG N23 protein was determined in complex with a synthetic peptide representing the fibrinogen  $\beta$ -chain N-terminus ( $\beta$ 6-20), which was bound in the trench between domains N2 and N3 (Figure 1.3; (Ponnuraj *et al.*, 2003)). Comparison of this structure to that of the apo-SdrG structure (no ligand bound)

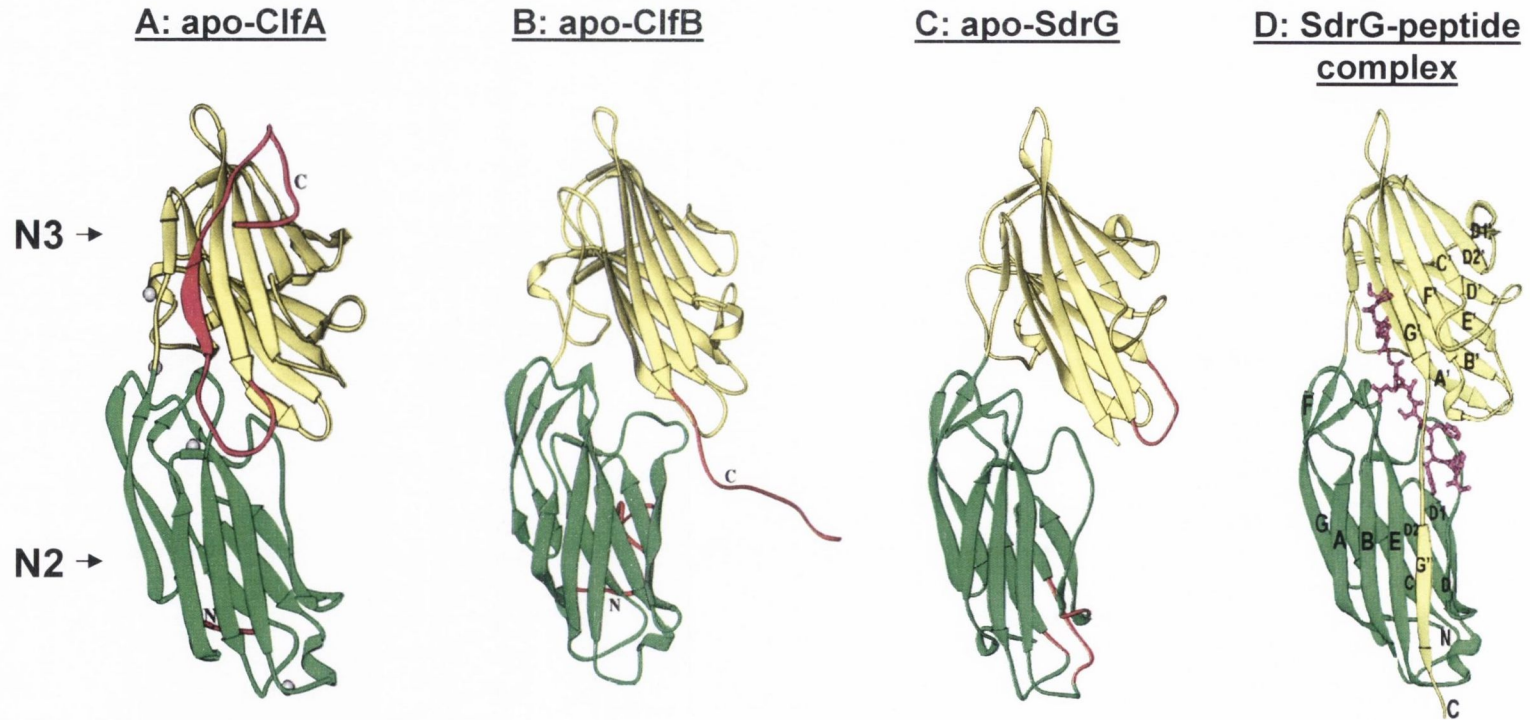


**Figure 1.3 Apo-structures of domains N23 of ClfA, ClfB and SdrG and SdrG-peptide complex.** Ribbon representations of rClfA<sub>(221-559)</sub>, rClfB<sub>(282-542)</sub> and rSdrG<sub>(276-597)</sub>. Regions of poor resolution are shown in red. Domains N2 (green) and N3 (yellow) are indicated. **A.** The C-terminus of rClfA<sub>(221-559)</sub> (latching peptide shown in red) loops back and folds into the N3 domain, partially blocking the proposed ligand-binding cleft. **B.** In rClfB<sub>(282-542)</sub> this peptide is located in the latching cleft of another rClfB molecule. **C.** In apo-SdrG the peptide (G'') is free in solution but interacts with N2 in the SdrG-peptide complex. **D:** Fibrinogen  $\beta$ -chain peptide analogue in complex with SdrG is shown in ball and stick form. The SdrG-peptide complex is taken from Ponnuraj *et al.*, 2003.



allowed a dynamic model for ligand binding to be proposed, namely the ‘dock, lock and latch’ model.

Initially, the fibrinogen peptide ‘docks’ in the trench that separates the N2 and N3 folded domains, and is stabilised by protein-protein interactions between residues in the trench and the ligand. This binding event triggers a structural rearrangement at the C-terminus of the N3 domain.  $\beta$ -strand G’’ (the latching peptide; Figure 1.3) in the apo-form of the structure extends into the solvent region. Upon ligand ‘docking’, the G’’ strand undergoes a directional change and crosses over the binding trench. The binding trench becomes covered by part of the G’  $\beta$ -sheet and the linker separating  $\beta$ -sheets G’ and G’’, thereby ‘locking’ the peptide in place. Hydrogen bonding between the bound fibrinogen peptide and  $\beta$ -strand G’/linker regions of the adhesin secures the ligand in the trench. The final step is  $\beta$ -strand complementation, where the C-terminal  $\beta$ -strand G’’ of the N3 domain ‘latches’ in on to the neighbouring N2 domain, where it inserts between strands E and D (the latching cleft) creating a new  $\beta$ -sheet in the N2 domain (Figure 1.3). This serves to stabilize the overall structure (Ponnuraj *et al.*, 2003). A conserved TYTFTDYVD-like motif forms the back of the latching cleft in rClfA and rClfB. This motif is likely to be involved in binding of the latching peptide to the latching cleft in domain N2 (Ponnuraj *et al.*, 2003). It is proposed that surface proteins bearing DEv-IgG folded domains that bind to fibrinogen (ClfA, ClfB, SdrG, Cna, and possibly FnBPA and FnBPB) all do so by the ‘dock, lock, latch’ mechanism.

#### **1.4.2 The tandem beta-zipper mechanism for fibronectin binding**

The binding of *S. aureus* to fibronectin is mediated by two closely related cell-surface proteins, fibronectin-binding proteins (FnBP) A and B. The expression of either FnBPA or FnBPB on the *S. aureus* surface is sufficient to promote bacterial adhesion to immobilized fibronectin (Greene *et al.*, 1995). These proteins are encoded by two closely linked but separately transcribed genes, *fnbA* and *fnbB* (Jonsson *et al.*, 1991; Signas *et al.*, 1989). Most *S. aureus* strains harbour both genes, although some strains are reported to contain only the *fnbA* gene (Peacock *et al.*, 2000). The FnBPs are composed of a number of domains that mediate interactions with host components. FnBPA and FnBPB contain N-terminal A domains of approximately 500 amino acids that share 45 % identity (Jonsson *et al.*, 1991). The

A domains have fibrinogen-binding and elastin-binding activity. C-terminal to the A domains are the CD domains that have fibronectin-binding activity (Massey *et al.*, 2001; Signas *et al.*, 1989) and share 95 % identity between FnBPA and FnBPB (Jonsson *et al.*, 1991). The primary recognition sequence in fibronectin for *S. aureus* FnBPs are the five type I modules in the N-terminus (Sottile *et al.*, 1991), although a second binding site has been identified in the heparin-binding type III module 14 (Bozzini *et al.*, 1992).

The structure of the B3 peptide of the *Strep. dysgalactiae* fibronectin-binding adhesin SfbI in complex with two of the N-terminal type I modules from fibronectin has recently been solved (Schwarz-Linek *et al.*, 2003). Fibronectin binding by B3 occurred by a tandem  $\beta$ -zipper interaction, where binding motifs in the B3 protein form additional antiparallel  $\beta$ -strands on adjacent type I modules of fibronectin (Schwarz-Linek *et al.*, 2003), shown in Figure 1.4. Eleven fibronectin-binding modules were identified in *S. aureus* FnBPA that stretch from the C-terminus of the A domain through to the D-repeats, each containing type I module-binding motifs (Schwarz-Linek *et al.*, 2003). This region of FnBPA (the BCD domain) has no discernable secondary structure, but upon binding to fibronectin type I modules this unfolded region adapts an ordered conformation (House-Pompeo *et al.*, 1996). It has also been demonstrated that one FnBPA molecule can accommodate two fibronectin molecules (Matsuka *et al.*, 2003). It is likely that *S. aureus* FnBPs bind to several fibronectin modules through a tandem  $\beta$ -zipper, accounting for the high affinity and specificity of this interaction (Schwarz-Linek *et al.*, 2003).

### 1.4.3 The 'collagen hug' mechanism

Collagen is the main component of the extracellular matrix of connective tissue. Some strains of *S. aureus* express a collagen-binding adhesin (Cna) that is necessary and sufficient for adhesion of *S. aureus* to collagen substrates and collagenous tissues (Patti *et al.*, 1992). Cna may be an important virulence determinant of infections involving collagen-rich bone tissue such as arthritis and osteomyelitis. It is a virulence factor in animal models of septic arthritis, endocarditis and osteomyelitis (Elasri *et al.*, 2002; Hienz *et al.*, 1996; Patti *et al.*, 1994), and vaccination against Cna is protective in septic arthritis (Nilsson *et al.*, 1998). However, the *cna* gene is only present in approximately 30 to 50 % of *S. aureus* isolates



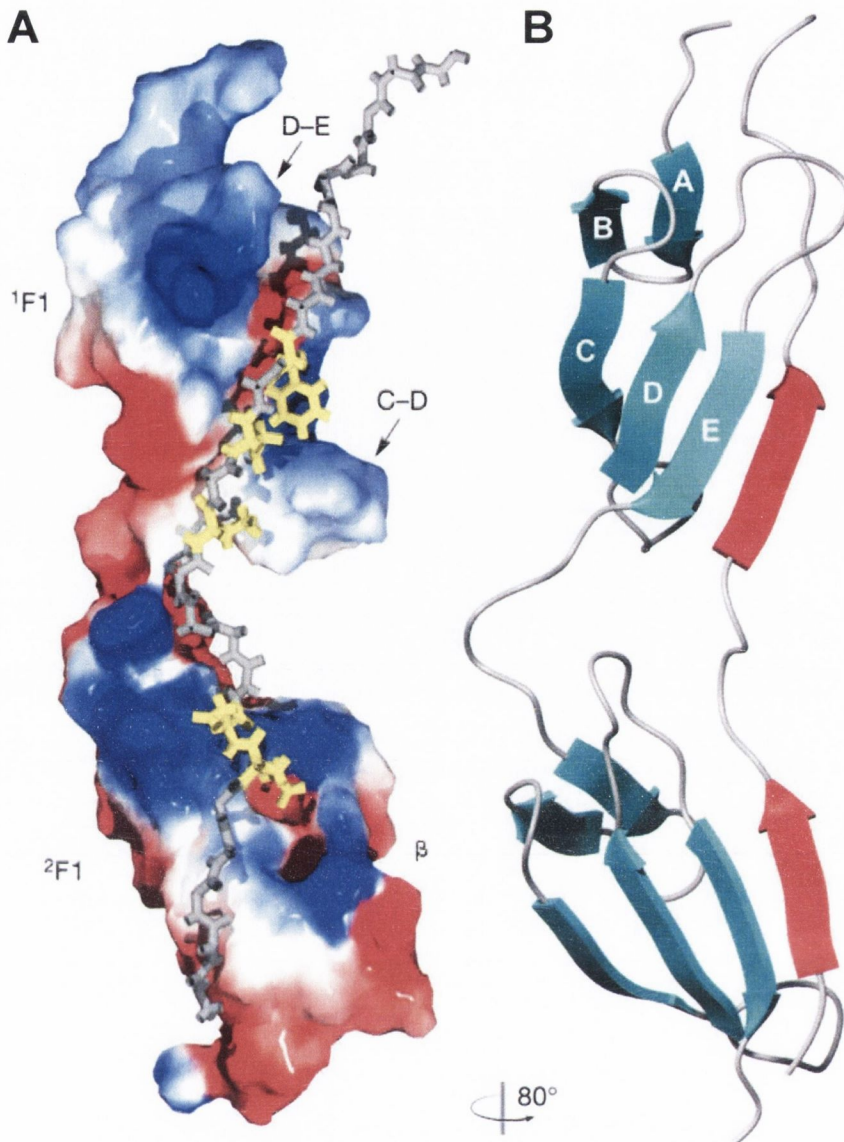


**Figure 1.4** Structure of the *Strep. dysgalactiae* B3 peptide in complex with  $^1\text{F1}^2\text{F1}$  type I fibronectin modules. **A.** Surface potential of  $^1\text{F1}^2\text{F1}$  fibronectin modules with bound B3 peptide (grey). Negatively and positively charged regions of the  $^1\text{F1}^2\text{F1}$  surface are shown in red and blue, respectively. Side chains of hydrophobic and acidic B3 residues are shown in yellow **B.** Ribbon diagram of the lowest-energy  $\beta$ -zipper structure showing strands of the F1 modules (cyan) and the fourth strand formed by B3 (red). The difference in orientation between the two views is indicated. Taken from Schwarz-Linek *et al.*, 2003.

(Arciola *et al.*, 2005; Peacock *et al.*, 2002; Smeltzer *et al.*, 1997) so it does not represent a useful target for vaccination or immunotherapy.

Collagen-binding activity is located in the A domain, an approximately 500 amino acid region, and the minimum ligand-binding truncate (Cna<sub>151-315</sub>) has been crystallized (Patti *et al.*, 1995; Symersky *et al.*, 1997). Cna<sub>151-315</sub> forms a DEv-IgG folded domain containing a surface trench in one of its  $\beta$ -sheets that can accommodate the collagen triple helix (Deivanayagam *et al.*, 2000; Symersky *et al.*, 1997). However, this minimum collagen-binding region has a 10-fold lower affinity for collagen when compared with the entire A domain, suggesting that regions flanking this central segment participate in collagen binding by Cna (Patti *et al.*, 1993; Xu *et al.*, 2004). For this reason, a Cna truncate comprising the minimum collagen-binding region and some flanking residues (Cna<sub>31-344</sub>) capable of binding a collagen peptide with high affinity was isolated for structural studies (Zong *et al.*, 2005). The crystal structure of the Cna<sub>31-344</sub>-collagen peptide complex revealed that the collagen peptide does indeed dock at the DEv-IgG fold in Cna<sub>31-344</sub>, much like the mechanism of fibrinogen-binding by *S. epidermidis* SdrG and presumably the *S. aureus* fibrinogen-binding surface proteins, discussed in section 1.4.1. However, the proposed model for collagen-binding is distinct from that of fibrinogen-binding. The collagen peptide initially associates with the N2 domain of Cna<sub>31-344</sub> and not the DEv-IgG fold. The N1 domain then ‘hugs’ the collagen peptide by folding over it and forming multiple hydrophobic contacts with the N2 domain, locking the bound peptide in place. Conformational changes in the long linker region between regions N1 and N2 of the Cna A-domain further secure the bound ligand. A C-terminal latch maintains the folded N1 domain in contact with N2 (Zong *et al.*, 2005). This is depicted in Figure 1.5.

## **1.5 Other *S. aureus* surface proteins**

### **1.5.1 Iron-regulated surface proteins**

A subset of *S. aureus* genes is expressed only under iron-limitation, resembling growth conditions in serum and within the host during infection. The genes encoding 5 of the iron-surface-determinant (Isd) proteins (IsdA, IsdB, IsdC) are found in a locus encoding an iron-transport system (Mazmanian *et al.*, 2003). The regulon also includes genes encoding IsdH and IsdI, located outside the main *isd* cluster (Dryla *et al.*, 2003). Expression is controlled by



the ferric-uptake-response (Fur) transcriptional regulator which inhibits transcription of *isdA*, *isdB*, *isdC* and *isdH* in the presence of  $\text{Fe}^{+3}$  (Dryla *et al.*, 2003; Horsburgh *et al.*, 2001; Mazmanian *et al.*, 2003). IsdA, IsdB and IsdH each contain the sortase A LPXTG sorting signal, while IsdC contains an NPQTN motif for sortase B-catalysed cell wall sorting (Dryla *et al.*, 2003; Mazmanian *et al.*, 2002). IsdA binds transferrin, haemoglobin, and heme (Clarke *et al.*, 2004; Mazmanian *et al.*, 2003; Taylor and Heinrichs, 2002). IsdA interacts with transferrin and heme (Mazmanian *et al.*, 2003; Taylor and Heinrichs, 2002; Vermeiren *et al.*, 2006). IsdB contains heme-binding and hemoglobin-binding activities (Mazmanian *et al.*, 2003; Torres *et al.*, 2006) and IsdH binds haptoglobin and haptoglobin-haemoglobin complexes (Dryla *et al.*, 2003). Expression of Isd proteins in response to limiting levels of free iron is believed to result in binding of heme-containing ligands to Isd proteins. Heme molecules are liberated and transferred across the cell wall and membrane into the cytoplasm (Mazmanian *et al.*, 2003; Skaar and Schneewind, 2004). IsdC appears to be buried in the cell wall and is not displayed on the cell surface (Mazmanian *et al.*, 2002). It is proposed to function in the passage of heme iron across the cell wall (Skaar and Schneewind, 2004). Several other iron-uptake mechanisms have been identified in *S. aureus*, including another heme-iron uptake system (*hts* locus) and numerous siderophore-dependent systems (Skaar *et al.*, 2004). This indicates that the Isd iron-uptake system is redundant in function, as evidenced by the ability of *isd* mutants to continue to utilize haem-iron (Mazmanian *et al.*, 2003).

Other ligands have been identified for some of the Isd surface proteins. IsdA is a physiologically relevant adhesin for fibrinogen and fibronectin when *S. aureus* is grown in iron-depleted conditions (Clarke *et al.*, 2004). IsdH has been shown to bind complement component C3 (N. Yanasigisawa, P. Speziale and T.J. Foster, unpublished data) which may interfere with complement deposition on the bacterial surface. The binding domains in IsdA and IsdH are known as NEAT domains (near transporter), which are found in variable numbers in bacterial proteins, the genes for which are in the vicinity of putative iron-siderophore transporters in Gram-positive bacteria (Andrade *et al.*, 2002). IsdA and IsdC contain a single NEAT domain, IsdB has two and IsdH bears three NEAT domains (Andrade *et al.*, 2002). The NEAT domains of IsdA and IsdH share only 20 % sequence identity (Clarke *et al.*, 2004), but the recently determined structures of NEAT domains (IsdH of *S. aureus*) revealed that all are members of the structurally related immunoglobulin (Ig) superfamily. All NEAT domains are expected to belong to this family, because the

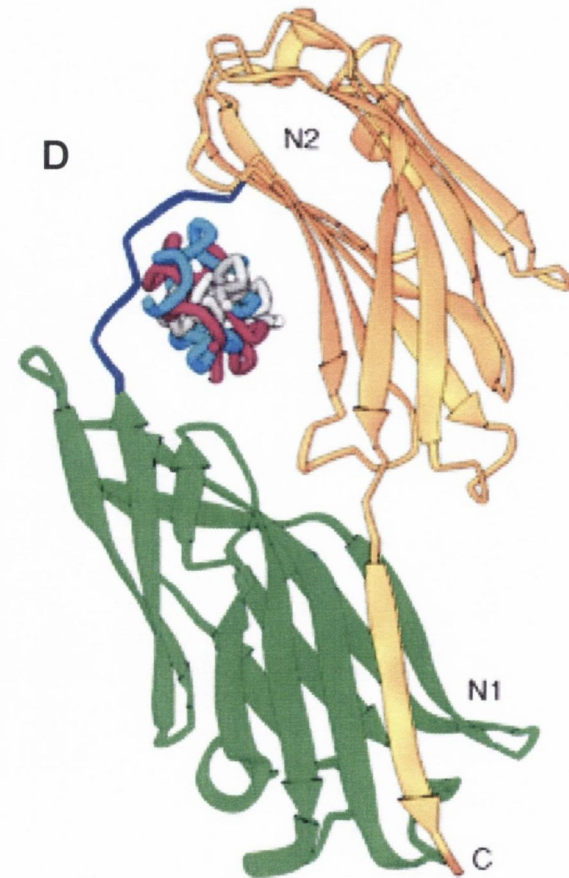
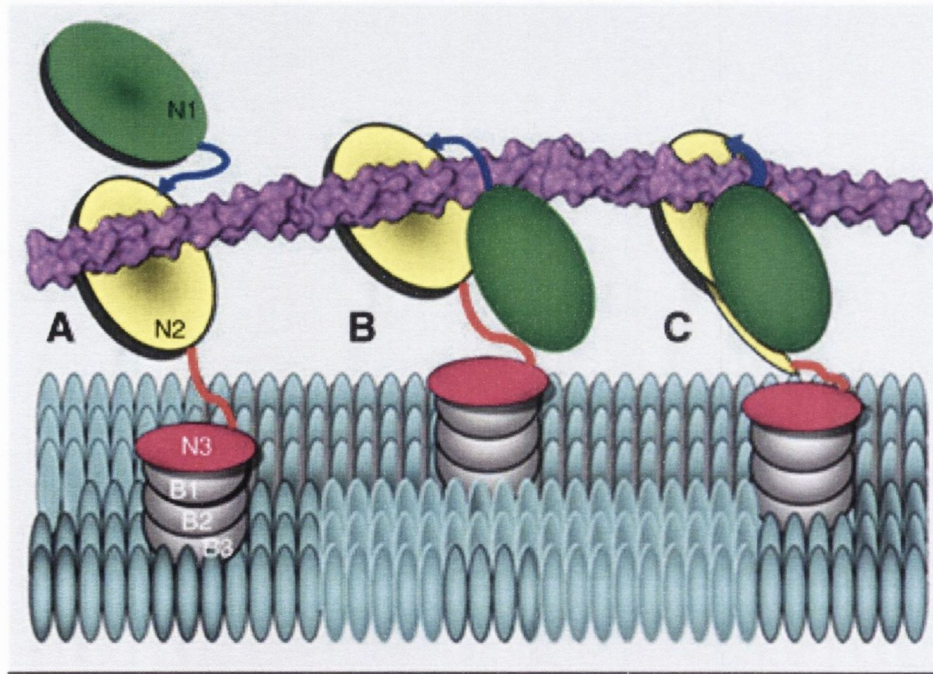


**Figure 1.5 The 'Collagen Hug' hypothesis model shown in a cartoon representation.** The collagen triple helix initially associates with the N2 domain (*A*) and is then wrapped by the N1–N2 linker and the N1 domain (*B*). *C*, The N1 domain interacts with the N2 domain via multiple hydrophobic interactions and finally the C-terminal latch is introduced in the N1 domain to secure the ligand in place. *D*, crystal structure of the collagen peptide in between N1 (green) and N2 (yellow) of *Cna*. Taken from Zong *et al.*, 2005.



hydrophobic residues that contribute to the core are highly conserved (Pilpa *et al.*, 2006). However, sequence diversity in other residues across the NEAT domains confers differences in ligand-binding (Clarke *et al.*, 2004; Dryla *et al.*, 2003).

### 1.5.2 Serine-aspartate repeat (Sdr) and novel *S. aureus* surface (Sas) proteins

*S. aureus* contains three genes (in addition to *clfA* and *clfB*) that encode surface proteins with Ser-Asp (SD) repeats (Josefsson *et al.*, 1998). The *sdrC*, *sdrD*, and *sdrE* genes are closely linked in a tandem-array in the *S. aureus* chromosome, although some strains do not contain all three genes (Josefsson *et al.*, 1998). A molecular function has not yet been revealed for SdrD and SdrE; however, these proteins are proposed to bind host extracellular matrix like other LPXTG-anchored proteins (Josefsson *et al.*, 1998; Patti *et al.*, 1994). Recently, it was shown that immunization with recombinant IsdA, IsdB, SdrD, and SdrE generated the highest level of protection in a murine renal infection model compared with 15 other *S. aureus* surface proteins (Stranger-Jones *et al.*, 2006).

Analysis of *S. aureus* genome sequences predicted 10 novel proteins harbouring the LPXTG motifs that are found in cell-wall associated surface proteins (Mazmanian *et al.*, 2001; Roche *et al.*, 2003). These were designated *S. aureus* surface (Sas) proteins. Antibodies against many Sas proteins have been detected in convalescent sera from patients with documented *S. aureus* infections (Roche *et al.*, 2003) indicating that expression of the Sas proteins occurs during infection. Like other *S. aureus* surface proteins, many of these proteins contain repeat domains. SasE, SasI and SasJ, which were present in all the genome sequences analysed, have been renamed IsdA, IsdH and IsdB, respectively (see section 1.5.1). SasG is homologous to the Pls (plasmin-sensitive) surface protein, which is encoded within the type I SCC*mec* element of some MRSA strains. Pls impairs bacterial adhesion to ligands such as fibrinogen or fibronectin (Savolainen *et al.*, 2001). In addition, SasG and Pls can promote *S. aureus* adherence to nasal epithelial cells (Roche *et al.*, 2003) which may be important for nasal colonization. SasA (also known as SraP) can promote *S. aureus* binding to platelets and is a virulence factor in the rabbit endocarditis model (Siboo *et al.*, 2005). No functions have been attributed to other Sas proteins (SasC, SasD, SasF, SasH, SasK).

## 1.6 Regulation of virulence determinants of *S. aureus*

Exoprotein production *in vitro* by *S. aureus* follows a temporal programme. In general, adhesins are produced before toxins and exo-enzymes (Chan *et al.*, 1998; Cheung *et al.*, 2004; Novick, 2003) which may also be the case *in vivo* (Novick, 2003). It is believed that the expression of adhesins at the beginning of the infectious process allows the bacteria to establish themselves at a focus of infection. *S. aureus* then secretes exoproteins that damage host tissue and thwart the immune response (see Section 1.3). These exoproteins can facilitate detachment and spreading throughout the body (McAleese *et al.*, 2001; McGavin *et al.*, 1997). Although it may not be strictly true, this is a useful paradigm for the study of surface proteins and secreted virulence factors. The bi-phasic pattern of expression is controlled by a density-sensing mechanism encoded by the *agr* locus, other two-component regulatory systems, transcription factors and alternative sigma factors (Bronner *et al.*, 2004; Cheung *et al.*, 2004).

### 1.6.1 Regulation of the *spa* promoter

Expression of the protein A (*spa*) gene is controlled in a complicated network by several regulators. Spa, like many of the *S. aureus* surface proteins, is expressed during the exponential phase of growth and then is transcriptionally down-regulated in the post-exponential growth phase. This process involves the Agr (accessory gene regulator) quorum-sensing global regulatory system (Benito *et al.*, 2000; Ji *et al.*, 1995). The Agr locus is comprised of two divergent transcriptional units. The first encodes a two-component regulatory system (*agrBDCA*). AgrB is a transmembrane protein that is responsible for the transport and processing of AgrD (Zhang *et al.*, 2002). AgrD is exported as a cyclic peptide, named the autoinducing peptide (AIP) (Ji *et al.*, 1995). Accumulation of AIP to a threshold concentration leads to it binding to AgrC, the sensor of the two-component system. Binding induces autophosphorylation of AgrC. The phosphate moiety is subsequently transferred to the transcription factor AgrA (Lina *et al.*, 1998). When activated, AgrA stimulates transcription from both of the *agr* locus promoters, P<sub>*agrBDCA*</sub> and the promoter for RNAIII. RNAIII is a 514 nucleotide RNA that encodes the delta toxin. RNAIII also binds to the ribosome-binding site of the *spa* mRNA, thereby recruiting endoribonuclease III which then degrades the *spa* mRNA (Huntzinger *et al.*, 2005; Janzon and Arvidson, 1990; Novick *et al.*, 1993). It most likely complexes with cytoplasmic protein(s) to form a transcriptional regulator that activates several



promoters (eg. *hla* which encodes  $\alpha$ -toxin) and represses others (such as *spa*). This occurs in the post-exponential phase of growth.

Several additional regulatory factors are also involved in the regulation of *spa* expression, including SarA (staphylococcal accessory regulator), SarS (initially designated SarH1), Rot (repressor of toxins), SarT, and the ArlR-ArlS two-component system (Bayer *et al.*, 1996; Cheung *et al.*, 1997; Cheung *et al.*, 1999; Cheung *et al.*, 2001; Cheung *et al.*, 2004; Chien *et al.*, 1999; Fournier *et al.*, 2001; Said-Salim *et al.*, 2003; Schmidt *et al.*, 2003; Tegmark *et al.*, 2000). SarA is a pleiotropic regulator for multiple genes (Chien *et al.*, 1999). Transcriptional profiling indicates that SarA represses transcription of a number of genes, including *spa*, and stimulates transcription of other genes, including *agr* (Chien and Cheung, 1998; Dunman *et al.*, 2001). Regulation by SarA can occur through Agr-dependent and Agr-independent mechanisms (Chien and Cheung, 1998). There is a SarA recognition sequence immediately upstream of the -35 box in the *spa* promoter (Chien *et al.*, 1999). The *sarS* gene is located immediately upstream of *spa*. SarS is a positive regulator of *spa* expression and is repressed by RNAIII (Cheung *et al.*, 2001; Tegmark *et al.*, 2000). Mutational analysis of the *spa* promoter suggests that SarS might stimulate *spa* transcription by competing with SarA (Gao and Stewart, 2004). In stationary phase, transcription of *sarA* is activated by a SigB-dependent promoter.

Other members of the Sar family of proteins, SarT and Rot appear to indirectly regulate *spa* transcription by up-regulation of *sarS* (Said-Salim *et al.*, 2003). Whether *rot* regulates gene transcription directly is not known, but the effect of *rot* on expression of several virulence genes seems to be opposite to that of RNAIII (Said-Salim *et al.*, 2003). Microarray analysis indicated a 15.6-fold enhancement of *spa* transcription by Rot. The ArlRS two-component regulatory system has been reported to affect *spa* expression (Fournier *et al.*, 2001). *spa* transcription is increased upon inactivation of *arlR* or *arlS*. The *arl* mutations did not affect *spa* transcription in an *agrA* or *sarA* mutant background, suggesting that the effect of the Arl proteins on *spa* expression occurs through other regulators in an indirect manner (Fournier *et al.*, 2001). In addition, the *mgrA*-encoded protein has been shown to act as a repressor of protein A production (Luong *et al.*, 2003).

The net effect of these numerous control pathways is that transcription of the *spa* and translation of the Spa protein is abruptly terminated when cells enter the stationary phase of growth. The regulatory elements involved in *spa* transcription are illustrated in Figure 1.6.

## 1.7 von Willebrand Factor

### 1.7.1 The von Willebrand Factor multimer

Plasma von Willebrand factor (vWF) is a multimeric protein that mediates adhesion of platelets to sites of vascular injury. vWF is synthesised in endothelial cells and megakaryocytes. The primary translation product of the *vwf* gene (pre-pro-vWF) is a 2813 residue peptide that includes a 22 amino acid signal peptide. In the endoplasmic reticulum vWF molecules are dimerised in a tail-to-tail configuration by disulfide bonding at the C-terminal ends to form pro-vWF dimers (Wagner *et al.*, 1987b). Pro-vWF dimers are transported to the Golgi apparatus where they are glycosylated and sulphated. They are next multimerized in a head-to-head configuration by the formation of additional disulfide-bonds at the N-terminal ends. After multimerisation, the propeptides are removed proteolytically by the enzyme furin and are released along with mature vWF from the endothelial cells (Fig. 1.7; (Sadler, 1998)).

Mature vWF comprises 2050 residues and the largest vWF multimers can comprise up to 80 subunits (Voorberg *et al.*, 1990). vWF produced by endothelial cells is either secreted constitutively or stored in Weibel–Palade bodies and released in response to thrombin, fibrin, histamine, and complement factors 5b-9. The constitutively secreted vWF is composed of dimers and small multimers whereas vWF released from Weibel–Palade bodies is of high molecular weight (Sporn *et al.*, 1986, , 1987; Wagner *et al.*, 1987a). The vWF multimeric structure is essential for its function (Fischer *et al.*, 1996). Structural studies on vWF performed using electron microscopy show that multimeric vWF consists of a repeating unit with a maximum extended length of 120 nm (Fowler *et al.*, 1985). Rotary-shadowed electron microscopy of vWF immobilised on mica revealed that 87% of multimeric vWF adopted a "ball of yarn" or "tangled" conformation with a mean diameter of 100–150 nm, whereas the remainder assumed an "extended form" with a mean length of 350 nm (Raghavachari *et al.*, 2000). However, studies using atomic force microscopy (AFM) on vWF immobilised to collagen suggested that the vWF structure determined depends on the surface on which it is deposited (Novak *et al.*, 2002).

Solution studies in which vWF was subjected to a shear force gradient in a cone-and-plate rotating device demonstrated the existence of long, uncoiled molecules when shear stress exceeded a threshold limit of 3.5 N/m<sup>2</sup> (Siedlecki *et al.*, 1996). These data support the



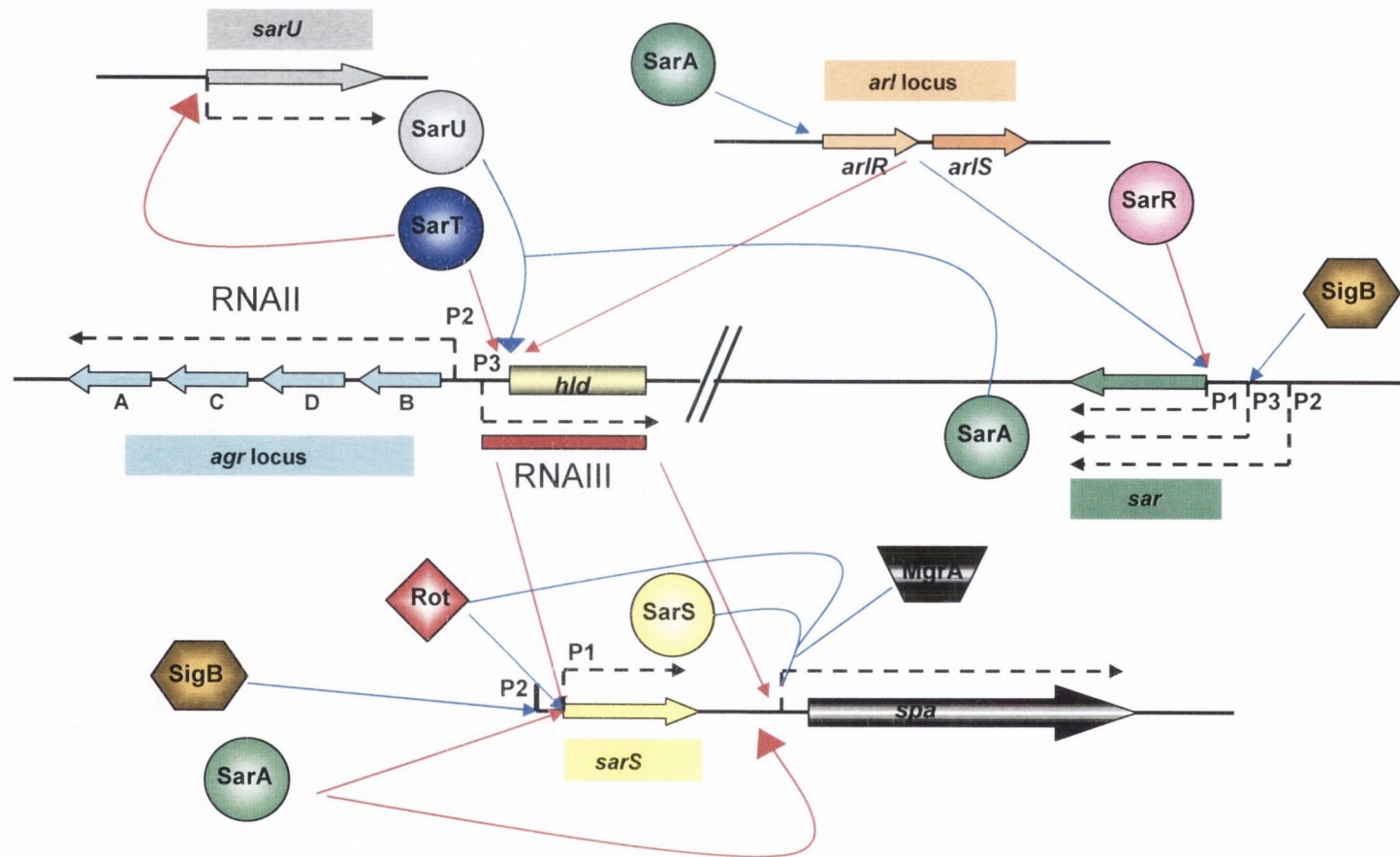


**Fig. 1.6 Schematic overview of the regulation of *spa*.** Arrows indicate activation (blue) or repression (red). *agr* (RNAIII) represses *sarS* expression and *spa*. *MgrA* stimulates *spa* expression through *sarS* and probably also directly. *Rot* directly stimulates both *sarS* and *spa* expression. *SarA* is a direct repressor of *sarS*, *spa* and also *arlRS*. *SarR* represses expression of *sarA*. *SarS* directly activates *spa*. *SarT* directly represses *sarU* (an activator of *agr* transcription).

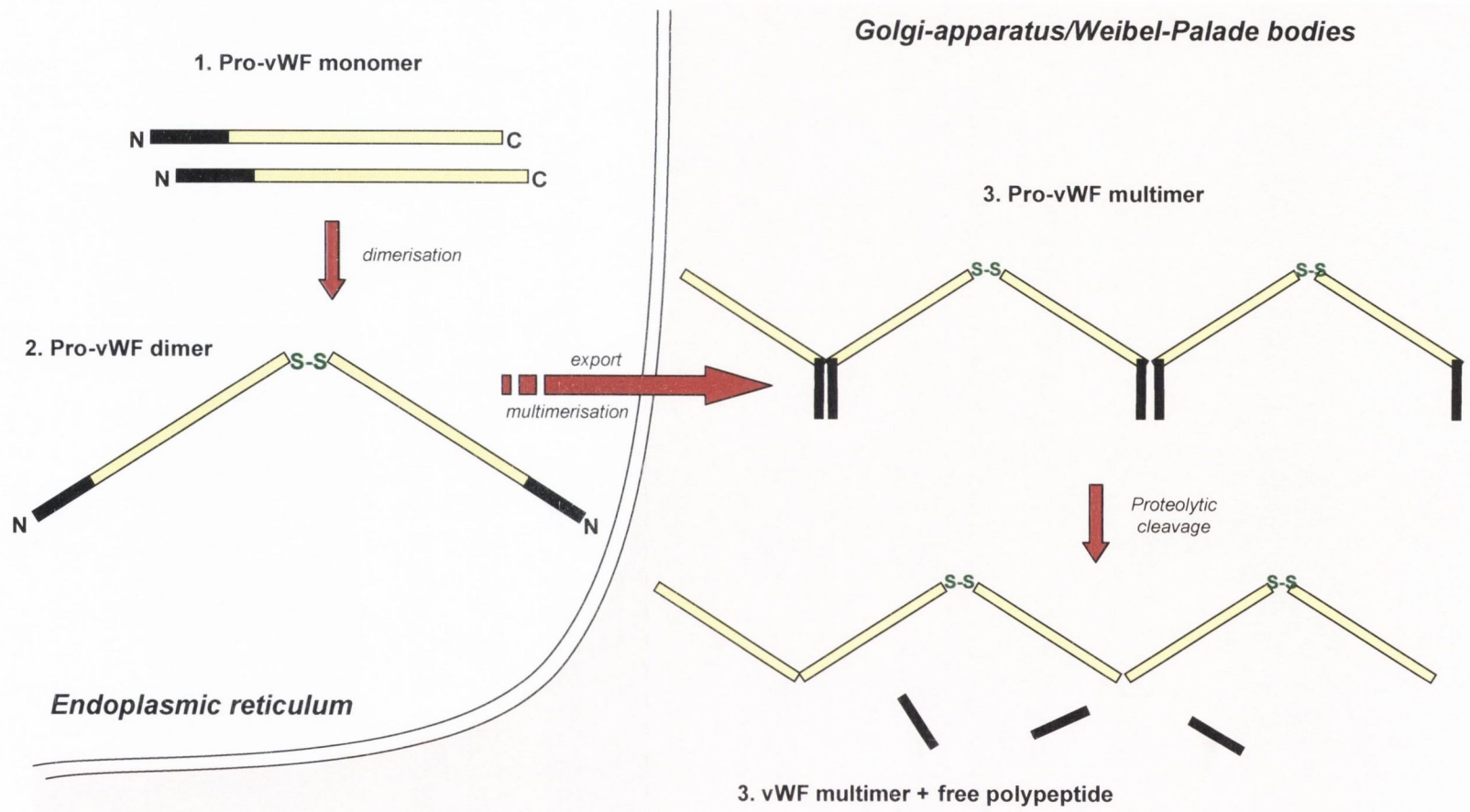


**Fig. 1.7. Biosynthesis of von Willebrand Factor.** Intersubunit disulfide bonds are formed near the carboxyl-termini of pro-vWF dimers in the endoplasmic reticulum. Additional intersubunit disulfide bonds are formed near the amino-terminus of the mature subunits to assemble multimers in the Golgi apparatus and finally, the N-termini are proteolytically removed. For details see text (section 1.7.1)

hypothesis of shear-induced modification in the three-dimensional structure of vWF. The vWF molecule was tethered to artificial material (octadecyl-trichlorosilane) which forms a self-assembling monolayer on glass. It provides an optimally flat surface for direct observation of protein molecules (Siedlecki *et al.*, 1996). However, these data could not be reproduced when vWF was attached to a collagen surface (Novak *et al.*, 2002).

### **1.7.2 The von Willebrand Factor monomer**

The vWF monomer is made up of four types of repeat domain (A, B, C, D) arranged in the order D'-D3-A1-A2-A3-D4-B1-B2-B3-C1-C2-CK (Fig. 1.8) from N- to C-terminus. The D3 domain contains cysteine residues involved in the formation of the N-terminal intermolecular disulfide bridges necessary for multimerisation. Intermolecular disulfide bridges are formed involving Cys379, and at least one cysteine of Cys459 Cys462-Cys464 (Dong *et al.*, 1994; Fujimura *et al.*, 1986). The CK domain contains the cysteine residues involved in C-terminal dimerisation, most likely through residues Cys2008, Cys2010 and Cys2048 (Katsumi *et al.*, 2000). The D' and the D3 domains are involved in binding and stabilizing coagulation factor VIII (Foster *et al.*, 1987; Kaufman *et al.*, 1999; Koedam *et al.*, 1990; Takahashi *et al.*, 1987). The A1 domain binds GpIb $\alpha$ , heparin, collagen type III and VI and sulfatides (Christophe *et al.*, 1991; Fujimura *et al.*, 1987; Hoylaerts *et al.*, 1997; Mazzucato *et al.*, 1999; Roth *et al.*, 1986; Sixma *et al.*, 1991). The A2 domain contains the proteolytic cleavage site for the vWF protease, ADAMTS-13 (Zheng *et al.*, 2001). The A3 domain contains the major collagen binding site of vWF (Lankhof *et al.*, 1996; Roth *et al.*, 1986). No specific function has been assigned for the D4 and B domains. The C domains contain the integrin recognition motif (Arg-Gly-Asp or RGD) beginning at position 1744 (Plow *et al.*, 2000).

### **1.7.3 Structural studies of the von Willebrand Factor A1 domain**

The vWF A1 domain comprises residues 497-716 of the mature vWF subunit and contains a disulfide bridge between Cys509 and Cys695 (Marti *et al.*, 1987; Nishio *et al.*, 1990; Shelton-Inloes *et al.*, 1986; Titani *et al.*, 1986). Its structure has been determined by X-ray crystallography (Emsley *et al.*, 1998) alone as well as in complex with the platelet receptor GpIb- $\alpha$  (Huizinga *et al.*, 2002), the snake venoms botrocetin (Fukuda *et al.*, 2005) and



biticetin (Maita *et al.*, 2003), and with a function blocking antibody Fab fragment Nmc-4 (Celikel *et al.*, 1998). The structure of a ternary complex of vWF A1, GpIb- $\alpha$  and botrocetin is also available (Fukuda *et al.*, 2005). The vWF A1 domain comprises an  $\alpha/\beta$  fold with a central  $\beta$  sheet flanked by three  $\alpha$ -helices on each side (Fig. 1.9), similar to the homologous type A domains of other proteins whose structure has been determined, which includes the integrin subunits  $\alpha_M$  (Lee *et al.*, 1995),  $\alpha_L$  (Qu and Leahy, 1995), and  $\alpha_2$  (Emsley *et al.*, 1997), as well as the VWF A3 domain (Bienkowska *et al.*, 1997; Huizinga *et al.*, 1997). All A-type domains adopt a so-called "Rossmann" or di-nucleotide binding fold, consists of a central hydrophobic  $\beta$ -sheet flanked on both sides by amphipathic  $\alpha$ -helices.

The N- and C-termini of vWF A1 are linked by a disulfide bridge formed by Cys509 and Cys695. The presence of this disulfide bridge is essential for the proper function of the vWF A1 domain and its removal causes a substantial reduction in the binding affinity for GpIb- $\alpha$  (Azuma *et al.*, 1993; Cruz *et al.*, 1993; Miura *et al.*, 1994; Miyata and Ruggeri, 1999). The A1 domain does not bind spontaneously to the platelet receptor GpIb- $\alpha$  because it needs to be activated. Removal of the *O*-linked glycans or desialisation of vWF A1 induces GpIb- $\alpha$  binding (Carew *et al.*, 1992; Cruz *et al.*, 1993; De Marco *et al.*, 1985). Similarly, binding of vWF A1 by the antibiotic ristocetin A, and the snake toxins botrocetin and bitiscetin result in activation. Immobilization of vWF to a surface (such as a blood vessel wall) also induces activation and platelet binding, most likely due to a conformational change in vWF. In the crystal structure of vWF A1 in complex with GpIb- $\alpha$ , two contact sites have been identified by structural, biochemical, and mutagenesis data (Cauwenberghs *et al.*, 2000; Cauwenberghs *et al.*, 2001; Huizinga *et al.*, 2002; Matsushita and Sadler, 1995). These regions lie on the concave face of GpIb- $\alpha$  that interacts with A1 (the so-called N-terminal  $\beta$ -hairpin) and a flexible loop at the C-terminal region termed the regulatory " $\beta$ -switch" region, which undergoes a conformational change upon binding vWF. It has been proposed that the increased affinity for GpIb- $\alpha$  of amino acid substitutions associated with type 2B von Willebrand's disease (VWD) is a result of displacement of the N- and C- termini of A1 that could otherwise be inhibitory in GpIb- $\alpha$  binding (Huizinga *et al.*, 2002).

Mutations affecting the vWF A1 domain associated with an active or inactive variant form of vWF A1 are categorized as type 2B and type 2M von Willebrand's disease (VWD), respectively. VWD is not actually a disease, but a heritable bleeding disorder. Type 2B VWD is characterised by an increased affinity of vWF for GpIb- $\alpha$  independent of activating factors



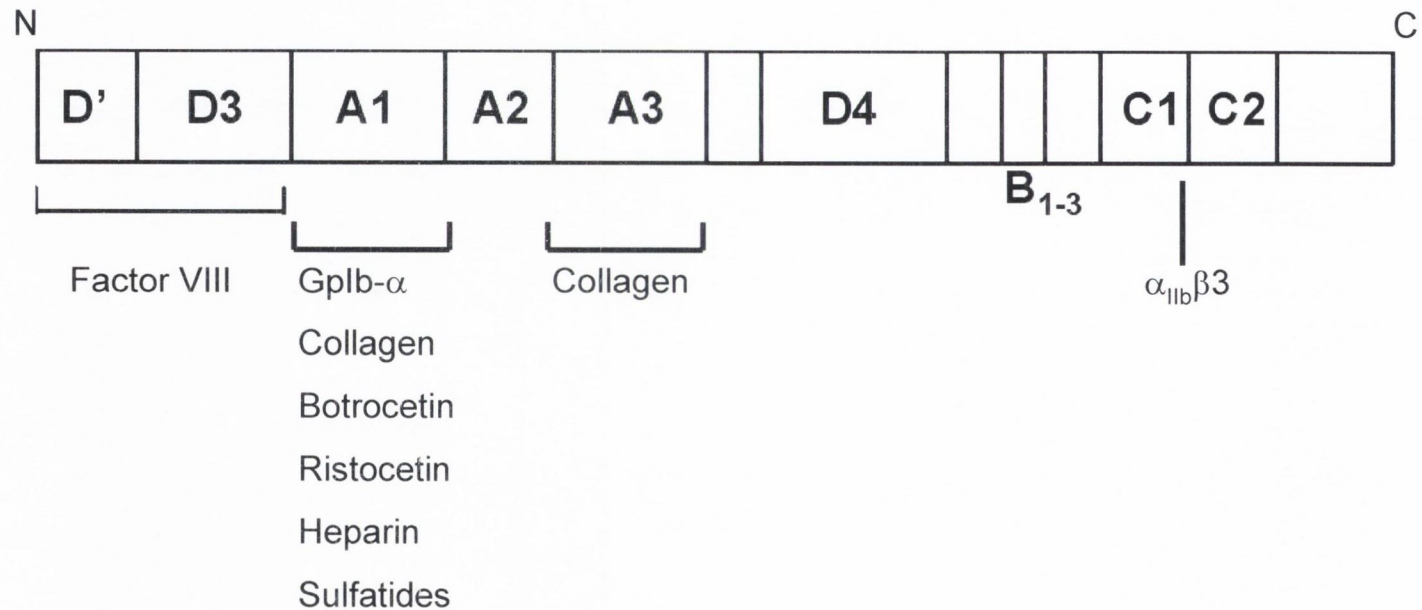


**Figure 1.8 Schematic representation of the von Willebrand factor monomer.** The locations of five kinds of the conserved structural domains (A, B, C, D) are indicated. Binding sites within the vWF subunit have been localised for several macromolecules as indicated. Activated platelet integrin  $\alpha_{IIb}\beta_3$  binds vWF through a segment that includes the tripeptide sequence Arg-Gly-Asp (RGD) in vWF domain C1.

(Ruggeri *et al.*, 1980). The majority of alterations cluster in a single disulfide loop of the VWF A1 domain between residues Cys509 and Cys695 (Fujimura *et al.*, 1986; Ginsburg and Sadler, 1993; Randi *et al.*, 1991; Sadler, 1991). Biochemical studies reveal binding sites for GpIb- $\alpha$ , heparin, and sulfatides within this region (Berndt *et al.*, 1992; Christophe *et al.*, 1991; Sobel *et al.*, 1992). Type 2M VWD mutations result in vWF with a decreased affinity for GpIb- $\alpha$ , presumably by inhibition of activator-induced conformational changes in vWF A1 (Morales *et al.*, 2006).

## 1.8 Structural studies on protein A

Staphylococcal protein A (Spa) comprises five approximately 58 residue homologous immunoglobulin-binding repeat domains (E, D, A, B and C from N- to C-terminus). Each repeat contains binding sites for the Fc $\gamma$  portion of IgG (Moks *et al.*, 1986) and Fab bearing V<sub>H</sub>3 heavy chains (Jansson *et al.*, 1998). Residues involved in binding sites for Fc or Fab have been identified and are highly conserved in all Spa domains (Fig 1.10 A) (Deisenhofer, 1981; Graille *et al.*, 2000). In addition, an analogue of the B domain (domain Z) has been engineered which binds Fc but not Fab due to the substitution Gly29Ala (Nilsson *et al.*, 1987). The Z domain was developed as an affinity purification tool due to its increased stability (Nilsson *et al.*, 1987). The solution structures of the Spa B domain (Gouda *et al.*, 1992), SpaE (Starovasnik *et al.*, 1996) and SpaZ domains (Tashiro *et al.*, 1997) have been solved and the structures of Spa domains in complex with an Fc (SpaB (Deisenhofer, 1981)) or V<sub>H</sub>3-Fab fragment (SpaD (Graille *et al.*, 2000)) have been determined. The overall structures of the Spa domains are similar. Each domain comprises three short antiparallel  $\alpha$ -helices (~ 10 aa) connected by five-residue loops. Helices 2 (residues 24-36) and 3 (residues 41-54) are anti-parallel and helix 1 (residues 9-18) is at a tilt of about 15° with respect to helices 2 and 3 (30° in the case of SpaB) (Fig. 1.10 B). The structure is stabilised by a core of hydrophobic residues (Cedergren *et al.*, 1993; Gouda *et al.*, 1992).

In the crystal complex of SpaB and Fc (Deisenhofer, 1981), SpaB interacts with two symmetric sites on Fc at the hinge region between the C<sub>H</sub>2 and C<sub>H</sub>3 domains. The binding interface is eleven residues in the B domain and nine residues of Fc. The binding site on SpaB is confined to residues on helices 1 and 2. Residues Leu17, Asn28, Ile31, and Lys35 are all

clustered at the binding interface in the crystal structure of the B-Fc complex and substitutions of these residues caused a 5- to 100-fold reduction in binding affinity (Deisenhofer, 1981; Jendeborg *et al.*, 1995). The structure of the SpaB in complex with Fc resolved as a two-helical bundle ( $\alpha$ -helices 1 and 2) in contrast to the solution structures of the unbound domains in which all three  $\alpha$ -helices were resolved. Furthermore, there was also an almost perfect antiparallel orientation of helices 1 (Gln9-Leu17) and 2 (Glu25-Asp36). It was first thought that the mechanism of binding Fc by the SpaB could involve unwinding or disordering of helix 3 (Torigoe *et al.*, 1990a; Torigoe *et al.*, 1990b) but it has since been shown that helix 3 remains intact in these complexes (Jendeborg *et al.*, 1996). Indeed, the X-ray crystal structure of a disulphide-stabilised two-helix derivative of SpaZ, Z34C, is available (Entrez's 3D structure database (PDB ID:1OQX, 1L6X)). This supports the notion that correct folding of helix three is important for ligand binding by native Spa (Starovasnik *et al.*, 1997).

The crystal structure of SpaD in complex with a  $V_H3$ -Fab was determined by Graille and co-workers (Graille *et al.*, 2000). The interaction occurs between helices 2 and 3 of Spa and a surface on Fab comprising four  $V_H$  region  $\beta$ -strands. Residues on Spa involved in contacts with Fab were confined to helices 2 and 3 (and the connecting loop) and were distinct from the Fc $\gamma$ -binding site. Superimposition of the two complexes revealed that a single Spa domain could bind both ligands. This supports experimental evidence that binding is non-competitive (Graille *et al.*, 2000; Roben *et al.*, 1995; Starovasnik *et al.*, 1999) (Fig.1.11). The interacting surfaces were composed predominantly of polar side chains, with three acidic residues on SpaD and two basic residues on Fab providing an overall electrostatic attraction between the two molecules (Graille *et al.*, 2000). This is in contrast to the Spa-Fc complex which is predominantly made up of hydrophobic contacts (Deisenhofer, 1981). The overall positions of the three helices of SpaD are very similar to the deduced structures of the other Spa domains with tilt angles of the helix 1 relative to the two parallel helices 2 and 3 of  $15^\circ$  (Gouda *et al.*, 1992; Graille *et al.*, 2000; Starovasnik *et al.*, 1996; Tashiro *et al.*, 1997). The SpaD-Fab complex clearly demonstrates how the substitution Gly29Ala in SpaZ would perturb the interaction as the C $\alpha$  of Gly is just 3.5 Å from a Fab contact.



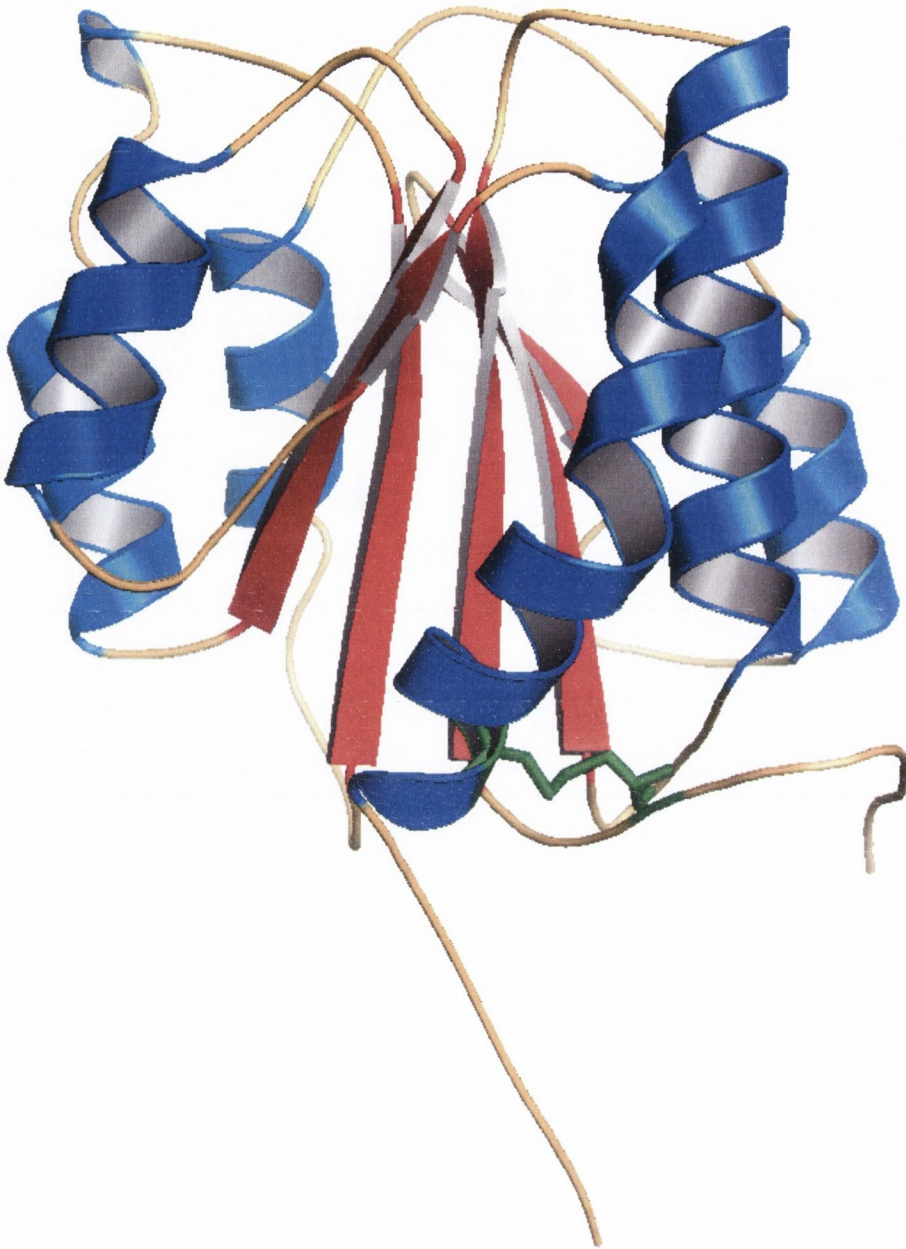


**Fig. 1.9. Ribbon representation of the crystal structure of vWF A1.**

$\alpha$ -helices (blue)  $\beta$ -sheets (red) and turns (orange) are indicated. The disulphide bond formed between Cys509 and Cys695 (green) is also indicated.

A

	←HELIX 1→	← HELIX 2 →	← HELIX 3 →	
D	ADAQQNNFNKDDQSAFYELNMPNLNEAQRNGFIQSLKDDPSQSTNVLGEAKKLNESQAPK			61
E	*-----QHDEA**N**QV*****AD*****A*****Q**D*****			56
A	**-----*****E**N*****E*****A*L*S*****			58
B	**---*K**E**N*****HL*****E*****A*L*A*****DA*****			58
C	**---*K**E**N*****HL*****E*****V*KEI*A*****DA*****			58

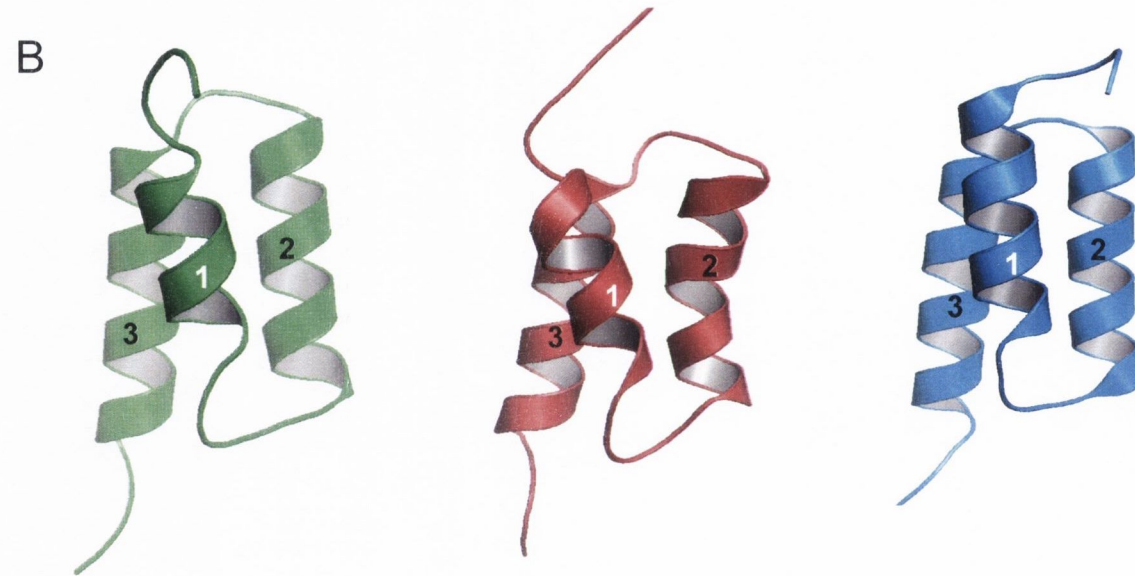


**Fig. 1.10 The Ig-binding domains of protein A.** *A*, alignment of the five Ig-binding domains of Spa, with positions of the  $\alpha$ -helices and residues involved in Fc (blue) or Fab (green) binding indicated. *B*, Ribbon diagrams showing overall chain folds for the E (green) B (red) and Z (blue) domains of Spa. Helices are numbered.

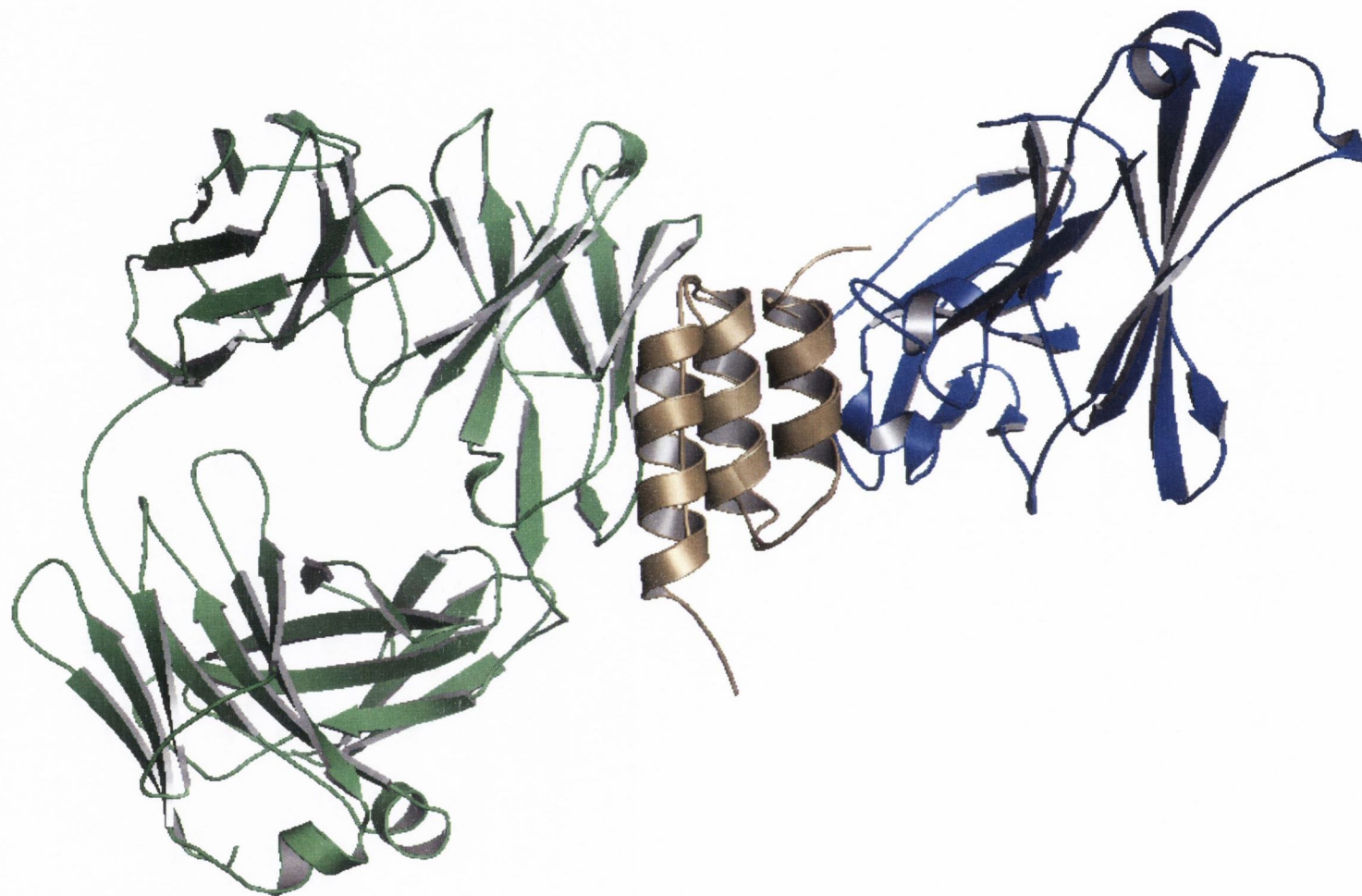


**Fig. 1.11. Composite figure of a single Spa domain interacting simultaneously with Fc and a V<sub>H3</sub>-Fab.** Spa is coloured gold, Fc in ble and VH3-Fab is coloured green. Figure is based on previously solved complexes (PDB IDs: 1FC2 and 1DEE).



Opportunistic bacterial pathogens occasionally gain entry to the human circulatory system resulting in a bacteraemic infection. Bacteraemia can lead to the development of serious cardiovascular complications, such as life-threatening infective endocarditis (IE), disseminated intravascular coagulation (DIC), thrombocytopenia, atherosclerosis and myocardial infarction. The interaction between bacterial pathogens and human blood platelets is postulated to play an important role in the development of IE, and may be important in the pathogenesis of other disease states (Fitzgerald *et al.*, 2006a). IE is characterised by the formation of vegetative growths on heart valves containing a collection of bacteria, platelets, fibrin and inflammatory cells which can serve to protect bacteria against the host immune response and antibiotics (Mylonakis and Calderwood, 2001).

Complications of IE include congestive heart failure as a result of infection-induced valvular damage, neurological complications such as stroke, and systemic embolism resulting in infection of organs such as the kidneys and spleen. Patients presenting with IE often have symptoms such as fever, weight loss, malaise and night sweats. IE is lethal if not aggressively treated with antibiotics, in combination with surgery where necessary. Despite this, a significant mortality rate is seen in studies of patients with IE. In particular IE due to *S. aureus* is associated with high mortality rates (25-47 %) (Mylonakis and Calderwood, 2001). Despite improvements in healthcare over the past 20 years the incidence of IE has not decreased. This is the result of a progressive change in risk factors and the emergence of antibiotic-resistant bacterial strains. Chronic rheumatic heart disease was the main risk factor in the pre-antibiotic era. Nowadays, new at-risk groups include intravenous drug users, patients with prosthetic valves, haemodialysis patients, elderly people with valve sclerosis and those exposed to nosocomial disease (Moreillon and Que, 2004). While many bacterial pathogens can cause IE, staphylococci, streptococci and enterococci together account for > 80 % of all instances of this disease (Moreillon and Que, 2004). Within this category, staphylococci are now recognised as the most common cause of IE (Mylonakis and Calderwood, 2001). Successful treatment of IE depends on effective antibiotic therapy. Endocarditis caused by methicillin-sensitive *S. aureus* (MSSA) is usually treated with nafcillin or oxacillin, while vancomycin is the treatment of choice when the causative bacterium is a methicillin-resistant *S. aureus* MRSA strain (Mylonakis and Calderwood, 2001). The emergence of *S. aureus* strains that have some degree of vancomycin resistance (VISA/VRSA strains (Cosgrove *et al.*, 2004; Kuroda *et al.*, 2001))

leads to cases of IE that cannot be treated by antibiotic intervention. Therefore a full understanding of the mechanisms of the pathogenesis of IE is crucial for the developments of novel non-antibiotic based therapeutics to combat this disease.

The ability of bacteria to bind to and activate platelets may contribute to IE development in a number of ways. Bacteria in the bloodstream could bind to activated platelets in a sterile developing thrombus on damaged valve surfaces, facilitating their colonisation. Bacteria within this thrombus may then capture and activate circulating platelets from the bloodstream, enhancing the vegetation. Alternatively, bacteria and platelets may co-localize at the site of damaged blood vessels resulting in activation leading to thrombus development. *S. aureus* is an important cause of IE in patients with no known valvular damage. In this scenario, the formation of bacteria-platelet micro-aggregates in the bloodstream and their subsequent deposition on the valve surface may be important in the initiation of IE. A role for platelets in the progression of IE is suggested by studies using the rabbit model of *S. aureus* endocarditis. Rabbits treated with aspirin, a cyclo-oxygenase inhibitor that prevents platelet aggregation, had significantly lower bacterial titres and smaller vegetations than control untreated rabbits (Kupferwasser *et al.*, 1999; Nicolau *et al.*, 1993).

### 1.9.1 Platelets

Platelets are non-nucleated cell particles, formed by the partial fragmentation of megakaryocyte cells. They are 2-4  $\mu\text{m}$  in diameter with a characteristic lentiform shape that resembles a discus (Longenecker *et al.*, 1985). Normal platelet counts in the human bloodstream range from  $1.5 \times 10^8$  to  $4.5 \times 10^8$  per ml (Marcus, 1999). The primary role of platelets is in hemostasis, although a number of other functions, including inflammation and anti-microbial defense, are attributed to them (Ni and Freedman, 2003). Damage to the vascular endothelium triggers the response of platelets, which eventually results in the formation of a hemostatic plug (thrombus) containing aggregated platelets and fibrin to arrest bleeding. Platelets contain a number of surface receptors that allow response to environmental factors. Deficiencies in either the platelet GPIb/V/IX complex (Bernard-Soulier Syndrome) or the platelet GPIIb/IIIa ( $\alpha_{\text{IIb}}\beta_3$ ) integrin (Glanzmann thrombasthenia) lead to bleeding disorders as a result of impaired platelet function (Bennett and Kolodziej, 1992). Granules within



platelets contain a number of important mediators, such as ADP, serotonin, vWF, fibrinogen and calcium that help regulate thrombus formation (Marcus, 1999).

The principle adhesive surface for platelets is the extracellular matrix (ECM) which becomes exposed in injured blood vessels (Shattil and Newman, 2004). Receptors recognizing exposed subendothelial components and extracellular matrix (ECM) proteins mediate platelet adhesion to sites of tissue damage and platelet spreading to cover the exposed tissue (Gibbins, 2004). Spreading is accompanied by secretion of several pro-thrombotic factors such as ADP and serotonin which serve to activate approaching platelets. Platelet activation results in inside-out signalling that up-regulates integrin affinity. Binding of fibrinogen to the activated  $\alpha_{IIb}\beta_3$  integrin results in the cross-linking of adjacent platelets into aggregates leading to thrombus assembly (Gibbins, 2004).

Thrombus formation at sites of vascular damage is a complex process, with many platelet receptors acting synergistically to regulate clot formation. Arguably the most important receptors involved in regulating thrombus formation are the  $\alpha_{IIb}\beta_3$  integrin and the GPIb/V/IX complex. Thrombus formation is initiated by platelet adhesion to exposed subendothelium. The nature of the adhesive ligand involved is determined by the prevailing conditions of shear stress. Under low shear conditions, such as those found in larger arteries and veins, platelet adhesion is mediated through collagens (platelet receptors  $\alpha_2\beta_1$  and GPVI), fibronectin (through  $\alpha_5\beta_1$ ) and laminin (through  $\alpha_6\beta_1$ ) (Jackson *et al.*, 2003). However, under high shear conditions found in small arteries and arterioles, platelet adhesion is critically dependent on binding of GPIb/V/IX to von Willebrand factor that has bound to the exposed subendothelium (Jackson *et al.*, 2003).

Following firm platelet adhesion, subsequent platelet-platelet cohesion (platelet aggregation) occurs on the layer of adherent platelets to form a haemostatic plug. Central to this process is  $\alpha_{IIb}\beta_3$ . Under conditions of high shear, von Willebrand factor is the major ligand promoting platelet aggregate formation by cross-linking activated platelets through  $\alpha_{IIb}\beta_3$ , with fibrinogen and/or fibrin playing a stabilizing role. At low shear rates, binding of the bivalent glycoprotein fibrinogen to  $\alpha_{IIb}\beta_3$  is the dominant factor mediating thrombus formation by bridging  $\alpha_{IIb}\beta_3$  receptors on adjacent platelets (Jackson *et al.*, 2003). Secretion of soluble agonists (e.g. ADP) from platelet granules and thrombin generation on the platelet surface increase the rate of platelet activation and aggregation (Ni and Freedman, 2003). ADP is thought to be involved in the progressive recruitment of platelets within developing



aggregates, while thrombin may be important in both promoting initial thrombus growth and in stabilising thrombi formed through fibrin formation (Jackson *et al.*, 2003).

Platelet aggregation is critically dependent on  $\alpha_{\text{IIb}}\beta_3$ . This receptor, like all integrins, is a heterodimeric type I transmembrane receptor consisting of an  $\alpha$  and a  $\beta$  subunit. Each subunit contains a relatively large extracellular domain, a single-pass transmembrane domain, and a short (20 – 60 amino acid) cytoplasmic tail.  $\alpha_{\text{IIb}}\beta_3$  exists in resting (low-affinity) and activated (high-affinity) conformations. The resting state is predominant in unstimulated platelets and the activated state in stimulated platelets. Platelet activation by an agonist generates intracellular signals that are transmitted to the  $\beta_3$  cytoplasmic tail (inside-out signaling). This leads to conformational changes in the extracellular domain of  $\alpha_{\text{IIb}}\beta_3$ , converting it to its activated form and increasing its affinity for adhesive ligands such as fibrinogen and von Willebrand factor. The X-ray crystal structure of  $\alpha_{\text{IIb}}\beta_3$  in its active form is available (Xiao *et al.*, 2004). Ligand binding to the extracellular face of  $\alpha_{\text{IIb}}\beta_3$  promotes integrin clustering and stimulation of protein tyrosine kinase activity (outside-in signaling). This drives further integrin activation by transmitting signals to the cytoplasmic tails of  $\alpha_{\text{IIb}}\beta_3$  stimulating conformational change. In this way,  $\alpha_{\text{IIb}}\beta_3$  ligand binding becomes progressively irreversible and results in irreversible platelet aggregation (Ni and Freedman, 2003; Shattil and Newman, 2004; Xiao *et al.*, 2004).

### 1.9.2 The interaction of bacteria and platelets

Many bacterial species have been shown to interact with platelets *in vitro*, including members of the genera *Staphylococcus*, *Streptococcus*, *Enterococcus*, *Helicobacter*, *Borrelia*, *Chlamydia* and *Listeria*. Staphylococci and streptococci, which are major causes of IE, are probably the most intensively studied with regard to their ability to interact with platelets. *In vitro*, some bacteria mediate platelet aggregation. This is thought to be the result of a multistep process, with initial bacterial adhesion to resting platelets triggering intracellular signaling resulting in platelet activation. Conformational modulation of  $\alpha_{\text{IIb}}\beta_3$  increases its affinity for fibrinogen, resulting in cross-linking of adjacent platelets into platelet aggregates.

*Helicobacter pylori* infection is associated with the development of peptic ulcers, gastric carcinoma and atrophic gastritis. Cardiovascular conditions such as arteriosclerotic vascular disease, myocardial infarction and thrombocytopenia are thought to be associated

with *H.pylori* infection. Remission of thrombocytopenia in patients has been observed upon eradication of *H.pylori* infection (Handin, 2003). Some strains of *H.pylori* have been shown to stimulate platelet activation and aggregation (Byrne *et al.*, 2003). *H.pylori* interaction with platelets involved binding to platelet GPIIb- $\alpha$  via a vWF bridge. IgG specific for *H.pylori* was also required for activation and aggregation by binding to the platelet IgG Fc receptor, Fc $\gamma$ RIIa (Byrne *et al.*, 2003).

### 1.9.2.1 *S. aureus*-platelet interactions

Bacteria must bind platelets to initiate subsequent platelet activation and aggregation (Clawson, 1973). The ability of *S. aureus* cells to bind directly to the platelet surface in the absence of plasma co-factors has been demonstrated in a number of studies (Herrmann *et al.*, 1993; Nguyen *et al.*, 2000; Siboo *et al.*, 2001; Siboo *et al.*, 2005; Sullam *et al.*, 1996; Yeaman *et al.*, 1992). Herrmann and co-workers reported that binding of *S. aureus* to platelets was extensively promoted in the presence of plasma, which would be more representative of *in vivo* conditions. Adhesion was sensitive to both an anti-fibrinogen antibody and an anti- $\alpha_{IIb}\beta_3$  monoclonal antibody, suggesting that fibrinogen acted as a bridging molecule between the *S. aureus* receptors (such as ClfA, ClfB, FnBPA or FnBPB) and  $\alpha_{IIb}\beta_3$  on the platelet. It was recently reported that soluble fibrin is a major mediator of *S. aureus* adhesion to activated platelets in solution, likely as a result of a similar bridging mechanism (Niemann *et al.*, 2004).

It is well established that *S. aureus* can induce platelet aggregation through surface-expressed proteins (Hawiger *et al.*, 1972; Hawiger *et al.*, 1979; Kessler *et al.*, 1991). ClfA has been shown to be an important factor in promoting platelet binding and aggregation *in vitro* (O'Brien *et al.*, 2002; Siboo *et al.*, 2001). It is also a virulence factor in experimental endocarditis (Moreillon *et al.*, 1995; Que *et al.*, 2005; Stutzmann Meier *et al.*, 2001; Sullam *et al.*, 1996). The molecular interaction between *S. aureus* and platelets under physiological hydrodynamic shear forces leading to thrombus formation required ClfA and platelet  $\alpha_{IIb}\beta_3$  (Pawar *et al.*, 2004). Another study examining real-time thrombus formation under shear conditions demonstrated thrombus formation upon exposure of whole blood to immobilized *S. aureus* Newman cells that was likely to be mediated by ClfA (Sjobring *et al.*, 2002). Indeed, ClfA can exert a potent pro-aggregatory effect when expressed on the surface of the non-aggregating surrogate host *Lactococcus lactis* (O'Brien *et al.*, 2002).



More recently, the molecular basis of platelet activation by ClfA has been investigated by extending this approach to different host strains and by studying cells in different phases of growth. It was shown that the major *S. aureus* determinants to promote rapid activation of platelets differ according to the phase of growth of the culture. ClfA is the dominant pro-aggregatory surface protein on stationary phase cells (Loughman *et al.*, 2005) whereas the fibronectin-binding proteins are the most important in the exponential phase of growth (Fitzgerald *et al.*, 2006b). This correlates with the regulation of expression of the genes that encode these proteins. By using a regulatable promoter to control expression of surface proteins in the surrogate host *L. lactis*, a threshold concentration of surface-expressed ClfA and FnBPA molecules was required on the bacterial surface before activation of platelets could occur. Once this is achieved, aggregation occurs rapidly (Loughman *et al.*, 2005).

The same study also identified the plasma and platelet components involved by using a mutant of ClfA that did not bind fibrinogen, inhibitors specific for platelet receptors and by analysing the soluble plasma proteins required in a reconstituted plasma-free system with washed platelets.  $\alpha_{IIb}\beta_3$  on resting platelets has a low affinity for fibrinogen but can still bind fibrinogen bound to bacteria. However, this is not sufficient to stimulate activation. ClfA-specific immunoglobulin must also be present to act as a bridge between the bacterial surface protein and the platelet immunoglobulin Fc receptor, Fc $\gamma$ RIIa (Loughman *et al.*, 2005).

FnBPA possesses two different but related mechanisms of binding to and activating resting platelets (Fitzgerald *et al.*, 2006b). The fibrinogen-binding A domain behaves in a similar fashion to ClfA and activates platelets through a fibrinogen bridge to  $\alpha_{IIb}\beta_3$  and an IgG bridge to Fc $\gamma$ RIIa. The fibronectin-binding region BCD of FnBPA can also activate platelets via fibronectin N-terminal type I domains that bind to the bacterial protein by the tandem  $\beta$ -zipper mechanism (see section 1.4.2) and to  $\alpha_{IIb}\beta_3$  through the integrin-binding RGD domain (Fitzgerald *et al.*, 2006b).

It was recently demonstrated that expression of SasA (also called SraP (Serine-rich adhesin for platelets)) by *S. aureus* contributed to direct platelet binding and virulence in experimental endocarditis (Siboo *et al.*, 2005). The gene encoding SraP is present in all isolates examined and was expressed by the majority of clinical isolates examined (Roche *et al.*, 2003; Siboo *et al.*, 2005). It was not determined whether SraP-mediated binding of *S. aureus* to platelets stimulates platelet aggregation.



Direct binding to platelets involving protein A (Spa) was recently characterized. Spa was shown to bind to the platelet C1q complement receptor gC1qR/p33 (Nguyen *et al.*, 2000). gC1qR/p33 expression on the platelet surface can only be detected following platelet activation by agonists such as epinephrine or ADP (Peerschke and Ghebrehiwet, 2001; Peerschke *et al.*, 2003). It is therefore more likely that this interaction plays a role in adherence to active platelets rather activation of resting platelets. Spa-mediated binding of *S. aureus* to gC1qR/p33 on activated platelets may play a role in the colonization of developing sterile thrombi *in vivo*. The ability of Spa to bind to von Willebrand factor (the major ligand for the platelet GPIb complex) appears to play a role in the interaction between *S. aureus* and platelets leading to their aggregation under high shear conditions, through the formation of a von Willebrand factor bridge linking SpA with GPIb (Hartleib *et al.*, 2000; Pawar *et al.*, 2004).

Spa can mediate adherence of staphylococci to immobilized collagen under flow in the presence of vWF (Mascari and Ross, 2003). Spa can mediate adherence of *S. aureus* to vWF-coated surfaces in conditions of low shear (Hartleib *et al.*, 2000). More recently, shear-dependent adhesion of *S. aureus* was demonstrated to occur as a result of Spa expressed on the bacterial surface binding vWF in a parallel plate flow chamber (George *et al.*, 2006). It is possible that Spa promotes bacterial binding to immobilized vWF, either bound directly to exposed subendothelial tissue or to platelets that had been previously captured. This opens the possibility that vWF contributes to the recruitment of Spa-expressing bacteria into vWF-rich platelet thrombi.

O'Brien and co-workers demonstrated roles for ClfB and SdrE in promoting platelet aggregation when expressed by *S. aureus* or *L. lactis* (O'Brien *et al.*, 2002). It has since been shown that expression of SdrCDE and ClfA are required for adherence to platelets via fibrinogen (George *et al.*, 2006). *S. aureus* appears to express a number of surface components that interact with platelets leading to their activation and aggregation. Such redundancy in function suggests that this plays an important role in pathogenesis.

At least one *S. aureus* factor, a secreted 15.8 kDa fibrinogen-binding protein named Efb (extracellular fibrinogen binding protein) interacts with platelets in a manner that prevents platelet aggregation (Shannon and Flock, 2004). The fibrinogen binding domain of Efb shares homology with the fibrinogen binding C-terminal repeats of staphylococcal coagulase (Boden and Flock, 1994). Efb binds to ADP-stimulated platelets by recognizing the  $\alpha$ -chain of platelet-bound fibrinogen (Palma *et al.*, 2001). It also appears that Efb binds directly to an as

yet unidentified receptor on activated platelets. The interaction(s) of Efb with activated platelets resulted in inhibition of platelet aggregation (Palma *et al.*, 2001; Shannon and Flock, 2004). In a rat wound-infection model, an *efb* mutant strain was less pathogenic than the Efb-producing parental strain, suggesting Efb contributes to a delay in wound healing, possibly through its inhibition of platelet function (Palma *et al.*, 1996). The anti-thrombogenic potential of Efb was used in a murine acute thrombosis model where intravenous administration of collagen and epinephrine results in rapid death due to massive systemic coagulation. Efb administration completely protected mice from collagen/epinephrine challenge. Mice treated with Efb also displayed significantly longer bleeding times than control mice suggesting the potential development of Efb as a novel anti-thrombotic agent (Shannon *et al.*, 2005).

The numerous mechanisms that *S. aureus* has evolved for binding to and activating platelets suggests that the interaction with platelets is an important aspect of *S. aureus* pathogenesis in the establishment of endocardial infections. It is clear that the interaction of *S. aureus* with platelets is a complex process and that a greater understanding of the mechanisms involved is required.

#### **1.10 *S. aureus* pathogenesis of the airway epithelium**

*Staphylococcus aureus* is a common cause of hospital-acquired pneumonia and strains isolated from individuals with airway infection show increased expression of surface proteins, particularly protein A (Goerke *et al.*, 2000; Hiramatsu *et al.*, 2001; Wann *et al.*, 1999). Recently community acquired MRSA (CA-MRSA) have been shown to cause a rapidly fatal necrotizing pneumonia (Mongkolrattanothai *et al.*, 2003). An examination of the interactions of *S. aureus* protein A and airway epithelial cells revealed that protein A has a major function in the recruitment of polymorphonuclear leukocytes (PMNLs) into the airway through activation of tumour necrosis factor receptor-1 (TNFR1) (Gomez *et al.*, 2004). TNFR1 is the receptor for the host cytokine, TNF- $\alpha$ , one of several cytokines that orchestrate events during bacterial infection in the lung. After entry into the lung, staphylococci can proliferate and eventually invade the epithelial linings of bronchioli and alveoli. Here, production and secretion of cytokines and chemokines, including TNF- $\alpha$ , IL-1 $\alpha$  and IL-1 $\beta$  is induced.



Chemokines bring about leukocyte migration to the site of infection leading to PMN and macrophage recruitment. These events damage host tissue and eventually contribute to the symptoms of disease (Gomez *et al.*, 2004; Normark *et al.*, 2004).

Signaling mediated by Spa binding to TNFR1 induced inflammation *in vivo* and played a crucial role in the development of pneumonia. TNFR1 is widely distributed and surface-expressed. Spa activates pro-inflammatory signalling through binding to TNFR1 and activation of TRAF2, the p38/c-Jun NH<sub>2</sub>-terminal kinase MAPKs, and NF- $\kappa$ B. Spa induces shedding of the TNFR1 ectodomain, presumably by activating TACE, the TNF-converting enzyme (or ADAM 17) through an as yet unidentified signalling pathway (Gomez *et al.*, 2004). Protein A-deficient mutants of *S. aureus* were less virulent in murine models of peritonitis, subcutaneous infections and arthritis. In addition, TNFR1 null mice are not susceptible to *S. aureus* pneumonia indicating that expression of protein A is essential in the pathogenesis of the disease (Gomez *et al.*, 2004).

### 1.11 Rationale for this study

*S. aureus* is the leading cause of infective endocarditis (Fowler *et al.*, 2005). This condition is associated with high mortality rates, even with aggressive antibiotic therapy (Mylonakis and Calderwood, 2001; Moreillon and Que, 2004). Mortality rates will no doubt increase with the emergence of multiple-resistant *S. aureus* strains that are refractory to treatment with clinically available antibiotics. It is widely believed that the ability of endovascular pathogens such as *S. aureus* to interact with platelets is a crucial virulence determinant in the pathogenesis of infective endocarditis (Sullam *et al.*, 1996). Platelet binding and activation by *S. aureus* resulting in the formation of platelet aggregates is likely to play a fundamental role in thrombus formation on the endocardial surface.

The surface protein Spa of *S. aureus* may play a significant role in colonisation of the vascular endothelium and/or platelet interactions under specific conditions. Recent studies in this laboratory demonstrated that clumping factor A and fibronectin-binding proteins FnBPA and FnBPB are the predominant pro-aggregatory factors expressed by exponentially and stationary grown bacteria, respectively under low shear stress (Fitzgerald *et al.*, 2006b; Loughman *et al.*, 2005). The role of protein A in this process is less well understood, but current understanding suggests that the interaction with von Willebrand factor may serve as a



bridge to platelets and collagen (George *et al.*, 2006; Hartleib *et al.*, 2000; Mascari and Ross, 2003; Pawar *et al.*, 2004). Spa has important functions in immune evasion and pathogenesis. Furthermore, it is expressed by most *S. aureus* isolates. This makes Spa an attractive target for anti-staphylococcal therapy. This study aims to gain a greater understanding of the nature of the interaction of Spa and vWF.

### **1.11.1 Aims and objectives**

This study aims to confirm that the vWF-binding region on Spa lies within the surface-expressed part of Spa. Recombinant truncates of the Spa Ig-binding domains will be constructed for comparative use in binding assays with vWF. Site-directed mutagenesis of Spa will be performed to identify the binding site on Spa for vWF. Recombinant vWF truncates will be employed in binding studies to localise the region(s) within the vWF molecule to which Spa binds. Finally, studies will be performed on ligand binding and cellular location of a novel Ig-binding protein of *S. aureus*, Sbi, which has protein A-like domains.

## **Chapter 2**

### **Materials and Methods**

## 2.1 Bacterial strains and growth conditions

Bacterial strains used in this study are listed in Table 2.1. *Escherichia coli* was routinely grown on L-agar or in L-broth at 37 °C or in Silva-Buddenhagen (SB) medium (3.0% Tryptone, 2.0% yeast extract, 1.0% MOPS free acid, 2.0% glucose) at 30 °C or 37 °C. *S. aureus* was grown on Trypticase Soy agar (TSA, Oxoid) or on Brain-Heart Infusion (BHI, Oxoid) agar or broth at 37 °C. *E. coli* and *S. aureus* broth cultures were grown in an orbital shaker at 200 rpm at 37 °C. *L. lactis* was grown on M17 agar or in M17 broth supplemented with 0.5 % (w/v) glucose (GM17). *L. lactis* broth cultures were grown statically at 30 °C. *S. aureus* cells were harvested in either exponential phase (OD<sub>600</sub> of 0.5 - 0.6) or stationary phase (16 h). *L. lactis* cells were harvested after 16 h. Stocks of bacterial strains were made by supplementing broth cultures with 20 % (v/v) glycerol and snap-freezing in liquid nitrogen, followed by storage at -70 °C.

Where appropriate, antibiotics were incorporated into growth media: ampicillin (Ap), 100 µg/ml; erythromycin (Em), 5 µg/ml; kanamycin (Kan), 100 µg/ml; tetracycline (Tet), 2 µg/ml. Antibiotics were purchased from Sigma Chemical Co.

## 2.2 Plasmids

Plasmids are listed in Table 2.2.

## 2.3 DNA manipulations

Standard methods were used for manipulation of DNA (Sambrook. J., 1989). Restriction endonucleases were purchased from New England Biolabs and Roche. DNA ligase and shrimp alkaline phosphatase were purchased from Roche. Materials for PCR were purchased from Promega Corp.

## 2.4 Transformation of bacterial cells with plasmid DNA

Competant *E. coli* cells were prepared by the CaCl<sub>2</sub> method (Sambrook. J., 1989). CaCl<sub>2</sub>-competant *E. coli* cells (100 µl) were incubated for 30 min on ice with 2 µl whole plasmid or 5-10 µl DNA ligation reaction. The mixture was then incubated at 42 °C for 1 min



followed by a further 1 min on ice. Next, 500 µl recovery medium (L-broth) was added and the mixture incubated for 1 h at 37 °C. 100 µl of the neat or diluted mixture was plated on agar containing the appropriate antibiotics and incubated at 37 °C for 16-24 h.

#### **2.4.1 Screening of transformants**

Putative XL-1 Blue transformant colonies were screened by a PCR-based strategy. Colonies were picked from agar plates and resuspended in 10 µl dH<sub>2</sub>O. Samples were boiled for 10 min followed by brief centrifugation to release DNA. 1 µl of supernatant was then used as a template for a PCR reaction using standard sequencing primers designed to anneal either side of the multiple cloning site. PCR products were analysed by agarose gel electrophoresis (2.9.1) to screen for DNA insertion in the multiple cloning site. A PCR reaction using empty vector was included as a control.

#### **2.5 PCR**

PCR reactions were performed in 100 µl volumes containing forward and reverse primers (100 pM) (Sigma Genosys), plasmid DNA (10 ng) or genomic DNA (20 ng) as template, dNTPs (2.5 mM) and *Pfu* polymerase (5 U) (Promega) in a standard *Pfu* reaction buffer (Promega). Oligonucleotides are listed in Tables 2.3 and 2.4. PCR amplification was carried out in a DNA thermal cycler (Techne). Reactions were carried out with a 1-min denaturation step at 94 °C, a 1-min annealing step at 54°C or 55 °C, and elongation at 72 °C, allowing 2 min per kb of DNA being amplified. This standard cycle was repeated 30 times followed by a final elongation at 72 °C for 10 min. Samples were then maintained at 4°C. DNA Sequencing was performed by GATC Biotech.

#### **2.6 DNA constructions**

Fragments of the region of *spa* encoding the extracellular immunoglobulin-binding domains were isolated and cloned as follows; plasmid pSPA7235 (Patel *et al.*, 1992) containing the entire coding region of the *spa* gene of *Staphylococcus aureus* 8325-4 was used

**Table 2.1 Bacterial strains**

Strain	Relevant Properties	Source/ Reference
<i>E. coli</i>		
XL-1 Blue	Propagation of plasmids	Stratagene
M15 (pREP4)	Protease deficient strain with LacI repressor used for recombinant protein expression	Qiagen
BL21 (DE3) Star	Protease deficient strain used for recombinant protein expression	Stratagene
<i>S. aureus</i>		
8325-4	NCTC 8325 cured of prophages	Novick, 1967
8325-4 <i>spa</i>	<i>spa</i> -defective mutant of 8325-4. Kan <sup>R</sup>	Patel <i>et al.</i> , 1987
Newman	NCTC8178	Duthie and Lorenz, 1952
Newman <i>spa</i>	<i>spa</i> -defective mutant of Newman. Kan <sup>R</sup>	Higgins <i>et al.</i> , 2006
SH1000	Functional <i>rsbU</i> derivative of 8325-4 <i>rsbU</i> <sup>+</sup>	Horsburgh <i>et al.</i> , 2002
SH1000 <i>spa</i>	<i>spa</i> -defective mutant of SH1000. Tet <sup>R</sup>	Laboratory strain
<i>L. lactis</i>		
MG1363	Plasmid-free derivative of strain NCDO712 Newman derivative deficient in protein A.	Gasson, 1983

**Table 2.2 List of plasmids.**

Plasmid	Features	Marker	Source/ Reference
pGEX-KG	Expression vector for N-terminal glutathione-S-transferase (GST) fusion proteins	Ap <sup>r</sup>	(Smith and Johnson, 1988)
pGEX-KG-SpaEDABC	pGEX-KG containing the region of <i>spa</i> encoding the EDABC domains	Ap <sup>r</sup>	This study
pGEX-KG-SpaEDAB	pGEX-KG containing the region of <i>spa</i> encoding the EDAB domains	Ap <sup>r</sup>	This study
pGEX-KG-SpaDABC	pGEX-KG containing the region of <i>spa</i> encoding the DABC domains	Ap <sup>r</sup>	This study
pGEX-KG-SpaEDA	pGEX-KG containing the region of <i>spa</i> encoding the EDA domains	Ap <sup>r</sup>	This study
pGEX-KG-SpaDAB	pGEX-KG containing the region of <i>spa</i> encoding the DAB domains	Ap <sup>r</sup>	This study
pGEX-KG-SpaABC	pGEX-KG containing the region of <i>spa</i> encoding the ABC domains	Ap <sup>r</sup>	This study
pGEX-KG-SpaED	pGEX-KG containing the region of <i>spa</i> encoding the ED domains	Ap <sup>r</sup>	This study
pGEX-KG-SpaDA	pGEX-KG containing the region of <i>spa</i> encoding the DA domains	Ap <sup>r</sup>	This study
pGEX-KG-SpaAB	pGEX-KG containing the region of <i>spa</i> encoding the AB domains	Ap <sup>r</sup>	This study
pGEX-KG-SpaBC	pGEX-KG containing the region of <i>spa</i> encoding the BC domains	Ap <sup>r</sup>	This study
pGEX-KG-SpaE	pGEX-KG containing the region of <i>spa</i> encoding the E domain	Ap <sup>r</sup>	This study
pGEX-KG-SpaD	pGEX-KG containing the region of <i>spa</i> encoding the D domain	Ap <sup>r</sup>	This study
pGEX-KG-SpaA	pGEX-KG containing the region of <i>spa</i> encoding the A domain	Ap <sup>r</sup>	This study
pGEX-KG-SpaB	pGEX-KG containing the region of <i>spa</i> encoding the B domain	Ap <sup>r</sup>	This study
pGEX-KG-SpaC	pGEX-KG containing the region of <i>spa</i> encoding the C domain	Ap <sup>r</sup>	This study
pGEX-KG-Spa-C-term	pGEX-KG containing the region of <i>spa</i> 3' of the coding region for the Ig-binding repeats	Ap <sup>r</sup>	This study
pGEX-KG-SpaD <sub>58</sub>	pGEX-KG containing a variant of <i>spaD</i> lacking codons 2-4	Ap <sup>r</sup>	This study
pGEX-KG-SpaD(F5A)	pGEX-KG containing a variant of <i>spaD</i> encoding the substitution F5A	Ap <sup>r</sup>	This study
pGEX-KG-SpaD(Q9A)	pGEX-KG containing a variant of <i>spaD</i> encoding the substitution Q9A	Ap <sup>r</sup>	This study



pGEX-KG-SpaD(Q10A)	pGEX-KG containing a variant of <i>spaD</i> encoding the substitution Q10A	Ap <sup>r</sup>	This study
pGEX-KG-SpaD(F13A)	pGEX-KG containing a variant of <i>spaD</i> encoding the substitution F13A	Ap <sup>r</sup>	This study
pGEX-KG-SpaD(Y14A)	pGEX-KG containing a variant of <i>spaD</i> encoding the substitution Y14A	Ap <sup>r</sup>	This study
pGEX-KG-SpaD(L17A)	pGEX-KG containing a variant of <i>spaD</i> encoding the substitution L17A	Ap <sup>r</sup>	This study
pGEX-KG-SpaD(N21A)	pGEX-KG containing a variant of <i>spaD</i> encoding the substitution N21A	Ap <sup>r</sup>	This study
pGEX-KG-SpaD(R27A)	pGEX-KG containing a variant of <i>spaD</i> encoding the substitution R27A	Ap <sup>r</sup>	This study
pGEX-KG-SpaD(N28A)	pGEX-KG containing a variant of <i>spaD</i> encoding the substitution N28A	Ap <sup>r</sup>	This study
pGEX-KG-SpaD(G29A)	pGEX-KG containing a variant of <i>spaD</i> encoding the substitution G29A	Ap <sup>r</sup>	This study
pGEX-KG-SpaD(F30A)	pGEX-KG containing a variant of <i>spaD</i> encoding the substitution F30A	Ap <sup>r</sup>	This study
pGEX-KG-SpaD(I31A)	pGEX-KG containing a variant of <i>spaD</i> encoding the substitution I31A	Ap <sup>r</sup>	This study
pGEX-KG-SpaD(Q32A)	pGEX-KG containing a variant of <i>spaD</i> encoding the substitution Q32A	Ap <sup>r</sup>	This study
pGEX-KG-SpaD(S33A)	pGEX-KG containing a variant of <i>spaD</i> encoding the substitution S33A	Ap <sup>r</sup>	This study
pGEX-KG-SpaD(L34A)	pGEX-KG containing a variant of <i>spaD</i> encoding the substitution L34A	Ap <sup>r</sup>	This study
pGEX-KG-SpaD(K35A)	pGEX-KG containing a variant of <i>spaD</i> encoding the substitution K35A	Ap <sup>r</sup>	This study
pGEX-KG-SpaD(D36A)	pGEX-KG containing a variant of <i>spaD</i> encoding the substitution D36A	Ap <sup>r</sup>	This study
pGEX-KG-SpaD(D37A)	pGEX-KG containing a variant of <i>spaD</i> encoding the substitution D37A	Ap <sup>r</sup>	This study
pGEX-KG-SpaD(Q40A)	pGEX-KG containing a variant of <i>spaD</i> encoding the substitution Q40A	Ap <sup>r</sup>	This study
pGEX-KG-SpaD(E47A)	pGEX-KG containing a variant of <i>spaD</i> encoding the substitution E47A	Ap <sup>r</sup>	This study
pQE30-vWFA1	pQE30 containing the coding region for the vWF A1 domain	Ap <sup>r</sup>	Cruz <i>et al.</i> , 1993
pQE30-vWFA1(R578Q)	pQE30 containing a variant of <i>vwfA1</i> encoding the substitution R578Q	Ap <sup>r</sup>	Dr. Jonas Emsley
pQE30-vWFA1(G561S)	pQE30 containing a variant of <i>vwfA1</i> encoding the substitution G561S	Ap <sup>r</sup>	This study
pQE30-vWFA1(S522F)	pQE30 containing a variant of <i>vwfA1</i> encoding the substitution S522F	Ap <sup>r</sup>	This study
pCOMB3::JMSpA3-08	pCOMB3 containing a DNA clone encoding a V <sub>H</sub> 3-Fab fragment of IgG	Ap <sup>r</sup>	Sasano <i>et al.</i> , 1993
pKS80	<i>L. lactis</i> vector for the heterologous expression of surface proteins	Erm <sup>R</sup>	Wells <i>et al.</i> , 1993
pKS80spa	Plasmid for constitutive expression of	Erm <sup>R</sup>	Hartford <i>et</i>

pKS80 <i>clfA</i>	Spa on the surface of <i>L. lactis</i> . Plasmid for constitutive expression of Spa on the surface of <i>L. lactis</i> .	Erm <sup>R</sup>	<i>al.</i> , 2001 a Hartford <i>et al.</i> , 2001 a
-------------------	--	------------------	--

as a template for amplification of specific regions of *spa*. Oligonucleotides were designed to a region 3' to the *spa* domains and to the flanking region of each individual domain to allow amplification of any combination of Ig-binding repeat region (Table 2.3). Cross-reaction of primers due to high sequence homology of the *spa* repeats was overcome by digestion of the *spa* template with unique restriction endonucleases prior to single domain amplifications. Restriction sites were incorporated at the 5' ends of the primers to facilitate directional cloning.

The region encoding a putative second Ig-binding repeat of the *sbi* gene was amplified using oligonucleotides listed in Table 2.3, and directionally cloned as in the *spa* constructs.

## **2.7 Site-directed mutagenesis**

### **2.7.1 Mutagenesis of a single *spa* domain**

Mutations were introduced into domain D of *spa* by PCR-based mutagenesis. Briefly, overlapping oligonucleotides (Table 2.4) carrying the desired mutation were combined with standard flanking primers to yield two overlapping mutant products. These were combined in a second round of PCR and amplified using the flanking primers alone to yield the mutant fusion product. In some cases, mutations were introduced using the Quikchange® method, according to manufacturer's instructions (Stratagene). Briefly, overlapping oligonucleotides carrying the desired mutation are designed to amplify the entire plasmid template. The template is digested with the restriction endonuclease *DpnI*, which only digests methylated and hemi-methylated DNA. The mutant PCR product can be cloned directly into *E. coli* XL1-Blue, which repairs nicked plasmid DNA. The following amino acid substitutions were constructed by mutation of the corresponding codon: F5A, Q9A, Q10A, F13A, Y14A, L17A, N21A, R27A, N28A, G29A, F30A, I31A, Q32A, S33A, L34A, K35A, D36A, D37A, Q40A and E47A. A variant lacking three additional codons unique to this *spa* domain was also created by PCR as previously described, generating a 58-residue variant, named D<sub>58</sub>.



### **2.7.2 Mutagenesis of the *vwf A1* domain**

Mutations were introduced into *vwf A1* by the Quikchange® method, according to manufacturer's instructions (Stratagene), using oligonucleotides listed in Table 2.4.

## **2.8 DNA purification**

Plasmid DNA was purified using the Wizard SV Plus Minipreps™ DNA purification system (Promega) according to the manufacturer's instructions. Linear DNA was purified using the Wizard™ SV gel and PCR cleanup system (Promega). When required, DNA was concentrated and purified using the SureClean™ system (Bioline).

Genomic DNA from *S. aureus* was isolated using the Genomic DNA purification kit (Edge Biosystems) as per the supplier's protocol, including an additional pre-treatment of cells with 200 µg lysostaphin (AMBI, New York) for 20 min at 37 °C to digest the cell-wall peptidoglycan.

## **2.9 Electrophoresis**

### **2.9.1 Agarose gel electrophoresis**

DNA was separated according to its size by agarose gel electrophoresis. Gels containing 0.5-2 % agarose, dissolved by boiling in TAE buffer (Invitrogen), were cooled to 65 °C and cast in mini trays (Life Technologies). DNA samples in loading buffer containing an electrophoretic dye were loaded into wells along with a standard DNA size marker (Bioline). Electrophoresis of samples was routinely performed at 90 v. Gels were bathed in ethidium bromide (10 mg/ml) for 10 min, washed and viewed under UV light. Gel images were analysed using Alpha Imager™ software.

### **2.9.2 SDS-PAGE**

Samples for SDS-PAGE were boiled for 5 min in an equal volume of final sample buffer (FSB) (10 % (v/v) glycerol, 5 % (v/v) β-mercaptoethanol, 3 % (w/v) SDS, 0.01 % bromophenol blue in 62.5 mM Tris-HCl, pH 6.8). 2-20 µl volumes were separated by SDS-

**Table 2.3. Oligonucleotides used for *spa* and *sbi* truncates<sup>a</sup>**

Name	Sequence (5'-3')
Fw_SpaE	CCG <b>GAA</b> TT <b>C</b> ATGCTGCGCAACACGATGAAG
Rv_SpaE	CCG <b>CC</b> AT <b>G</b> GT <b>T</b> ATTTTGGTGCTTGAGAGTCA
Fw_SpaD	CCG <b>GAA</b> TT <b>C</b> AAGCTGATGCGCAACAAAATAAC
Fw_SpaA	CCG <b>GAA</b> TT <b>C</b> AAGCTGATAACAATTTCAACAAAG
Rv_SpaD/A	CCG <b>CC</b> AT <b>G</b> GT <b>T</b> ATTTTCGGTGCTTGAGATT <b>C</b> G
Fw_SpaB	CCG <b>GAA</b> TT <b>C</b> AAGCGGATAACAAATTCAACAAAG
Fw_SpaC	CCG <b>GAA</b> TT <b>C</b> AAGCTGACAACAAATTCAACAAAG
Rv_SpaB/C	CCG <b>CC</b> AT <b>G</b> GT <b>T</b> ATTTTGGTGCTTGAGCAT <b>C</b> AT
Fw_SpaD <sub>58</sub>	CCG <b>GAA</b> TT <b>C</b> AAGCTGATAATAACTTCAACAAAG
Fw_Spa-C-term	GG <b>C</b> GA <b>AT</b> T <b>C</b> AGGAAGACAATAACAAGCCTGG
Rv_Spa-C-term	CCG <b>CC</b> AT <b>G</b> GT <b>T</b> ATAGTTCGCGACGACGT <b>C</b> C
Fw_Sbi-1	CCG <b>GG</b> AT <b>CC</b> ACTCAAACA <b>ACT</b> ACGTAACAGA
Rv_Sbi-1	CCG <b>AAG</b> CTTTTACTTGCTGTCTTTAAGTGATT <b>C</b> AG
Fw_Sbi-2	CCG <b>GG</b> AT <b>CC</b> AACCCAGAACCGACGTGTT <b>G</b> C
Rv-Sbi-2	CCG <b>AAG</b> CTTTTATTTATCCGCATTTTCAATATTT <b>G</b>

<sup>a</sup> restriction sites are indicated in boldface type.

**Table 2.4 Oligonucleotides used for *spaD* and *vwfA1* variants<sup>a,b</sup>.**

Name	Forward Primer (5'-3')
Fw_F5A	GCAACAAAATAAC <u>GCG</u> AACAAAGATC
Fw_Q9A	CTTCAACAAAGAT <u>GCA</u> CAAAGCGCC
Fw_Q10A	CAACAAAGATCAAG <u>CA</u> AGCGCCTTC
Fw_F13A	CAAAGCGCC <u>GCG</u> TATGAAATC
Fw_Y14A	GCGCCTTC <u>GCG</u> GAAATCTTG
Fw_L17A	CTATGAAATC <u>GCG</u> AACATGCC
Fw_N21A	GAACATGCCT <u>GCG</u> TAAACGAAG
Fw_R27A	GAAGCGCAAG <u>GCT</u> AACGGCTTC
Fw_N28A	CCAACGT <u>GCG</u> GGCTTCATTC
Fw_G29A	GCAACGTAAC <u>GCG</u> TTCATTCA
Fw_F30A	GTAACGGC <u>GCG</u> ATTCAAAGTC
Fw_I31A	GTAACGGCTTC <u>GCG</u> CAAAGTC
Fw_Q32A	GGCTTCATT <u>GCG</u> AGTCTTAAAG
Fw_S33A	GCTTCATTCAAG <u>GCG</u> CTTAAAGAC
Fw_L34A	TCATTCAAGC <u>GCG</u> GAAAGACCC
Fw_K35A	GTCTT <u>GCG</u> GACGACCCAAG
Fw_D36A	GTCTTAAAGC <u>GCG</u> GACCCAAGCC
Fw_D37A	CTTAAAGAC <u>GCG</u> CCAAGCC
Fw_Q40A	GACGACCCAAGC <u>GCA</u> AGCACTAACG
Fw_E47A	CGTTTTAGGT <u>GCA</u> GCTAAAAAATTAAACG
Fw_vWFA1-G561S	GTACCACGAC <u>AGCT</u> CCCACG
Rv_vWFA1-S522F	GGATGGCT <u>CGT</u> CCAGGCTGTC

<sup>a</sup> reverse primers for all variants is the reverse complement of forward primer.

<sup>b</sup> underlined bases indicate a changed codon.



PAGE (Laemmli, 1970) using 4.5 % stacking and 12.5 % separating acrylamide gels, except in the case of cell wall and cell envelope extracts, which were separated through 10 % separating acrylamide gels. Prestained protein molecular weight markers were purchased from New England Biolabs or Invitrogen. Protein samples were subjected to electrophoresis at 120 V until the dye front reached the bottom of the gel. After separation, proteins were either visualised by Coomassie blue protein staining or electroblotted onto methanol-activated PVDF membranes (Roche) at 100 V for 1h using a wet transfer cell (BioRad) for immunodetection or ligand blotting.

## **2.10 Protein detection**

### **2.10.1 Protein labelling and antibodies**

#### **2.10.1.1 Protein labelling**

Recombinant vWF truncates were biotylated using the EZ-Link TFP-PEO-biotin (Pierce). The reaction was stopped by addition of ammonium chloride (10 mM) and free biotin removed by dialysis in PBS.

#### **2.10.1.2 Antibodies**

Antibodies and antibody fragments are listed in Table 2.5. Note that the Fc region of chicken IgY does not interact with Spa.

### **2.10.2 Protein staining**

Acrylamide gels were bathed in Coomassie blue protein stain solution (2.5 % (w/v) Coomassie blue, 45 % (v/v) methanol, 10 % (v/v) acetic acid) overnight. Non-specific staining was removed by repeated bathing in a destain solution (45 % (v/v) methanol, 10 % (v/v) acetic acid) and gels were analysed under white light using Alpha Imager™ software. When greater sensitivity was required, proteins were visualised by silver staining (Ansorge, 1985).

### **2.10.3 Western immunoblotting**

PVDF membranes containing electroblotted proteins were incubated in blocking buffer (10 mM Tris-HCl pH 7.4, 150 mM NaCl 5 % (w/v) skimmed milk (Marvel)) for 16 h at 4°C. Membranes were washed three times with gentle agitation for 15 min in TBS-Tween (10 mM Tris-HCl pH 7.4, 150 mM NaCl, 0.05 % (v/v) Tween 20 (Sigma)) Next, horseradish-peroxidase conjugated antibodies were diluted appropriately in blocking buffer and incubated with the membrane for 1.5 h at room temperature with gentle agitation. Antibodies and antibody fragments and their working dilutions are listed in Table 2.6. Unbound antibody was removed by washing the membrane three times in TBS-Tween. Membranes were developed in the dark using the chemiluminescent substrate LumiGlo (New England BioLabs) as recommended by the manufacturer and exposed to X-Omat autoradiographic film (Kodak). The exposed films were fixed and developed manually or using a Kodak X-OMAT 1000 Processor developing machine.

### **2.10.4 Western ligand affinity blotting**

PVDF membranes containing electroblotted protein samples were blocked and washed as in Western immunoblotting (2.10.1). Membranes were then incubated with the appropriate ligand (200 nM) in blocking buffer for 3.5 h with gentle agitation at room temperature. Membranes were washed as before followed by incubation with the appropriate secondary antibody or peroxidase-conjugated streptavidin (1:5,000) for 1.5h at room temperature with shaking. Membranes were washed and developed as in Western immunoblotting (2.10.1).

### **2.10.5 Dot immunoblotting**

Nitrocellulose membranes were dotted with solutions containing 1 µg of protein and the spots allowed to dry. The Western immunoblotting (2.10.1) or Western ligand affinity blotting (2.10.2) was then followed.

**Table 2.5 Antibodies and antibody fragments**

<b>Antibody</b>	<b>Relevant features</b>	<b>Working dilution</b>	<b>Source</b>
Chicken anti-GST	Chicken IgY (non-Spa reactive), HRP-conjugated	1: 500	Gallus Immunotech
Chicken anti-Spa	Chicken IgY (non-Spa reactive), HRP-conjugated	1: 4,000	Gallus Immunotech
Chicken anti-IgG (human) (H+L chains)	Chicken IgY (non-Spa reactive), HRP-conjugated	1: 4,000	Gallus Immunotech
Chicken anti-IgM (human) (H+L chains)	Chicken IgY (non-Spa reactive), HRP-conjugated	1: 2,000	Gallus Immunotech
Monoclonal anti-6xHis	Mouse IgG1 (weakly Spa reactive), HRP-conjugated	1: 500	Roche
Rabbit anti-vWF F(ab') <sub>2</sub>	No Fc region, HRP-conjugated	1: 500	Dako
Rabbit IgG	Spa-reactive, HRP-conjugated	1: 5, 000	Dako
Rabbit anti-Sbi	Raised against recombinant Sbi-E	1: 10,000	Dr. J. van den Elsen
Goat anti-rabbit IgG	Secondary antibody with low Sbi-reactivity	1: 5,000	Dako



## **2.11 Protein expression and purification**

### **2.11.1 Small-scale protein induction**

Overnight cultures of *E. coli* BL21 DE3 or M15 (pREP4) cells (0.5 ml) were inoculated into fresh medium (1.5 ml) and grown to an OD<sub>600</sub> of 0.5. Isopropyl β-D-thiogalactopyranoside (IPTG) was added to a concentration of 1.5 mM and the culture was allowed to grow for a further 3 h. 250 μl cells were harvested by centrifugation at 16,000 x g for 5 min and resuspended in 50 μl final sample buffer. Samples were analysed by SDS-PAGE and stained as described (2.10.1). Recombinant proteins expressed from pGEX-KG contained an N-terminal glutathione-S-transferase (GST) fusion of 26 kDa. Proteins expressed from pQE30 contained an N-terminal hexahistidine tag. An uninduced sample was included to facilitate identification of induced proteins. Samples that contained an induced protein of expected size and that were confirmed by DNA sequencing were next used for large-scale protein induction and purification.

### **2.11.2 Large-scale protein induction**

#### **2.11.2.1 Expression and purification of recombinant Spa**

For expression of recombinant Spa, pGEX-KG constructs were purified from *E. coli* XL1-Blue and transformed into *E. coli* BL21 DE3 cells. Overnight cultures (20 ml) were inoculated into fresh medium (1:50) and grown to an OD<sub>600</sub> of 0.5. IPTG was added to a concentration of 1.5 mM and the culture was grown for a further 3 h. Cells were harvested by centrifugation at 7,000 rpm for 10 min at 4 °C in a Sorvall GS-3 rotor. The pellet was resuspended in PBS containing protease inhibitor (Roche), lysozyme (200 μg/mL) and DNase I (3 μg/mL) and allowed to stand on ice for 1 h. Cells were lysed by repeated passage through a French Pressure Cell. Cell debris was removed by centrifugation at 17,000 rpm for 30 min at 4 °C in a Sorvall SS-34 rotor and the supernatant was filtered through a 0.45 μm filter. The GST-fusion proteins were purified using a GSTrap™ column (Amersham) according to the manufacturer's instructions using a peristaltic pump (Amersham). Proteins were eluted using 10 mM glutathione in 50 mM Tris-HCL, pH 8.0 in 2ml fractions and samples were analysed

by SDS-PAGE for presence of the recombinant protein. Positive fractions were pooled and dialysed against phosphate-buffered saline (PBS). Recombinant GST-fusion proteins had approximate  $M_w$ s ranging from 59 kDa (five-domain Spa) to 32 kDa (single Spa domains).

#### **2.11.2.2 Expression and purification of recombinant untagged Sbi-II and Spa**

*E. coli* BL21 DE3 cells expressing Sbi-II or the desired Spa construct were induced, lysed and loaded onto a GSTrap™ column (Amersham) as described above (2.11.2.1). Recombinant proteins were released by on-column thrombin cleavage of the GST tag as follows; after repeated washing of the column, PBS containing human  $\alpha$ -thrombin (5  $\mu$ g/ml) was added and the column sealed and incubated for 18-24 h at 4 °C. The untagged proteins were eluted using PBS and a Benzamidine™ column (Amersham) was attached downstream of the column to remove thrombin. GST was eluted using 10 mM glutathione in 50 mM Tris-HCL, pH 8.0.

#### **2.11.2.3 Expression and purification of recombinant vWF A1**

*E. coli* M15 (pREP4) expressing vWF A1 from pQE30 was purified according to previously published methods (Cruz *et al.*, 2000; Emsley *et al.*, 1998).

#### **2.11.2.4 Expression and purification of recombinant V<sub>H</sub>3-Fab**

*E. coli* XL1-Blue expressing V<sub>H</sub>3-Fab (clone JMSpA3-08) from pCOMB3 was expressed essentially according to (Sasano *et al.*, 1993). Overnight cultures grown in L-broth were used to inoculate fresh SB medium and allowed to reach an OD<sub>600</sub> of 0.2 in an orbital shaker (200 rpm) at 37 °C. IPTG was added to a final concentration of 0.5 mM and cultures were grown overnight at 30 °C with shaking (200 rpm). Cells were harvested and lysed as described (2.11.2.1) and the lysate used directly or was filtered through a 0.45  $\mu$ m filter and passed over a protein A-sepharose column (Amersham) and eluted with (0.1 M Citric acid, pH 2.5) dropwise into (1 M Tris-NaCl, pH 9.0) followed by dialysis against PBS.

## **2.12 Determination of protein concentration**

Protein concentrations were determined using the BCA protein assay kit (Pierce) according to the manufacturer's protocol.

## **2.13 Antibody fragmentation**

Fc and F(ab)<sub>2</sub> fragments were generated using the X kit (Pierce).

## **2.14 Solid-phase binding assays**

### **2.14.1 Protein-protein binding assays**

Microtitre plates (Sarstedt) were coated with 100 µl recombinant protein (10 µg/ml) in PBS for 16 h at 4 °C. Wells were washed three times with Tween 20 (0.05 % v/v) in PBS and blocked at 37 °C for 2 h with 200 µl 3 % (w/v) bovine serum albumin (BSA) in PBS. Wells were again washed and varying concentrations of appropriate ligand in 3 % (w/v) BSA were added. Plates were incubated for 1 h at 37 °C. Unbound protein was removed by washing. Wells were incubated with the appropriate antibody (100 µl at recommended dilution) in 3 % BSA and incubated for 1 h at 37 °C. After washing, 100 µl of a chromogenic substrate solution (1 mg/ml tetramethylbenzidine and 0.006 % H<sub>2</sub>O<sub>2</sub> in 0.05 M phosphate citrate buffer pH 5.0) was added, and plates were developed for 10-15 min. The reaction was stopped by the addition of 2 M H<sub>2</sub>SO<sub>4</sub> (50 µl/well), and plates were read at 450 nm. Data was graphed and analysed using GraphPad Prism version 4.00 for Windows, GraphPad Software, San Diego, California, USA.

#### **2.14.1.1 Inhibition studies**

Microtitre plates were coated and blocked as before. Wells were incubated with mixtures containing increasing concentrations of inhibitor and a standard concentration of ligand corresponding to its half-maximal binding to the coated protein as determined



previously by solid-phase binding assays. Wells were washed and residual ligand binding was detected as before. Percentage inhibition was calculated from the percentage of bound protein detected in the absence of inhibitor.

#### **2.14.2 Bacterial-protein binding assay**

Cultures of *L. lactis* (stationary phase) or *S. aureus* (mid-exponential or stationary phase) were washed and adjusted to an OD<sub>600nm</sub> of 1.0 in PBS. Cells (100 µl) were coated onto microtitre plates (Nunc) by incubation at 4 °C for 16 h. Non-adherent cells were removed by washing plates with PBS and plates were blocked at 37 °C with 3 % (w/v) BSA in PBS (200 µl). Plates were washed and serial dilutions of ligand or antibody diluted in PBS (100 µl) were added followed by incubation at 37 °C for 1 h. This step was repeated with a secondary antibody if required and plates were developed as described before (2.14.1).

#### **2.14.3 Platelet adherence assay**

Adhesion of resting, non-activated platelets to bacterial cells was performed as previously described (Kerrigan *et al.*, 2002). Overnight cultures of *L. lactis* cells were harvested by centrifugation and washed twice in PBS. Bacteria were adjusted to an OD<sub>600</sub> of 1.0 in PBS and the bacterial suspension (100 µl) coated onto 96-well flat-bottomed plates (Nunc) by incubation for 2 h at 37°C. Triplicate wells were also coated with human fibrinogen (5 µg/ml), which binds platelets. Wells were blocked with 2 % (w/v) BSA in PBS for a further 2 h at 37 °C. During this incubation, washed GFPs were prepared as described in section 2.15. When desired, GFP samples were treated with the  $\alpha_{11b}\beta_3$  inhibitor tirofiban (5 nM, Merck) for 20 min at 37 °C. Wells were washed three times with JNL buffer (6 mM Dextrose, 130 mM NaCl, 9 mM NaCl<sub>2</sub>, 10 mM Na citrate, 10 mM Tris base, 3 mM KCl, 0.8 mM KH<sub>2</sub>PO<sub>4</sub> and 0.9 mM MgCl<sub>2</sub>; pH 7.4) (150 µl/well) and platelet preparations (1 x 10<sup>7</sup> platelets) were added to the wells followed by incubation for 30 min at 37 °C. Unbound platelets removed by washing three times with JNL buffer. Adherent platelets were detected by using a lysis buffer containing a substrate for acid phosphatase (100 mM Na acetate, 0.1 % (v/v) Triton-X-100, 10 mM *p*-nitrophenol phosphate (Sigma)). Plates were incubated in the dark at 37 °C for 2 h or until a straw-yellow colour had developed in the control well. Plates were then read in an ELISA plate reader at 405 nm.

## 2.15 Preparation of human platelets

Blood was drawn from healthy human volunteers that had abstained from non-steroidal anti-inflammatory drugs during the previous 10 days using a 19-gauge butterfly needle. For the preparation of platelet-rich plasma (PRP), 54 ml of blood was drawn into 6 ml of 3.8 % (w/v) Na citrate. The blood was centrifuged for 10 min at 150 x g. The PRP contained in the upper layer of each tube was carefully removed using a pasteur pipette. Platelet-poor-plasma (PPP) was prepared by centrifugation of the remaining blood at 720 x g for 10 min.

For the preparation of washed gel-filtered platelets (GFP), 51 ml of blood was drawn into 9 ml ACD buffer (25 mM citric acid, 75 mM Na citrate, 135 mM D-glucose) and PRP isolated as before. The PRP was adjusted to pH 6.5 with ACD and prostaglandin E1 (Sigma) was added at a final concentration of 1  $\mu$ M. The PRP was centrifuged at 630 x g for 10 min to pellet the platelets. The supernatant (PPP) was removed using a pasteur pipette and the platelet pellet was carefully resuspended in 1 ml of JNL buffer. The washed platelet suspension was filtered by gel-filtration on a Sepharose 2B column (Sigma) containing 10 ml packed sepharose that had been equilibrated in JNL buffer. Flow-through fractions containing the GFPs were collected in 15 ml tubes.

## 2.16 Platelet aggregation

PRP was prepared as described above. Activation of platelet aggregation was measured by light transmission at 37 °C using a PAP-4 aggregometer (BioData). PPP was used as the 100 % light transmission reference. Reactions were performed in siliconized flat-bottom glass cuvettes (BioData) at 37 °C with stirring (900 rpm). PRP (200  $\mu$ l) was pre-incubated with recombinant protein (25  $\mu$ l) for 15 min at 37 °C followed by addition of 1 U platelet agonist (ristocetin, botrocetin, thrombin, ADP, TRAP) (25  $\mu$ l) and aggregation measured. When necessary, bacterial cells were washed and adjusted to OD<sub>600nm</sub> of 1.6 in PBS (approximately 2 x 10<sup>9</sup> cells/ml). The bacterial suspension (25  $\mu$ l) (1 x 10<sup>8</sup> cells) was added to the PRP/protein mixture (225  $\mu$ l) and the aggregation measured.

## **2.17 Bacterial perfusion studies**

### **2.17.1 Preparation of flow chamber slides**

A 500 $\mu$ l solution of purified vWF (100  $\mu$ g/ml) was applied to glass slides (75 x 25 mm) and allowed to attach for 2 h at room temperature in a humidity chamber. Slides were washed 3 times in PBS buffer to remove any unbound protein and blocked with 1% (w/v) BSA for 1 h at 37 °C.

### **2.17.2 Videomicroscopy**

Overnight cultures of *L. lactis* or *L. lactis* Spa<sup>+</sup> were washed twice in PBS and resuspended to an OD<sub>600</sub> of 1. Next, cells were perfused over immobilized vWF at various shear rates. A syringe pump (Harvard Biosciences, MA, USA) was used to aspirate bacteria through the flow chamber. Bacterial adhesion was visualised by phase contrast microscopy (63X LD-Achroplan objective) through the flow chamber (GlycoTech) mounted on a Zeiss Axiovert-200 epi-fluorescence microscope (Carl Zeiss). Images were captured every second up to 300 s by a liquid chilled Quantix-57 CCD camera (Photometrics Ltd.). Bacterial adhesion was analysed using MetaMorph (Universal Imaging Corp.).

## **2.18 Isolation of *S. aureus* cell wall and cell envelope components**

### **2.18.1 Preparation of staphylococcal whole cell lysates**

Overnight cultures of *S. aureus* were washed in PBS and adjusted to an OD<sub>600nm</sub> of 100 in PBS containing protease inhibitors (Roche) and Dnase (80  $\mu$ g/ml). Cell walls were digested by incubation at 37 °C for 30 min with lysostaphin (200  $\mu$ g/ml). Lysostaphin digests were mixed with an equal volume of FSB, boiled for 10 min and analysed by SDS-PAGE and Western immunoblotting.



### **2.18.2 Preparation of the staphylococcal cell wall**

Stationary-phase cultures of *S. aureus* (50 ml) were harvested by centrifugation at 7,000 rpm for 10 min at 4 °C in a Sorvall GS-3 rotor, washed and adjusted to 100 OD<sub>600nm</sub> units in PBS and harvested by centrifugation. Cells were resuspended in 1 ml digestion buffer (50 mM Tris-HCL, 20 mM MgCl<sub>2</sub>, 30 % (w/v) raffinose, pH 7.5) containing protease inhibitors (Roche). Cell wall proteins were released by digestion with lysostaphin (200 µg/ml) at 37 °C for 15 min. Protoplasts were harvested by centrifugation at 6,000 rpm for 15 min and the supernatant was retained as the cell wall fraction.

### **2.18.3 Preparation of the staphylococcal protoplast and cytoplasm**

Protoplast pellets were isolated as described above. The pellets were resuspended in 1 ml 50 mM Tris-HCL, 20 mM MgCl<sub>2</sub>, pH 7.5 with protease inhibitors (Roche). This sample was retained as the stabilised protoplast fraction. Protoplasts were also fractionated into membrane and cytoplasmic fractions. Protoplast pellets were washed once in digestion buffer and resuspended in ice-cold 50 mM Tris-HCL, pH 7.5 containing protease inhibitors (Roche) and DNase (80 µg/ml). Protoplasts were lysed on ice by vortexing followed by centrifugation in a SM-24 rotor (Sorvall) at 40,000 rpm for 1 h at 4 °C. The supernatant was retained as the cytoplasmic fraction. The pellet was washed once with ice-cold 50 mM Tris-HCL, pH 7.5 and the pellet containing the protoplast membrane fraction finally resuspended in 50 mM Tris-HCL, pH 7.5.

### **2.18.4 Preparation of extracellular proteins of *S. aureus***

Overnight cultures of *S. aureus* (50 ml) were harvested and the supernatant was concentrated 25-fold using Centricon™ centrifugal filtration devices (Amicon). This sample represents the extracellular protein fraction at approximately the same concentration as other *S. aureus* components isolated.

## 2.19 Proteomics tools for prediction of protein topology

Membrane-spanning regions and topology of Sbi and EbpS based on their primary protein sequence was performed using the following online computer programs;

Kyte-Doolittle Hydropathy plotting: <http://gcat.davidson.edu/rakarnik/kyte-doolittle.htm>,

Prediction of transmembrane  $\alpha$ -helices: TMHMM (<http://www.cbs.dtu.dk/services/TMHMM>),

DAS (<http://www.sbc.su.se/~miklos/DAS/>).

## **Chapter 3**

### **Analysis of the Interaction between Protein A and von Willebrand Factor using Recombinant Protein Truncates**



### 3.1 Introduction

*S. aureus* has the ability to express a number of cell wall-anchored surface proteins that bind to plasma proteins or to components of the extracellular matrix. This facilitates evasion of immune responses, colonization of damaged tissue and adhesion to host cells and to platelets. The interaction between *S. aureus* and platelets is a critical step in *S. aureus*-induced endocarditis (Sullam *et al.*, 1996). It has been demonstrated previously that the plasma proteins fibrinogen and fibronectin can act as bridges between bacterial cells and the platelet intergrin  $\alpha_{IIb}\beta_3$  on resting platelets, through interactions with staphylococcal surface proteins Clumping Factor A (ClfA), and Fibronectin Binding Proteins (FnBPs) (Fitzgerald *et al.*, 2006; Loughman *et al.*, 2005). In each case, specific antibodies to the surface protein are also required to form a bridge to the platelet surface, via the platelet IgG receptor, Fc $\gamma$ RIIa. This can lead to infective vegetations in the vascular endothelium. *S. aureus*-platelet interactions are discussed in more detail in section 1.9.2.1.

Protein A (Spa) is a major surface protein of *S. aureus*. Spa is known to bind human von Willebrand factor (vWF), a plasma protein that is essential for haemostasis (Hartleib *et al.*, 2000). The Spa-vWF interaction has a  $K_d$  of 15 nM as measured by surface plasmon resonance (SPR) using full-length recombinant protein A and vWF that had been purified from plasma. This interaction was shown to occur in the presence of physiological concentrations of IgG, despite avid IgG-binding by Spa ( $K_d \sim 9$  nM) (Hartleib *et al.*, 2000). The main function of vWF is to capture platelets by binding to the platelet receptor GPIb- $\alpha$ , and immobilise them to a damaged blood vessel. This stimulates the formation of a blood clot. von Willebrand's disease, a common genetic disorder in which vWF functions abnormally or vWF is produced at very low levels, can cause severe haemophilia. During biosynthesis, vWF is proteolytically cleaved and multimerised through disulfide bridging. Larger vWF multimers are more efficient in platelet capture and thrombus initiation. The vWF monomer consists of four types of repeat domain denoted A, B, C and D. Domains are arranged in the sequence D'-D3-A1-A2-A3-D4-B1-B2-B3-C1-C2-CK in the mature protein. Binding of circulating vWF to collagen in exposed sub-endothelial matrix of damaged blood vessels under high shear stress stimulates a conformational change in vWF. This promotes platelet-vWF interactions via GpIb- $\alpha$  on the platelet surface. Circulating platelets are captured and activated, stimulating the thrombus formation (for review see section 1.7).

The ability of *S. aureus* to bind vWF could potentially contribute to the adherence of the bacterium to platelets or to damaged blood vessels *in vivo*. Studies using a Spa-

deficient mutant of *S. aureus* have shown that the Spa-vWF interaction is necessary for efficient recruitment of *S. aureus* by platelets under high shear stress in whole blood (Pawar *et al.*, 2004). In addition, fluid-shear adhesion experiments suggested that vWF-binding by Spa promotes adherence of circulating *S. aureus* cells to immobilised collagen *in vitro* (Mascari and Ross, 2003). This interaction occurs at low shear, presumably because collagen-bound vWF is already conformationally active.

In this chapter the interaction between Spa and vWF is reported. The ability of surface-expressed Spa to promote bacterial adhesion under flow was investigated in the absence of any other *S. aureus* surface proteins. Investigation of bacterial-expressed Spa binding to immobilised vWF in conditions of shear-stress is more physiologically relevant than under static conditions as it may more accurately reflect the conditions in blood vessels. Previous studies have demonstrated that *S. aureus* deficient in Spa is not captured by vWF-coated surfaces under flow (Hartleib *et al.*, 2000). It is not known whether Spa alone can trigger this process through the vWF interaction. This was achieved by heterologous expression of Spa on the surface of the food-grade Gram-positive organism *Lactococcus lactis* which was used as a surrogate host. *L. lactis* has been successfully used to express other *S. aureus* surface proteins such as ClfA, ClfB and SdrE (O'Brien *et al.*, 2002). As in *S. aureus*, proteins are sorted by the Sec pathway and anchored to cell-wall peptidoglycan via their C-terminal LPXTG motif, as described in section 1.2. The Spa-vWF interaction was also analysed using recombinant protein truncates. These comprised vWF truncates and variants with deletions of all of the major ligand-binding regions of the vWF molecule. The Spa truncates comprised varying numbers of the five surface-exposed Ig-binding repeats E, D, A, B and C, which make up most of the surface-exposed region of Spa when it is anchored to the bacterial cell wall. It was postulated that these domains contained the binding site(s) for vWF. The Spa repeats are highly homologous, sharing between 75 and 89 % amino-acid identity (Graille *et al.*, 2000). Adjacent repeats are more similar while domain E is the most divergent. It is possible that the vWF-binding region on Spa is contained in a conserved region of each Ig-binding domain or that it spans multiple domains. To investigate this, different combinations of domains were constructed to investigate their ability to bind vWF. The purified proteins were employed in solid-phase binding assays with vWF. Solid-phase binding assays were performed by firstly immobilising a protein in 96-well ELISA plates. After blocking the remaining protein binding sites, the immobilised protein was incubated with the ligand, usually diluted to a range of different concentrations. The plates were washed and any bound ligand detected

using specific antibody. The Spa-vWF interaction was also investigated by ligand affinity blotting.



## 3.2 Results

### 3.2.1 Surface-expression of Spa on *Lactococcus lactis*

It has previously been shown that protein A-expressing *S. aureus* strains can bind to vWF, while their isogenic *spa* mutants cannot. To determine whether expression of protein A on the cell surface is sufficient for adhesion of bacteria to immobilized vWF under flow, *L. lactis* or *L. lactis* expressing Spa from plasmid pKS80 were used. Open-reading frames cloned in-frame into the plasmid pKS80 are constitutively expressed from the strong lactococcal bacteriophage C2 promoter, LPS2 (Hartford *et al.*, 2001). Surface expression of protein A from pKS80 in *L. lactis* was investigated by whole cell dot immunoblotting as described in 2.10.5. Briefly, overnight *L. lactis* cultures were washed and corrected to an OD<sub>600</sub> of 1.0. Serial dilutions of the washed cultures were made and 5 µl of each dilution was spotted onto nitrocellulose membrane. The membrane was probed with chicken anti-Spa antibody. A positive reaction was only detected in *L. lactis*(pKS80*spa*) (Figure 3.1 A). *L. lactis*(pKS80*spa*) therefore contains a surface-exposed protein reactive with anti-Spa antibody that is not on the surface of *L. lactis*(pKS80). To test this further, whole-cell lysates of overnight cultures of *L. lactis*(pKS80) and *L. lactis*(pKS80*spa*) were analysed by Western immunoblotting using chicken anti-Spa antibody. Figure 3.1 B shows a reactive band of 55 kDa, the approximate Mr of Spa, in the whole-cell lysate of *L. lactis*(pKS80*spa*) strain that was absent in the sample of *L. lactis* containing the empty pKS80 vector. This confirms that full-length Spa is expressed and surface exposed in *L. lactis* from the pKS80 plasmid.

### 3.2.2 Surface expression of Spa on *Lactococcus lactis* is sufficient for bacterial adhesion to vWF-coated surfaces under flow

Perfusion studies with vWF were performed using overnight cultures of *L. lactis*(pKS80) and *L. lactis*(pKS80*spa*) that had been corrected to OD<sub>600</sub> of 1.0 in PBS. vWF (100 µg/ml) was coated on glass slides and slides were placed in a perfusion chamber maintained at 37 °C. The perfusion system works by forcing bacteria over the vWF-coated slides at a selected shear rate using a syringe pump. A microscope mounted on the flow chamber allows adherent bacteria to be visualised in real-time and images to be recorded every second for 300 s by video microscopy as detailed in section 2.17.2. Adherent bacteria were observed only in the case of the *L. lactis* strain expressing protein A. Binding occurred at low shear rates (50 s<sup>-1</sup>) (Fig. 3.2), in agreement with previous studies

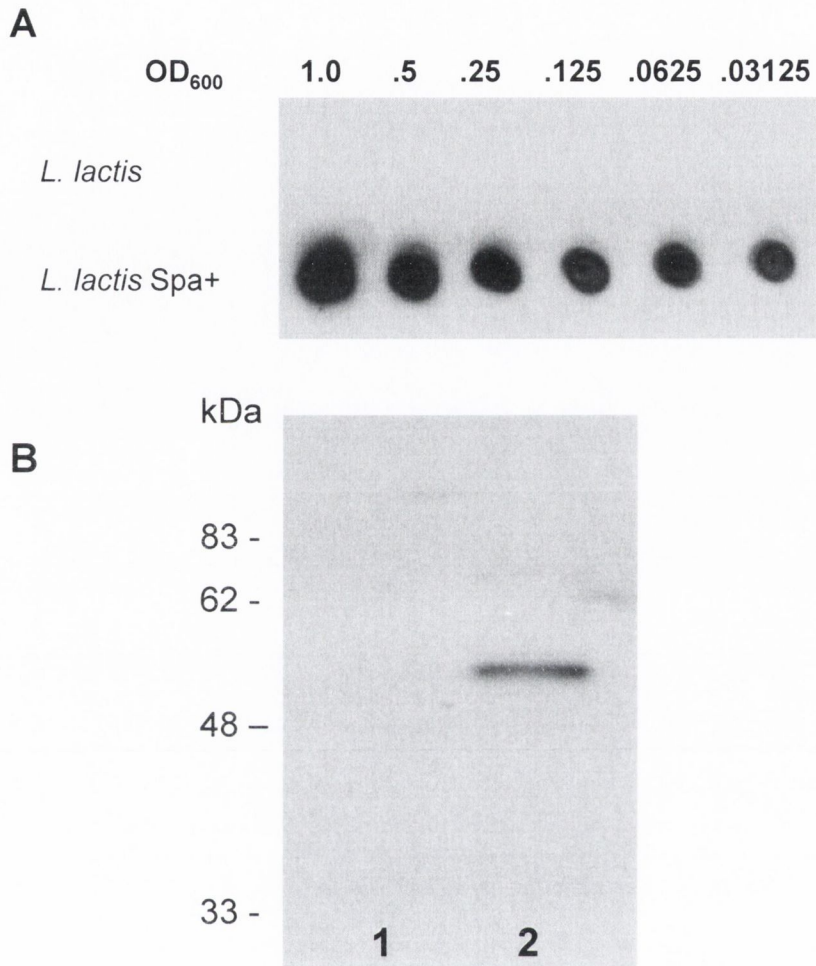
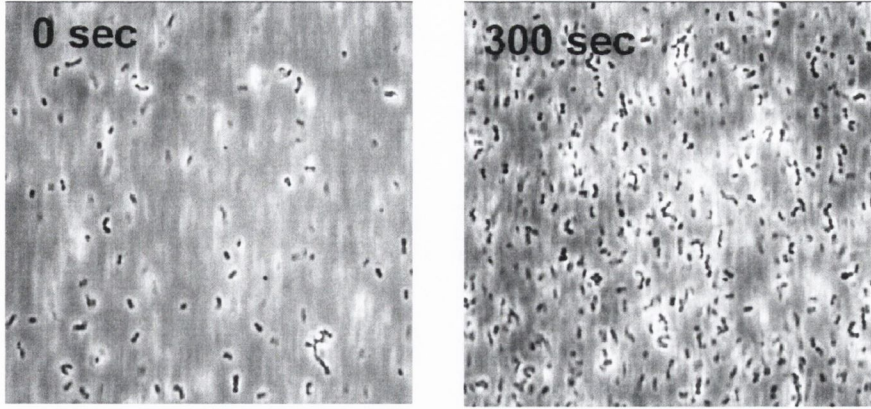


**Fig. 3.1. Surface expression of Spa on *L. lactis*.** *A*, overnight cultures of *L. lactis* pKS80 or *L. lactis*(pKS80spa) were washed and corrected to an OD<sub>600</sub> of 1.0. Doubling dilutions of this culture were then spotted onto nitrocellulose membrane as indicated, and probed with chicken anti-Spa antibody. *B*, Whole cell lysates of *L. lactis* pKS80 (1) and *L. lactis*(pKS80spa) (2) were resolved by SDS-PAGE, and analysed by Western immunoblotting using peroxidase-conjugated chicken anti-Spa antibody. Bound antibody was detected using chemiluminescent substrate.

A



B

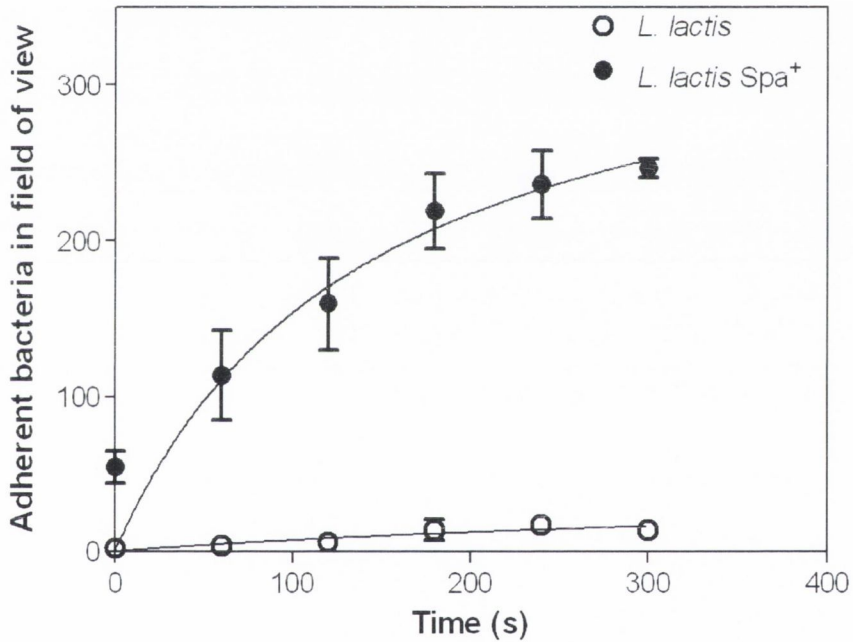


**Fig. 3.2. Perfusion of *L. lactis* expressing Spa over vWF-coated slides.** *L. lactis* or *L. lactis* expressing Spa were perfused over glass slides coated with full-length vWF (100  $\mu\text{g/ml}$ ). Live imaging of adherent cells was performed by videomicroscopy. *A*, images of *L. lactis Spa*<sup>+</sup> after 0 and 300 seconds of perfusion over vWF. *B*, Adherent bacterial cells were counted from three independent fields of view at 60 second intervals for both *L. lactis* and *L. lactis Spa*<sup>+</sup>.



using immobilised vWF perfused with *S. aureus*. Quantitative analysis was performed by counting adherent cells from at least three separate fields at 60-second time intervals. It can be seen in Figure 3.2 B that the number of adherent bacteria increased with time until saturation occurred after approximately 300 s. A recording from one field of view accompanies this thesis. These data support previous work suggesting that Spa on the surface of *S. aureus* is necessary for efficient attachment of bacteria to a vWF-collagen complex at low shear rates by demonstrating that it is sufficient for this process (Hartleib *et al.*, 2000; Mascari and Ross, 2003).

### 3.2.3 Recombinant GST-Spa truncates

This study and work by others has demonstrated that expression of Spa on the bacterial surface is both necessary and sufficient for adherence to vWF. To localise the region on Spa responsible for vWF-binding, a series of recombinant Spa truncates were constructed by PCR-amplification of fragments of the *spa* gene, which were cloned into the GST-fusion protein expression vector, pGEX-KG (Fig. 3.3). DNA fragments cloned into pGEX-KG produce N-terminal GST-fusion proteins under the control of the IPTG-inducible  $P_{tac}$  promoter. Purification of GST-fusion proteins was performed in a single step by affinity chromatography with glutathione sepharose. GST-fusion proteins bound to immobilised glutathione columns were eluted using a glutathione solution. A rapid protein purification procedure was desirable because of the number of constructs to be expressed and purified. Another benefit of the GST fusion-tag system is that recombinant proteins can be detected with anti-GST antibody. Detection of bound protein using anti-Spa antibodies would generate data that would be difficult to compare meaningfully because of the varying number of domains present.

To create the *spa* constructs, oligonucleotides were designed against each individual repeat of *spa* allowing the generation of five-, four-, three-, two- and single-repeat constructs. The region of the *spa* gene encoding the cell wall-spanning region was also amplified. Restriction sites were incorporated into the 5' extensions of the primers to facilitate directional cloning. The entire *spa* gene was used as a template for generation of the five-, four- and three-domain constructs, and for the 3' region of *spa*. Amplification of the two- and one-domain repeats required smaller DNA templates, due to high sequence homology between the five *spa* repeats. Despite highly homologous DNA sequences between the repeats of *spa*, there are a number of unique endonuclease recognition sites (Fig. 3.4 A). Digestion of the *spa* template with the appropriate endonucleases generated

fragments that could be identified by size and isolated for use as a PCR template to amplify specific regions (Fig. 3.4 B).

The cloned *spa* fragments were sequenced and plasmids transformed into the *E. coli* protein expression strain BL21. The ability of this strain to express the GST-fusion proteins was confirmed by IPTG induction of 2 ml cultures as described in section 2.11.1. Lysates were resolved by SDS-PAGE and compared to an uninduced control culture for expression of recombinant protein. Putative positive clones were also analysed by Western immunoblotting using a chicken anti-GST antibody. Recombinant GST-Spa-expressing clones were then induced in 1L batch cultures and purified using the GSTrap system as described (2.11.2.1). Samples from the following steps in the purification procedure were retained and analysed by SDS-PAGE; a lysate of induced cells, the soluble fraction prior to addition to the column, the 'flow-through', the first and final 10 ml of wash buffer, each of ten 2 ml elution fractions. In this way, the recombinant protein can be monitored at each stage of the purification. A typical GST-Spa purification (for a single-domain construct) is shown in Figure 3.5. In this case, the elution fractions 2-6 were pooled and dialysed against PBS.

### 3.2.4 Functional analysis of recombinant GST-Spa constructs

Protein A is known to bind the Fc region of IgG from most mammals, along with a number of other ligands. In the case of the Fc region of Ig, the best characterised interaction, it has been demonstrated that each individual Spa domain is capable of ligand binding with similar affinity (Inganas *et al.*, 1981). The crystal structure of a Spa domain in complex with human Fc has been solved (Deisenhofer, 1981). This indicates that correct folding of Spa is necessary for optimal binding, as contact residues for Fc are located on two anti-parallel  $\alpha$ -helices. The ability of the GST-Spa truncates to bind IgG would give an indication of correct folding. The protein solutions were dialysed into PBS and the concentrations determined by the BCA protein assay (Pierce). Protein stocks were then normalised to an equal concentration. Samples were separated by SDS-PAGE and stained (Fig. 3.6). Samples were also coated on microtitre plates at an equal concentration (5  $\mu$ g/ml) and probed with chicken anti-GST antibody. Figure 3.7 shows a similar level of antibody binding to each GST-Spa truncate. The protein concentrations thus were assumed to be equal. Each GST-Spa truncate was then tested for binding to rabbit IgG in a solid phase assay, in which a peroxidase-conjugated rabbit antibody was tested for binding to

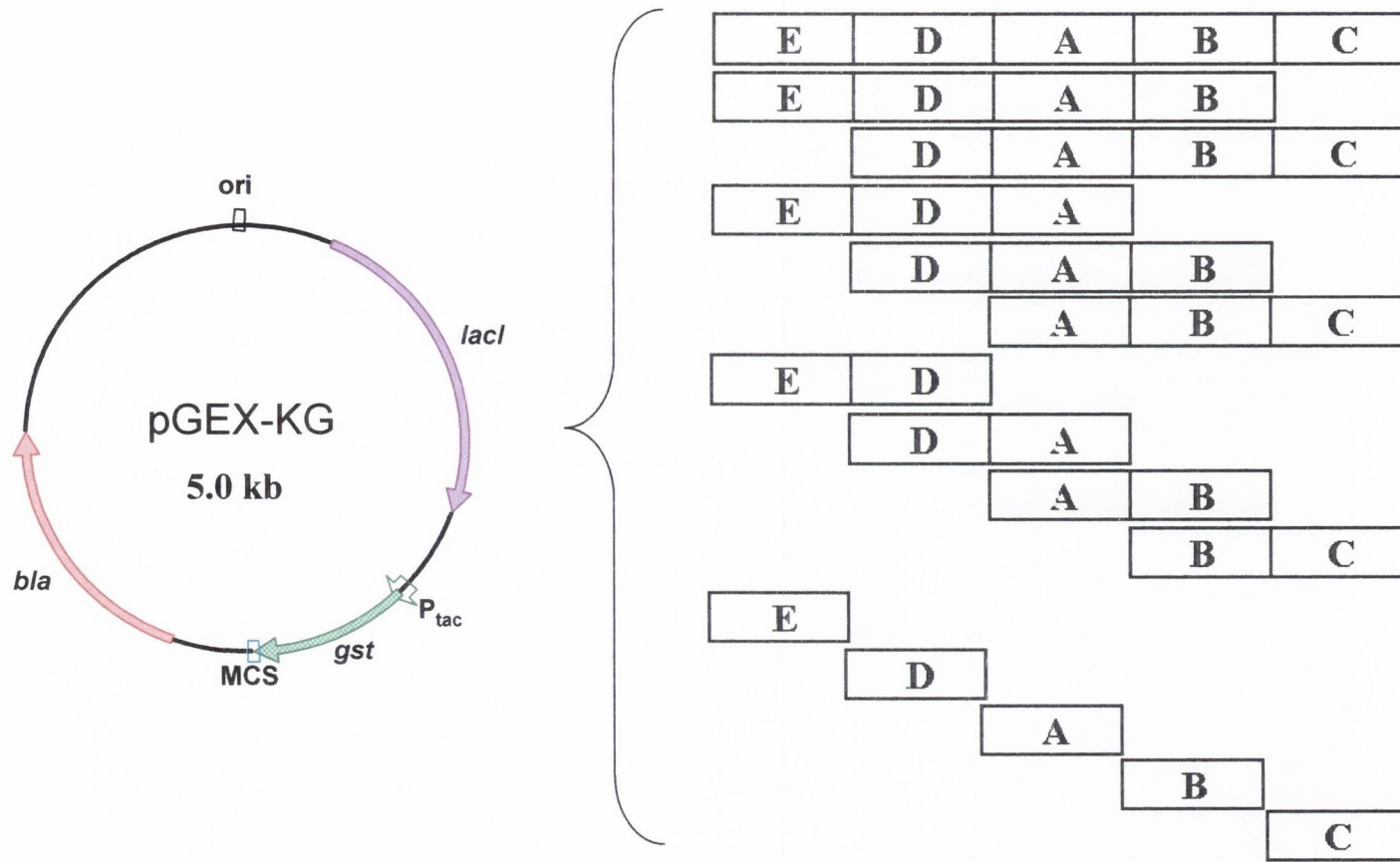


**Fig. 3.3 Plasmid pGEX-KG and recombinant GST-Spa truncates.** Schematic representation of the Spa domain constructs generated for cloning into the GST-fusion expression vector pGEX-KG (left). 5-, 4-, 3-, 2-, and single-domain constructs were generated by PCR and directionally cloned into pGEX-KG. Cloning into the multiple cloning site (MCS) creates an N-terminal 26 kDa GST-fusion which allows one-step protein purification on glutathione-sepharose columns.



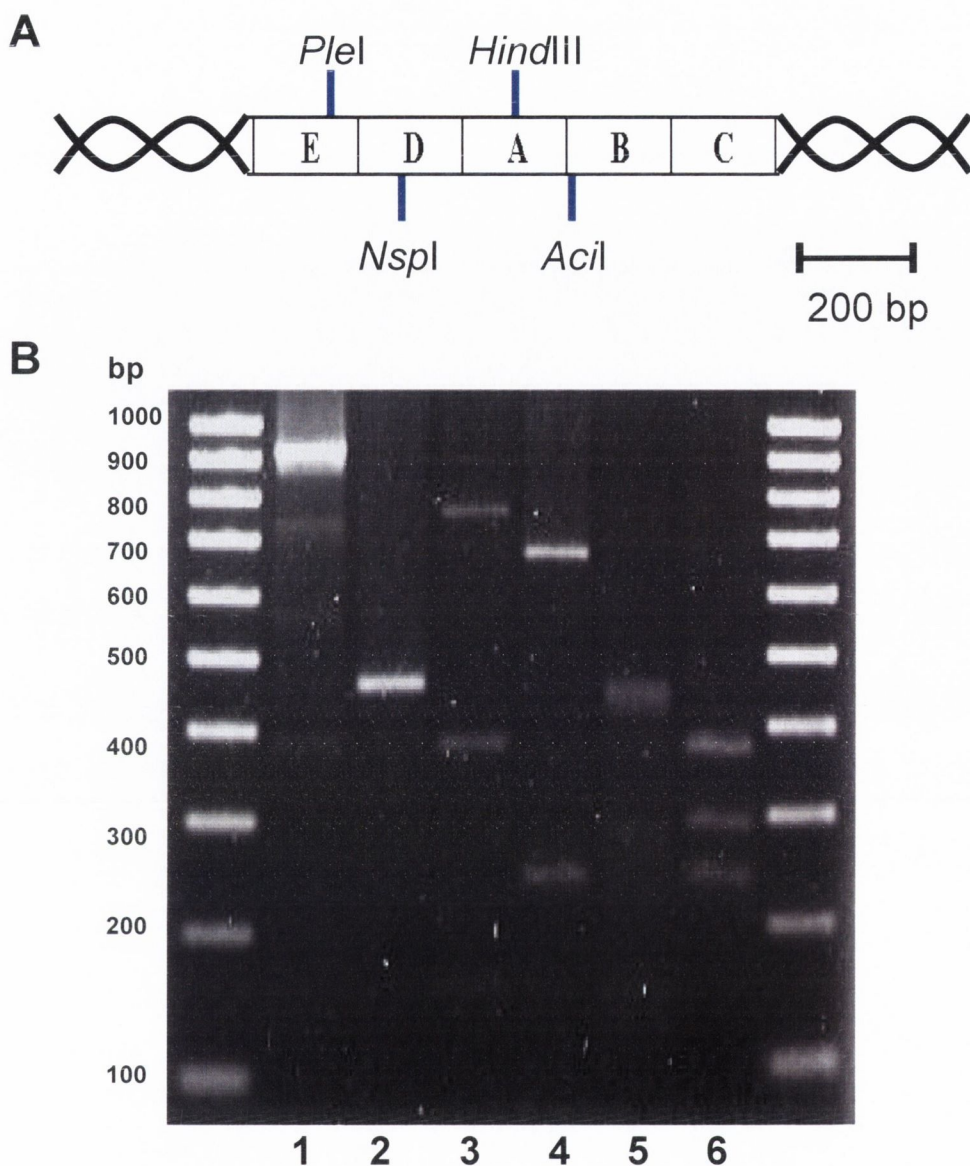


**Fig. 3.4 Procedure for amplification of *spa* fragments.** *A*, the DNA region encoding the *spaEDABC* repeats contains a number of unique restriction sites. Digestion of the *spaEDABC* template with one or more of these enzymes facilitates DNA amplification of double and single *spa* repeats. *B*, agarose gel of *spaEDABC* restriction digests (1, uncut *spaEDABC* (920 bp) 2, *Hind*III (domains ED - 462bp, domains BC and B - 420 bp) 3, *Ple*I, *Ac*il (domains DA - 375 bp, domain C - 348 bp) 4, *Nsp*I (domains AB - 644 bp, domain E - 241 bp) 5, *Ple*I, *Hind*III (domain D - 162 bp) 6, *Nsp*I, *Ac*il (domain A - 296 bp).

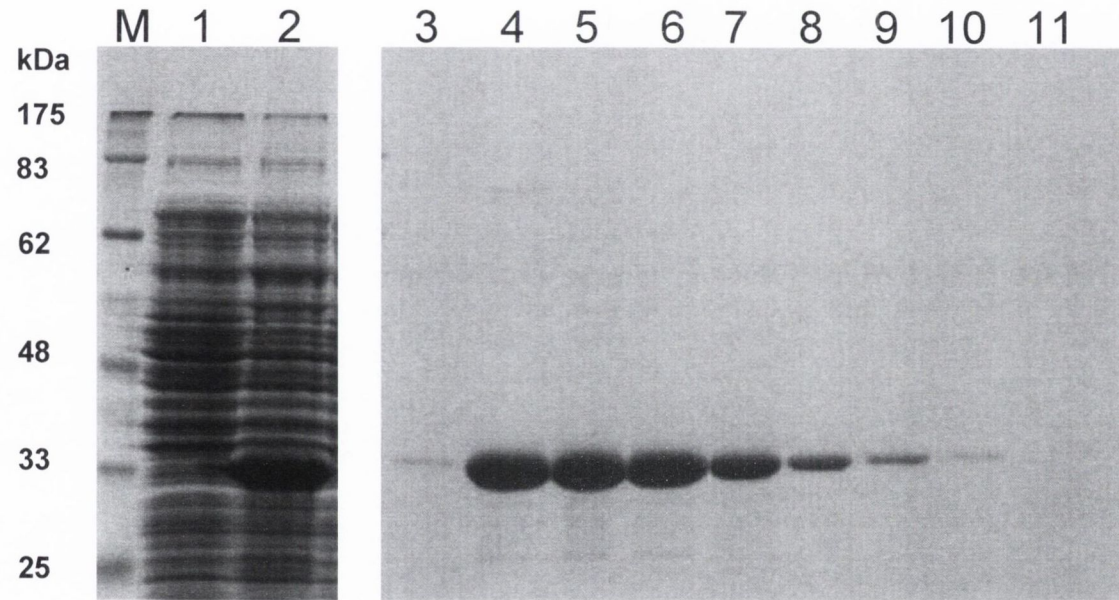


**Fig. 3.5. Purification of GST-fusion proteins.** Samples of *E. coli* BL21(DE3) cells uninduced (1) or induced (2) for production of GST-fusion proteins by addition of IPTG (GST-SpaD, 33 kDa) and samples from 2 ml elution fractions from GSTrap columns (3-11) were separated by SDS-PAGE and stained using Coomassie Blue. A standard protein marker (M) was included. GST-fusion proteins were induced and purified as described in section 2.11.2.1.

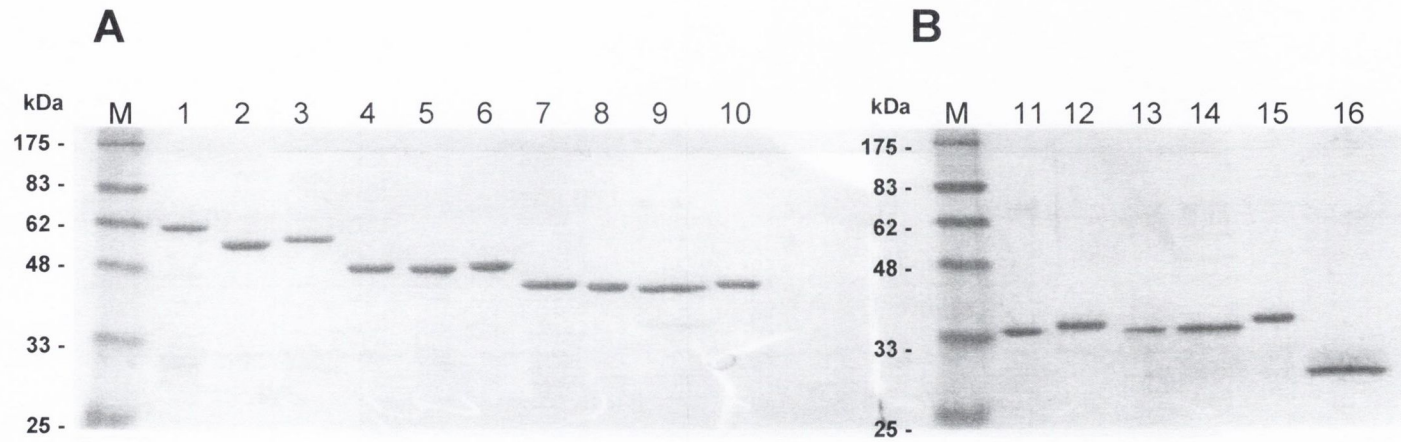


**Fig. 3.6. SDS-PAGE analysis of GST-Spa truncates.** Each of the GST-Spa constructs used in this study were subjected to SDS-PAGE and stained with Coomassie Blue in the order; *A*, M, molecular weight marker lane 1, GST-EDABC (59 kDa) lane 2, GST-EDAB (51.5 kDa) lane 3, GST-DABC (52 kDa) lane 4, GST-EDA lane 5, GST-DAB (45 kDa) lane 6, GST-ABC (46 kDa) lane 7, GST-ED lane 8, GST-DA lane 9, GST-AB (all 39 kDa) lane 10, GST-BC (40 kDa). *B*, M, molecular weight marker lane 11, GST-E (32 kDa) lane 12, GST-D (32.5 kDa) lane 13, GST-A (32 kDa) lane 14, GST-B (32 kDa) lane 15, GST-C (33 kDa) lane 16, GST (26 kDa).



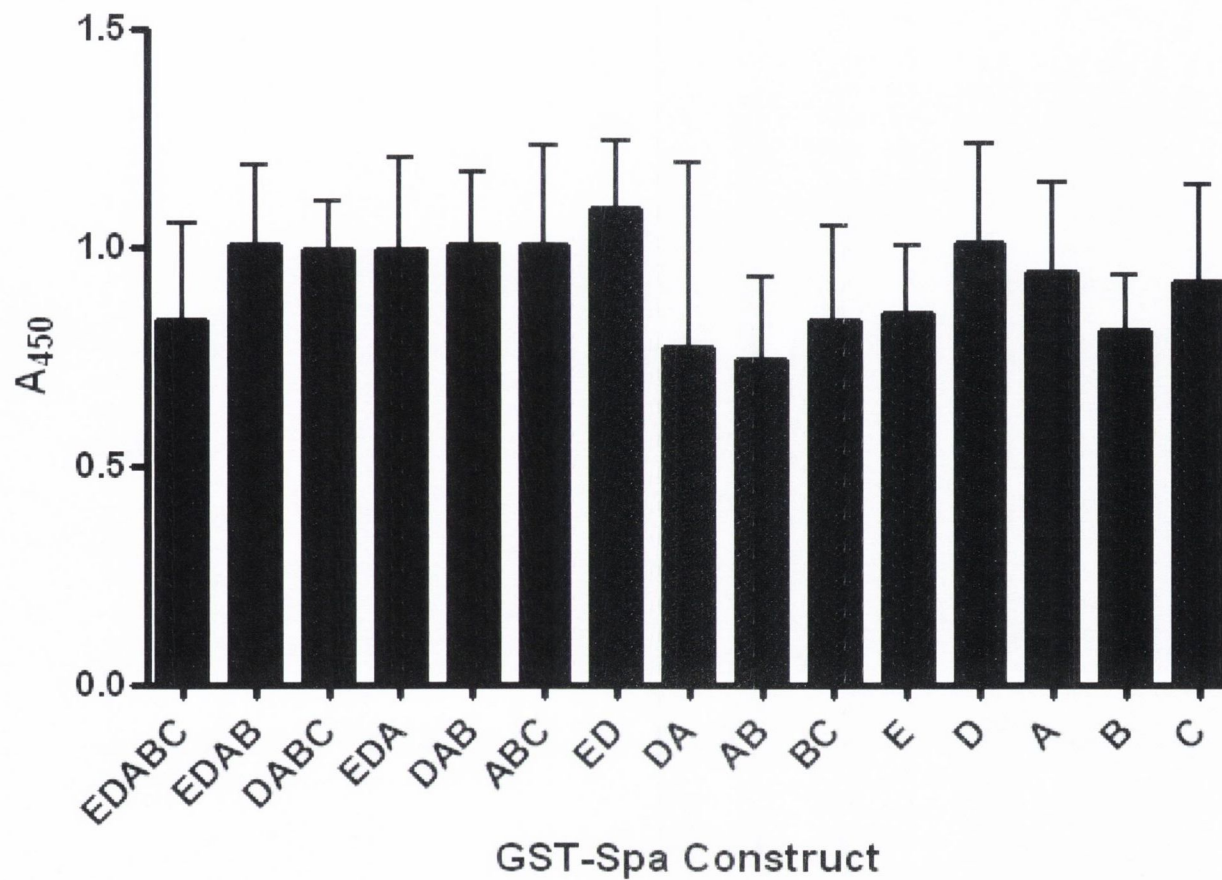


**Fig. 3.7 Relative protein concentrations of GST-Spa truncates.** GST-Spa constructs were dialysed in PBS and protein concentrations of each constructs was estimated. Protein stocks were diluted to 5  $\mu\text{g}/\text{ml}$  in 100  $\mu\text{l}$  aliquots. Each sample allowed to coat on microtitre plates for 16 h and was probed using peroxidase-conjugated chicken anti-GST antibody followed by development for 15 min in a chromogenic substrate solution, described in 2.14.1. Absorbance at 450 nm was recorded using a plate-reader.

immobilised GST-Spa truncates. All truncates bound the rabbit IgG with high affinity, indicating that they were most likely folded correctly (Fig 3.8). Single Spa domains bound IgG with slightly lower affinity when compared to constructs containing multiple repeats. In agreement with previous reports, the single Spa domains bound IgG with similar affinity.

### 3.2.5 Interaction of GST-SpaEDABC with von Willebrand Factor

Previously it was shown by surface plasmon resonance (SPR) that commercial protein A bound to von Willebrand Factor that had been purified from plasma (Hartleib *et al.*, 2000). SPR utilises the change in light resonance of monochromatic light a gold chip coated with analyte as a result of a ligand binding when passed over the chip. A thin layer of metal (gold) on the chip causes the light to be monochromatic and p-polarized. The intensity of this reflected light is reduced at a specific incident angle producing a sharp shadow (called surface plasmon resonance) due to the resonance energy transfer between evanescent wave and surface plasmons. A linear relationship exists between resonance energy and mass concentration of biochemically relevant molecules such as proteins, sugars and DNA. The SPR signal (expressed in resonance units) therefore measures the increase of mass concentration at the sensor chip surface. This means that the analyte and ligand association and dissociation can be observed and ultimately rate constants (as well as equilibrium constants) can be calculated. This technique is extremely sensitive and can be used to accurately measure  $K_d$  values. The estimated  $K_d$  value for the Spa-vWF interaction was determined to be 15 nM by this method. While these data indicate avid binding, it is possible that small amounts of contaminating Ig present in the vWF preparation could contribute to the reported  $K_d$  value. Protein A-Ig interactions would not be distinguished from those with vWF by surface plasmon resonance. This can be overcome by using recombinant vWF. Therefore, GST-SpaEDABC was tested for binding to recombinant von Willebrand factor in a solid-phase assay. This technique cannot be used to determine  $K_d$  values accurately. However, it was desirable to verify that a specific interaction was occurring, and half-maximal binding values should be comparable to the reported dissociation constant. Both GST-SpaEDABC and vWF were tested for dose-dependent and saturable binding as described in section 2.14.1. Firstly, GST-SpaEDABC and the region of Spa encoding the cell wall-spanning region, GST-Spa-C-term (10  $\mu$ g/ml), were coated on 96-well microtitre plates. Immobilised proteins were incubated with increasing concentrations of recombinant vWF ranging from 625 pM to 640 nM. Bound



vWF was detected using peroxidase-conjugated rabbit anti-vWF (Fab)<sub>2</sub> fragments. The anti-vWF (Fab)<sub>2</sub> fragments were prepared by pepsin digestion of polyclonal rabbit anti-vWF antibody followed by removal of Fc fragments using protein A-sepharose. Control experiments showed that the rabbit anti-vWF (Fab)<sub>2</sub> fragments did not interact with Spa, while the whole rabbit IgG bound with high affinity (Fig. 3.9). Soluble recombinant vWF bound in a dose-dependent, saturable manner to GST-SpaEDABC, with half maximal binding estimated at 30 nM (Fig. 3.10 A). No interaction was seen between soluble vWF and immobilised GST-Spa-c-term. This confirms that the extracellular Ig-binding repeats of Spa contain the binding site for vWF. In the reverse assay, immobilised vWF (10 µg/ml) was incubated with increasing concentrations of GST-SpaEDABC, ranging from 625 pM to 640 nM. Adherent GST-SpaEDABC was detected using peroxidase-conjugated chicken anti-GST IgY. The Fc region of chicken IgY does not bind Spa (Fig. 3.9). Dose-dependent and saturable binding occurred with a half-maximal binding estimated at 30 nM from the resultant binding curve (Fig. 3.10 B). This is in close agreement with the previously estimated  $K_d$  value of 15 nM (Hartleib *et al.*, 2000).

To demonstrate specificity of this interaction, inhibition studies were also performed. The ability of soluble, biotinylated proteins to bind to immobilised ligand in the presence of increasing concentrations of the non-biotinylated protein was tested. The use of biotinylated proteins circumvented the need to use antibodies to detect bound protein, which could be confused by the interaction between the Fc region of IgG and Spa. Proteins were biotinylated as described in section 2.10.1.1. Solid-phase binding of soluble vWF-biotin at its half-maximal binding value (30 nM) to immobilised GST-SpaEDABC in the presence unlabelled vWF, ranging from 30 nM to 2 µM, was measured. Bound biotinylated vWF was detected using peroxidase-conjugated streptavidin. Figure 3.10 shows dose-dependent and saturable inhibition to approximately 60 %, indicating a specific interaction between GST-SpaEDABC and vWF. In the reverse assay, binding of soluble GST-SpaEDABC-biotin to immobilised vWF was also specifically inhibited by up to 60 % using increasing concentrations (30 nM to 2 µM) of unlabelled GST-SpaEDABC. Unlabelled GST-Spa-C-term ranging from 30 nM to 2 µM did not inhibit vWF-binding by soluble GST-SpaEDABC (Fig. 3.11). These data taken together demonstrate that the interaction between Spa and vWF occurs with high affinity through the N-terminal EDABC domains of Spa and is specific. Notably, recombinant human vWF behaved in a similar fashion to plasma-derived protein used in previous studies.



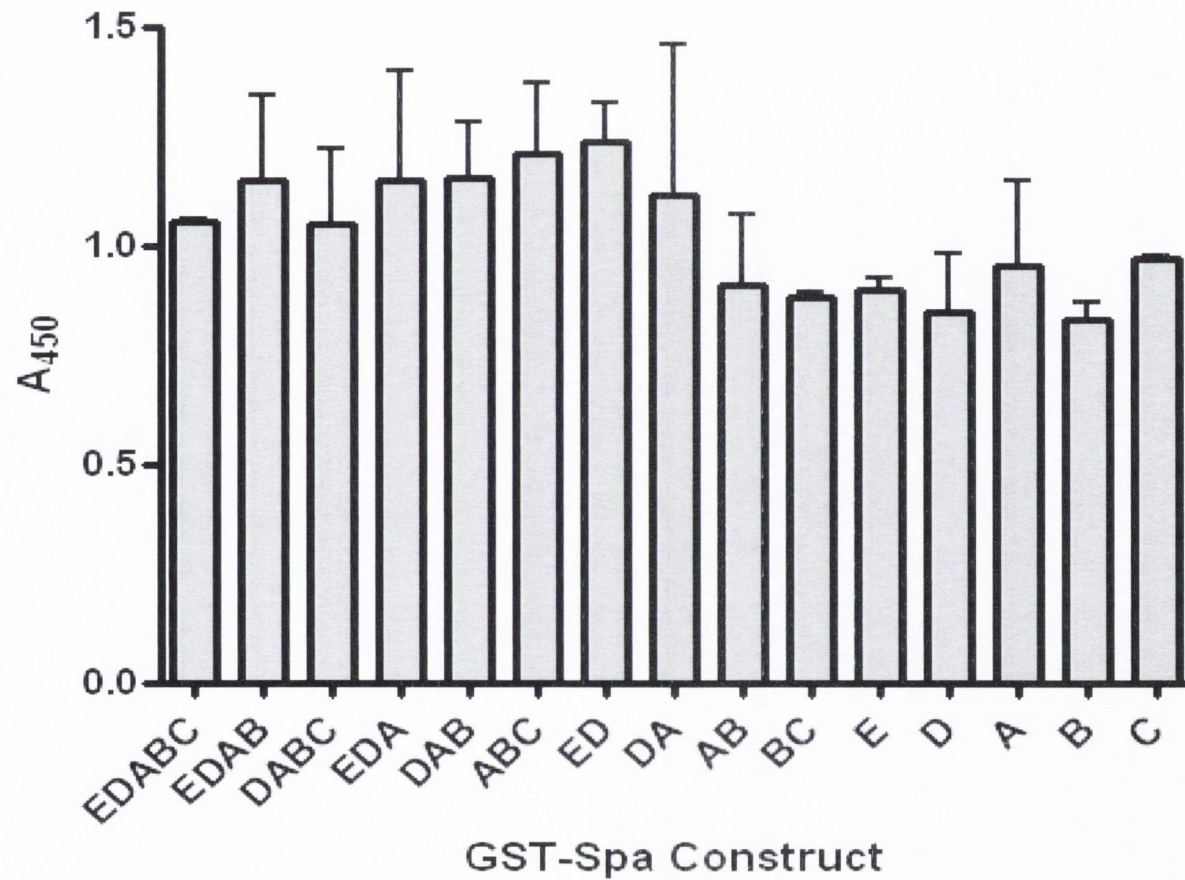


**Fig. 3.8 IgG binding by GST-Spa truncates.** 100  $\mu$ l of each GST-Spa construct (5  $\mu$ g/ml) was coated onto microtitre plates for 16 h and incubated with peroxidase-conjugated rabbit IgG and developed using a chromogenic substrate solution, described in 2.14.1. Absorbance at 450 nm was recorded using a plate-reader.

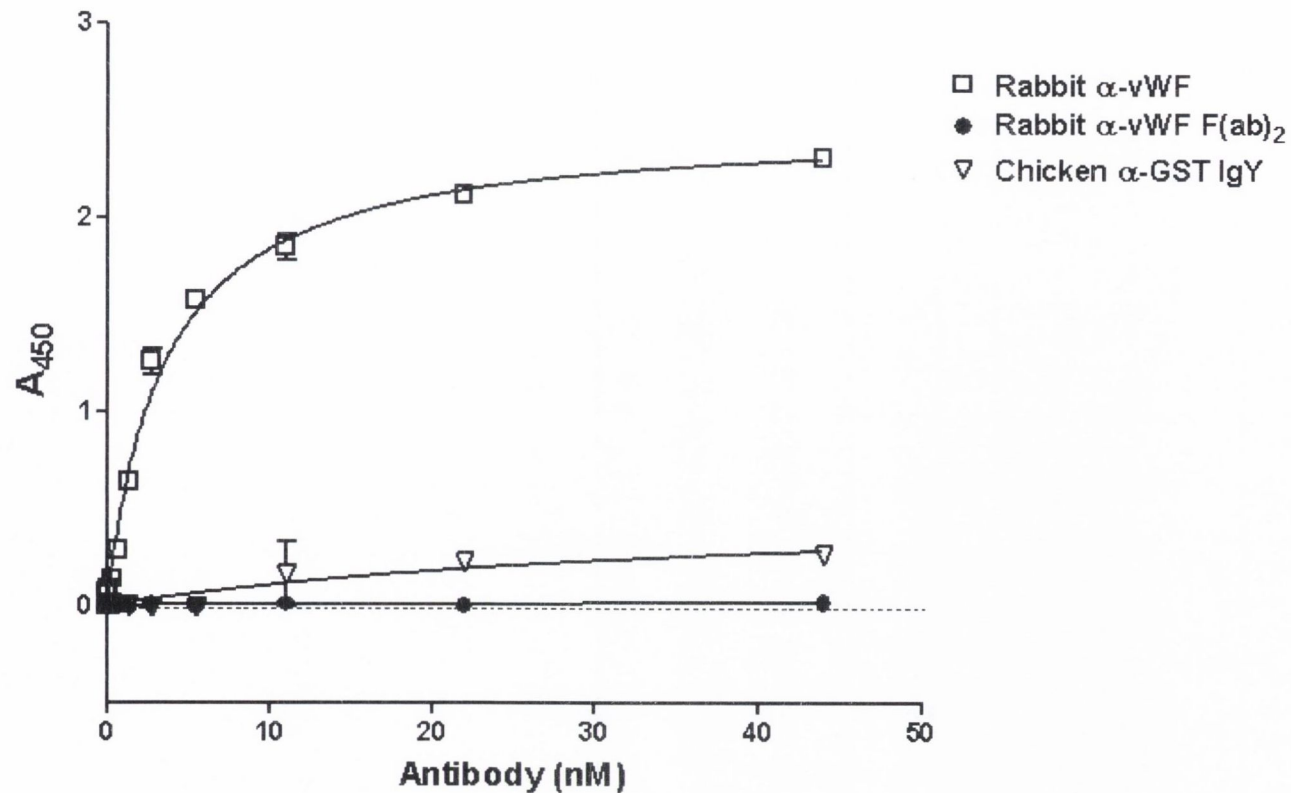


**Fig. 3.9 Interaction of GST-SpaEDABC with rabbit and chicken immunoglobulin.** 96-well plates coated with GST-SpaEDABC (10  $\mu$ g/ml) were incubated with increasing concentrations of peroxidase-conjugated rabbit anti-vWF, rabbit anti-vWF F(ab)<sub>2</sub> fragments, or chicken anti-GST. Bound antibody was detected directly by incubation with a chromogenic substrate solution (section 2.14.1). Experiments were performed in triplicate, data represents the mean  $\pm$  standard deviation of three independent experiments.

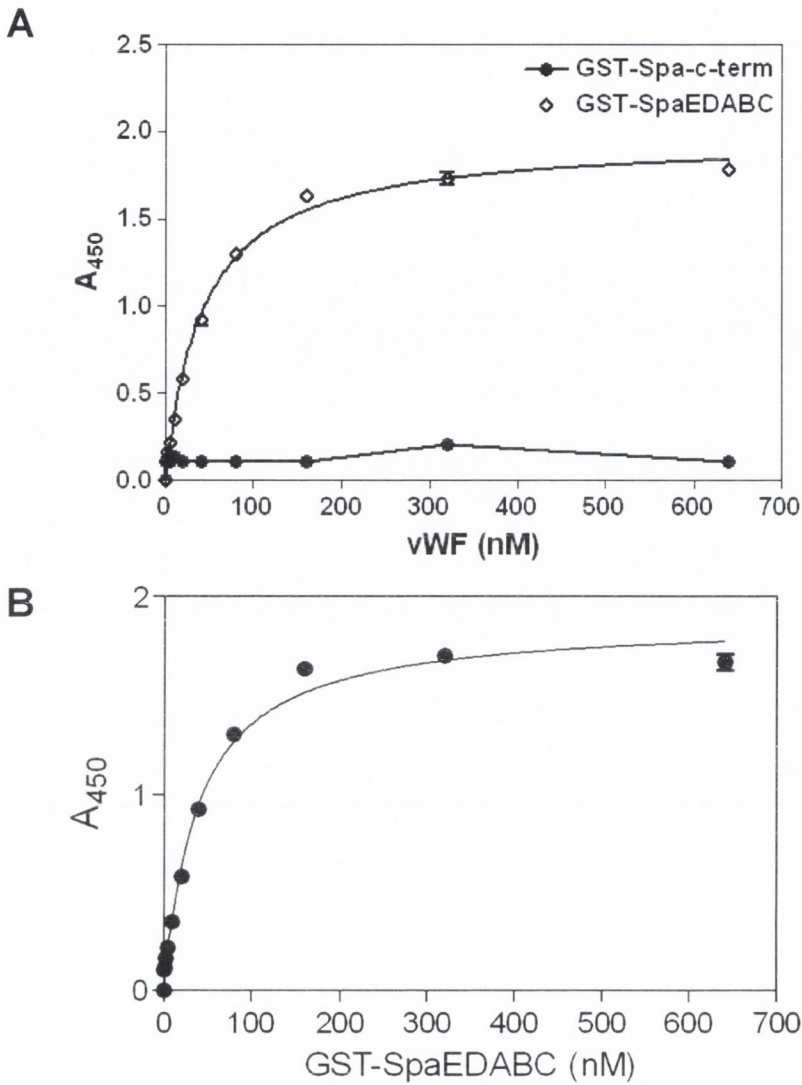


**Fig. 3.10. Interaction of full-length vWF with GST-SpaEDABC.** *A*, Microtitre plates were coated with GST-SpaEDABC (10  $\mu\text{g}/\text{mL}$ ) followed by incubation with serial dilutions of soluble vWF (640 nM to 625 pM). Bound vWF was detected using peroxidase-conjugated rabbit anti-vWF (Fab)<sub>2</sub> fragments and developed by incubation in a chromogenic substrate. *B*, Microtitre wells were coated with vWF (10  $\mu\text{g}/\text{mL}$ ) and incubated with serial dilutions of GST-SpaEDABC (open diamonds) or GST-Spa-c-term (filled circles) ranging from 640 nM to 625 pM. HRP-conjugated chicken anti-GST antibody was used to detect bound protein followed by development in chromogenic substrate as outlined in 2.14.1. Values are the means  $\pm$  standard deviation of triplicate wells. The experiment was performed three times in triplicate with similar results.



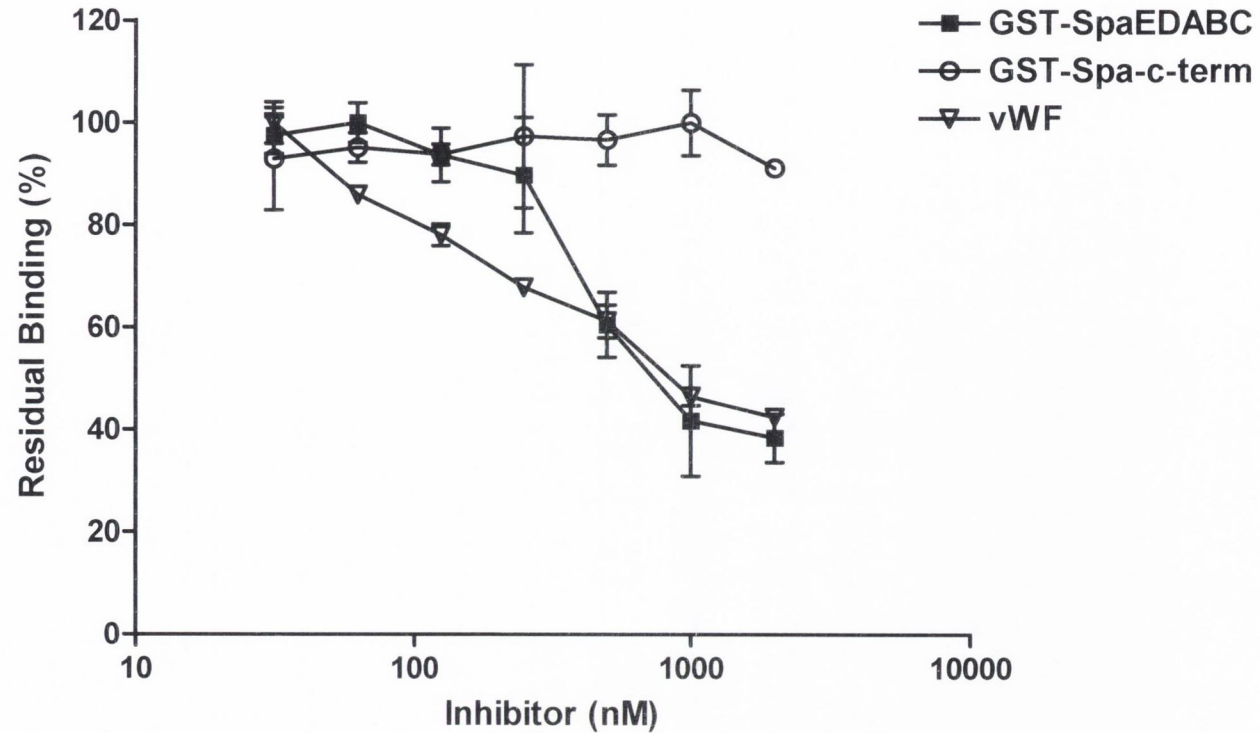


**Fig. 3.11 Inhibition of GST-SpaEDABC binding to vWF.** 96-well plates coated with GST-SpaEDABC (10  $\mu\text{g/ml}$ ) were incubated with biotinylated vWF at a concentration corresponding to its half maximal binding value to SpaEDABC (30 nM) and increasing concentrations of unlabelled vWF (30 nM to 2  $\mu\text{M}$ ) and residual binding measured (open triangles). In the reverse assay, immobilised vWF (10  $\mu\text{g/ml}$ ) was incubated with biotinylated GST-SpaEDABC (30 nM) and increasing concentrations of non-biotinylated GST-SpaEDABC from, 30 nM to 2  $\mu\text{M}$  (filled squares) or non-biotinylated GST-Spa-c-term (30 nM to 2  $\mu\text{M}$ , open circles). Experiments were performed in triplicate, data represents the mean  $\pm$  standard deviation of three independent experiments.

### 3.2.6 GST-SpaEDABC binds the vWF D'-D3 and A1-domains

In order to characterise the interaction of Spa with vWF and in particular to localise the binding domain(s) within the mammalian protein, the ability of GST-SpaEDABC to bind recombinant vWF domain truncates and deletions was investigated. The laboratory of Dr. Peter Lenting in the University Medical Centre, Utrecht, the Netherlands have constructed a number of vWF truncates and deletions, which are produced as recombinant hexahistidine-tagged proteins in baby hamster kidney (BHK) cells, *Pichia pastoris* or *E. coli*. The constructs focussed on the major ligand-binding regions of vWF and include the variant vWF-RGG, which contains a glycine substitution in the RGD motif, which is known to be the site on vWF responsible binding to the platelet glycoprotein,  $\alpha_{IIb}\beta_3$ . The vWF truncates and deletions used in this study are illustrated in Figure 3.12. vWF constructs were biotinylated and adjusted to approximately equal concentrations. Proteins were analysed by SDS-PAGE and stained using Coomassie blue or silver staining. The vWF proteins were analysed for binding by Western ligand affinity dot blotting with soluble GST-SpaEDABC. The results were somewhat unclear, but Figure 3.13 indicates an interaction between GST-SpaEDABC and full-length vWF, the RGG variant and truncates harbouring the vWF D'-D3 and A1 domains. The vWF A3 domain did not interact with Spa. These results were treated with caution, as the full-length vWF did not produce the expected strong reaction with GST-SpaEDABC. No significant reaction was seen with any of the A-domain deletions of vWF, including  $\Delta A3$ . It is possible that domain cause conformational changes in the binding region(s) on the vWF protein. The positive reaction observed for vWF D'-D3 and A1 containing truncates justified further analysis.

### 3.2.7 Interaction of GST-Spa truncates with vWF D'-D3 and A1

#### 3.2.7.1 Production of recombinant vWF A1 in *Escherichia coli*

To facilitate further studies on the interaction between protein A and vWF D'-D3 and A1 domains, it was desirable to produce large amounts of functional recombinant vWF protein in an efficient manner. This is not possible in the case of the D'-D3 domain, which was produced in BHK cells. However, the vWF A1 domain has been produced in *E. coli* by Dr. Jonas Emsley's group, and used successfully in functional studies (Cruz *et al.*, 2000; Emsley *et al.*, 1998). Indeed, structures of vWF A1 alone and in complex with its

platelet receptor, GpIb, were solved using *E. coli*-derived protein (Dumas *et al.*, 2004; Emsley *et al.*, 1998). Dr. Jonas Emsley of the University of Nottingham provided the expression vector, pQE30-vWF A1. Recombinant vWF A1 containing an N-terminal 6xHis tag was induced, refolded and purified as described (Cruz *et al.*, 1993; Emsley *et al.*, 1998). This procedure produced a high yield of soluble vWF A1 (approximately 1 mg/l).

The functionality of the recombinant vWF A1 was demonstrated by its ability to inhibit platelet aggregation, by competing for GpIb- $\alpha$  binding sites with native A1 domains in plasma vWF. This phenomenon has been demonstrated previously (Cruz *et al.*, 2000). Aggregation of platelets in platelet-rich plasma (PRP) can be initiated by the addition of ristocetin, which binds to the A1 domain of vWF and induces a conformational change. This causes vWF to bind platelets and thus, cause their activation and aggregation. This is known as ristocetin-induced platelet aggregation (RIPA). The percentage platelet aggregation was measured as the decrease in turbidity using an aggregometer, relative to the light transmission in a platelet-poor plasma (PPP) preparation. Pre-incubation of PRP with vWF A1 domain (2  $\mu$ M) is known to inhibit RIPA (Cruz *et al.*, 2000). The *E. coli*-produced vWF A1 used in this study inhibited RIPA at this concentration (Fig. 3.14), demonstrating its ability to compete with native vWF in whole blood for ristocetin. Platelet aggregation induced by the addition of ADP, which binds to receptor P2Y<sub>12</sub> on the platelet surface occurs independently of vWF and thus was not inhibited by addition of vWF (Fig. 3.14).

### 3.2.7.2 Interaction of GST-Spa truncates with vWF domains D'-D3 and A1

Solid-phase binding assays were performed to compare the avidity of Spa for the D'-D3 and A1 domains. Immobilised GST-SpaEDABC was incubated with increasing concentrations of vWF D'-D3 (11.7 nM to 1.5  $\mu$ M), A1 (9.375 nM to 1.2  $\mu$ M), and the A3 domain (9.375 nM to 1.2  $\mu$ M). Bound vWF was detected using a peroxidase-conjugated murine monoclonal anti 6xHis IgG1 antibody. Murine IgG1 contains a single substitution in the Fc region when compared to most mammalian IgG and has a markedly lower reactivity with Spa (Nagaoka and Akaike, 2003). Triplicate wells lacking vWF were included in each binding assay to normalise for background Spa-mouse IgG1 binding. Specific dose-dependent and saturable binding was seen for both vWF D'-D3 and A1 domains (Fig. 3.15). The half-maximal binding was calculated to be 250 nM and 100 nM for the D'-D3 and A1 domains, respectively. No interaction was observed when the vWF A3 domain was incubated with GST-SpaEDABC (Fig. 3.15). In addition, comparative



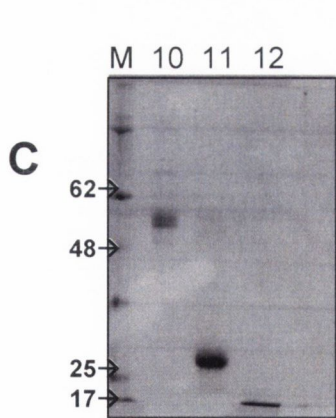
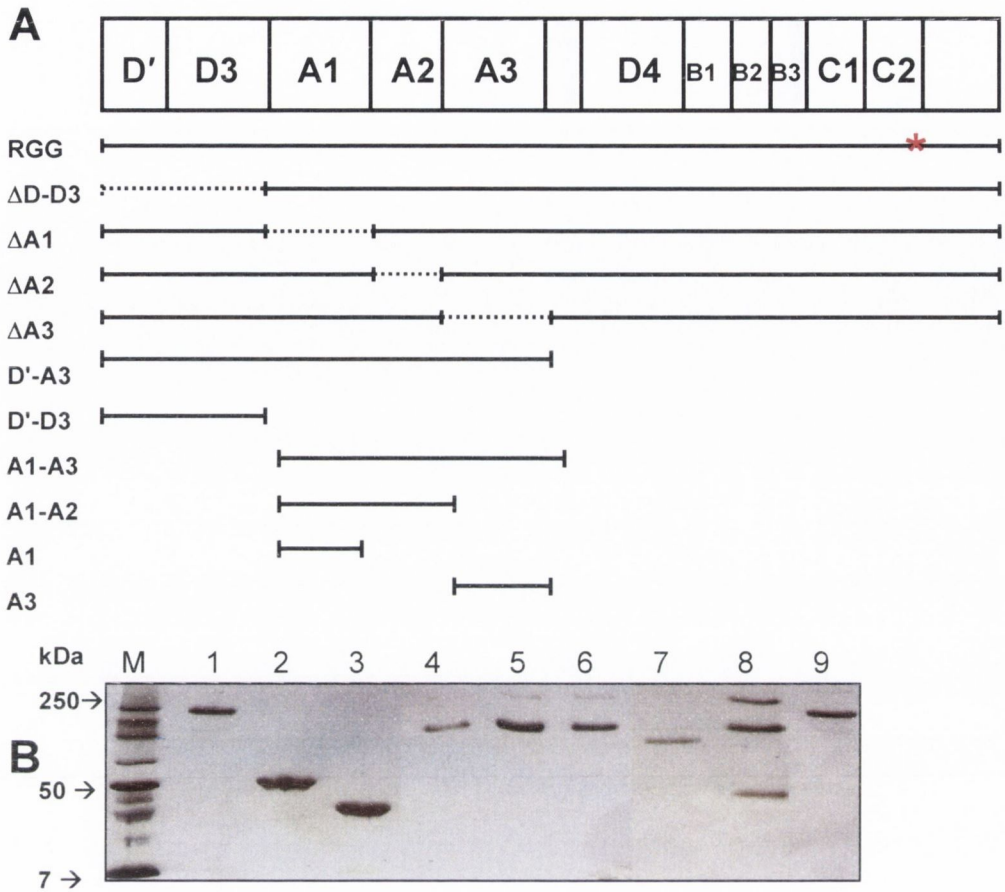


**Fig. 3.12 Recombinant vWF constructs.**

*A*, schematic figure of a vWF monomer and recombinant vWF constructs. vWF constructs used in this study are denoted by lines under the relevant region of the vWF monomer. Deleted regions are denoted by dotted lines. Variant RGG is indicated by a red asterisk. *B*, recombinant proteins were resolved by SDS-PAGE and silver-stained in the order; molecular weight marker (M) lane 1, full-length vWF (1) lane 2, A1-A3 lane 3, A1-A2 lane 4, ΔA1 lane 5, ΔA2 lane 6, ΔA3 lane 7, D'-A3 lane 8, ΔD'-D3 lane 9, variant RGG. *C*, Coomassie Blue-stained acylamide gel of vWF truncates in the order; molecular weight marker (M) lane 10, D'-D3 lane 11, A1 lane 12, A3.

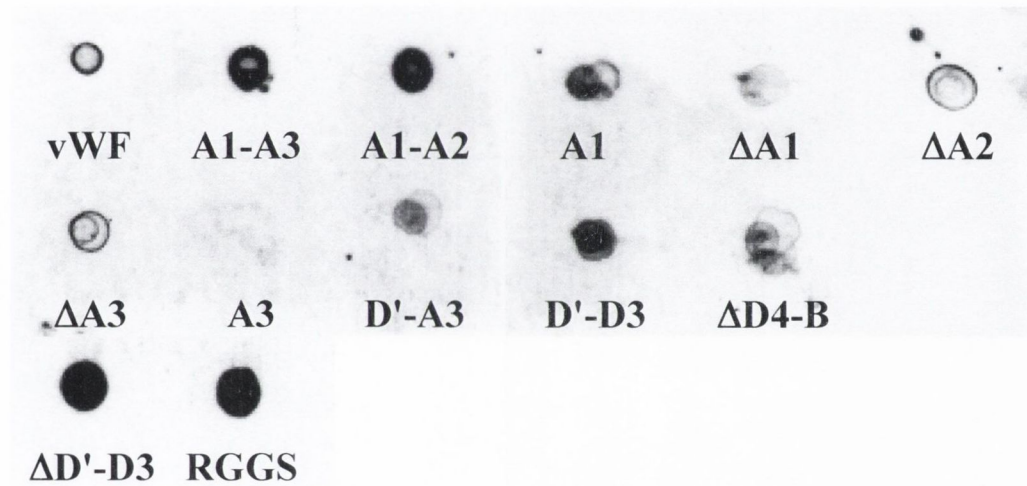


**Fig. 3.13. Interaction of SpaEDABC with recombinant vWF truncates.** Recombinant vWF truncates (1  $\mu$ g) were spotted on nitrocellulose and incubated with GST-SpaEDABC. Bound Spa was detected using chicken anti-Spa antibody.

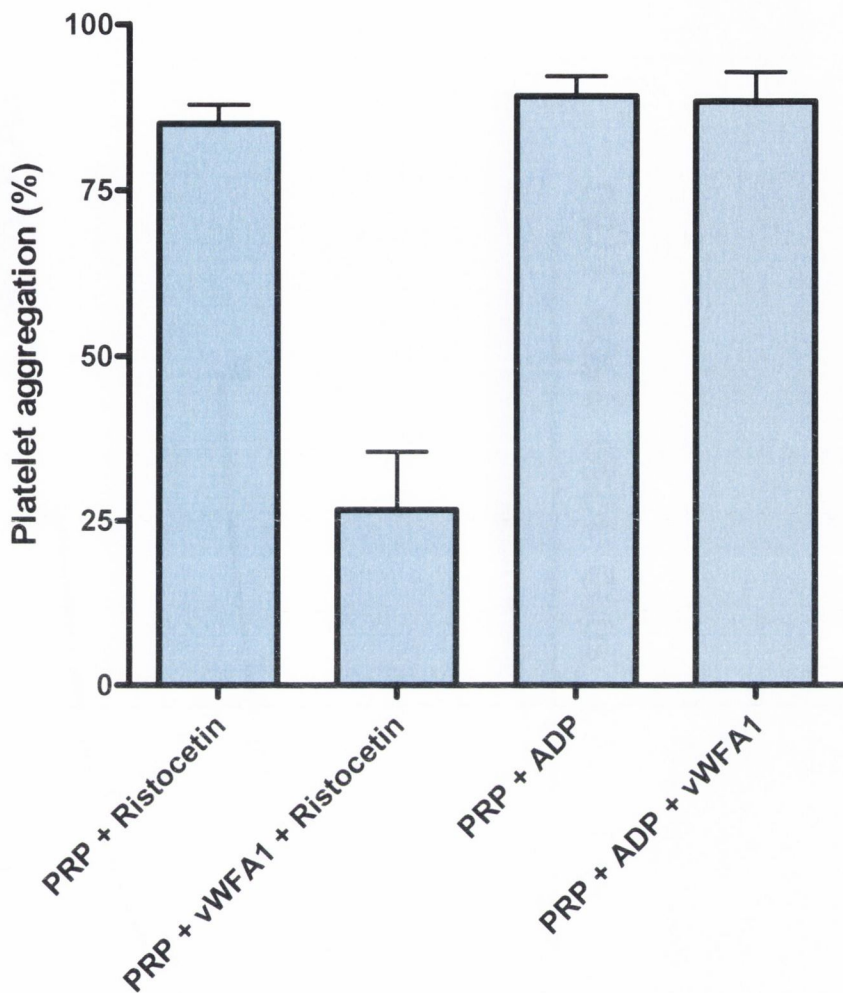


**Fig . 3.14. Inhibition of platelet aggregation by the vWF A1 domain.** Aggregation of platelet-rich plasma (PRP) was induced using the agonists ristocetin or ADP in the presence or absence of recombinant vWF A1 (2  $\mu$ M) and the percentage aggregation after 15 minutes was measured. Ristocetin binds to and activates vWF A1 domain, which, in turn binds platelets, causing their aggregation. ADP triggers platelet aggregation through the platelet receptor, P2Y<sub>12</sub>, independently of vWF.



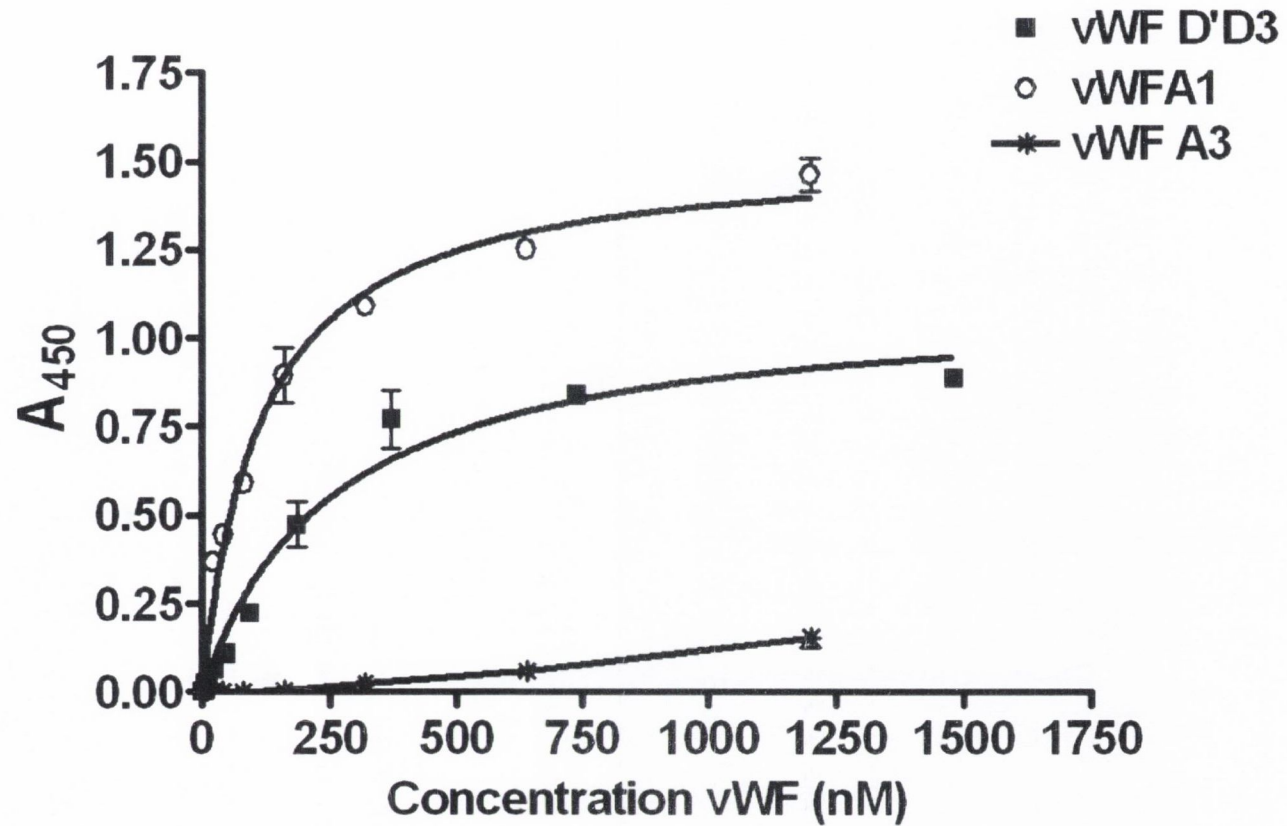


**Fig. 3.15 Interaction of GST-SpaEDABC with vWF D'-D3, A1 and A3.** Microtitre plates were coated with GST-SpaEDABC (10  $\mu\text{g}/\text{mL}$ ) and incubated with increasing concentrations of vWF D'D3, A1 or A3. Bound vWF constructs were detected with HRP-anti-His monoclonal antibody, using a chromogenic substrate as described in 2.14.1. Half-maximal binding for vWF A1 and D'-D3 truncates is at 100 nM and 250 nM, respectively. Values are the means  $\pm$  standard deviation of three separate experiments.

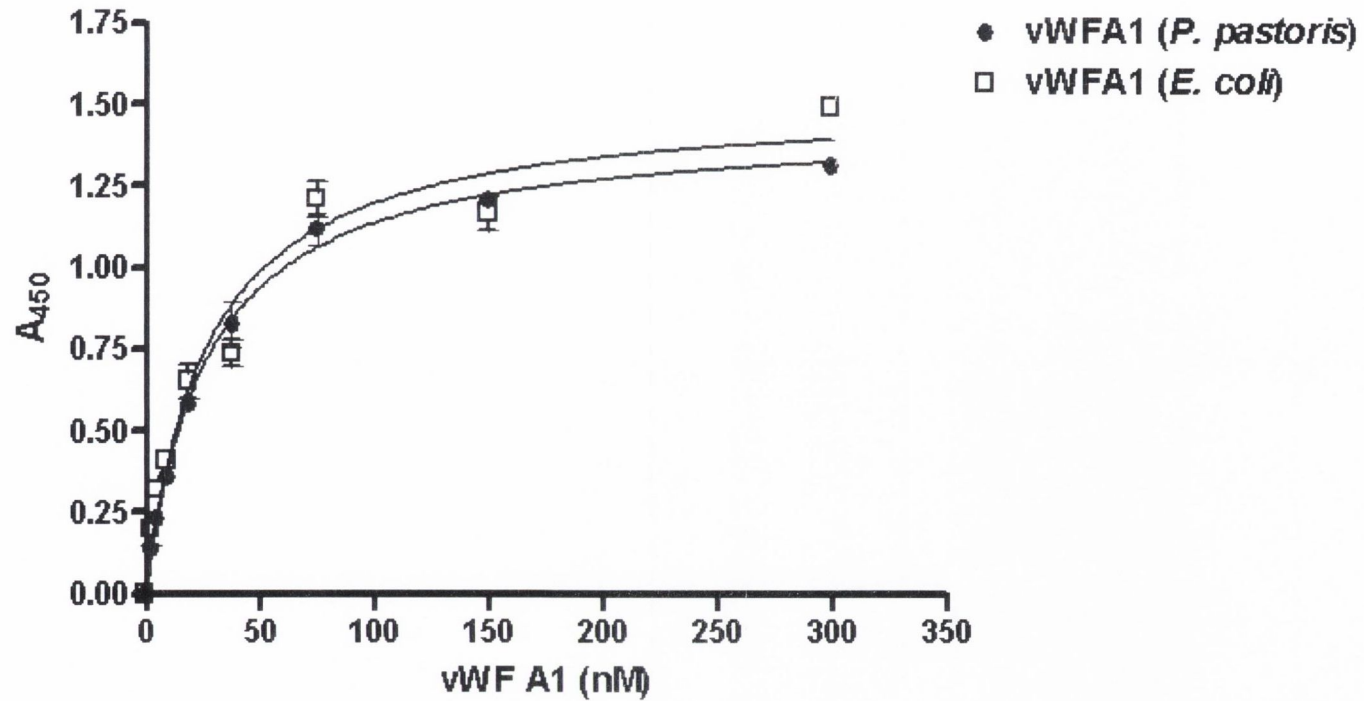


**Fig. 3.16 Comparative binding of *P. pastoris* and *E. coli*-produced rvWF A1 to GST-SpaEDABC.** Microtitre plates coated with GST-SpaEDABC (10  $\mu\text{g/ml}$ ) and were incubated with increasing concentrations of vWF A1 produced from either *P. pastoris* or *E. coli*. Bound vWF was detected using peroxidase-conjugated murine monoclonal anti-6xHis IgG1 and developed with chromogenic substrate as described (2.14.1). Experiments were performed in triplicate, data represents the mean  $\pm$  standard deviation of three independent experiments.

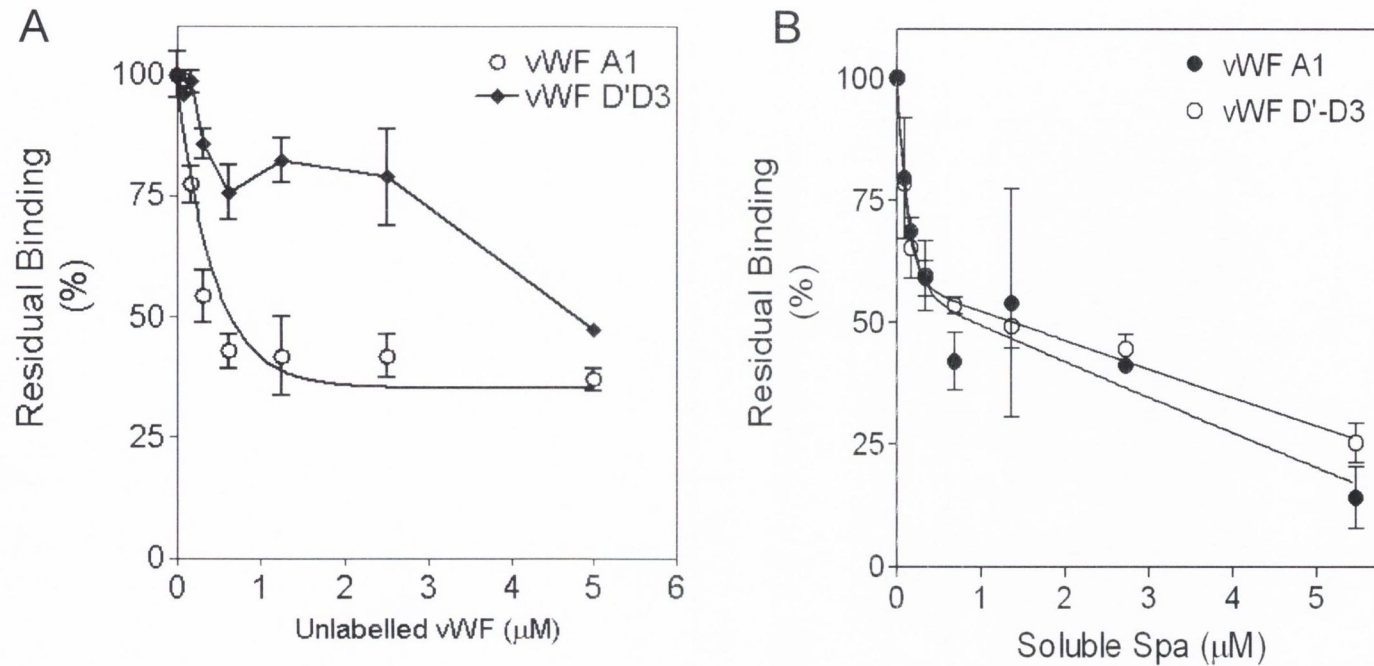


**Fig. 3.17. Inhibition studies using vWF A1 and D'-D3.** *A*, microtitre plates were coated overnight with GST-SpaEDABC (10  $\mu\text{g/ml}$ ) and incubated with biotinylated vWF A1 or D'D3 (100 nM or 250 nM, respectively) in the presence of increasing concentrations of the corresponding non-biotinylated truncate. *B*, soluble vWF A1 and D'-D3 (100 nM or 250 nM, respectively) were also tested for binding to immobilised GST-SpaEDABC in the presence of increasing concentrations of soluble GST-SpaEDABC. Percentage binding relative to vWF binding in the absence of competitor/inhibitor protein was calculated. Values represent the means  $\pm$  standard deviation of three separate experiments.



binding studies using *P. pastoris*- and *E. coli*-derived vWF A1 showed no significant difference in affinity for GST-SpaEDABC (Fig 3.16). This indicates that the interaction does not require glycosylation of the vWF A1 domain.

Inhibition assays were performed to study the specificity of binding. The ligand was used at the concentration corresponding to its half-maximal binding value as determined by solid-phase binding studies. Binding of biotinylated D'-D3 and A1 domains was inhibited by up to 70 % in a dose-dependent and saturable manner by incubation with increasing concentrations, ranging from 40 nM to 5  $\mu$ M, of the corresponding non-biotinylated vWF truncate (Figure 3.17 A). Soluble GST-SpaEDABC, at concentrations ranging from 42 nM to 5.4  $\mu$ M, inhibited binding of the soluble vWF truncates to immobilised Spa in a dose-dependent and saturable manner (Fig. 3.17 B). Taken together, these data indicate a specific protein: protein interaction.

As the vWF A1 domain binds to GST-SpaEDABC most avidly, this vWF truncate was used for binding studies with smaller GST-Spa truncates. All GST-Spa truncates of five-, four-, three-, two-, and one-domain were tested for binding to vWF A1. The GST-Spa constructs (250 ng) were subjected to SDS-PAGE and either stained with Coomassie Blue or used in a ligand affinity blot with vWF A1 (250 nM). GST alone was also included. Ligand blotting revealed that all domain combinations of Spa bound vWF A1, including single Spa domains, with the exception domain E (GST-SpaE) (Fig. 3.18). It is noteworthy that the E-domain is the most divergent protein A domain. Purified GST did not interact with vWF A1.

Binding of individual Spa domains to vWF A1 was also investigated by solid-phase binding assays. Each GST-Spa domain was immobilised on microtitre plates and tested for its ability to bind soluble vWF A1 ranging in concentration from 9.375 nM to 1.2  $\mu$ M. Soluble vWF A1 bound dose-dependently to saturation with similar affinity to all five Spa domains (Fig. 3.19 A). Half-maximal binding values estimated from the binding curves were each approximately 100 nM. Interestingly, GST-SpaE behaved in a similar fashion to the other GST-Spa constructs. The apparent lower affinity of the E domain for vWF A1 in ligand blotting could be explained by slower or improper renaturation of the protein after transfer from the SDS-PAGE gel to the PVDF membrane. To investigate this further, Western ligand affinity blotting was performed using increased amounts of GST-SpaE and GST-SpaD that were subjected to SDS-PAGE and either stained with Coomassie Blue or tested for binding vWF A1 (100 nM) by Western ligand affinity immunoblotting. Figure 3.19 B shows that proteins were of equal concentration while ligand affinity blotting with vWF A1 indicates that binding occurs when increased amounts of GST-SpaE were used,

but binding was approximately ten-fold lower than that observed for GST-SpaD (Fig. 3.19 C).

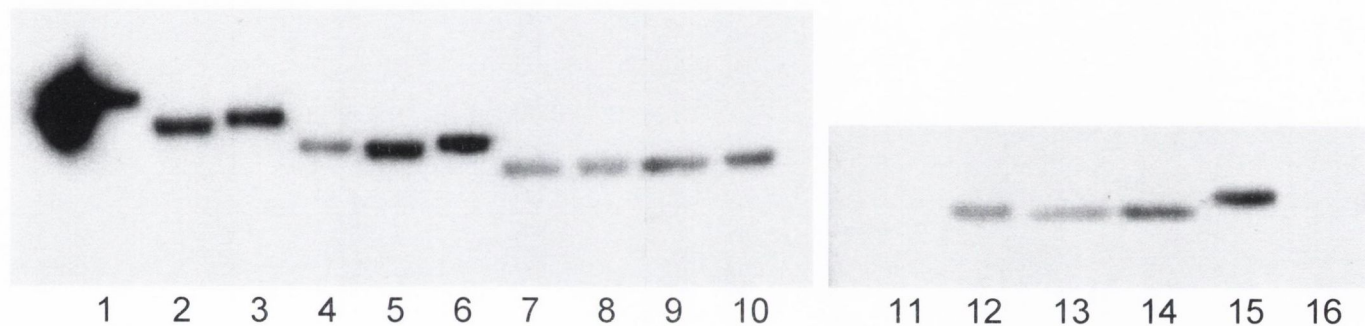


**Fig. 3.18. Interaction of GST-Spa truncates with vWF A1.** All GST-Spa truncates were transferred onto PVDF membranes and analysed by ligand affinity blotting for binding to biotinylated vWF A1 (200 nM) after a 3.5 h incubation. Bound vWF A1 was detected by incubation with peroxidase-conjugated streptavidin followed by development with chromogenic substrate as described in section 2.10.4. GST-Spa truncates were loaded in the order; lane 1 GST-EDABC lane 2, GST-EDAB lane 3, GST-DABC lane 4, GST-EDA lane 5, GST-DAB lane 6, GST-ABC lane 7, GST-ED lane 8, GST-DA lane 9, GST-AB lane 10, GST-BC lane 11, GST-E lane 12, GST-D lane 13, GST-A lane 14, GST-B lane 15, GST-C lane 16, GST.



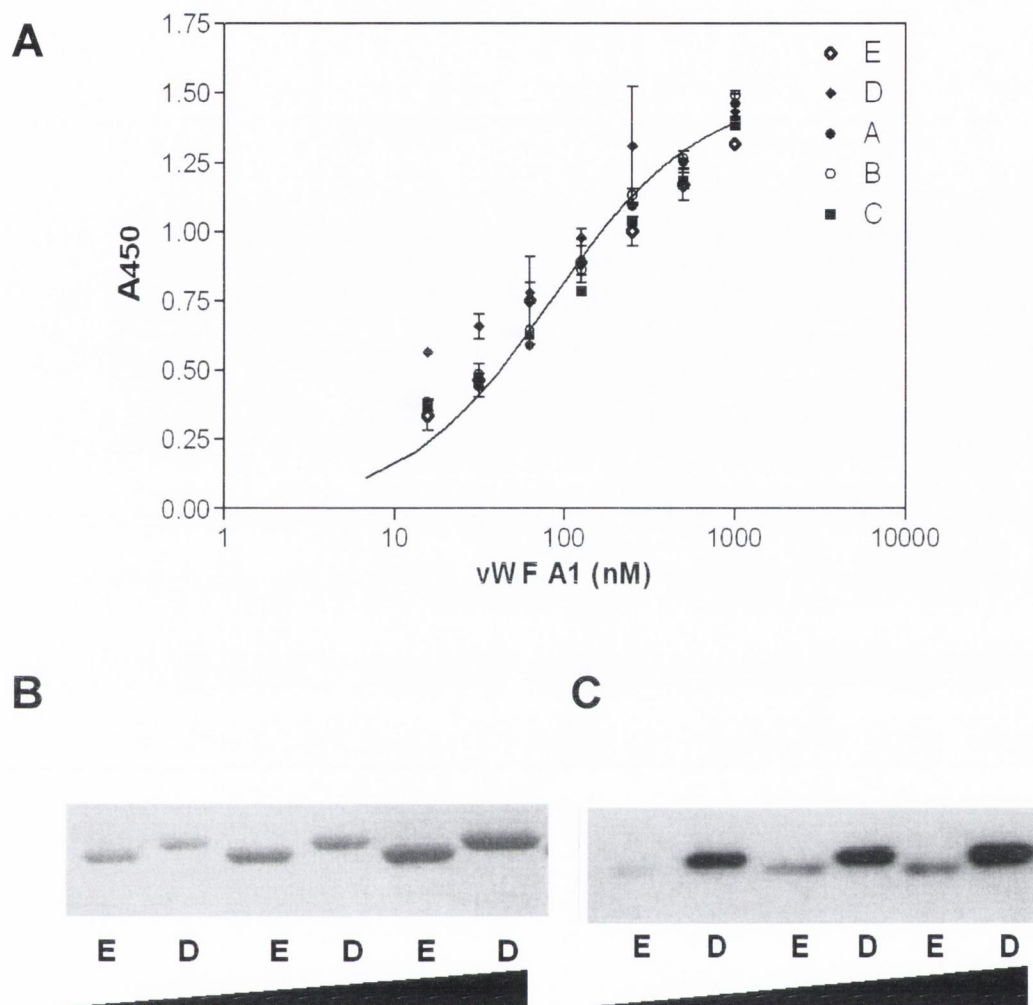


**Fig. 3.19. Interaction of single GST-Spa domains with vWF A1.** *A*, interaction of GST-SpaE, GST-SpaD, GST-SpaA, GST-SpaB and GST-SpaC domains with soluble vWF A1 as determined by ELISA-type assay. Values represent the mean of triplicate determinations. Binding curve represents average of all data values from GST-Spa truncates. Bottom, increasing concentrations of domains GST-SpaE and GST-SpaD (500 ng, 1  $\mu$ g, 2  $\mu$ g) were separated by SDS-PAGE and stained with Coomassie Blue (*B*) or assayed for vWF A1 binding by ligand affinity blotting (*C*). Experiments were performed three times.

### 3.3 Discussion

A number of surface proteins expressed on the surface of *S. aureus* are known to interact with plasma proteins that provide a bridge between the bacterium and circulating platelets. The interaction between *S. aureus* and human platelets is believed to be an important step in the development of infective endocarditis (Sullam *et al.*, 1996). Clumping factor A (ClfA) binds fibrinogen with high affinity as determined by surface plasmon resonance using a fragment of the A-domain, residues 221-550 ( $K_d$  of 0.51 +/- 0.19  $\mu$ M) (McDevitt *et al.*, 1997). Fibrinogen acts as a bridge between ClfA on the surface of *S. aureus* and the platelet integrin  $\alpha_{IIb}\beta_3$ . In addition, anti-ClfA antibodies are required to bind the platelet Fc receptor Fc $\gamma$ R<sub>IIa</sub> and trigger apoptosis (Loughman *et al.*, 2005). ClfA is expressed at high levels in stationary phase by *S. aureus* and is the dominant factor for *S. aureus*-induced platelet aggregation on cells in this growth phase. The fibronectin binding proteins (FnBPs), which are only expressed in exponential growth phase, can mediate platelet aggregation through fibrinogen or fibronectin bridges to  $\alpha_{IIb}\beta_3$ . Both FnBPA and FnBPB are capable of inducing platelet aggregation. Again, FnBP-specific IgG is required (Fitzgerald *et al.*, 2006). Several other *S. aureus* surface proteins (SraP, SdrE, ClfB) and secreted proteins ( $\alpha$ -toxin, Efb) can also promote binding or trigger activation by other mechanisms (discussed in section 1.9.2.1).

Protein A is postulated to induce platelet binding and activation by using vWF as a bridge to GpIb on resting platelets. However, studies characterising the roles for the FnBPs and ClfA suggest that these proteins are the major mechanisms of platelet aggregation by staphylococci in exponential and stationary growth phase, respectively. However, these studies were performed in solution at low shear rates, thereby excluding the role of vWF. Immobilised vWF can adhere to and activate platelets, as can soluble vWF, but only at high shear rates. Indeed, fluid-shear experiments by other groups have suggested a function for Spa in promoting bacterial adherence to platelets in whole blood under high shear rates in solution (5000  $s^{-1}$ ) such as those found in stenotic blood vessels (Pawar *et al.*, 2004). ClfA was demonstrated to be of importance in a low shear regime (100  $s^{-1}$ ). This is further supported by perfusion studies with *S. aureus* using vWF immobilised to a collagen surface in which Spa-expressing *S. aureus* were captured by the immobilised vWF, while isogenic *spa* mutants were not (Mascari and Ross, 2003). This was performed at low shear (100  $s^{-1}$ ). The requirement of Spa to be present on the *S. aureus* surface for bacterial adherence to vWF and platelets does not rule out a role for other surface proteins. To address whether protein A-expression alone is sufficient for this process, a surrogate



expression system in *Lactococcus lactis* was employed. This study demonstrated that expression of protein A on the surface of *L. lactis* in the absence of other surface proteins of *S. aureus* is sufficient to support bacterial adherence to immobilized vWF under low shear conditions ( $50 \text{ s}^{-1}$ ) representing normal venous shear rates (Fig. 3.1). This is in agreement with previous studies using *S. aureus* cells that indicated that Spa was necessary for efficient binding. Perfusion of whole blood at low shear rates over immobilized *S. aureus* leads to platelet capture and thrombus formation that was shown to be triggered by clumping factor A (Kerrigan *et al.*, unpublished data). It is more likely that Spa promotes bacterial binding to immobilized vWF, either bound directly to exposed sub-endothelial tissue or to platelets that had been previously captured. This raises the possibility that vWF contributes to the recruitment of Spa-expressing bacteria into vWF-rich platelet thrombi.

Since the Spa-vWF interaction was first reported (Hartleib *et al.*, 2000), there has been no further characterisation of the nature of this interaction. This study set out to determine the region(s) on vWF involved in Spa-binding and the site on Spa that interacts with vWF. Firstly, the interaction was confirmed using recombinant Spa and vWF. This was necessary as the original study used a plasma-derived vWF preparation, which may have contained immunoglobulin. While it was clearly demonstrated that an interaction occurred, the affinity of Spa for vWF, as estimated by surface plasmon resonance (SPR), may be inaccurate. Solid-phase binding studies demonstrated dose-dependent, saturable binding of soluble vWF to immobilised Spa, and soluble Spa to immobilised vWF. The estimated half-maximal binding values were similar in both cases (30 nM), and in close agreement with the  $K_d$  value determined previously by SPR (15 nM (Hartleib *et al.*, 2000)) (Fig. 3.10). This demonstrates that i) the plasma-purified vWF used by others was of high purity and ii) the Ig-binding repeat region of protein A contains the binding site for vWF.

To identify the region within vWF responsible for binding Spa, a number of recombinant vWF truncates and domain deletions were employed in solid-phase binding studies with GST-SpaEDABC. The following vWF truncates and deletions were used, representative of the major ligand-binding domains of vWF; D'-D3, A1, A1-A2, A1-A3, A3, D'-A3,  $\Delta$ D'-D3,  $\Delta$ A1,  $\Delta$ A2,  $\Delta$ A3,  $\Delta$ D4-B and a variant of vWF lacking the integrin-binding RGD motif, named vWF-RGG. This study identified two binding regions on vWF, domains D'-D3 and A1 (Fig. 3.15). The specificity of the interactions was demonstrated by the ability of soluble GST-SpaEDABC to compete for binding to immobilised Spa (Fig. 3.17). The D'-D3 region of vWF is involved in binding and stabilising blood coagulation Factor VIII (Foster *et al.*, 1987; Takahashi *et al.*, 1987). The A1 domain contains the binding site for the platelet receptor GpIb- $\alpha$  and for collagen (Fujimura *et al.*, 1987;



Mazzucato *et al.*, 1999). Spa binds to the D'-D3 and A1 domains with estimated half-maximal binding values of 250 and 100 nM, respectively, estimated from solid-phase binding assays. vWF binds coagulation factor VIII through the D'-D3 region with dissociation constants of 200-400 pM. However, it is estimated that only 2 % of available vWF sites bind to Factor VIII (Vlot *et al.*, 1995; Vlot *et al.*, 1996). Therefore, it is possible that D'-D3 provides a more available, lower affinity site for Spa on vWF. The availability of binding sites on vWF is probably also limited by its globular shape, particularly under conditions of low shear. The vWF A3 domain and the C-terminal RGD motif were not involved in binding Spa (Figs. 3.13 and 3.15).

The vWF domains D'-D3 and A1 were used to characterise the vWF-binding region on Spa. Solid-phase binding studies require relatively large amounts of protein when compared to more sensitive techniques such as SPR. Therefore, vWF A1 was produced in *E. coli* to increase protein yield. vWF A1 is produced by *E. coli* in inclusion bodies and must be solubilised with guanidine hydrochloride. Functionality was confirmed by the ability of recombinant vWF A1 to inhibit ristocetin-induced platelet aggregation when 2  $\mu$ M vWF A1 is mixed with PRP (Fig. 3.14). The vWF D'-D3 domain was produced in BHK cells.

Recombinant Spa domain constructs were generated by PCR using the smallest possible *spa* template, to reduce the possibility of amplification of the wrong repeat. This was achieved by restriction digestion of the template in naturally occurring single sites prior to PCR amplification. This technique was successful in generating all possible domain truncates of Spa. The vWF A1 domain was tested for binding to recombinant five-, four-, three-, two- and single-domain Spa constructs by Western ligand affinity blot. All multiple Spa domain constructs showed similar binding to vWF A1. Indeed, with the exception of Spa-E, the most divergent domain, binding to vWF A1 was detected for each individual domain. However, an interaction was observed when increased amounts of Spa E were used (Fig. 3.19). When single Spa domains were tested for binding to vWF A1 by solid phase binding, individual domains bound with equal affinity (Fig. 3.19), suggesting that the reduced vWF binding observed may be due to the reported lower stability of domain E under denaturation-refolding conditions. Solid-phase binding studies also demonstrated that each Spa domain also bound vWF D'-D3. Single Spa domains bound vWF A1 and D'-D3 with estimated half-maximal binding values of 100 nM and 250 nM. This is comparable to the affinity seen for the five-domain Spa construct, GST-SpaEDABC. Although each Spa repeat can bind vWF, there may still be a 1:1 stoichiometry when all five domains are present. Single Spa domains have a lower affinity

for IgG when compared with multiple Spa repeats. Each Spa domain can bind IgG. However, full-length Spa, which contains five binding sites, is thought to interact with a maximum of two IgG molecules (Jendeberg *et al.*, 1997; Yang *et al.*, 2003).

In conclusion, a direct role for Spa in adherence to surfaces through its interaction with vWF under flow was demonstrated. Spa binds to at least two regions of vWF, D'-D3 and A1, and does not bind to the A3 domain or the C-terminal RGD sequence.

## **Chapter 4**

### **Mapping the Protein A-von Willebrand Factor Binding Site**



## 4.1 Introduction

It has been previously shown that individual domains of protein A bind the Fc $\gamma$  region of most mammalian IgGs and the Fab region of Ig bearing heavy chains of the V<sub>H3</sub>-subgroup (Inganas *et al.*, 1981; Jansson *et al.*, 1998). Structural studies on single protein A domains revealed three short  $\alpha$ -helices (~ 10 aa) connected by five-residue loops. Each  $\alpha$ -helix is orientated anti-parallel to the next and the structure is stabilised by a core of hydrophobic residues (Deisenhofer, 1981). This three-helix bundle structure gives the Spa domains three 'faces' lying between helices 1-2, 2-3 and 3-1, as illustrated in Figure 4.1. The complex formed between the B domain of Spa and a human Fc $\gamma$  antibody fragment has been solved. The binding surface on Spa lies between helices 1 and 2 and binding is mainly made up of hydrophobic interactions (Deisenhofer, 1981). The key contacts involved were confirmed by mutational analysis of SpaB (Cedergren *et al.*, 1993). The co-crystal structure of SpaD in complex with a human V<sub>H3</sub>-Fab fragment revealed a different binding interface on Spa, involving residues on helices 2 and 3. This interaction is made up of polar contacts (Graille *et al.*, 2000). In both cases binding is avid, with K<sub>d</sub> values in the low nanomolar range (Jendeberg *et al.*, 1995; Sasano *et al.*, 1993).

Previous work suggested that a single Spa domain can bind Fc $\gamma$  and V<sub>H3</sub>-Fab simultaneously; single Spa domains that were captured on IgG-coupled sepharose were still capable of depleting V<sub>H3</sub>-Fab from solution (Starovasnik *et al.*, 1999), and 'sandwich' ELISAs in which microtitre plates coated with purified Fc $\gamma$  fragments were used to capture Spa domains which could in turn capture V<sub>H3</sub>-Fab (Roben *et al.*, 1995). Alignment of the co-complexes of single Spa domains with Fc $\gamma$  and V<sub>H3</sub>-Fab revealed that there is no steric hindrance of a dual interaction by a single protein A domain (Figure 1.11).

Residues on Spa involved in binding Fc $\gamma$  and V<sub>H3</sub>-Fab are conserved in all five Spa domains (Graille *et al.*, 2000). Since all individual Spa domains can bind vWF (section 3.2.7.2), it is possible that the vWF-binding site on Spa overlaps the binding site for Fc $\gamma$  or V<sub>H3</sub>-Fab. It may be the case that a single Spa domain can bind both to vWF and an antibody fragment simultaneously. Inhibition studies could localise the binding region on Spa to one face of the three-helix bundle. Ligands of vWF A1 domain whose binding sites are known would also provide useful information about the Spa binding site on vWF A1. A co-crystal of a protein A domain in complex with vWF A1 would identify the binding interface between Spa and vWF A1. Crystal structures have been solved for Spa and vWF A1, indicating that correct conditions for crystallisation are known for both proteins. The vWF-binding site on Spa could also be mapped by substitution of residues that are

conserved in all five Spa domains. Structural data demonstrated how correct folding of Spa is necessary for binding to Fc $\gamma$  and V<sub>H</sub>3-Fab.

The role of protein A in *S. aureus*-induced platelet aggregation is still unclear. There is increasing data to support a role for the protein A-vWF interaction in bridging staphylococci and platelets (George *et al.*, 2006; Pawar *et al.*, 2004). von Willebrand Factor can form a bridge between *S. aureus* cells and collagen exposed in the basal lamina of damaged blood vessels (Mascari and Ross, 2003). Binding to the vascular endothelium presumably facilitates persistence and colonisation by *S. aureus*. Adherence to the endothelium by surface proteins possibly including Spa is also an important prerequisite for transmigration through the endothelial barrier. The bridging of *S. aureus* to platelets through vWF may allow *S. aureus* to bind to platelets under conditions of high shear in the bloodstream when the bridge to *S. aureus* surface proteins ClfA, FnBPA and FnBPB cannot form. This is supported by the observation that *S. aureus*-platelet interactions under high shear require vWF and expression of Spa on the bacterial surface (Pawar *et al.*, 2004). However, studies have focussed on bacterial adherence and not subsequent activation and aggregation of the bound platelets. The role of the Spa-vWF interaction in platelet aggregation is studied in this chapter.

In addition to vWF, protein A has recently been shown to bind the receptor for tumour necrosis factor- $\alpha$ , TNFR1 (Gomez *et al.*, 2004). This interaction promotes inflammation in the airway epithelium and contributes to the pathogenesis of pneumonia caused by *S. aureus*. This chapter describes the isolation of truncates of Spa and mutants of a single domain of Spa that were used to map the binding site for Spa on the A1 domain of vWF and TNFR1.



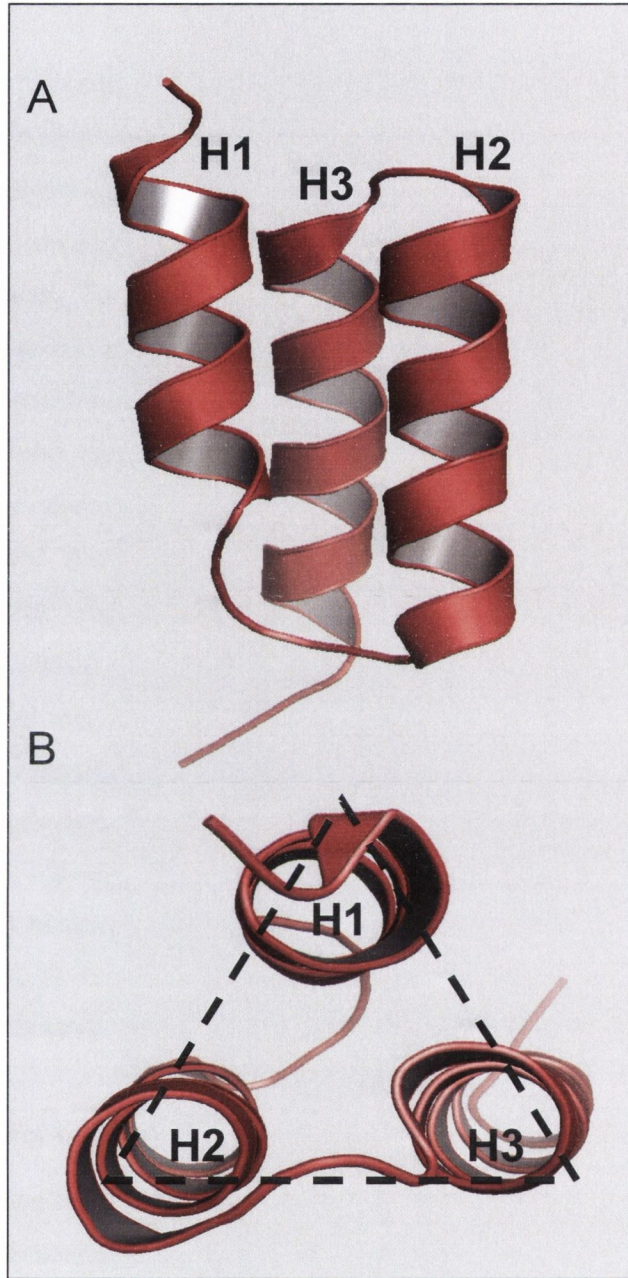


**Fig. 4.1 Architecture of a Spa domain.** Ribbon representation of a single Spa domain viewed (A) from the side or (B) above from the crystal structure of SpaD (1DEE). Each domain is made up of three anti-parallel  $\alpha$ -helices (H1, H2, H3) packed in a three-helix bundle. This structure provides Spa domains with three 'faces' available for ligand binding at the interface of each pair of helices.



## 4.2 Results

### 4.2.1 The binding site on protein A for von Willebrand factor

#### 4.2.1.1 The protein A-vWF interaction is blocked by IgG and V<sub>H</sub>3-IgM

Protein A binds vWF in the presence of physiological concentrations of IgG although some inhibition of the interaction mediated by IgG was reported (Hartleib *et al.*, 2000). This suggests a possible shared binding region on Spa between the Fc $\gamma$  region of IgG and vWF. However, this study used a pooled human IgG that could have contained anti-Spa antibodies. To investigate whether Fc and vWF compete for a shared binding region on Spa, rabbit IgG was tested for inhibition of vWF A1 binding to a single Spa domain (GST-SpaD). IgM bearing V<sub>H</sub>3 heavy chains were also tested. A V<sub>H</sub>4-bearing IgM that does not bind Spa was included as a control. Binding to Fc $\gamma$  and V<sub>H</sub>3-derived immunoglobulin occurs through distinct binding regions on Spa and is non-competitive, as was demonstrated from the structures of complexes and by sandwich ELISA assays (Roben *et al.*, 1995). Microtitre plates were coated with GST-SpaD (10  $\mu$ g/ml) and were tested for their ability to bind vWF A1 (100 nM) in the presence of concentrations of inhibitor proteins ranging from 40  $\mu$ g/ml to 312.5 ng/ml. Figure 4.2 shows that dose-dependent and saturable inhibition to approximately 95 % occurred with either IgG or V<sub>H</sub>3-IgM. The IgM-bearing heavy chains of the V<sub>H</sub>4 subgroup did not inhibit the Spa-vWF interaction. This indicates that when Spa is in complex with IgG or V<sub>H</sub>3-IgM, the binding site for vWF A1 binding is not available. However, it is possible that inhibition in either or both cases is due to steric blocking of the vWF A1 binding site and is not due to a direct competition for contact residues on Spa.

#### 4.2.1.2 Fc $\gamma$ but not V<sub>H</sub>3-Fab specifically blocks protein A-vWF binding

The inhibition of the Spa-vWF interaction by both IgG and V<sub>H</sub>3-IgM is either due to a shared vWF-binding region on Spa for both ligands or because the large Ig molecules (150 kDa and 800 kDa, respectively) sterically block vWF A1 binding when in complex with Spa. To address this, human IgG Fc $\gamma$  fragments and a recombinant human V<sub>H</sub>3 heavy chain fragment were used in inhibition studies with vWF A1. The V<sub>H</sub>3-Fab was expressed in *E. coli* from the IPTG-inducible expression vector pCOMB3:JMSpA3-08 as described in section 2.11.2.4. Soluble Fab heavy and light chains are produced under the control of separate *lacZ* promoters and are directed to the periplasmic space for functional assembly of heavy and light chains by the N-terminal fusion of *pelB* leader sequences. The V<sub>H</sub>3-Fab

expressing phagemid has a pBluescript plasmid backbone. pCOMB3:JMSpA3-08 is illustrated in Figure 4.3. Recombinant V<sub>H3</sub>-Fab fragments were isolated from bacterial lysates by affinity chromatography using protein A-sepharose. The V<sub>H3</sub>-Fab heavy and light chain fragments resolved as bands of 22 kDa and 25 kDa when subjected to SDS-PAGE and stained using Coomassie Blue (Fig. 4.4), in agreement with a previous study (Sasano *et al.*, 1993). However the 25 kDa fragment was less evident by Coomassie Blue staining. In order to confirm that both human Fc $\gamma$  and V<sub>H3</sub>-Fab fragments bind GST-SpaD, solid-phase binding assays were performed. Fc $\gamma$  or V<sub>H3</sub>-Fab (10  $\mu$ g/ml) were immobilised on microtitre plates and incubated with serial dilutions of GST-SpaD (1.2  $\mu$ M to 4.7 nM). Bound GST-SpaD was detected by incubation with peroxidase-conjugated chicken anti-GST antibody followed by a chromogenic substrate as described in section 2.14. GST-SpaD bound dose-dependently and saturably to both immunoglobulin fragments with half-maximal binding estimated at 20 nM (Fc $\gamma$ ) and 75 nM (V<sub>H3</sub>-Fab) of ligand. These data indicate a specific high affinity interaction between GST-SpaD and the immunoglobulin fragments (Fig. 4.5). The lower affinity interaction between Spa and V<sub>H3</sub>-Fab could be attributed to a low yield of the 25 kDa Fab fragment (Fig. 4.4).

Inhibition studies were performed using the immunoglobulin fragments. Mixtures of vWF A1 (200 nM) and increasing concentrations of Fc $\gamma$  or V<sub>H3</sub>-Fab (2.3  $\mu$ g/ml to 150  $\mu$ g/ml) were incubated with immobilised GST-SpaD (10  $\mu$ g/ml) on microtitre plates. Bound vWF was detected using a peroxidase-conjugated murine monoclonal anti-6xHis IgG1 antibody. This revealed that the Fc $\gamma$  fragment blocked vWF A1 binding in a dose-dependent and saturable manner while the V<sub>H3</sub> fragment did not, suggesting that vWF A1 binds to a region on Spa overlapping the binding site for the Fc fragment of IgG (Figure 4.6).

#### **4.2.2 Variants of the D domain of Spa**

Inhibition studies using the protein A ligands Fc $\gamma$  and V<sub>H3</sub>-Fab suggest that the vWF A1-binding site on Spa overlaps the Fc $\gamma$ -binding site, but not that of V<sub>H3</sub>-Fab. To investigate this further and to identify the specific residues on Spa involved in binding vWF A1, GST-SpaD variants bearing substitutions in residues known to be involved in Fc $\gamma$  or V<sub>H3</sub>-Fab binding were generated. The D domain of Spa was chosen for mutagenesis because its crystal structure has been solved (Graille *et al.*, 2000). SpaD is the largest Spa domain (61 aa) due to three additional residues (alanine-glutamine-glutamine), at its N-

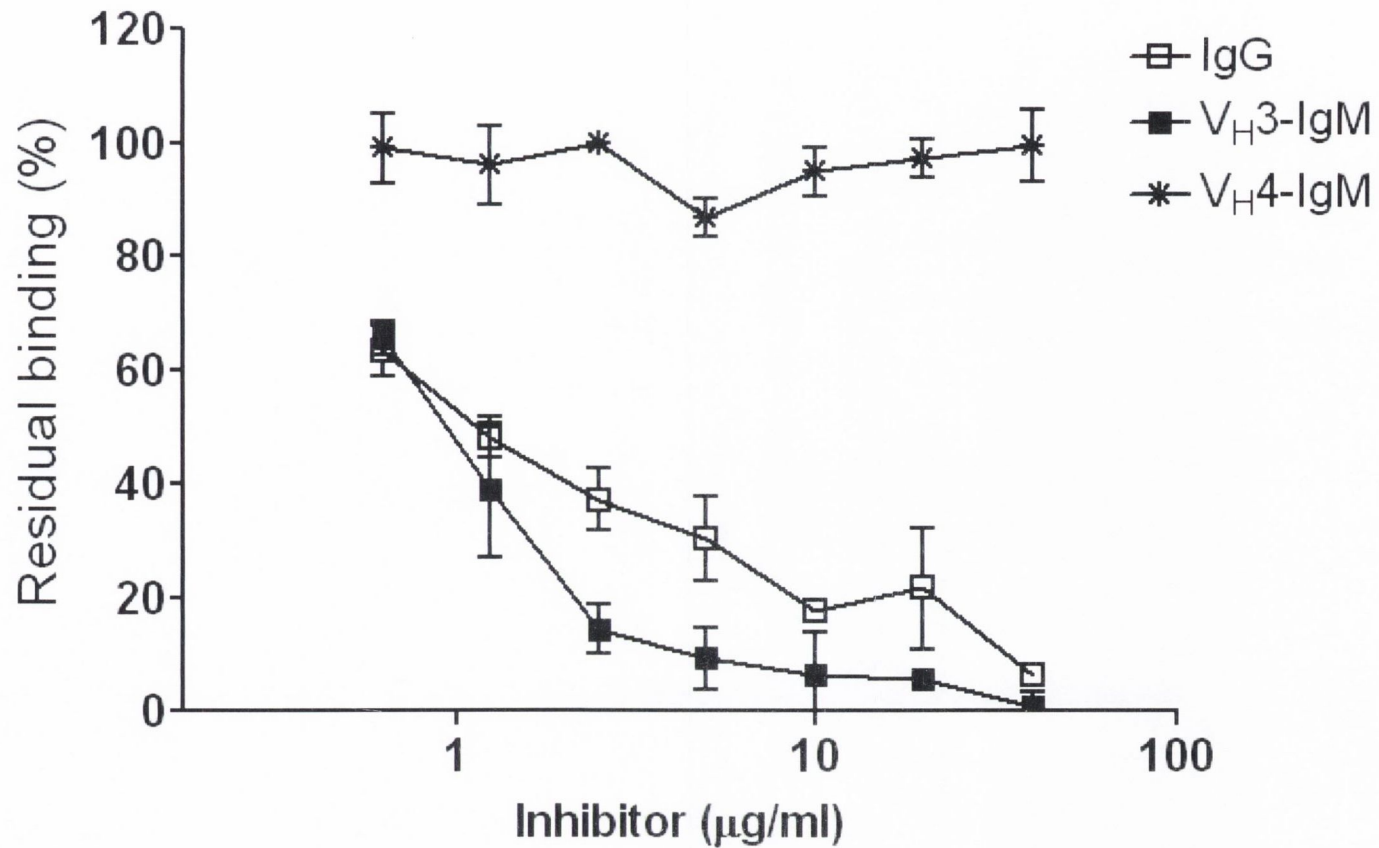


**Fig. 4.2. Inhibition of Spa binding to vWF A1 by IgG and IgM.** 96-well plates were coated with GST-SpaD (10 µg/mL) and were incubated with a mixture of vWF A1 (100 nM) and various concentrations of rabbit IgG or IgM bearing V<sub>H</sub>3-chains. V<sub>H</sub>4-bearing IgM which does not bind Spa, was also included. Bound vWF was monitored using a HRP-conjugated anti-Hisx6 antibody. The percentage inhibition was calculated relative to vWF bound in the absence of inhibitor. The experiment was performed three times with similar results.



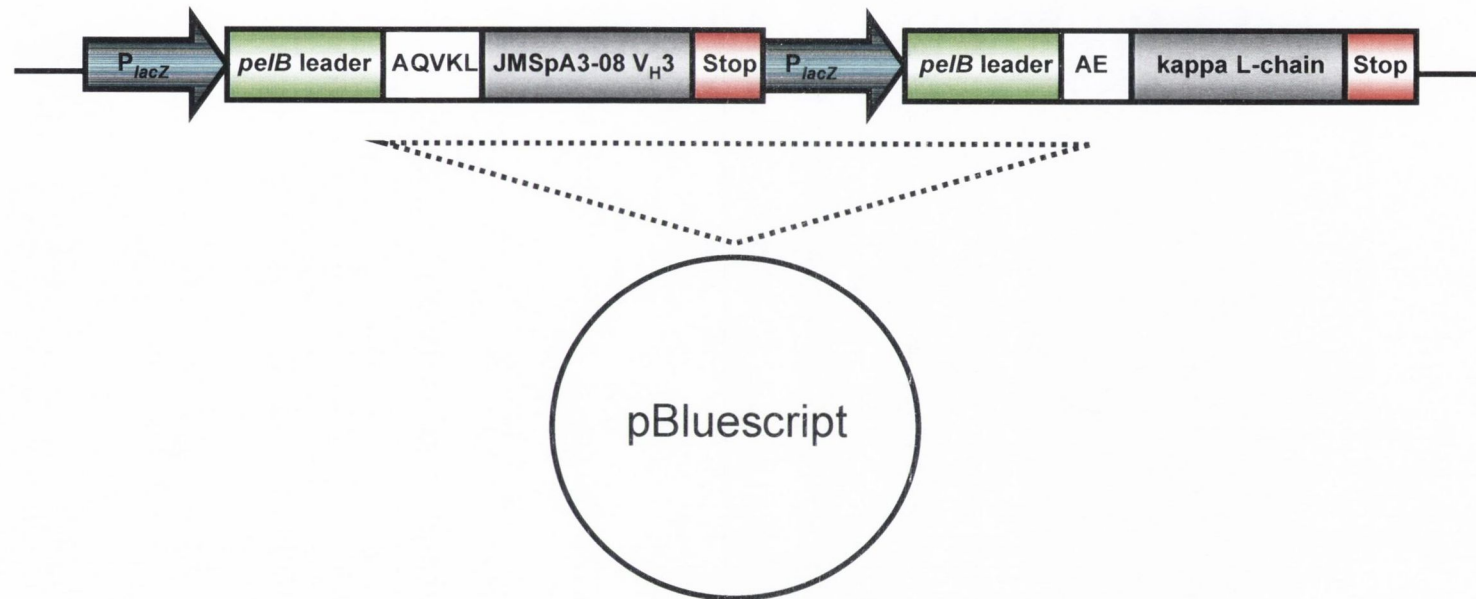


**Fig. 4.3 The pComb3:JMSpA3-08 soluble Fab-producing phagemid vector.** Expression of the V<sub>H</sub>3 heavy chain, JMSpA3-08 and a kappa light chain are under the control of the *lacZ* promoter and preceded by a *pelB* leader sequence to allow functional assembly of the Fab in the *E. coli* periplasm.

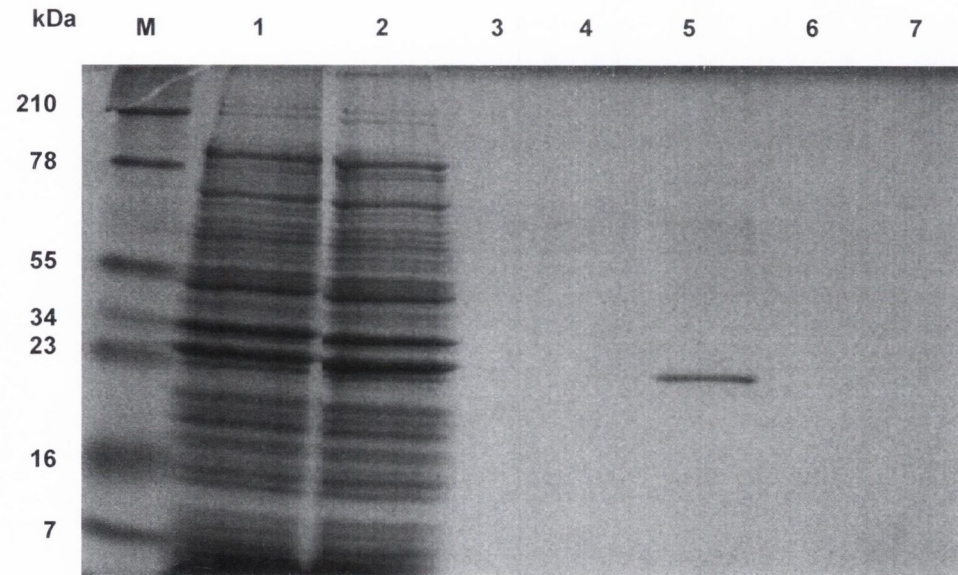


**Figure 4.4 Purification of V<sub>H</sub>3-Fab.** Overnight cultures of *E. coli* XL1 blue cells containing pComb3:JMSP A3-08 that had been induced for V<sub>H</sub>3-Fab expression were purified as described in section 2.11.2.4. and samples analysed by SDS-PAGE in the following order; (M) molecular weight marker, (1) uninduced cell lysate, (2) induced cell lysate, (3-7) 1 ml elution fractions from protein A-sepharose. Lane 5 contains the V<sub>H</sub>3-Fab, which can be resolved into two bands of 22 kDa and 25 kDa.

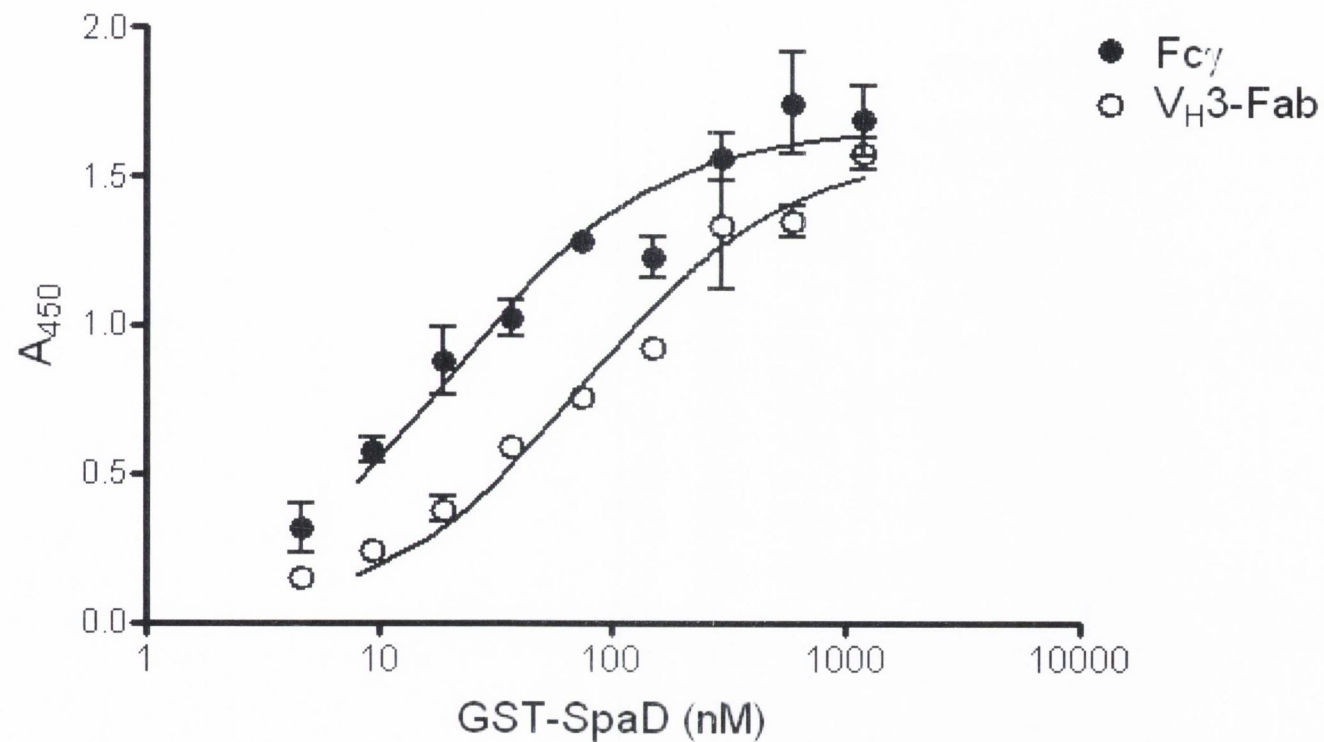


**Fig. 4.5 Binding of GST-SpaD to Fc $\gamma$  and V<sub>H</sub>3-Fab.** Microtitre plates were coated with Fc $\gamma$  or V<sub>H</sub>3-Fab (10  $\mu$ g/mL) and incubated with increasing concentrations of GST-SpaD. Bound GST-SpaD was detected with HRP-chicken anti-GST antibody, using a chromogenic substrate. Half-maximal binding for Fc $\gamma$  and V<sub>H</sub>3-Fab was calculated at 20 nm and 75 nm, respectively. Values are the means  $\pm$  standard deviation of three separate experiments.



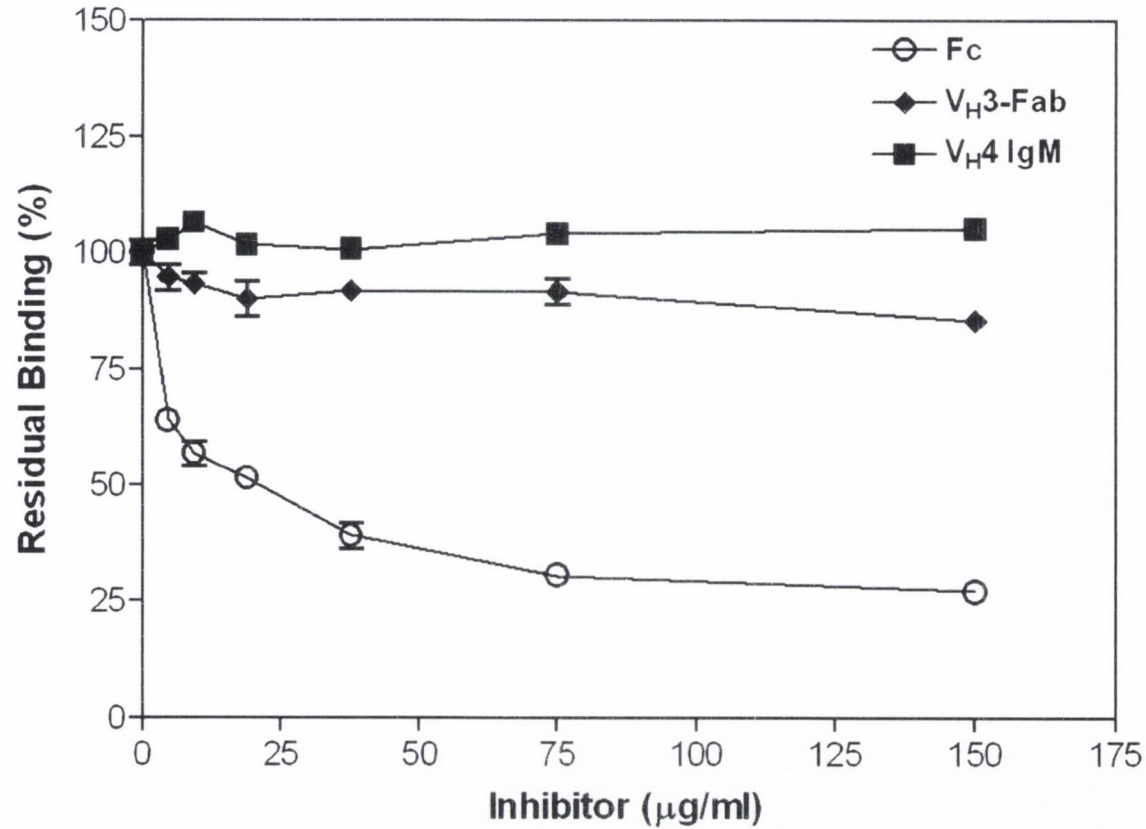


**Fig. 4.6. Inhibition of Spa binding to vWF A1 by Fc and V<sub>H</sub>3-Fab.** 96-well plates coated with GST-SpaD (10 μg/ml) were incubated with a mixture of vWF A1 (100 nM) and various concentrations of Fcγ or V<sub>H</sub>3-Fab. A V<sub>H</sub>4-bearing IgM, which does not bind Spa, was also included. Bound vWF was monitored using a HRP-conjugated anti-Hisx6 antibody. Percentage inhibition was calculated relative to vWF bound in the absence of inhibitor. The experiment was performed three times with similar results.

terminus preceding helix 1. It has been reported that this insertion impairs Fc $\gamma$ -binding by SpaD, thereby conferring a preferential V<sub>H3</sub>-binding by this domain (Roben *et al.*, 1995). In order to investigate the role of the N-terminal extension in vWF binding, a 58-residue variant of GST-SpaD (GST-SpaD<sub>58</sub>) lacking the additional N-terminal residues unique to SpaD was generated. A comprehensive set of Spa domain variants was constructed to map the vWF-binding region as accurately as possible. Residues were selected from the reported Fc $\gamma$  binding region, the V<sub>H3</sub>-Fab-binding region, and conserved residues not involved in either Fc $\gamma$  or V<sub>H3</sub>-Fab interactions (Fig. 4.7).

The GST-SpaD variants were created by PCR using pGEX-KG-SpaD as a DNA template with the oligonucleotides listed in Table 2.4 as described in section 2.7.1. Two PCR strategies were employed. The Quikchange® method in which overlapping primers carrying the desired mutation are designed to copy the entire plasmid template. After amplification, the restriction endonuclease *DpnI* is added to digest the plasmid template. The non-methylated mutant plasmid is not a substrate for *DpnI* digestion. The mixture can then be transformed directly into *E. coli* and transformants selected. This method was used when the desired codon was located at either end of the *spaD* fragment. Overlap-extension (OE-) PCR was used if the codon to be mutated was central in *spaD*. In this technique, overlapping oligonucleotides carrying the desired mutation were used with standard primers flanking *spaD* to yield two overlapping PCR products. These were combined in a second round of PCR using the flanking *spaD* primers to create the mutant fusion product. Restriction sites were incorporated into the *spaD* flanking primers to facilitate cloning of *spaD* mutants into pGEX-KG. All *spaD* mutants were verified by DNA sequencing. The mutant GST-SpaD fusion proteins were produced in the same manner as the GST-Spa domain constructs (section 2.11.2.1). The protein concentration of the purified GST-SpaD variants was determined as described in section 2.12. Protein solutions were diluted to the same concentrations for comparative binding studies. To confirm that each sample was of equal concentration and of high purity, 2  $\mu$ g of each protein was subjected to SDS-PAGE and stained with Coomassie Blue (Fig. 4.8).

#### 4.2.2.1 Interaction of GST-SpaD variants with IgG and V<sub>H3</sub>-Fab

In order to confirm the effect of the amino acid substitutions and to test each GST-SpaD variant for functionality, binding assays were performed with IgG and V<sub>H3</sub>-Fab. The distinct binding regions on Spa for Fc $\gamma$  and V<sub>H3</sub>-Fab suggest that impaired binding to both IgG and V<sub>H3</sub>-Fab by a single amino acid change may be due to that substitution

destabilising the three-helix bundle structure. Each Spa variant was tested for binding to IgG and V<sub>H</sub>3-Fab to investigate this. To test IgG Fc $\gamma$  binding, the GST-SpaD variants (10  $\mu$ g/ml) were coated on microtitre plates and incubated with peroxidase-conjugated rabbit IgG1 (200 nM). Bound IgG was measured by 15 minute incubation with a chromogenic substrate as described in section 2.14.1 and the percentage binding of each variant relative to native GST-SpaD was calculated.

The results shown in Figure 4.9 are in good agreement with previous data from structural and functional studies on the Spa-Fc $\gamma$  interaction. In agreement with previous work the SpaD variant lacking the N-terminal three-residue insertion unique to SpaD, GST-SpaD<sub>58</sub> bound IgG1 with a higher affinity than the wild-type GST-SpaD (Roben *et al.*, 1995). A two-fold or greater decrease in binding was observed for GST-SpaD variants with the substitutions Q10A, F13A, Y14A, L17A, N28A and I31A. GST-SpaD(K35A) also showed significantly reduced IgG1 binding. All of these amino acid substitutions have previously been implicated in Fc $\gamma$  binding (Cedergren *et al.*, 1993; Deisenhofer, 1981). Substitutions in F5 and Q9 of SpaD, which are proposed from structural studies to be involved in the Fc $\gamma$  interaction (Deisenhofer, 1981), did not show reduced binding to rabbit IgG1. The variant GST-SpaD(Q32A) bound IgG1 with the same affinity as GST-SpaD. It is unlikely that residue Q32 is essential for normal Fc $\gamma$  or V<sub>H</sub>3-Fab binding as a single Spa domain can simultaneously bind both ligands. All of the GST-SpaD variants that are proposed to be involved in the Spa-V<sub>H</sub>3-Fab interaction bound IgG at levels similar to the wild-type GST-SpaD protein. With the exception of GST-SpaD(L34A), which bound Fc $\gamma$  with greatly reduced affinity (20 % compared to GST-SpaD), substitutions in conserved residues that are not involved in either Fc $\gamma$  or V<sub>H</sub>3-Fab binding (N21A and R27A) did not cause a reduction in IgG binding. This suggests that these substitutions have not altered the tertiary structure of the Spa domain. When the residues on SpaD shown to be important in IgG binding were mapped onto the SpaD crystal structure (PDB ID: 1DEE) they are seen to cluster on the helix 1-2 face (Fig. 4.10). Superimposing the human Fc $\gamma$  fragment from the SpaB co-complex (PDB ID: 1FC2) demonstrated that data obtained from the IgG1 binding studies are in good agreement with previous structural data (Fig. 4.10 B, (Deisenhofer, 1981)). The unexpected decrease in Fc $\gamma$  binding by variant GST-SpaD(L34A) may be due to it destabilising the overall folding of SpaD, as the crystal structure indicates that its hydrophobic side-chain is orientated towards helix 1 (Deisenhofer, 1981).



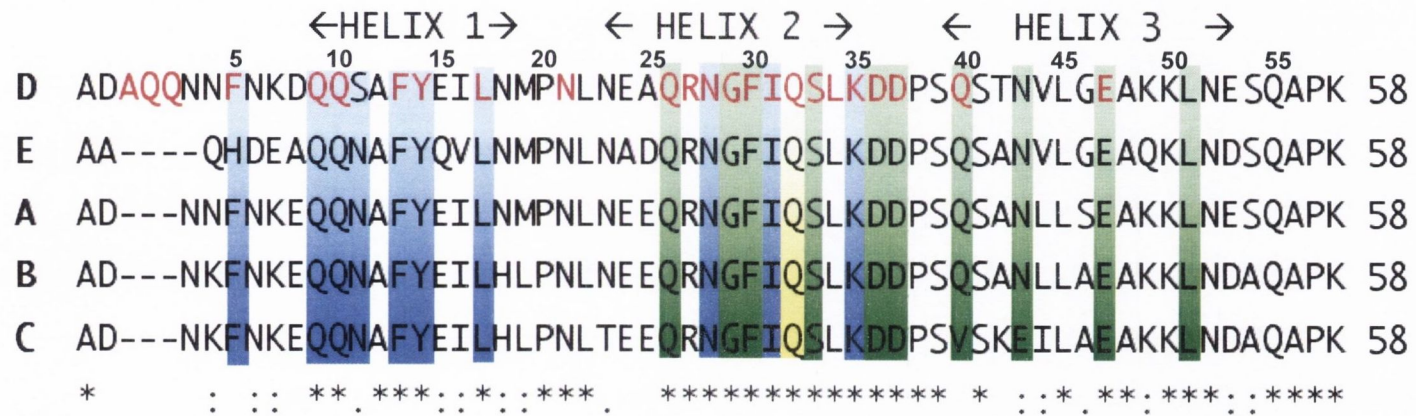


**Fig 4.7. SpA variants used in this study.** Alignment of the five domains of protein A. Residues are numbered according to (Nilsson *et al.*, 1987) and those reported to be involved in Fc $\gamma$  and V<sub>H</sub>3-Fab binding are highlighted blue and green, respectively. Q32, proposed to contribute to both interactions, is highlighted yellow. Conserved residues are denoted by an asterisk (\*), conserved substitutions in residues by a colon (:), and semi-conserved residues by a stop (.). Residues substituted or deleted by site-directed mutagenesis are highlighted red.

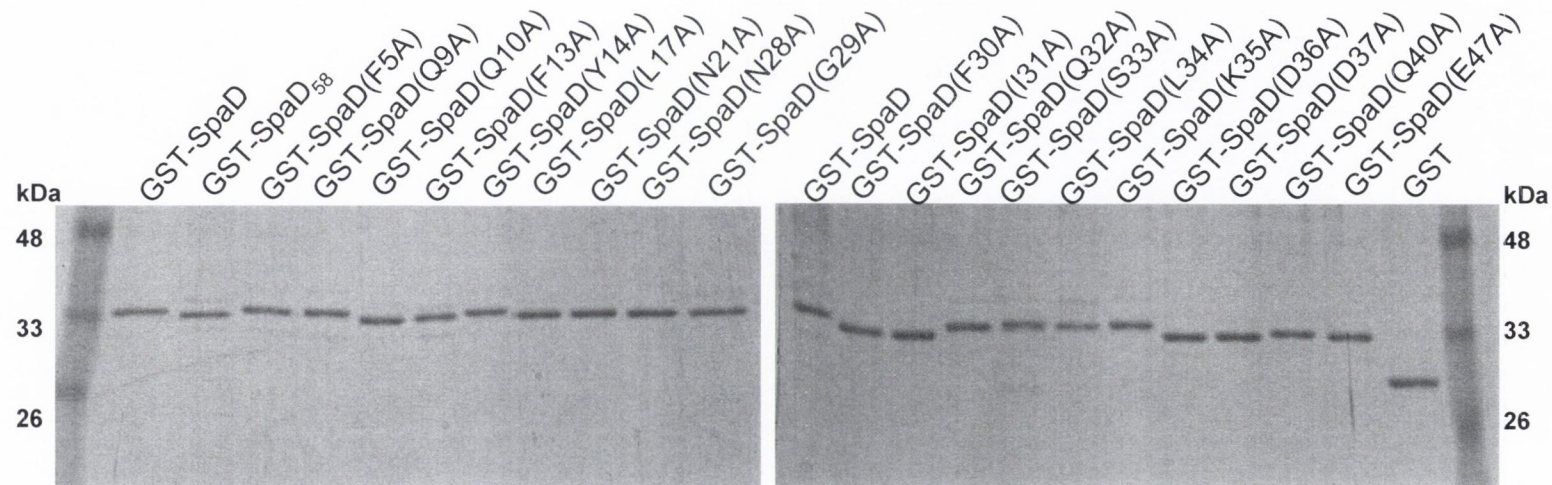


**Fig. 4.8 Recombinant GST-SpaD variants.** GST-SpaD variants were purified and normalised to equal concentrations and samples (2  $\mu$ g) analysed by SDS-PAGE followed by staining with Coomassie Blue in the order indicated. M, molecular weight marker. Variants resolved at approximately 33 kDa.

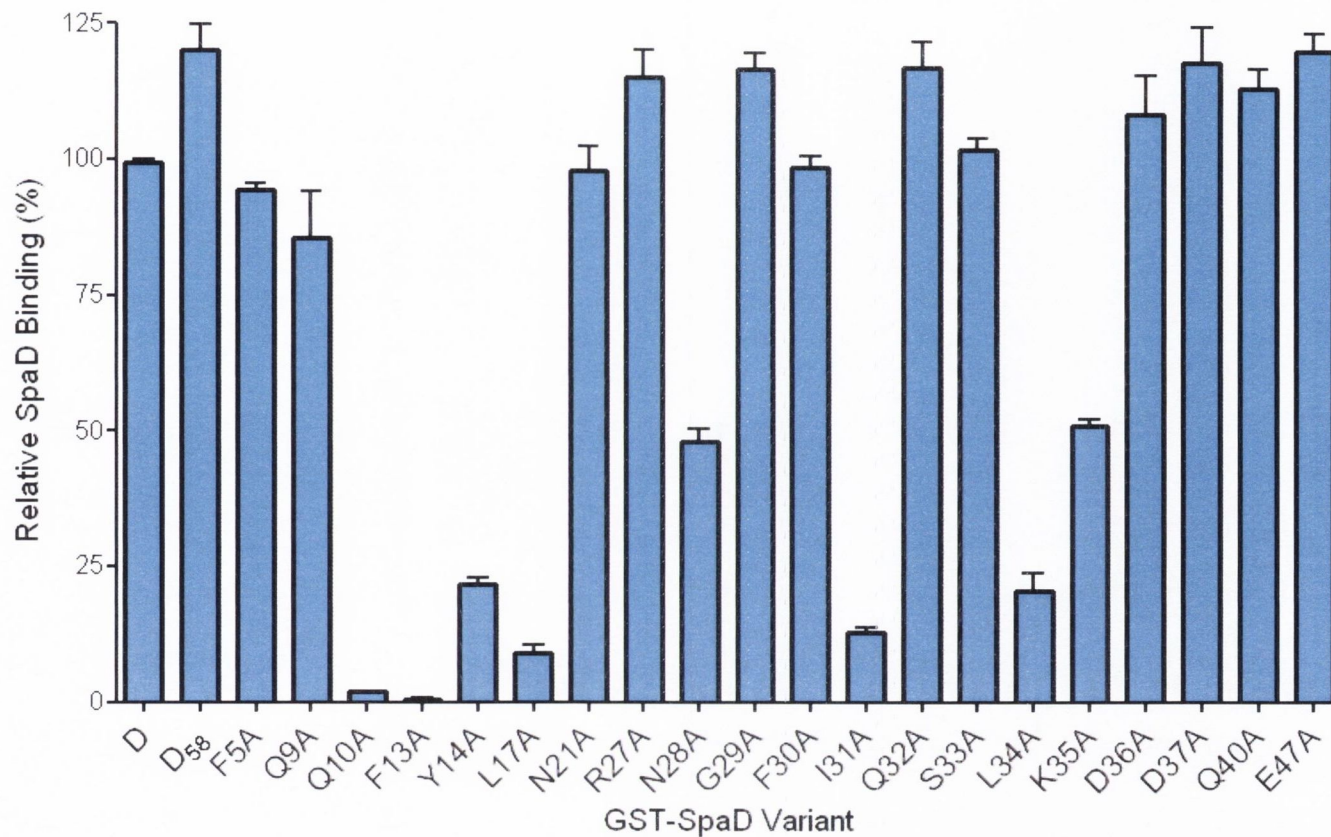


**Fig. 4.9 Binding of IgG to GST-SpaD variants.** 96-well plates were coated with GST-SpaD variants (10  $\mu\text{g/ml}$ ) followed by incubation with peroxidase-conjugated rabbit IgG (200 nM). Bound IgG was detected by incubation with chromogenic substrate and calculated as a percentage of the binding to wild-type SpaD. Experiments were performed in triplicate on three separate occasions. Figures represent the mean  $\pm$  SD from three independent experiments.



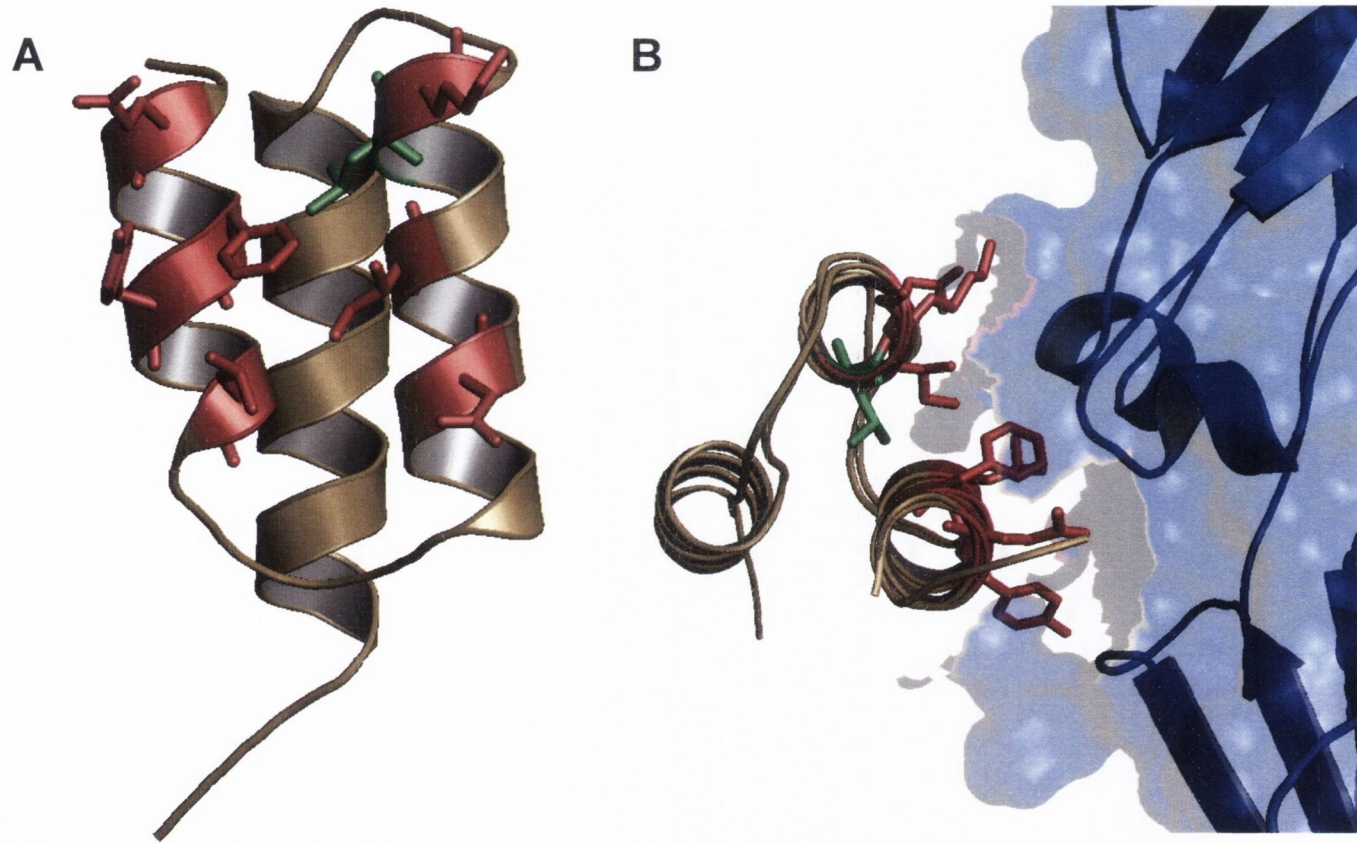


**Fig. 4.10** The Fc $\gamma$ -binding region on Spa determined by mutagenesis of SpaD. Amino acids which showed a two-fold or greater decrease in IgG binding when changed to alanine are highlighted in red and shown from (A) the side or (B) from above in complex with Fc $\gamma$  (blue). L34, which showed an 80 % reduction in IgG binding when substituted to alanine but is not directly involved in the interaction, is shown in green.

Binding studies were performed in a similar manner to study the interaction of the GST-SpaD variants with V<sub>H3</sub>-Fab. 96-well microtitre plates were coated with GST-SpaD (10 µg/ml) and incubated with a V<sub>H3</sub>-bearing IgM (50 µg/ml). Bound IgM was detected by incubation with peroxidase-conjugated chicken anti-human IgM followed by development in a chromogenic substrate. The A<sub>450</sub> values for each GST-SpaD variant was calculated as a percentage of the value obtained for wild-type GST-SpaD. The results correlate well with the X-ray crystal structure of the SpaD-V<sub>H3</sub>-Fab co-complex (Graille *et al.*, 2000). However, none of the GST-SpaD variants bound V<sub>H3</sub>-bearing IgM with the same affinity as wild-type GST-SpaD (Fig. 4.11). Residues G29, F30, D36, D37, Q40 and E47 show greatly decreased binding to V<sub>H3</sub>-IgM when substituted to alanine. However there was also decreased V<sub>H3</sub>-IgM binding of GST-SpaD variants Q9A, Q10A, and I31A which are involved in the Fcγ interaction. The observed reduction in binding may be due to structural changes caused by these substitutions. Mapping the residues important in V<sub>H3</sub>-IgM binding to the crystal structure shows a generally good agreement between the crystal co-complex and the binding of each GST-SpaD variant (Fig. 4.12).

#### 4.2.2.2 Interaction of GST-SpaD variants with vWF

The relative binding of each Spa domain substitution to Fcγ or V<sub>H3</sub>-Fab proteins was generally in agreement with the current knowledge of the binding of antibody fragments. In order to identify the residues on Spa that are important for binding to vWF, solid-phase binding studies were performed. Microtitre plates were coated with each GST-SpaD variant (10 µg/ml) and incubated with recombinant hexahistidine-tagged vWF A1 (100 nM). Bound vWF was detected using a murine anti-6xHis monoclonal IgG1 and a chromogenic substrate as described before (section 2.14.1). The binding of vWF-A1 to each GST-SpaD variant relative to that of wild-type GST-SpaD was calculated as before (section 4.2.2.1). Data in Figure 4.13 shows residues in Spa that are important for vWF A1 binding occur in helices 1 and 2 but not helix 3. Many of the residues demonstrated to be of importance in binding IgG1 were also important in the interaction with vWF A1. Increased vWF-binding was observed when GST-SpaD<sub>58</sub> was tested. GST-SpaD substitutions that showed a two-fold or greater decrease in binding to vWF A1 were Q10A, F13A, Y14A, L17A, N28A, F30A, I31A and K35A. Notably, vWF A1-binding of GST-SpaD(R27A) was 54 % that of GST-SpaD. These residues were mapped on the X-ray crystal structure of SpaD where they formed a cluster between helices 1 and 2 (Fig. 4.14). With the exceptions of R27 and F30, these residues coincide with those involved in IgG



Fc $\gamma$  binding. The side-chain of R27 also projects toward the helix 1-2 face of Spa (Fig. 4.14). F30 is involved in V<sub>H3</sub>-binding by Spa. In agreement with the data from inhibition studies, it can be seen from the SpaD structure that binding to vWF A1 and Fc $\gamma$  is competitive due to a shared binding region between helices 1 and 2. Residues involved in the V<sub>H3</sub>-IgM binding (G29, Q32, S33, D36, D37, Q40, E47) did not alter vWF binding when they were substituted. A similar binding profile was observed when a selection of the GST-SpaD variants were analysed for binding to vWF D'-D3 (Figure 4.15). Taken together, these data indicate that the Fc $\gamma$ - and vWF-binding sites on Spa are located on the helix 1-2 face and share numerous contact residues. This is supported by the observed inhibition of vWF A1 binding to Spa by Fc $\gamma$ . Only one residue that is involved in the Spa-V<sub>H3</sub>-IgM interaction was shown to have importance in the vWF-binding, F30. However, it may be that F30 is involved in stabilising the tertiary structure of Spa rather than it contacting the ligand.

### **4.2.3 The protein A binding site on vWF A1**

#### **4.2.3.1 Inhibition studies**

##### **4.2.3.1.1 Anti-vWF A1 monoclonal antibodies**

To investigate the region on vWF A1 responsible for binding to Spa, a similar approach was taken to that used to identify the binding site on Spa for vWF. The vWF A1 binding site for Spa was investigated rather than that of vWF D'-D3 because the vWF D'-D3 domain has a lower affinity for protein A than vWF A1 and there is little or no information on its structure or the location of its ligand binding sites for heparin or Factor VIII. In contrast, the vWF A1 domain is well characterised as a result of numerous structural and functional studies (Dumas *et al.*, 2004; Emsley *et al.*, 1998; Fukuda *et al.*, 2005; Huizinga *et al.*, 2002; Maita *et al.*, 2003; Morales *et al.*, 2006). Ligands include the platelet membrane receptor GpIb- $\alpha$ , collagen, and snake venom toxins. X-ray crystal structures of vWF A1 alone (PDB ID: 1AUQ (Emsley *et al.*, 1998)), and in complex with GpIb- $\alpha$  (PDB ID: 1M10 (Huizinga *et al.*, 2002), the snake venoms botrocetin (PDB ID: 1U0O (Fukuda *et al.*, 2005)) and biticetin (PDB ID: 1UEX (Maita *et al.*, 2003)), and with a function blocking Fab fragment Nmc-4 (PDB ID: 1OAK (Celikel *et al.*, 1997)) have been solved. A ternary complex of vWF A1, GpIb- $\alpha$  and botrocetin is also available (PDB ID: 1U0N (Fukuda *et al.*, 2005)).



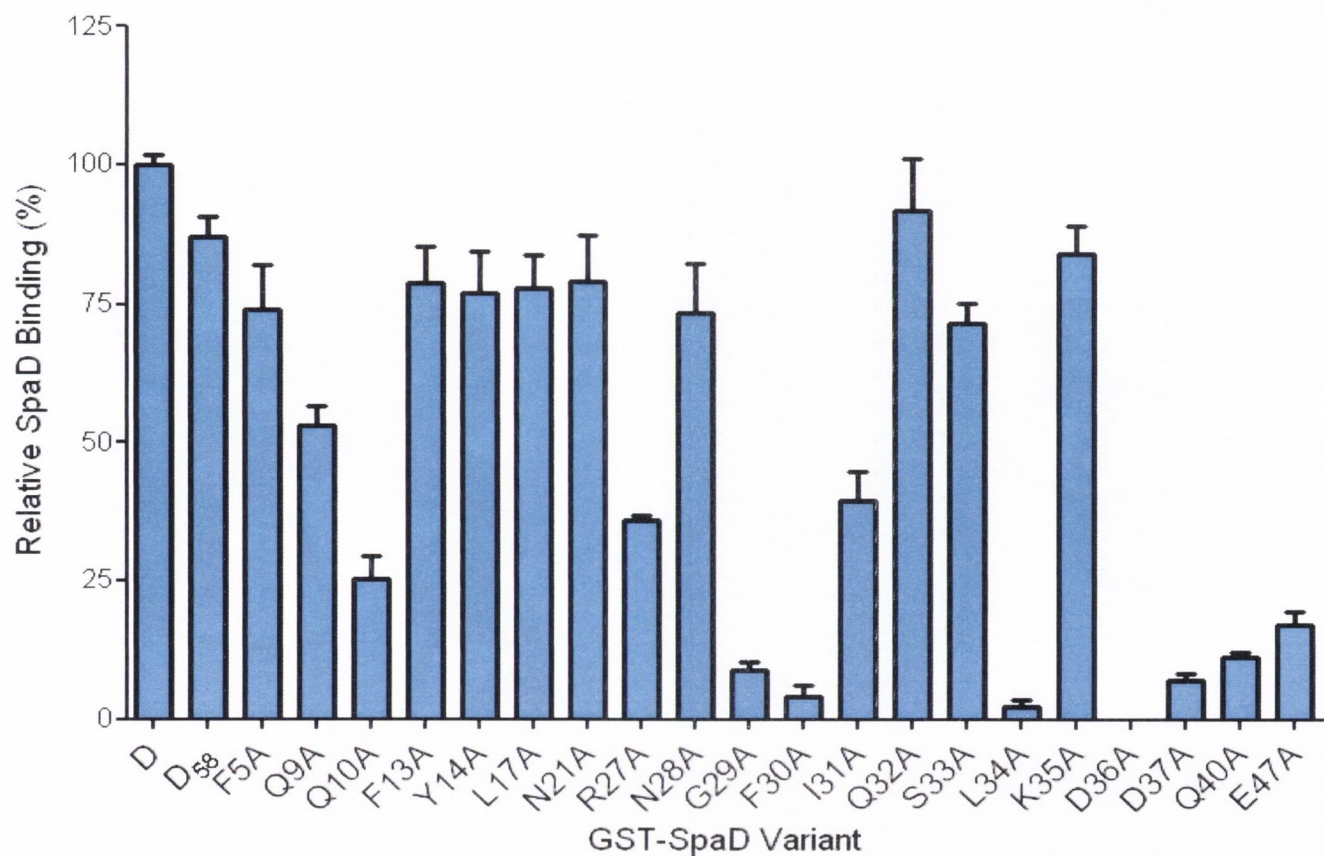


**Fig. 4.11 Binding of V<sub>H</sub>3-IgM to GST-SpaD variants.** ELISA plates were coated with GST-SpaD variants (10 µg/ml) followed by incubation with human IgM bearing V<sub>H</sub>3-heavy chains (50 µg/ml). Bound IgM was detected by incubation with peroxidase-conjugated chicken anti-human IgM followed by incubation in chromogenic substrate and calculated as a percentage of binding to SpaD. Experiments were performed in triplicate on three separate occasions. Figures represent the mean ± SD from three independent experiments.

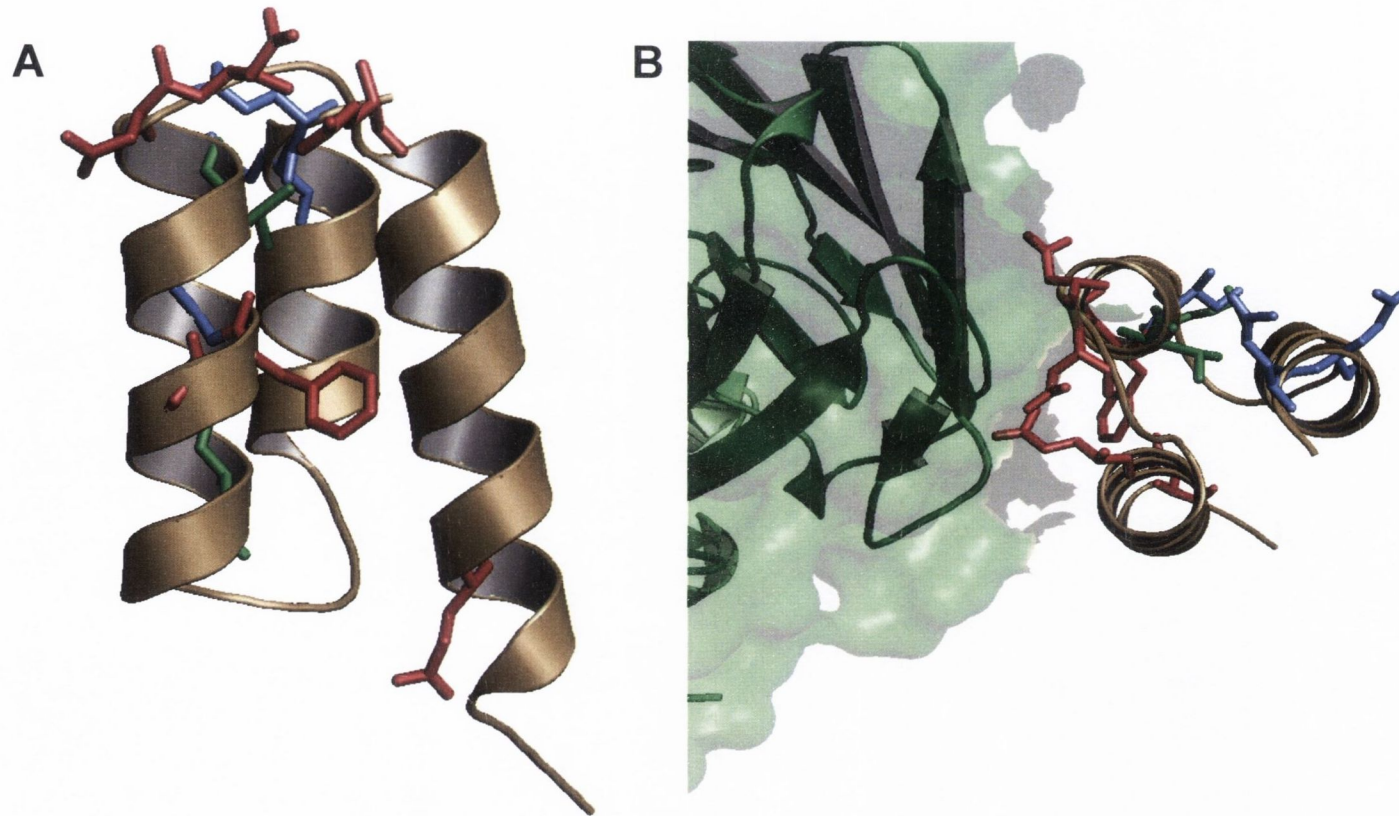


**Fig. 4.12 The  $V_H3$ -Fab binding region on Spa determined by mutagenesis of SpaD.** Amino acids which showed a two-fold or greater decrease in  $V_H3$ -Fab binding when changed to alanine are highlighted in red and are shown from (A) the side or (B) above in complex with  $V_H3$ -Fab (green). Residues involved in  $Fc\gamma$ -binding that were defective in  $V_H3$ -Fab-binding when substituted are coloured blue and residues not involved in  $V_H3$ -Fab or  $Fc\gamma$  binding to Spa which had reduced binding when substituted are coloured green.

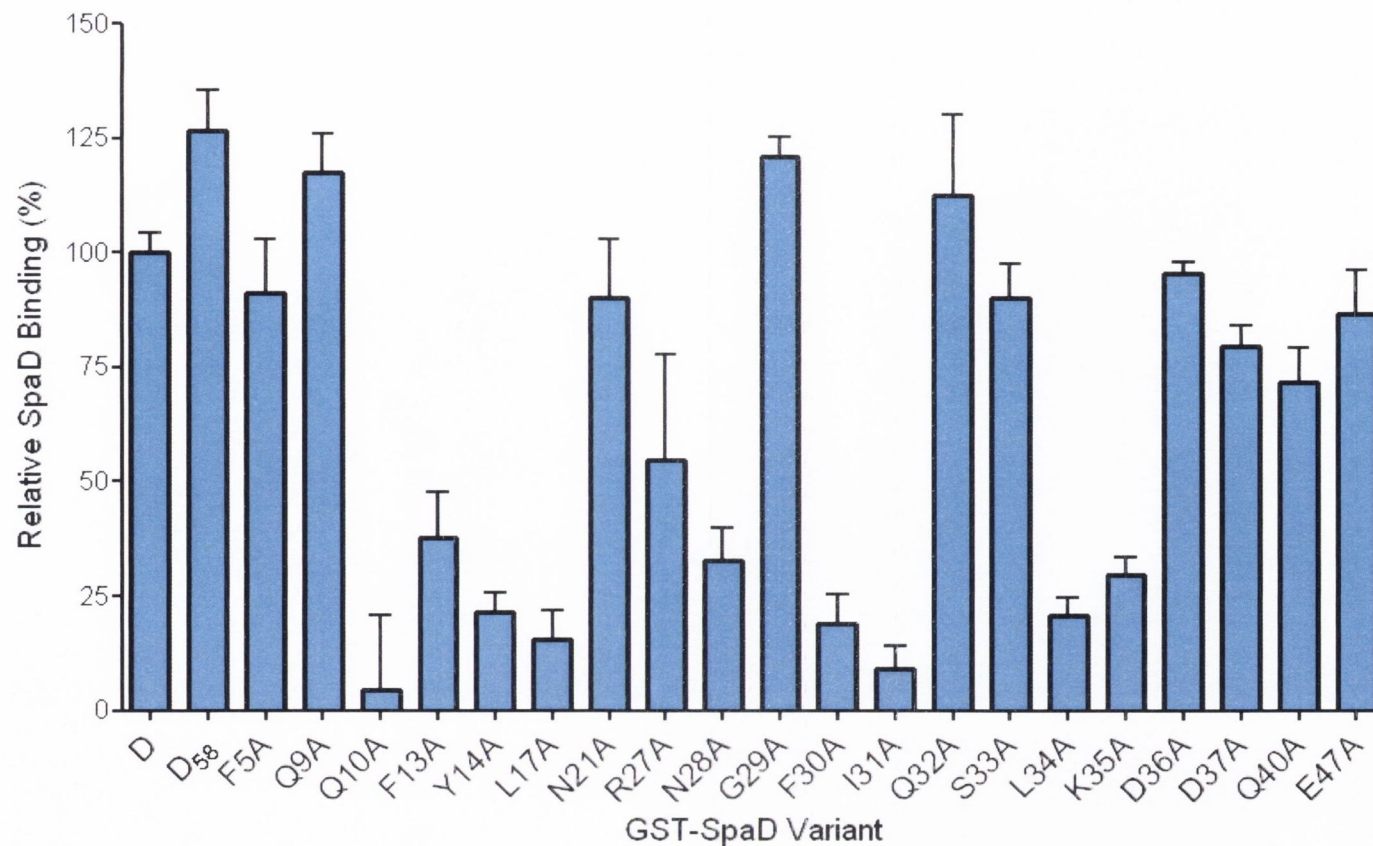


**Fig. 4.13 Binding of vWF A1 to GST-SpaD variants.** Microtitre plates were coated with GST-SpaD variants (10  $\mu\text{g/ml}$ ) followed by incubation with vWF A1 (100 nM). Bound vWF was detected by incubation with peroxidase-conjugated murine monoclonal anti-6xHis antibody followed by incubation in chromogenic substrate and calculated as a percentage of SpaD binding. Experiments were performed in triplicate on three separate occasions. Figures represent the mean  $\pm$  SD from three independent experiments.



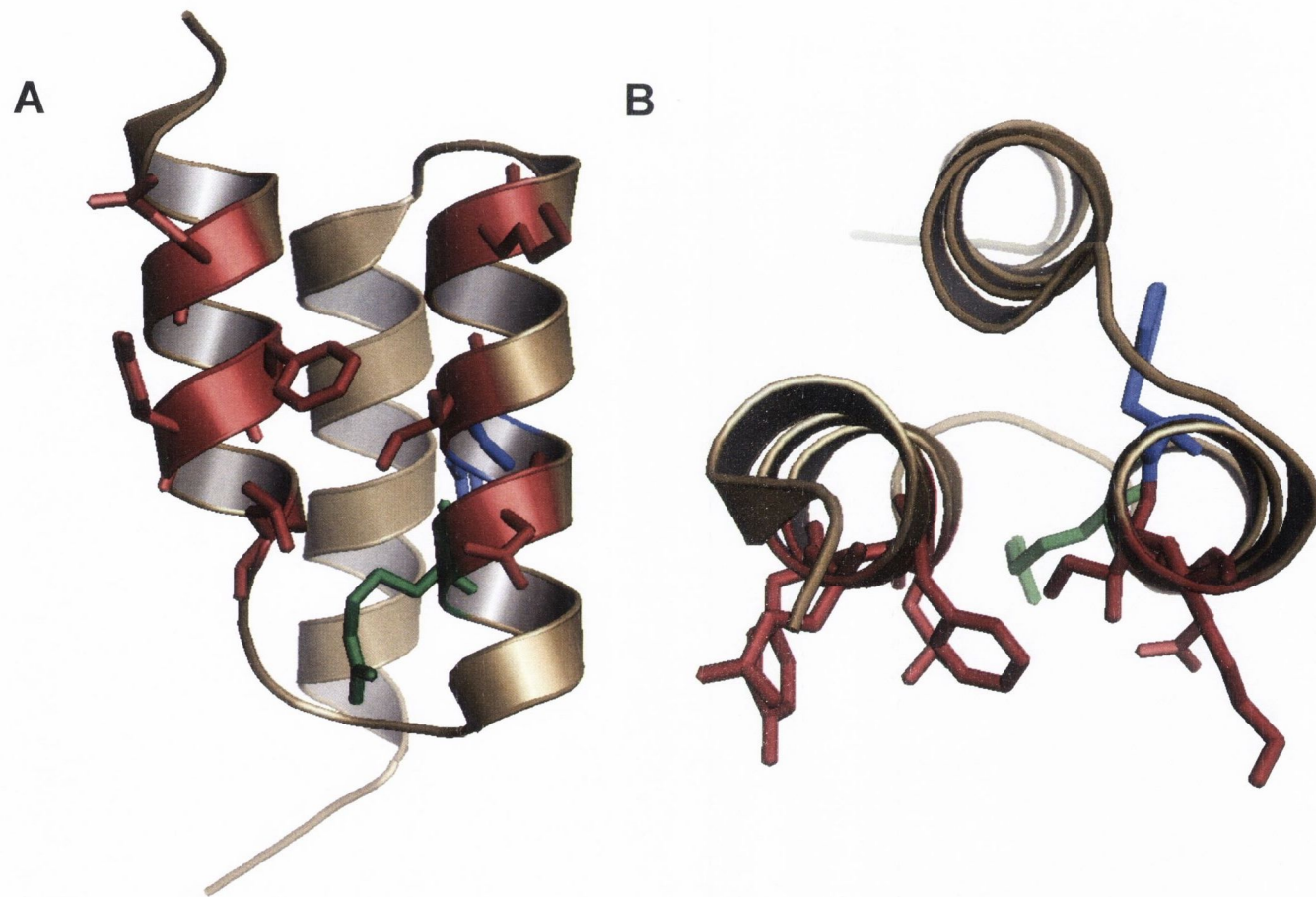


**Fig. 4.14. The vWF-binding region on Spa.** Ribbon structure of SpaD shown from (A) the side or (B) from above. Residues on Spa important for vWF-binding are highlighted. Residues coloured red are also involved in Fc $\gamma$ -binding. R27 (green) is important in vWF binding but is not involved in the Fc $\gamma$  interaction. Substitution of F30 (blue) also leads to reduced vWF-binding by Spa.

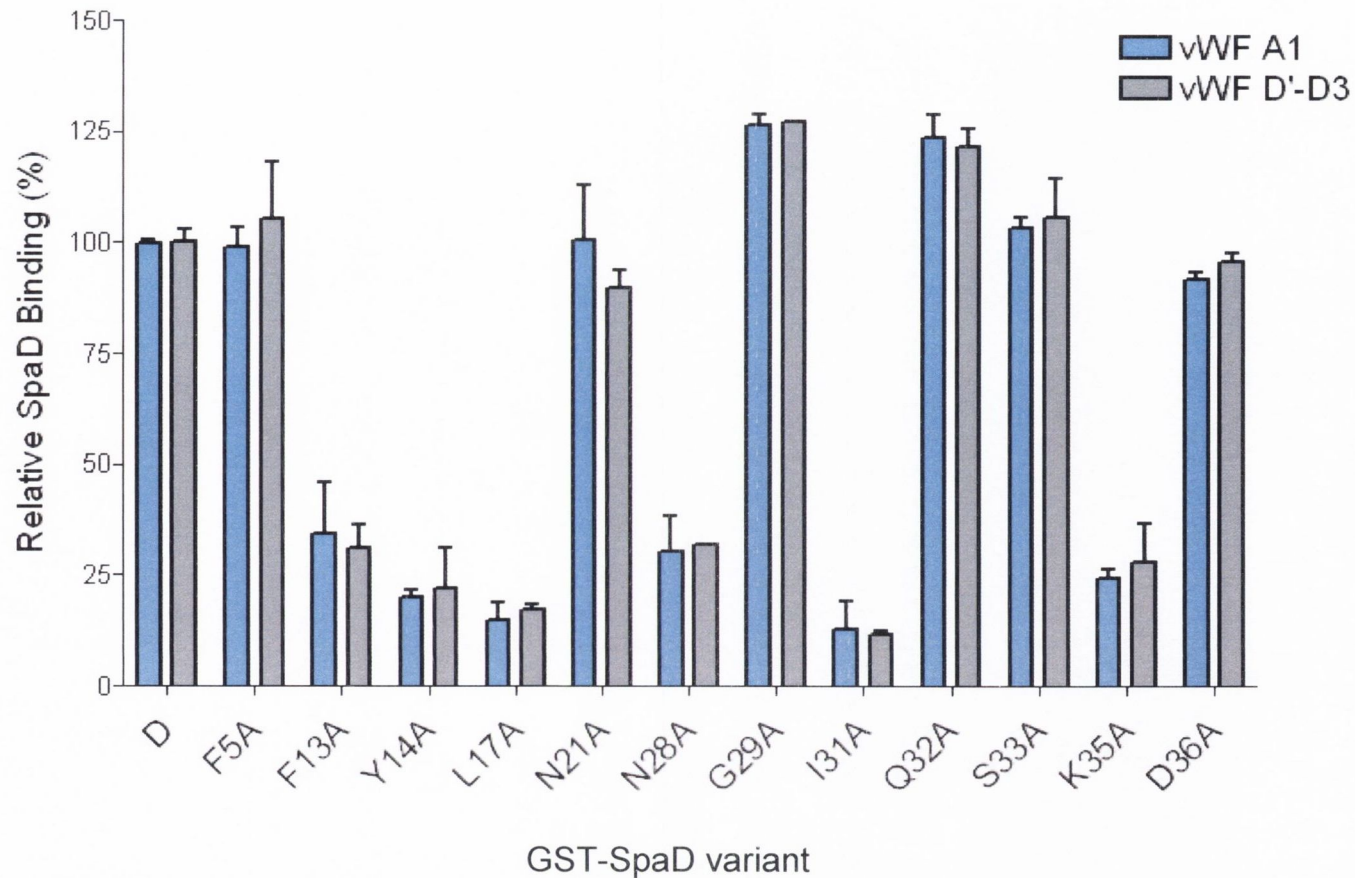


**Fig. 4.15 Binding of Spa to vWF D'-D3 and A1 domains.** 96-well plates were coated with GST-SpaD variants (10  $\mu\text{g/ml}$ ) and incubated with vWF D'-D3 (250 nM) or A1 (100 nM). Bound vWF was detected by incubation with peroxidase-conjugated murine monoclonal anti-6xHis antibody followed by incubation in chromogenic substrate and calculated as a percentage of binding to SpaD. Experiments were performed in triplicate on three separate occasions. Figures represent the mean  $\pm$  SD from three independent experiments.

Mutagenesis studies identified important regions in vWF A1 for the binding of collagen and GpIb- $\alpha$  (Matsushita and Sadler, 1995; Morales *et al.*, 2006). In addition, a number of murine monoclonal antibodies (mAbs) have been raised against vWF A1. These can be used in inhibition studies to localise the region for Spa binding on vWF A1. Dr. Jean-Pierre Girma kindly provided a collection of vWF A1-binding mAb Fab fragments for this study named 700, 701, 710, 723 and 724. Murine IgG1 Fab fragments react with Spa because they lack an Fc $\gamma$  region. Previous work by Dr. Girma's group to localise the vWF A1 binding regions of the mAbs is summarised in Table 4.1. Here, the antibodies were used to block vWF A1 binding to SpaD. Microtitre plates were coated with GST-SpaD (10  $\mu$ g/ml) followed by incubation with a mixture of vWF A1 (100 nM) and serial dilutions of each mAb ranging from 20  $\mu$ g/ml to 78 ng/ml. The bound vWF A1 was detected as previously described in this chapter (section 4.3.2.2). The results shown in Figure 4.16 show no inhibition of vWF A1 binding to GST-SpaD by any of the mAbs tested. An increase of vWF A1 binding by up to 35 % was observed when mAbs 700 and 724 were used.

#### 4.2.3.1.2 Ligands of vWF A1

Inhibition studies using mAbs directed against specific regions of vWF A1 failed to identify the binding site of Spa. Binding of vWF A1 to Spa was investigated in the presence of the snake-venom protein botrocetin, the bacterial glycopeptide ristocetin and type I collagen. Each binds to distinct regions on vWF A1 and induces the binding of vWF A1 to GpIb- $\alpha$ . The binding site of botrocetin is well characterised and X-ray crystal structures have shed light on how botrocetin binding to the A1 domain of vWF increases its affinity for GpIb- $\alpha$  by  $\sim$ 300-fold (Fukuda *et al.*, 2005). The botrocetin-binding site on vWF A1 comprises residues on the  $\alpha$ -helices  $\alpha$ 5 and  $\alpha$ 6 (Fig. 4.17). The binding of ristocetin to vWF A1 also induces binding to platelets via GpIb- $\alpha$ , presumably through conformational changes in vWF A1, although the interaction is less well understood. The binding site for ristocetin on vWF A1 has not been identified but is thought to bind the proline-rich sequences Cys474-Pro488 and Leu694-Pro708 ((Fujimura *et al.*, 1991; Hoylaerts *et al.*, 1995) Fig. 4.17). This is supported by the observation that a mAb recognising the region Glu700-Asp709 inhibits ristocetin from binding to vWF A1 (De Luca *et al.*, 2000). This mAb also blocks collagen binding by vWF A1. There is little other information on the binding site on vWF A1 for collagen. It is completely distinct from the



GpIb- $\alpha$  binding site and is in close proximity to or overlaps the site recognised by ristocetin. The vWF A1-binding regions of botrocetin, ristocetin and collagen are listed in Table 4.1.

To investigate if any of the ligands that bind vWF share the binding site of Spa on vWF A1, inhibition studies were performed. For comparative purposes, the concentrations of vWF ligands were measured by units of cofactor activity, where 1 U/ml is sufficient to induce platelet aggregation in a standard PRP sample. This corresponds to 2  $\mu$ g/ml botrocetin, 1 mg/ml ristocetin and 190  $\mu$ g/ml collagen. GST-SpaD (10  $\mu$ g/ml) was coated on 96-well ELISA plates followed by incubation with mixtures of vWF A1 (100 nM) and botrocetin, ristocetin or collagen ranging from 2 U/ml to 7 mU/ml. It can be seen from Figure 4.18 that ristocetin and collagen inhibited GST-SpaD-vWF A1 binding by 91 % and 58 %, respectively. In the case of collagen, complete inhibition might have been achieved with higher concentrations. Botrocetin did not block the interaction at any of the concentrations tested. These data suggested that the binding site for Spa on vWF A1 may be located close to the proline-rich regions, Leu694-Pro708 and Cys474-Pro488. However, it cannot be ruled out that the inhibition is due to ristocetin- or collagen-induced conformational changes in vWF A1 rather than an overlapping or shared binding site.

#### 4.2.3.2 vWF A1 variants

The conformation of vWF A1 is essential for its ability to bind to GpIb- $\alpha$  on platelets. Binding of vWF to collagen that has been exposed in damaged vascular endothelium causes the A1 domain to assume an active conformation and to bind to resting platelets. This is the primary step in thrombus formation at sites of vascular damage. High shear stress can cause vWF to bind to platelets independently of collagen binding, presumably through conformational changes in vWF A1 (Dong *et al.*, 2001). Ristocetin may also induce structural changes in vWF A1 that promote binding to GpIb- $\alpha$  on platelets. In addition, a number of naturally occurring mutations affecting vWF A1 can lead to abnormally active or inactive vWF conformations. The vWF alterations define specific categories of von Willebrand's disease (VWD). Type 2M VWD results from loss of GpIb- $\alpha$  binding by vWF A1 and is characterised by decreased binding of vWF to platelets and a reduction in the laboratory test for ristocetin-induced platelet aggregation (RIPA). Ristocetin binds to the A1 domain in vWF and induces a conformational change that activates vWF. This stimulates platelet binding and activation and aggregation without the need for high shear. vWF from patients with Type 2B VWD has an increased affinity

**Table 4.1. Properties of vWF A1 ligands used in this study.**

<b>vWF A1 ligand</b>	<b>Properties/binding region on vWF A1</b>	<b>Reference/source</b>
Murine mAb 700	Binds vWF A1	Dr. J. P. Girma
Murine mAb 701	Blocks ristocetin- or botrocetin-induced binding to GpIb- $\alpha$	Obert <i>et al.</i> , 1999
Murine mAb 710	Ser593-Ser678. Blocks ristocetin-induced binding to GpIb- $\alpha$	Pietu <i>et al.</i> , 1994
Murine mAb 723	Ser 523-Gly588 Promotes vWF-induced shear-dependent platelet aggregation. Blocks botrocetin and botrocetin-induced binding to GpIb- $\alpha$ . Blocks heparin binding and reduces collagen binding.	Pietu <i>et al.</i> , 1994
Murine mAb 724	Binding promotes active conformation. Proposed site within Cys474-Pro488 and Leu694-Pro708	Christophe <i>et al.</i> , 1995
Ristocetin	Binding promotes active conformation. Binds residues on the $\alpha$ -helices $\alpha$ 5 and $\alpha$ 6	Fujimura <i>et al.</i> , 1991
Botrocetin Collagen	Binding promotes active conformation. Distinct site from GpIb- $\alpha$ , overlaps that of ristocetin. Blocked by mAb against Glu700-Asp709.	Fukuda <i>et al.</i> , 2005 Morales <i>et al.</i> , 2006

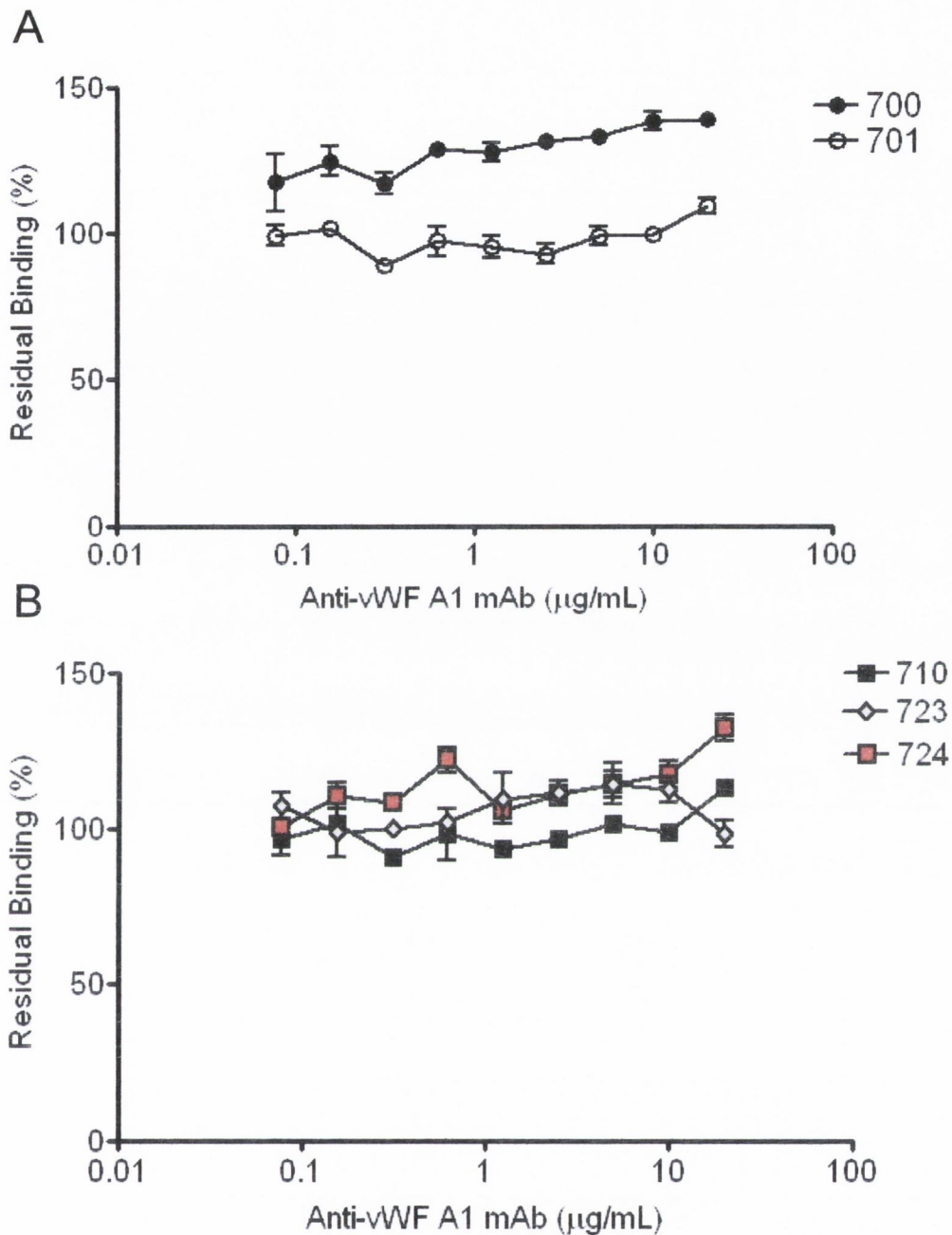


**Fig. 4.16. Effect of anti-vWF A1 monoclonal antibodies on the binding of Spa to vWF A1.** 96-well plates were coated with GST-SpaD (10 µg/mL) and were incubated with a mixture of vWF A1 (100 nM) and various concentrations of anti-vWF A1 mAbs 700, 701 (A) and 710, 723, 724 (B). Relevant properties of the mAbs are outlined in Table 4.2. Bound vWF A1 was monitored using a HRP-conjugated anti-Hisx6 antibody. The percentage inhibition was calculated relative to vWF bound in the absence of antibody. The experiment was performed three times with similar results.



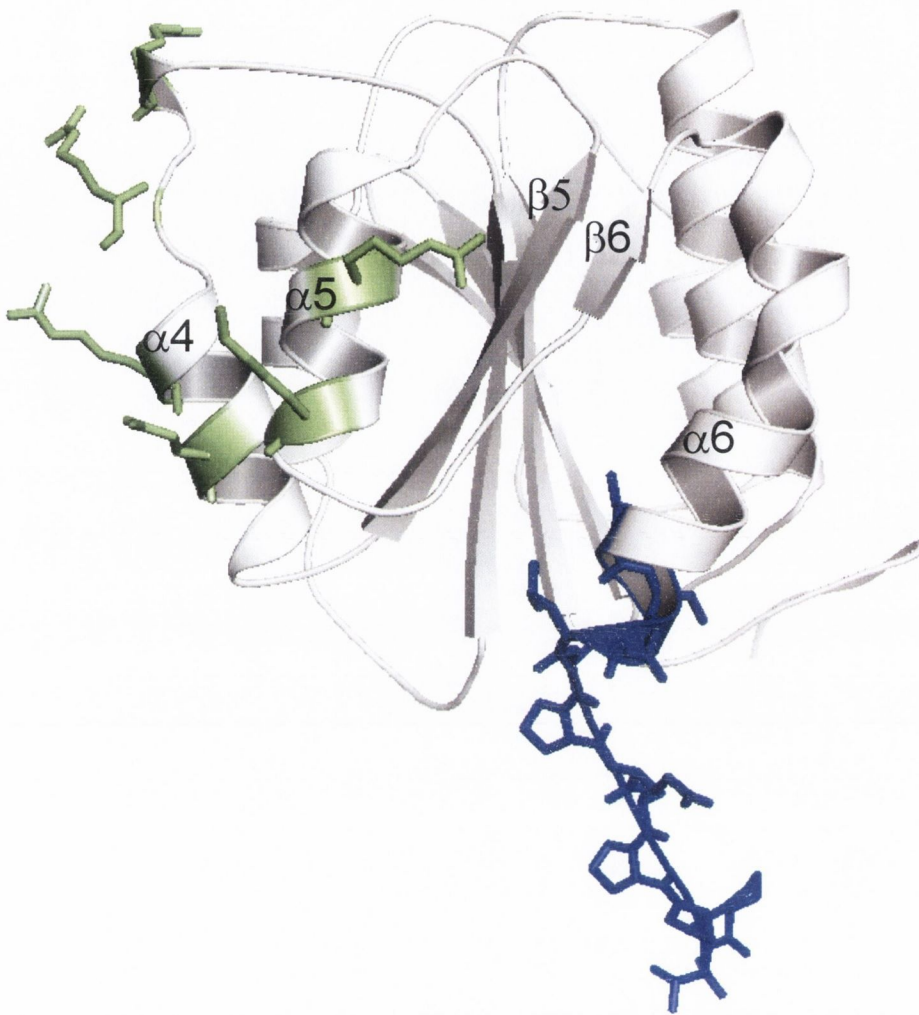


**Fig. 4.17 The binding regions on vWF A1 for botrocetin, ristocetin and collagen.** The crystal structure of vWF A1 (PDB ID: 1AUQ) with the binding regions for botrocetin (green), ristocetin and collagen (blue).  $\alpha$ -helices and  $\beta$ -sheets are numbered according to Celikel *et al.*, 1998.

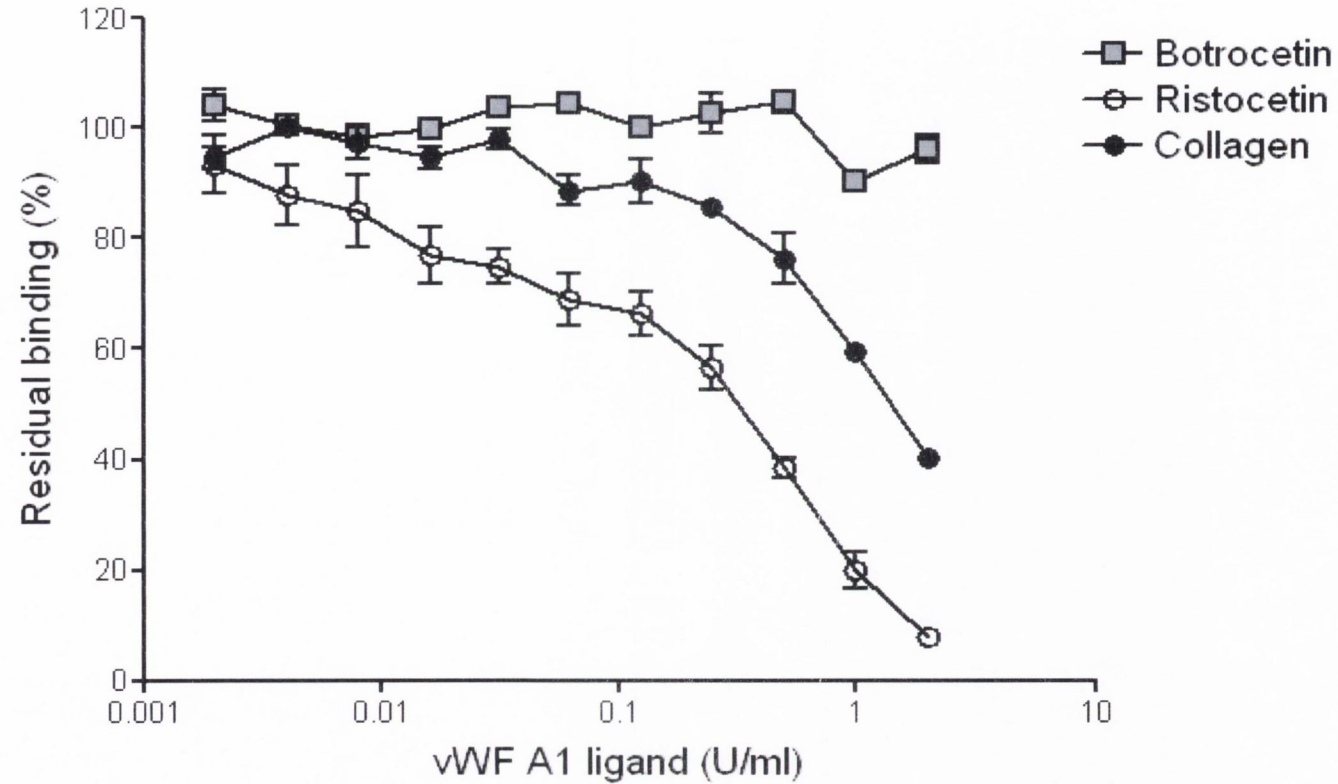


**Fig. 4.18. Inhibition studies on the Spa-vWF A1 interaction using vWF ligands.** 96-well plates were coated with GST-SpaD (10 $\mu$ g/mL) and were incubated with a mixture of vWF A1 (100 nM) and the vWF ligands botrocetin, ristocetin or collagen at a range of concentrations. Bound vWF was detected using a HRP-conjugated anti-Hisx6 antibody. The percentage inhibition was calculated relative to vWF bound in the absence of inhibitor. The experiment was performed three times with similar results.

for platelet GpIb- $\alpha$  and smaller amounts of ristocetin are required to induce platelet aggregation (Michiels *et al.*, 2006). To study the effect on binding to Spa resulting from conformational changes in vWF A1 causing type 2M or 2B VWD, substitutions in vWF A1 associated with these phenotypes were generated. The vWF A1 substitutions vWF A1(S522F) and vWF A1(G561S) conferred a loss of GpIb- $\alpha$  binding associated with type 2M VWD (Morales *et al.*, 2006; Stepanian *et al.*, 2003). A type 2B VWD substitution in vWF A1 contained on plasmid pQE30-vWFA1(R578Q) was a kind gift from Dr. Jonas Emsley. The position of each variant residue on vWF A1 is shown in Figure 4.19 A. The vWF A1 variants contained an N-terminal hexahistidine tag and were induced and purified from *E. coli* M15 pREP4 by immobilised metal chelate chromatography in the same way as wild-type vWF A1 (Cruz *et al.*, 2000; Emsley *et al.*, 1998). Recombinant proteins were subjected to SDS-PAGE and stained with Coomassie Blue. The mutant proteins had the same molecular weight as the wild-type and were intact (Fig. 4.19 B).

#### 4.2.3.2.1 Functional analysis of vWF A1 variants

Plasma from patients with type 2B VWD contains mutated vWF that has increased reactivity with platelets. In PRP their platelets can be agglutinated (activated) at lower ristocetin concentrations than normal. It has been reported that vWF A1 harbouring the substitution R578Q (type 2B VWD) has an increased affinity for GpIb- $\alpha$  on platelets whereas the substitutions S522F and G561S in vWF A1 (type 2M VWD) show a marked decrease in platelet interactions (Randi *et al.*, 1992). The greatly reduced platelet binding by the vWF A1(G561S) variant may be due to the position of Gly-561 on vWF A1 which is surface-exposed at the centre of the GpIb- $\alpha$  binding surface. However there are numerous possible reasons why substitution of Gly in a tight  $\beta$ -turn close to the GpIb- $\alpha$  binding site could affect the vWF A1 structure and its packing against GpIb- $\alpha$ . Ser-522 is not directly involved in the GpIb- $\alpha$  interaction but the substitution S522F induces a conformational change in vWF A1 resulting in abnormal binding to the platelet receptor (Stepanian *et al.*, 2003). To confirm this, inhibition of ristocetin-induced platelet agglutination (RIPA) by each of the vWF A1 variants was analysed. Wild-type vWF A1 at a concentration of 2  $\mu$ M completely inhibited RIPA in a standard PRP preparation. The type 2B VWD disease variant R578Q also completely inhibited RIPA whereas inhibition of RIPA by the type 2M variants, vWF A1(S522F) and vWF A1(G561S) was 59 % and 85 % of wild-type vWF A1, respectively (Fig. 4.20). These data are in close agreement with



previous studies using full-length vWF or recombinant vWF A1 variants harbouring these substitutions (Ajzenberg *et al.*, 2000; Morales *et al.*, 2006; Stepanian *et al.*, 2003).

#### **4.2.3.3 Interaction of vWF A1 variants with SpaD**

Inhibition studies have suggested that Spa binds to vWF A1 at a site overlapping the ristocetin and/or collagen binding sites. However, binding by these ligands induces a conformational change in vWF A1. To investigate whether the inhibition of Spa binding is due to a shared binding site or to an unfavourable vWF structural conformation, vWF A1 mutants that are active or inactive for GpIb- $\alpha$  binding were employed in binding studies with GST-SpaD. The substitution R578Q represents an active vWF A1 conformation that is demonstrated by increased platelet binding by vWF in patients with this mutation. The vWF A1 variants S522F and G561S have reduced GpIb- $\alpha$  binding activity. The G561S substitution impairs the structural change induced by collagen in vWF A1. The vWF variants were tested for binding to immobilised GST-SpaD. Immobilised GST-SpaD (10  $\mu\text{g/ml}$ ) was incubated with serial dilutions of each vWF variant ranging from 1.2  $\mu\text{M}$  to 18.75 nM. Bound vWF A1 was detected with peroxidase-conjugated monoclonal anti-6xHis mouse IgG1 followed by 15 min incubation with a chromogenic substrate. Data from binding curves indicate that none of the vWF substitutions caused decreased binding by GST-SpaD binding (Fig. 4.21). Taken together, these data suggest that the Spa-binding region on vWF A1 may overlap that of collagen and ristocetin. The Spa binding site does not overlap the botrocetin-binding region or the recognition sites of mAbs 700, 701, 710, 723 or 724. Data from the vWF A1 inhibition and mutagenesis studies including the proposed Spa binding site is summarised in Figure 4.22.

#### **4.2.4 Structural studies on the Spa-vWF complex**

An X-ray crystal structure of SpaD in complex with vWF A1 would identify the residues involved in binding and may provide other valuable information about the nature of the interaction. This project was undertaken in collaboration with Dr. Jonas Emsley's research group in the University of Nottingham. GST-Spa domain truncates comprising 5, 3, 2 and 1 domain(s) were purified and the N-terminal GST-fusion tag removed by thrombin cleavage as described in section 2.11.2.2. Briefly, GST-Spa proteins were immobilised onto glutathione-sepharose columns and washed. The columns were

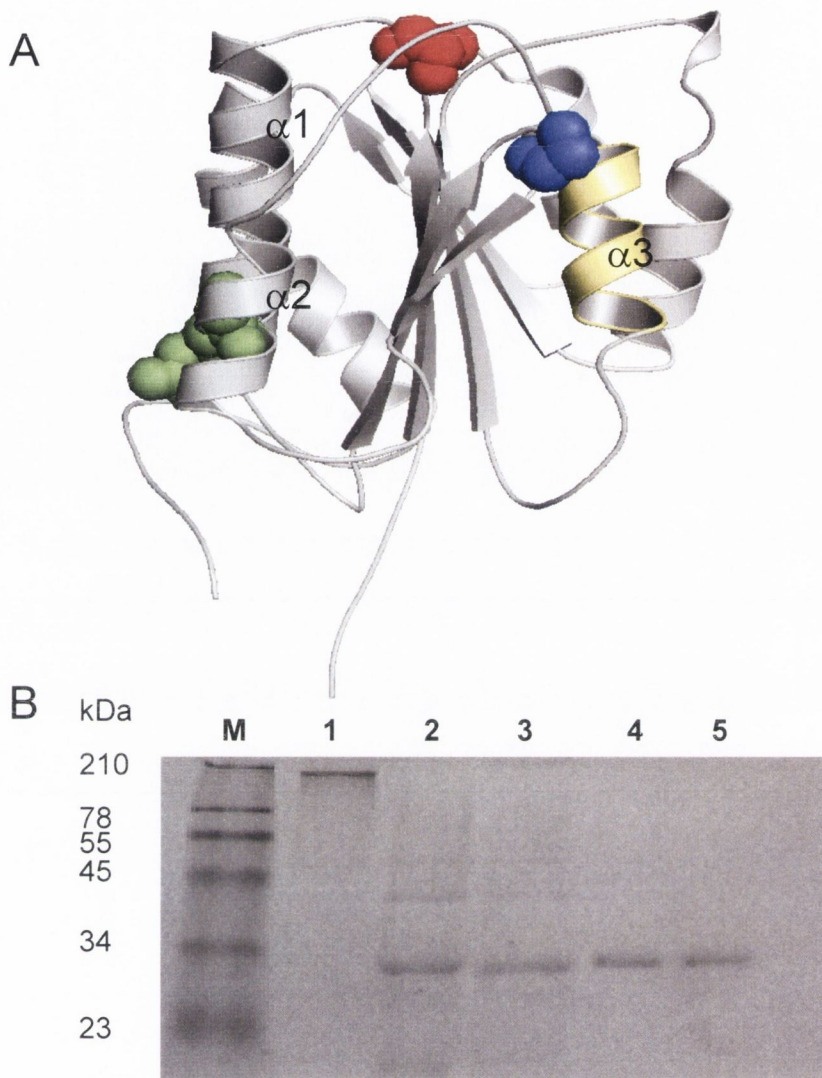


**Fig. 4.19. vWF A1 variants used in this study.** The position of residues Ser522 (red) Gly561 (blue) and Arg578 (green) which were substituted to Phe, Ser and Glue, respectively (A). Substitution of these residues causes abnormal GpIb- $\alpha$  binding by vWF through conformational changes in vWF A1. None of the substitutions lie in the GpIb- $\alpha$  binding site (yellow). B, vWF A1 variants were resolved by SDS-PAGE and stained with Coomassie Blue. Proteins were loaded in the following order, M, molecular weight marker, lane 1 full-length vWF, lane 2 vWF A1, lane 3 vWF A1(S522F), lane 4, vWF A1(G561S), lane 5 vWF A1(R578Q)

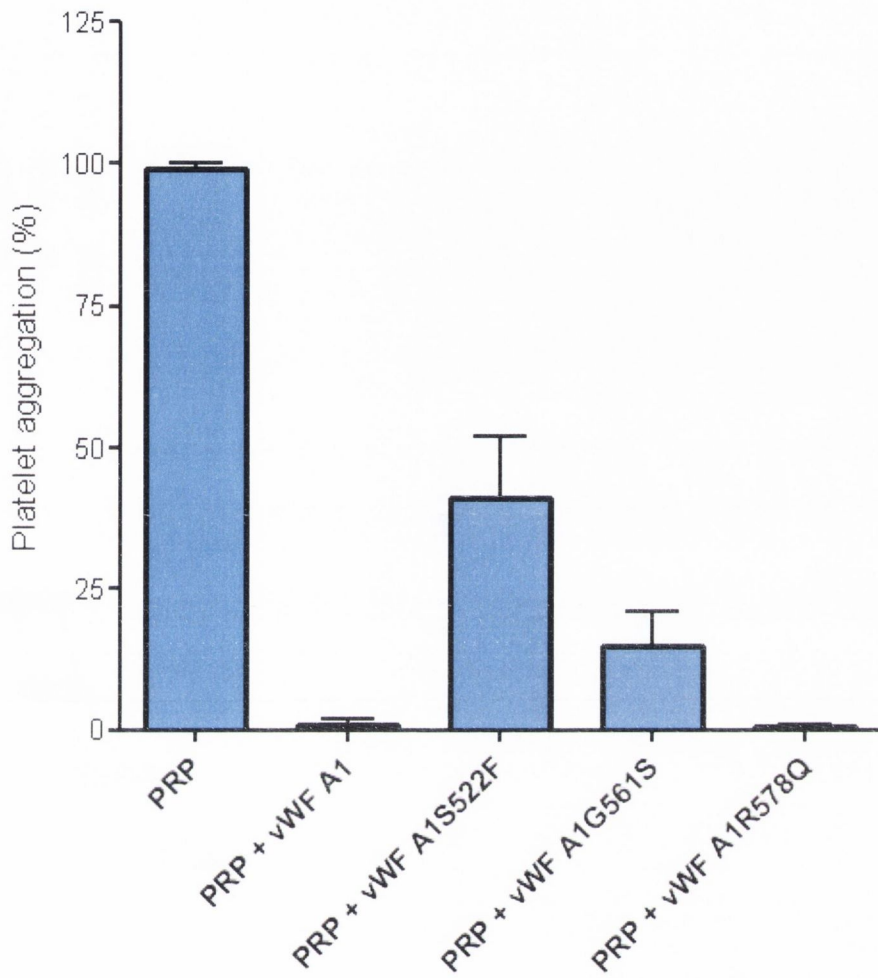


**Fig. 4.20. Effect of vWF A1 variants on ristocetin-induced platelet aggregation.** Platelet-rich plasma (PRP) was induced for platelet aggregation by addition of ristocetin (1 mg/ml) and the percentage platelet aggregation was measured after 15 min without prior incubation with vWF A1, or after 15 min incubation with 2  $\mu$ M vWF A1, vWF A1(S522F), vWF A1(G561S) or vWF A1(R578Q)



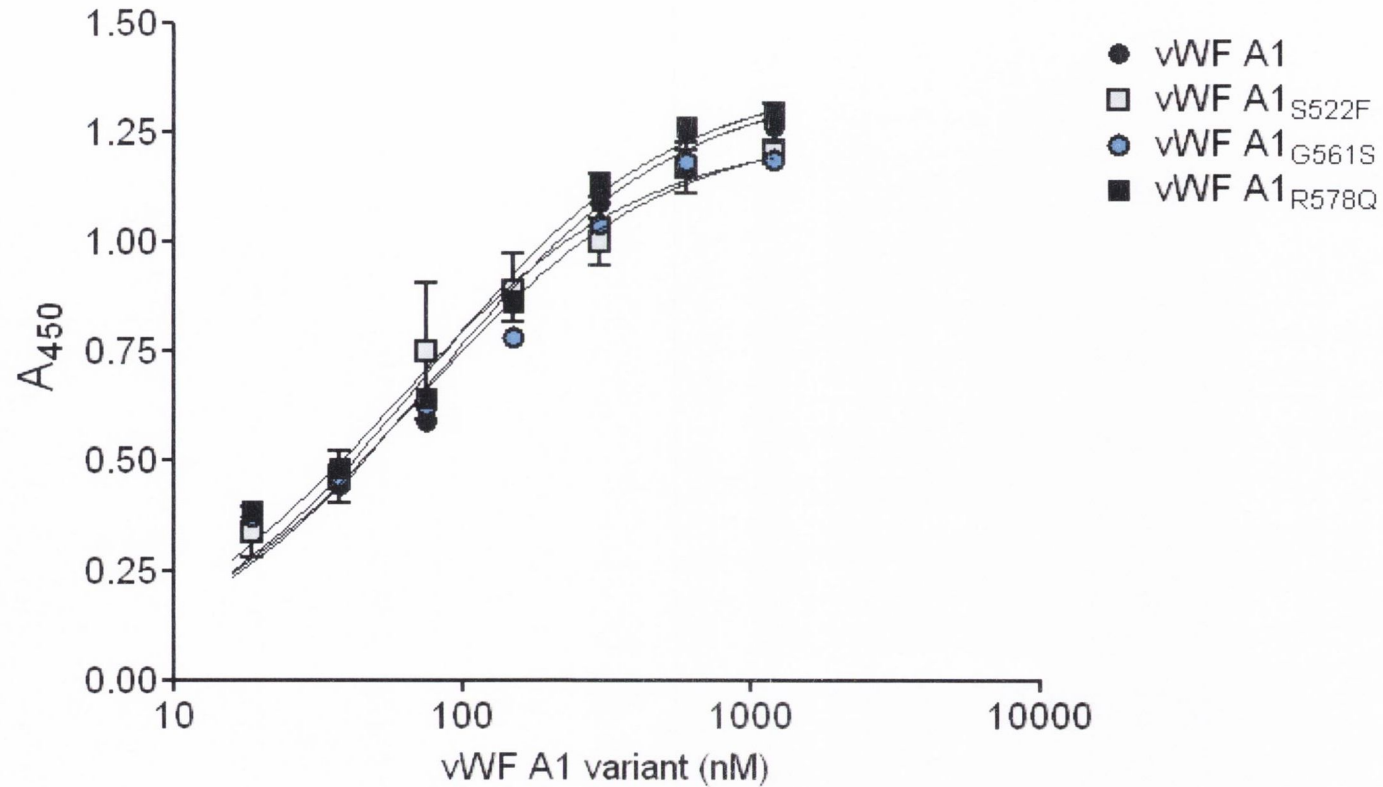


**Fig. 4.21. Interaction of vWF A1 variants with GST-SpaD.** Microtitre plates were coated with GST-SpaD (10  $\mu\text{g}/\text{mL}$ ) and incubated with increasing concentrations of vWF A1 or vWF A1 variants S522F, G561S or R578Q. Bound vWF was detected using monoclonal anti-6xHis antibody. Half-maximal binding for vWF A1 and each vWF A1 variant was calculated at approximately 100 nM. Values are the means  $\pm$  standard deviation of three separate experiments.

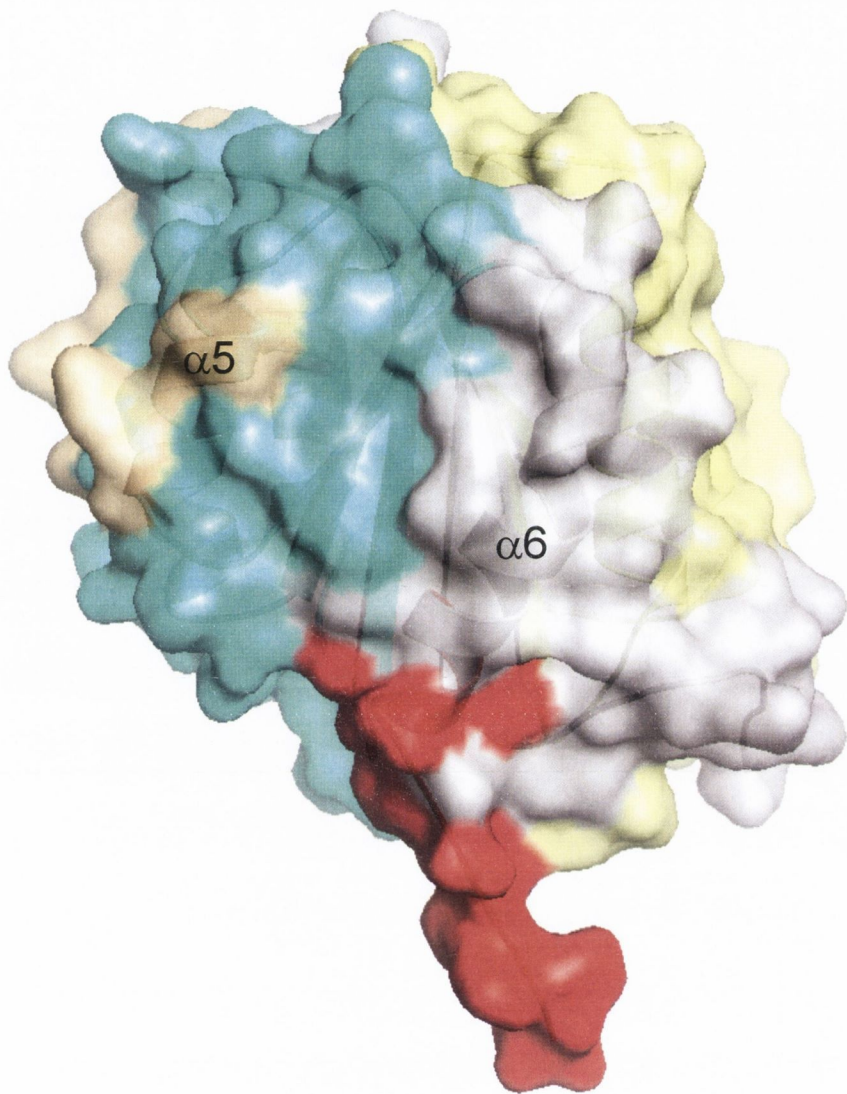


**Fig. 4.22 Proposed Spa binding region on vWF A1.** The site on vWF proposed to be involved in Spa binding based on inhibition and mutagenesis studies is shown coloured red. This region is also the proposed ristocetin/collagen binding domain. Regions of vWF A1 that are unlikely to form part of the Spa binding site based on inhibition studies using botrocetin (orange) and monoclonal anti-vWF antibodies 710 (cyan) and 723 (yellow) are also highlighted.

incubated for 18-24 h at 4 °C in a buffered solution containing human  $\alpha$ -thrombin (5  $\mu$ g/ml). The GST-fusion expressed by pGEX-KG has a thrombin-cleavage site between the GST moiety and the fusion protein. Untagged Spa was released and was passed over a benzamidine-sepharose column to remove human  $\alpha$ -thrombin from the preparation. The highly purified Spa was collected and used directly or stored at -20 °C. The Spa truncates studied were SpaEDABC, SpaDAB, SpaDA and SpaB. Recombinant vWF A1 harbouring an N-terminal 6xHis tag was purified as before (Cruz *et al.*, 2000; Emsley *et al.*, 1998). Despite specific binding between Spa and vWF A1 in solid-phase assays, X-ray crystallography trials performed by Dr. Jonas Emsley's group did not yield Spa-vWF A1 crystals in any of the conditions tested. Alternative binding studies in solution could shed more light on the conditions necessary for sufficient binding to occur to obtain crystals; tryptophan fluorescence quenching and isothermal titration calorimetry are possible alternatives. Also, creation of a C-terminal tagged protein may better represent the presentation of Spa domains *in vivo*. A study of the X-ray crystal structure of SpaD in complex with human V<sub>H</sub>3-Fab reported that SpaD was homodimeric in solution (Graille *et al.*, 2000). This may be an artifact of crystallization due to the hydrophobic residues of helices 1 and 2 in an aqueous environment. The helix 1-2 Fc $\gamma$ -binding region on SpaD was involved in dimerisation. Since this region also makes up the vWF-binding site, it may account for the absence of a Spa-vWF A1 complex in solution.

To investigate this, untagged Spa domain truncates were analysed by gel filtration (by Dr. Emsley's group). Data from gel filtration is shown in Figs. 4.23 (SpaEDABC and SpaDAB), 4.24 (SpaDA and SpaB) and 4.25 (vWF A1 and vWFA1/SpaEDABC). In all cases, the true peak volume is 2 ml less than the x-axis co-ordinate due to column calibration. Molecular weights were calculated using the calibration equation  $y = -0.1645x + 6.4375$  where  $y$  is the log of the molecular mass (in daltons) and  $x$  is the peak elution volume. In all cases data suggested that the Spa truncates were forming homo-dimers in solution. Filtration data for SpaEDABC and SpaDAB in Figure 4.23 show single peaks corresponding to 62 kDa and 37.9 kDa, respectively. However, the predicted masses of SpaEDABC (33 kDa) and SpaDAB (20 kDa) are approximately half those values. Similarly, the calculated molecular weight of SpaDA (14 kDa) was 28 kDa protein and SpaB (7 kDa) had an estimated molecular weight of 16.5 kDa (Fig. 4.24). These data showed that all Spa truncates tested formed dimers in solution which may explain the failure to form a complex between Spa and vWF A1. In order to confirm that there was no complex formation between Spa and vWF A1 in this setting, SpaEDABC and vWF A1 were mixed and incubated for 1 h at 37 °C. The mixture was analysed by gel filtration for



the presence a complex. Figure 4.25 shows gel filtration data obtained for vWF A1 (25 kDa) alone and for the vWF A1-SpaEDABC mixture. A complex with a 1:1 stoichiometry would be expected to form a peak at 58 kDa and if the SpaEDABC dimer was capable of binding vWF A1, a peak corresponding to 86 kDa would be recorded. However, only peaks corresponding to the SpaEDABC homo-dimer (62 kDa) and uncomplexed vWF A1 (22 kDa) were recorded. Further studies including NMR using Spa and vWF A1 under conditions of high shear will be performed in the future.

## 4.2.5 The interaction of protein A and platelets

### 4.2.5.1 The role of protein A in platelet aggregation

*S. aureus* cells bind to the surface of resting platelets and stimulate rapid activation and aggregation. The major pro-aggregatory surface proteins are ClfA and the FnBPs (Fitzgerald *et al.*, 2006; Loughman *et al.*, 2005). These proteins bind to platelets in a process that requires plasma fibrinogen or fibronectin to form a bridge between the bacterial adhesin and the low-affinity form of the platelet integrin  $\alpha_{IIb}\beta_3$  (also called GpIIb/IIIa). In addition antibody bound to the bacterial surface engages the platelet Fc receptor, Fc $\gamma$ R<sub>IIa</sub> which triggers signal transduction and activation. Previous work by light transmission aggregometry suggested that protein A did not have a prominent role in promoting *S. aureus* binding to or aggregation of platelets in plasma under the low shear conditions used (O'Brien *et al.*, 2002). However, more recent experiments have identified a role for Spa in promoting interactions with platelets under shear stress conditions where vWF in plasma is induced to form an active conformation that can bind the platelet receptor GpIb- $\alpha$  (Pawar *et al.*, 2004). Here the possible role of protein A in promoting *S. aureus* binding to platelets or in stimulating platelet activation and aggregation was investigated further. The ability of *S. aureus* Newman and *S. aureus* Newman *spa* (defective in expression of protein A) to stimulate aggregation was compared. Also, in order to examine any possible role for Spa in promoting activation that might be obscured by the potent pro-aggregatory surface protein clumping factor A (ClfA), the surrogate host *L. lactis* expressing Spa on its surface was studied. For comparison, *L. lactis* expressing ClfA was studied.

To confirm that Spa does not directly induce platelet aggregation, the ability of Spa to activate platelet aggregation was tested. *S. aureus* Newman is a potent activator of human platelets. Therefore the ability of Newman and Newman *spa* to induce platelet

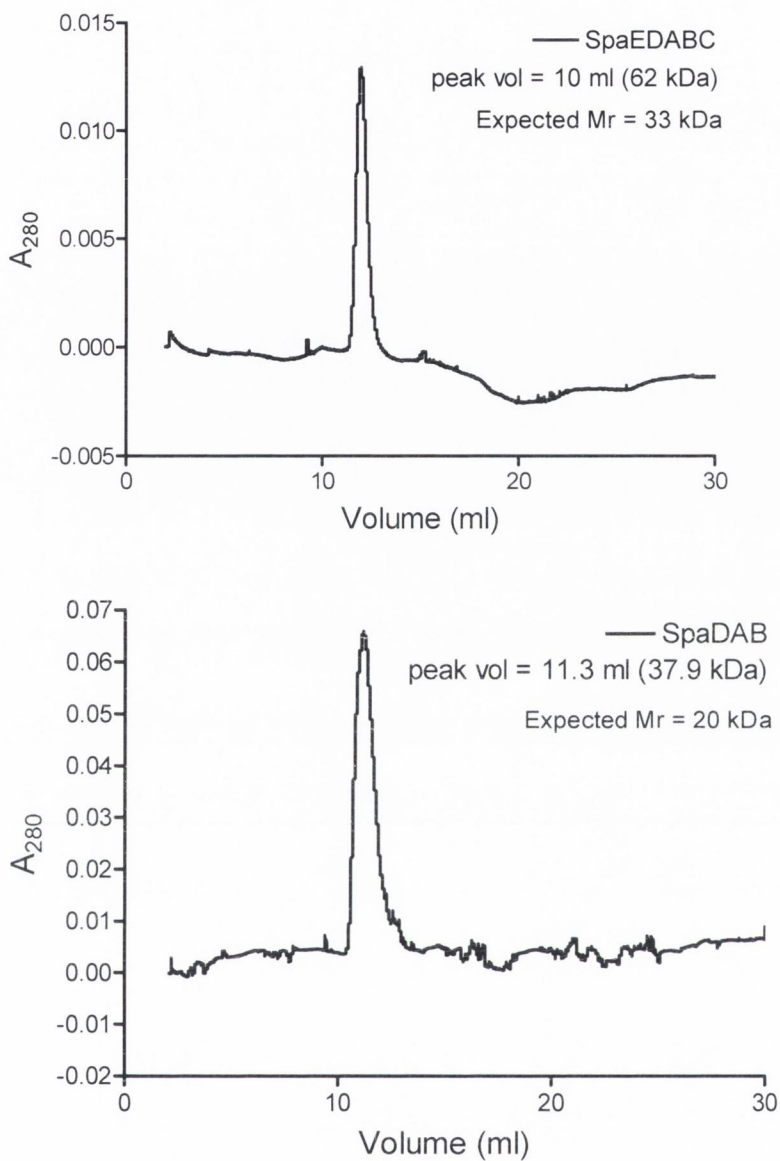


**Fig. 4.23. Gel filtraion analysis of SpaEDABC and SpaDAB.** 2 ml of untagged SpaEDABC and SpaDAB in TBS (100  $\mu$ g/ml) was applied to Superdex 75 10/300 GL columns and the fractions were analysed at 280 nm using a Bio-Logic HR FPLC (BioRad). The peak volume was used to calculate the molecular weight of the sample using the calibration equation  $y = -0.1645x + 6.4375$  where  $y$  is the log of the molecular mass (in daltons) and  $x$  is the peak elution volume. The expected molecular weights of SpaEDABC and SpaDAB are 33 kDa and 20 kDa, respectively.

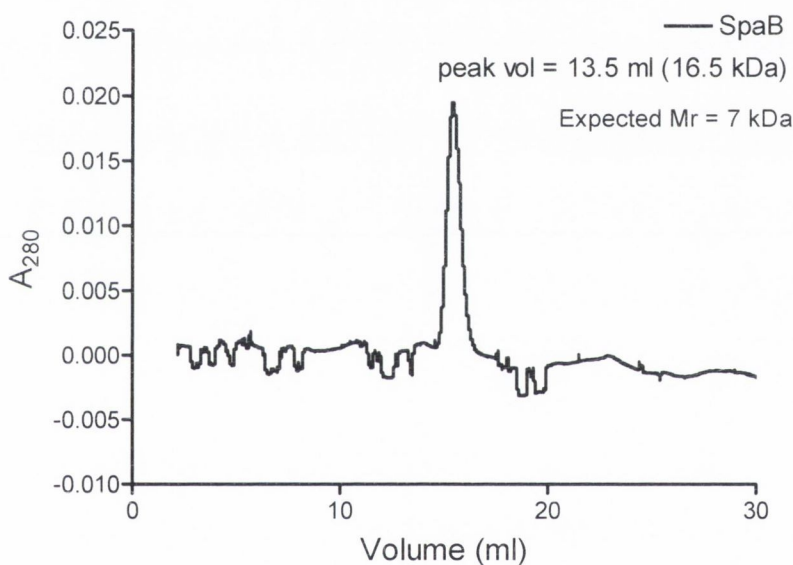
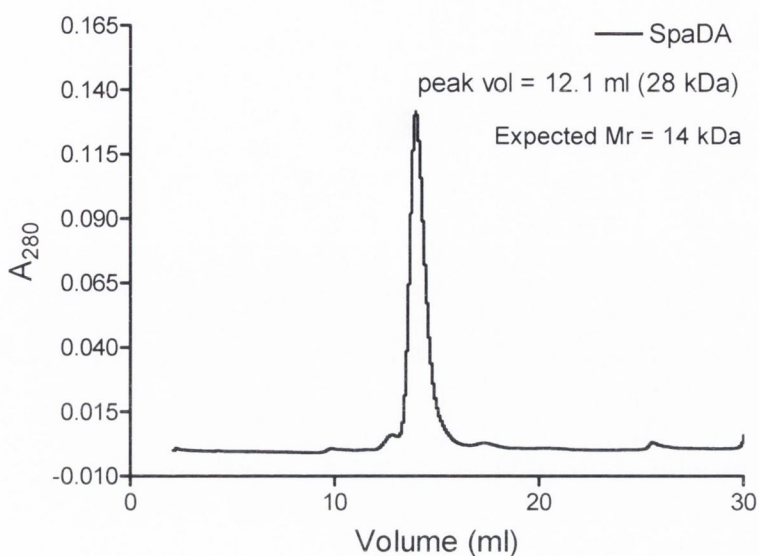


**Fig. 4.24. Gel filtration analysis of SpaDA and SpaB.** 2 ml of untagged SpaDA and SpaB in TBS (100  $\mu\text{g/ml}$ ) was applied to Superdex 75 10/300 GL columns and the fractions were analysed at 280 nm using a Bio-Logic HR FPLC (BioRad). The peak volume was used to calculate the molecular weight of the sample using the calibration equation  $y = -0.1645x + 6.4375$  where  $y$  is the log of the molecular mass (in daltons) and  $x$  is the peak elution volume. The expected molecular weights of SpaDA and SpaB are 14 kDa and 7 kDa, respectively.



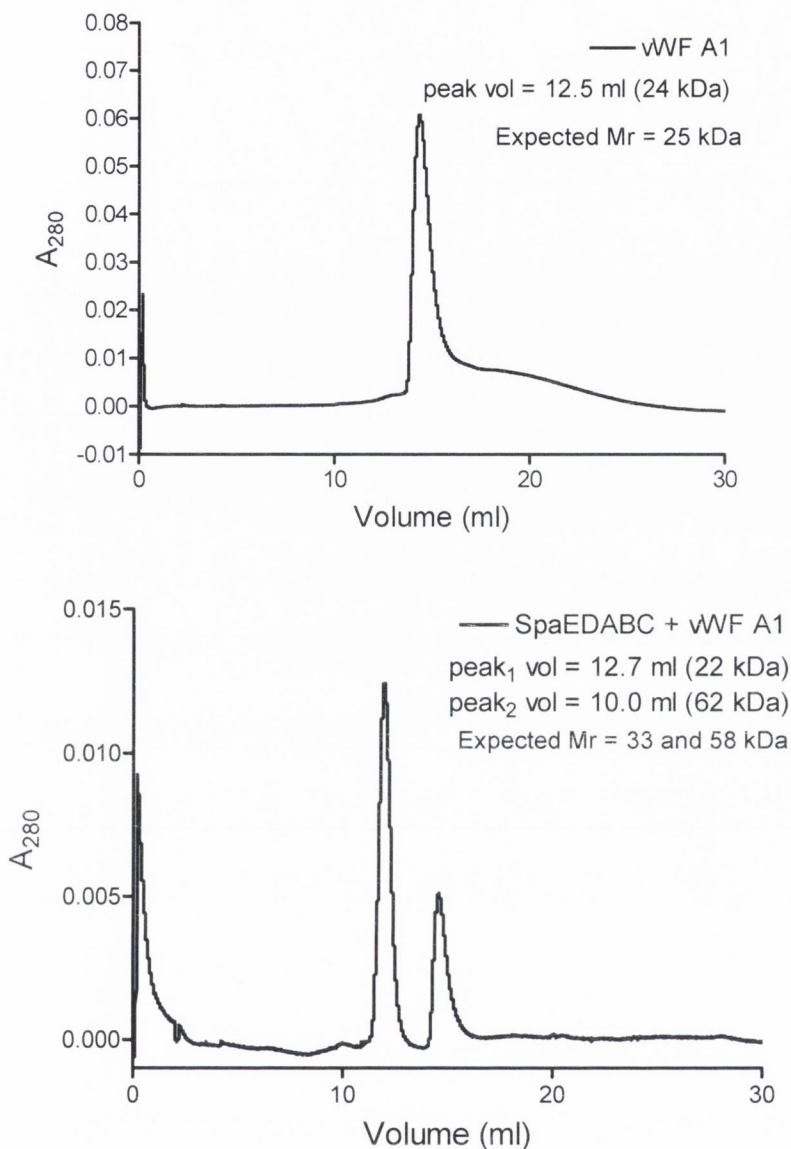


**Fig. 4.25. Gel filtration analysis of vWF A1 and SpaEDABC/vWF A1.** 2 ml of vWF A1 in TBS (100  $\mu\text{g/ml}$ ) or a mixture of SpaEDABC/vWF A1 that had been incubated at 37  $^{\circ}\text{C}$  for 1h in TBS (100  $\mu\text{g/ml}$ ) was applied to Superdex 75 10/300 columns and the fractions were analysed at 280 nm using a Bio-Logic HR FPLC (BioRad). The peak volumes were used to calculate the molecular weight of the sample using the calibration equation  $y = -0.1645x + 6.4375$  where  $y$  is the log of the molecular mass (in daltons) and  $x$  is the peak elution volume. The expected molecular weights of vWF A1, SpaEDABC and a SpaEDABC/vWF A1 complex are 25 kDa, 33 kDa and 58 kDa, respectively.

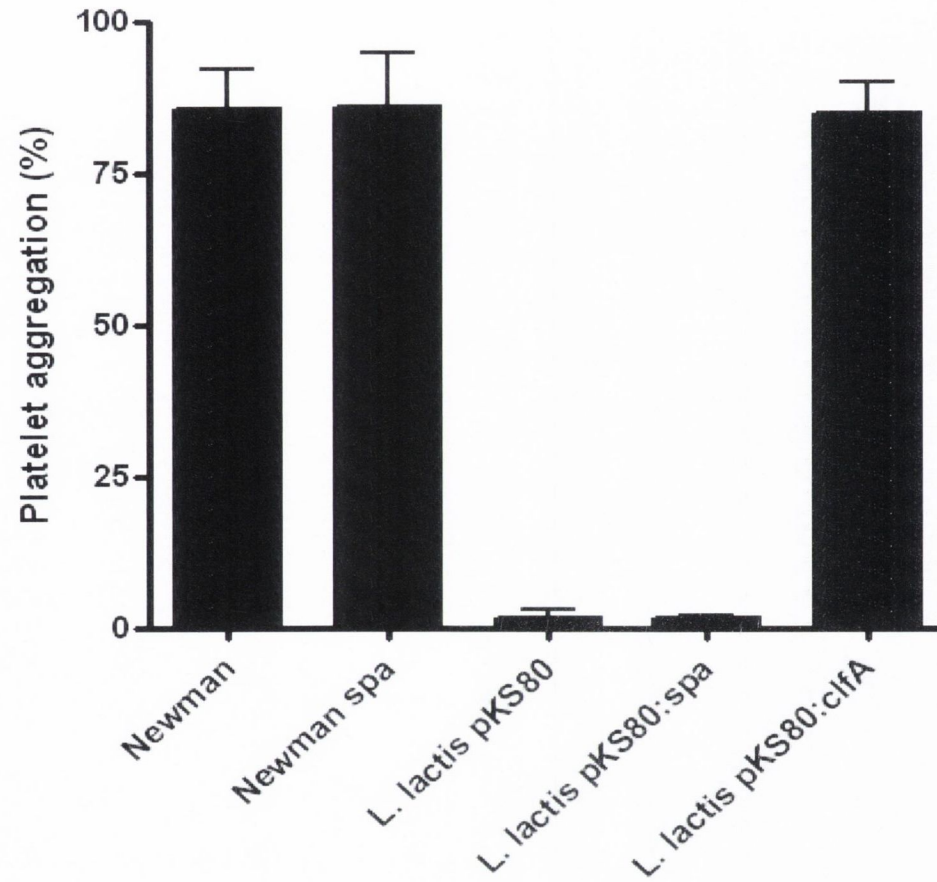


**Fig. 4.26. The effect of Spa expression on platelet aggregation.** Platelet-rich plasma (PRP) was incubated with *S. aureus* Newman, Newman *spa*, *L. lactis*(pKS80), *L. lactis*(pKS80*spa*) or *L. lactis*(pKS80*clfA*) at an OD<sub>600</sub> of 0.16 and the percentage aggregation measured after 15 min in a platelet aggregometer. Where platelet aggregation occurred, the lag time to aggregation was under 3 min. Experiments were performed three times using different donors and the mean  $\pm$  SEM calculated.

aggregation was compared. Platelet aggregation studies using *L. lactis* (pKS80), *L. lactis* (pKS80:*spa*) and *L. lactis* (pKS80:*clfA*) were also performed. Bacterial cells were grown to stationary phase (16 h), washed and resuspended in PBS to an OD<sub>600</sub> of 1.6 as described (section 2.16). The ability of the bacteria to induce platelet agglutination in PRP was tested. Data are in agreement with previously published observations. Newman, Newman *spa* and *L. lactis* (pKS80:*clfA*) caused 80-100 % platelet aggregation with very short lag times (1-2 min) whereas *L. lactis* pKS80 and *L. lactis* pKS80:*spa* did not induce platelet aggregation (Fig. 4.26).

It is possible that Spa enhances *S. aureus*-induced platelet aggregation in conditions that favour vWF-platelet interactions since the low shear rates present in a standard aggregometer (300 s<sup>-1</sup>) do not promote binding of vWF to platelets via GpIb- $\alpha$ . To investigate this, the effect of pre-incubation of PRP with soluble Spa on ristocetin-induced platelet aggregation (RIPA) was tested. Ristocetin binds to the A1 domain on vWF, induces a conformational change that activates vWF and stimulates platelet binding, activation and aggregation without the need for high shear. PRP was incubated with recombinant Spa (4  $\mu$ M) for 15 min at 37 °C, followed by the addition of ristocetin (1 mg/ml). The results show ristocetin-induced platelet aggregation did not occur in the presence of soluble Spa (Fig. 4.27). That Spa completely abolished this may be due to a shared binding site on vWF A1 for ristocetin. Ristocetin inhibits GST-SpaD binding to recombinant vWF A1 (Fig. 4.18). To investigate whether the observed inhibition is dependent on active vWF, the effect of Spa on platelet aggregation induced by the modulators botrocetin, ADP, thrombin-receptor activating peptide (TRAP), the platelet activating ligand collagen and by *S. aureus* Newman (OD<sub>600</sub> of 1.6) was tested. Modulators were used at recommended concentrations. Botrocetin and Spa do not compete for binding on vWF A1 (Fig. 4.18) and ADP, TRAP and collagen induce platelet aggregation independently of vWF. Stationary phase *S. aureus* Newman activates and aggregation platelets through ClfA and fibrinogen and ClfA-specific IgG binding to Fc $\gamma$ R<sub>IIa</sub>. Pre-incubation of PRP with Spa inhibited platelet agglutination for all of the modulators tested, including *S. aureus* Newman (Fig. 4.28). These data open up the possibility that protein A binds a platelet receptor without inducing platelet activation.

#### 4.2.5.2 Protein A binds directly to resting platelets

Inhibition of platelet aggregation by pre-incubation of platelets with Spa suggests a direct interaction with Spa and resting platelets. The previously reported interaction



between Spa and the complement receptor gC1qR/p33 interaction is unlikely to account for this as this receptor is poorly expressed on resting platelets (Nguyen *et al.*, 2000). To investigate if a direct interaction occurs between Spa and platelets, a platelet adherence assay was performed. *L. lactis* pKS80 and *L. lactis* pKS80:*spa* were grown to stationary phase, washed and resuspended in PBS to an OD<sub>600</sub> of 1.0 and adherence of gel-filtered platelets (GFPs) to the immobilised bacteria was tested as described in section 2.14.3. Adherence of platelets to fibrinogen-coated wells was also measured as a positive control. Resting platelets are known to adhere to fibrinogen via  $\alpha_{IIb}\beta_3$  when it has been immobilised on a surface (Polanowska-Grabowska *et al.*, 1999; Shiba *et al.*, 1991). GFP preparations do not contain any plasma proteins and can be used to assay for direct platelet interactions. Adherent platelets were detected by using a lysis buffer containing a chromogenic substrate for acid phosphatase, which is released from lysed platelets. Platelets adhered to *L. lactis* (pKS80:*spa*) but not to *L. lactis* (pKS80) (Fig. 4.29).

Given the inhibitory effect on platelet aggregation by Spa, one possible ligand is the platelet membrane glycoprotein,  $\alpha_{IIb}\beta_3$ . Aggregation of platelets occurs through cross-linking of activated platelets mediated by the interaction of fibrinogen and von Willebrand factor with  $\alpha_{IIb}\beta_3$ . To investigate this, platelets were incubated with tirofiban (5 nM), an  $\alpha_{IIb}\beta_3$ -blocking peptide prior to binding studies with immobilised to *L. lactis* (pKS80:*spa*). The addition of tirofiban inhibited the binding of platelets to  $\alpha_{IIb}\beta_3$ , suggesting that Spa can interact directly with  $\alpha_{IIb}\beta_3$  on resting platelets (Fig. 4.29). This is further supported by data from Dr. Peter Lenting's research group who have observed a specific interaction between recombinant Spa and purified  $\alpha_{IIb}\beta_3$  by surface plasmon resonance (personal communication).

#### 4.2.6 Studies on the interaction between protein A and TNFR1

It has recently been reported that protein A binds tumour necrosis factor receptor-1 (TNFR1) (Gomez *et al.*, 2004). This interaction is central to *S. aureus*-induced inflammation of airway epithelial cells and plays key role in the pathogenesis of staphylococcal pneumonia. Two major steps in the inflammation process are TNFR1-dependent CXCL8 production and TNFR1 shedding. A collaborative effort was made to determine the TNFR1 binding site on Spa with Dr. Alice Prince's group who first reported the interaction. It was demonstrated that recombinant Spa induced TNFR1 mobilisation and receptor shedding from airway epithelial cells. Shedding of TNFR in response to Spa

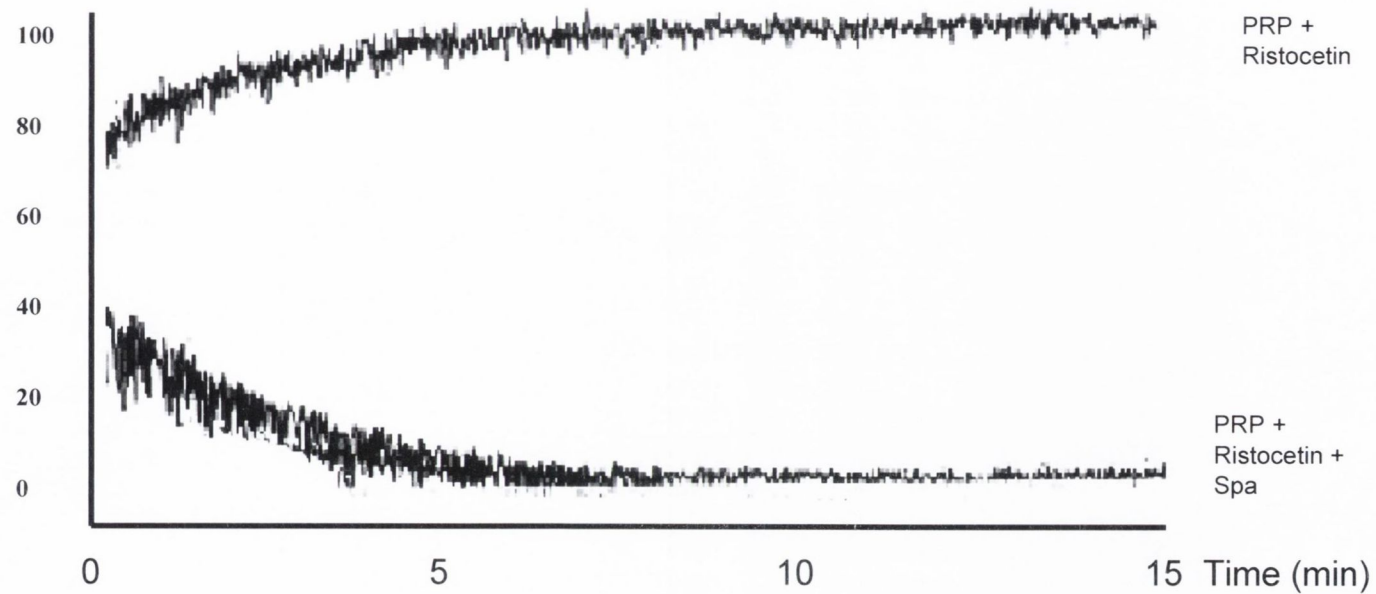


**Fig. 4.27 The effect of Spa on ristocetin-induced platelet aggregation.** Aggregation of platelet-rich plasma (PRP) or PRP that had been incubated with recombinant Spa ( $4 \mu\text{M}$ ) was induced by the addition of ristocetin ( $2 \mu\text{M}$ ) and aggregation was measured in a platelet aggregometer for 15 min. The experiment was performed three times using three different donors and a representative aggregometer trace is shown.

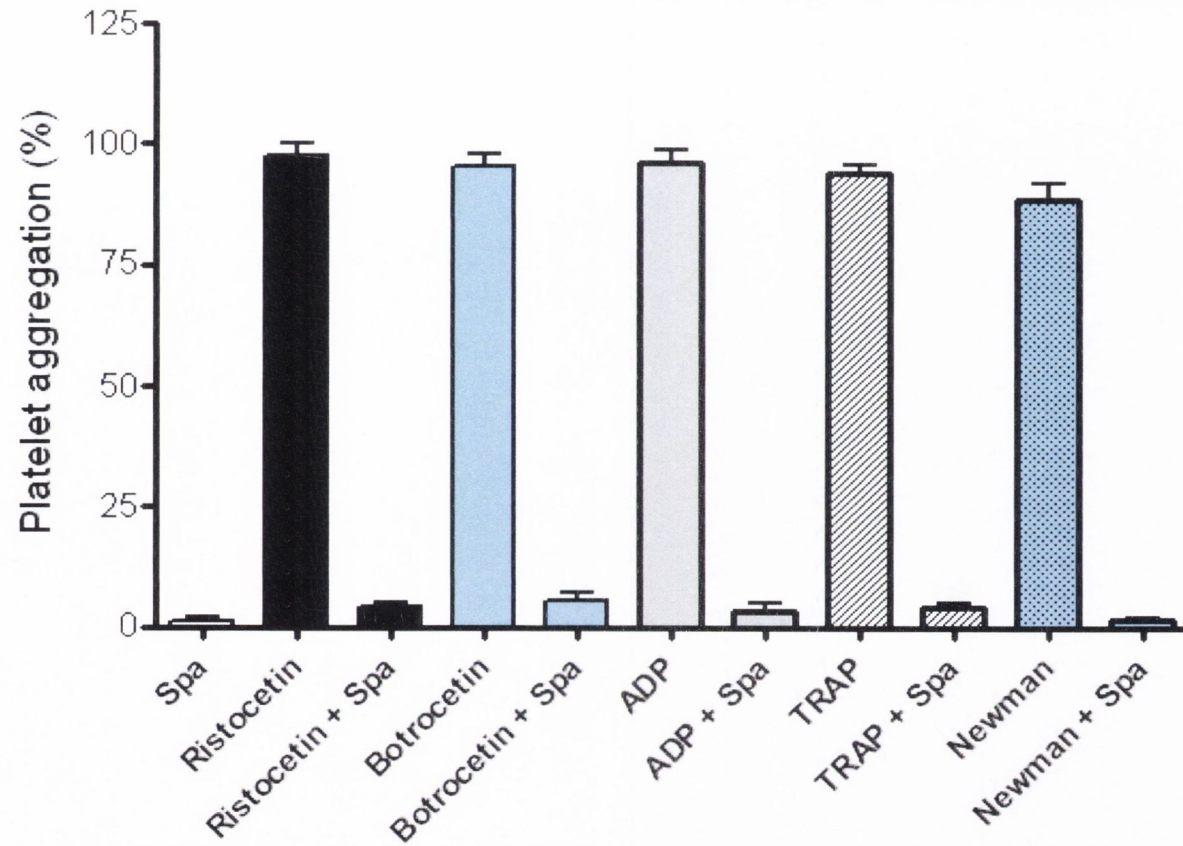


**Fig. 4.28. Inhibition of platelet aggregation by Spa.** Aggregation of platelet-rich plasma (PRP) or PRP that had been incubated with recombinant Spa (4 mM) was induced by the addition of the pro-aggregatory agents ristocetin, botrocetin, ADP, thrombin receptor-activating peptide (TRAP) and *S. aureus* Newman. Platelet aggregation was measured in a platelet aggregometer for 15 min. The experiment was performed three times using different plasma donors and the mean percentage aggregation and the mean  $\pm$  SEM after 15 min calculated.



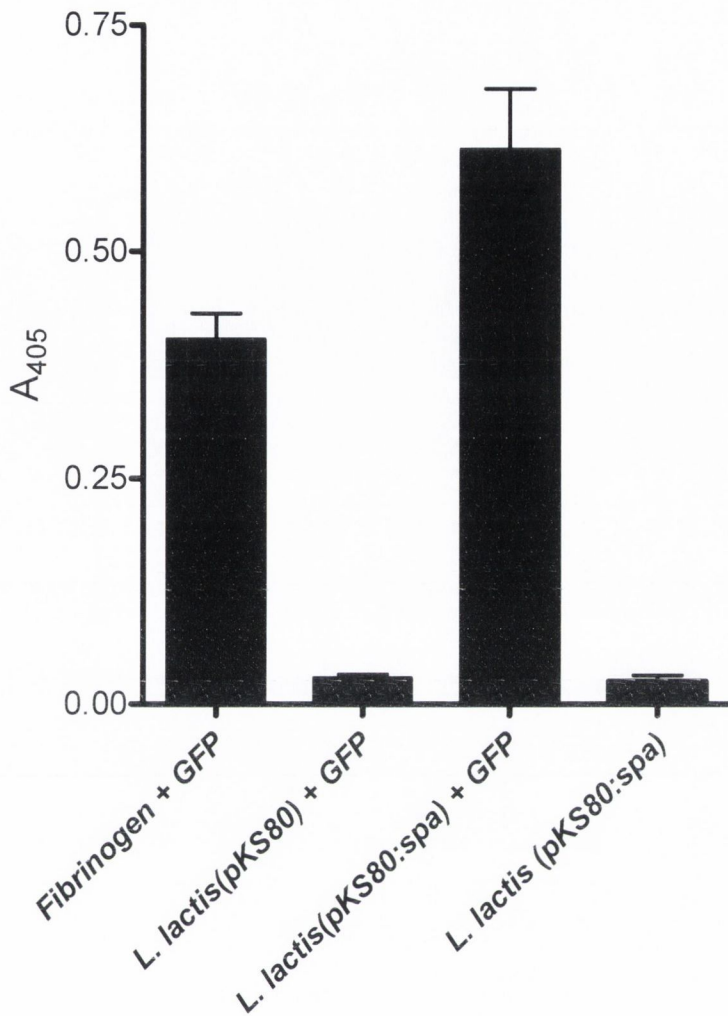


**Fig. 4.29. Adherence of platelets to bacteria expressing Spa.** Microtitre plates coated with human fibrinogen (10  $\mu\text{g/ml}$ ) or 100  $\mu\text{l}$  of a suspension ( $\text{OD}_{600}=1.0$ ) of *L. lactis*(pKS80), *L. lactis*(pKS80:spa) were incubated with gel-filtered (washed) platelets (GFPs) ( $1 \times 10^7$  platelets) or GFPs containing the specific  $\alpha_{\text{IIb}}\beta_3$ -blocker, tirofiban (5 nM) and platelet adherence was measured. The experiment was performed three times with different donors and the mean platelet adherence  $\pm$  SEM calculated.

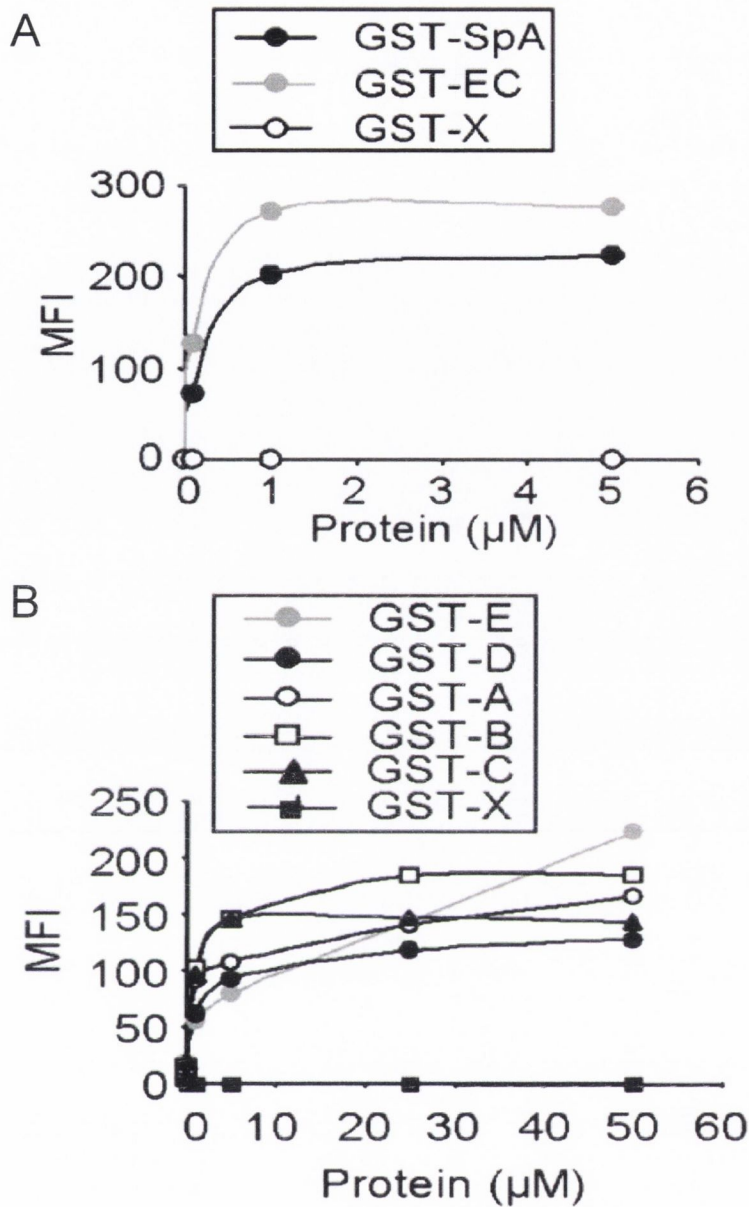


**Fig. 4.30 Interaction of Spa truncates with TNFR1-expressing airway epithelial cells.** Epithelial cells were incubated with GST-Spa fusion proteins as follows: GST-SpA, full-length Spa; GST-EC Spa domains EDABC; and GST-X, Spa residues C-terminal of domains EDABC (A) and GST-E, Spa domain E, GST-D, Spa domain D, GST-A, Spa domain A, GST-B, Spa domain B and GST-C, Spa domain C (B). Binding of the protein constructs to the surface was quantified by flow cytometry. *MFI*, mean fluorescence intensity. One representative experiment of three is shown. Figure taken from Gomez *et al.*, 2006.

was due to a metalloprotease, the tumour necrosis factor- $\alpha$  converting enzyme (TACE) which is activated (by phosphorylation) in response to protein A exposure.

In a similar approach to that taken for mapping the vWF binding site on Spa, GST-SpaEDABC and GST-Spa-C-term (a control protein comprising the portion of Spa C-terminal of the Ig-binding repeat region designated GST-X in Fig. 4.30 A) were tested for binding airway epithelial cells by confocal fluorescent microscopy and staining for GST-Spa and TNFR1. Binding was detected for GST-SpaEDABC but not GST-Spa-C-term, indicating that the Ig-binding region of Spa is also responsible for interacting with TNFR1 (Fig. 4.30 A). To investigate whether individual Spa domains could bind TNFR1, the interaction of fluorescent GST-SpaE, GST-SpaD, GST-SpaA, GST-SpaB and GST-SpaC with surface of airway epithelial cells was quantified by flow cytometry. All individual domains bound, but with a lower affinity than the GST-SpaEDABC construct (Fig. 4.30 B). A selection of GST-Spa variants generated in this study was assayed for binding airway epithelial cells by flow cytometry in order to map the TNFR1-binding site on Spa. The binding region was localised to the helix 1-2 interface of SpaD, the region also responsible for binding to Fc $\gamma$  and vWF. Substitution of residues on the helix 2-3 face involved in V<sub>H</sub>3-Fab binding did not affect the Spa-TNFR1 interaction (Fig. 4.31). Interestingly, The GST-SpaD variants L17A and F5A retained the ability to induce IL-8 induction but not TNFR1 shedding.

In addition to binding TNFR1, Spa has been shown to bind the epidermal growth factor receptor (EGFR) which is apically expressed in airway epithelial cells. GST-SpaD(F5A) and GST-SpaD(L17A) were analysed for their ability to bind EGFR. There was no interaction, demonstrating that the binding regions for TNFR1 and EGFR are distinct and that the Spa-EGFR interaction is essential for receptor shedding. Indeed, the Spa-EGFR interaction was responsible for TACE activation by phosphorylation of EGFR. These data strongly suggest a multifunctional role of Spa in staphylococcal pathogenesis in different environmental niches in the host.



### 4.3 Discussion

The experiments described in this chapter set out to identify the sites on Spa and vWF A1 involved in their binding. In addition, the possibility that Spa could bind directly to platelets was investigated. To investigate the vWF-binding site on Spa, inhibition studies were employed using well-characterised ligands for Spa. A single Spa domain has binding sites for the Fc $\gamma$  region of most mammalian IgGs and the Fab region of Ig bearing heavy chains of the V<sub>H3</sub> subgroup. The binding site on Spa for Fc $\gamma$  and V<sub>H3</sub>-Fab comprises residues on helices 1 and 2 and helices 2 and 3, respectively. Structural studies have demonstrated how a single Spa domain can simultaneously bind Fc $\gamma$  and V<sub>H3</sub>-Fab (Graille *et al.*, 2000). Binding studies using both ligands and a Spa domain supported this *in silico* observation (Roben *et al.*, 1995; Starovasnik *et al.*, 1999).

Studies using rabbit IgG and human IgM bearing V<sub>H3</sub> heavy chains to inhibit SpaD binding to vWF A1 showed that both ligands blocked the interaction (Fig. 4.2). Since the binding sites on Spa for these factors are distinct, the observed inhibition by either or both ligands may have been due to steric blocking of the vWF-binding site. Smaller Ig fragments were used to overcome this. A commercial preparation of human Fc $\gamma$  and *E. coli*-expressed V<sub>H3</sub>-Fab were less likely to cause steric blocking of vWF binding (Fig. 4.5). It was shown that Fc $\gamma$  but not V<sub>H3</sub>-Fab blocked the binding of Spa to vWF A1 in a dose-dependent and saturable manner (Fig. 4.6). This suggested that the vWF binding site occurred on Spa overlaps or is in close proximity to the Fc $\gamma$ -binding site.

Variants of GST-SpaD were generated to identify the residues on Spa that are important for vWF-binding. Residues from the Fc $\gamma$ - and V<sub>H3</sub>-Fab-binding regions and a selection of residues that are conserved in each Spa domain were substituted. In addition, a SpaD variant devoid of three N-terminal residues unique to this domain was constructed (Fig. 4.7). The affinity for IgG of the GST-SpaD variants was generally in agreement with previous structural and mutagenesis studies and important residues clustered onto the NMR complex of Fc $\gamma$  and Spa (Fig. 4.10). Residues Q10, F13, Y14, L17, N28, I31 and K35 which are known to be involved in the Fc $\gamma$  interaction were shown to be defective in IgG binding when substituted to alanine. Variants F5A and Q9A did not show reduced IgG binding in the current study but have been proposed to participate in Fc $\gamma$ -binding. Similarly, GST-SpaD(Q32A) bound IgG with the same affinity as the wild-type GST-SpaD. Q32 is the only residue implicated in binding to both Fc $\gamma$  and V<sub>H3</sub>-Fab. The 58-residue variant of SpaD bound IgG with higher affinity than the 61 residue wild-type

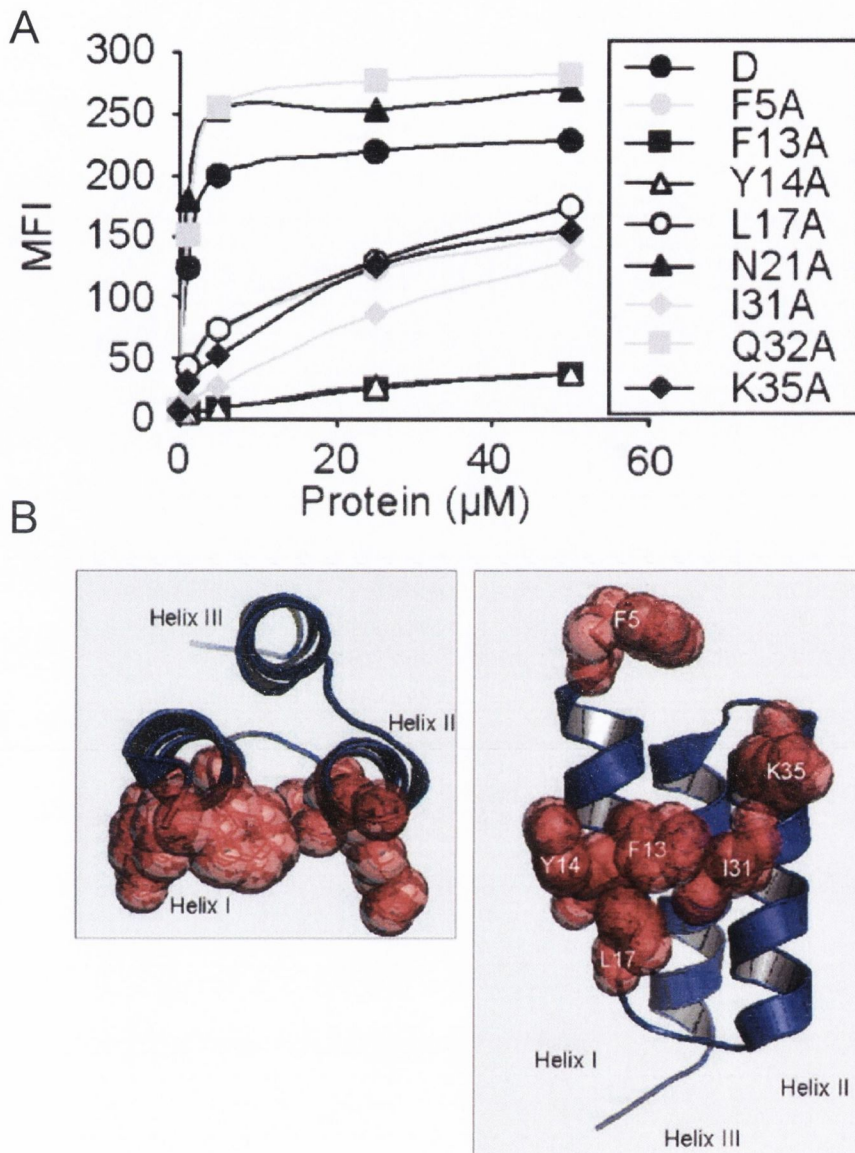


**Fig. 4.31. The TNFR1 binding region on Spa.** *A*, epithelial cells were incubated with GST-SpaD or GST-SpaD variants and binding to the surface was quantified by flow cytometry. *MFI*, mean fluorescence intensity. One representative experiment of three is shown. (*B*) SpaD viewed from above (*left*) and from the side (*right*) with residues shown to be important in TNFR1 binding highlighted in *red*. Taken from Gomez *et al.*, 2006.



SpaD, in agreement with work by others. This is likely due to hindrance of the Spa helix 1 contact residues for Fc $\gamma$  by the N-terminal Ala-Glu-Glu in this domain. Substitution of residues known to be involved in V<sub>H3</sub>-Fab-binding had no effect on the interaction of Spa with Fc $\gamma$  interaction. The reduced IgG binding of GST-SpaD(L34A) was unexpected. L34 is conserved in all Spa domains but is not involved in binding to either Fc $\gamma$  and V<sub>H3</sub>-Fab. Analysis of the structure of SpaD shows that the hydrophobic side-chain of L34 may stabilise the packing of helices 1 and 2 (Fig. 4.10). The L34A substitution may cause reduced affinity for Fc $\gamma$  by destabilising the Spa three helix bundle. A misfolded Spa domain would also be defective in binding to V<sub>H3</sub>-Fab.

The ability of GST-SpaD variants to bind to V<sub>H3</sub>-Fab was also investigated. The GST-Spa variants G29A, F30A, D36A, D37A, Q40A and E47A bound V<sub>H3</sub>-Fab with reduced affinity (Fig. 4.11). Substitution of acidic residues D36, D37 and E47 disrupts the polar contacts responsible for the majority of the Spa V<sub>H3</sub>-Fab interface (Graille *et al.*, 2000). The substitution G29A has been previously shown to eliminate binding to V<sub>H3</sub>-Fab most likely due to steric blocking by the side chain of alanine. In addition to reduced affinity for IgG, variant L34A was also defective in binding to V<sub>H3</sub>-Fab. This strongly suggests that substitution of L34 disrupts the folding of Spa. Variants of the Fc $\gamma$ -binding region Q9A, Q10A and I31A bound V<sub>H3</sub>-Fab with a lower affinity than wild-type SpaD. It is unclear why a reduction in V<sub>H3</sub>-Fab binding is seen in the case of GST-SpaD(Q9A) which does not exhibit reduced Fc $\gamma$  binding. The side-chain of GST-SpaD(Q10A) does not appear to be involved in stabilising SpaD or interacting with any residues on V<sub>H3</sub>-Fab. The side-chain of I31 makes up part of the hydrophobic core of Spa and may therefore affect V<sub>H3</sub>-Fab-binding when substituted to alanine. Reduced binding was also seen for variant GST-SpaD(R27A) which also does not map to the Spa V<sub>H3</sub>-Fab binding interface (Fig. 4.12). It is possible that V<sub>H3</sub>-Fab binding is more sensitive to structural changes in Spa than the Fc $\gamma$  interaction.

The GST-SpaD variants were next assayed for vWF A1 binding. Inhibition studies using Fc $\gamma$  and V<sub>H3</sub>-Fab suggested that the vWF A1 binding region on SpaD overlaps that of Fc $\gamma$  and is unlikely to involve residues involved in V<sub>H3</sub>-Fab binding. The relative binding of each SpaD variant to vWFA1 mapped the vWF A1 binding site to the helix 1-2 face of Spa (Fig. 4.14). Similar studies on the binding of GST-SpaD variants to vWF D'-D3 indicated that the same region on protein A is responsible for binding vWF A1 and D'-D3 (Fig. 4.15). Variants Q10A, F13A, Y14A, L17A, N28A, F30A, I31A and K35A showed a two-fold or greater decrease in vWF A1 binding and substitution of R27 to



alanine reduced binding by 46 % (Fig. 4.13). With the exception of R27 and F30, all variants affecting the vWF A1 interaction also had defective IgG binding. The phenyl ring of Phe30 is sandwiched between residues Leu44 and Leu51 of helix 3 in the solution structures of the B and Z domains, contributing to the tightly packed hydrophobic core (Cedergren *et al.*, 1993; Deisenhofer, 1981). Substitution of F30 to alanine is reported to result in binding affinities for Fc $\gamma$  essentially identical to those of wild-type domains. Replacement of Phe30 by alanine apparently disrupts this hydrophobic core and may destabilize the protein structure under certain conditions (Cedergren *et al.*, 1993). It is possible F30 supports the tertiary structure of Spa by stabilising the hydrophobic core at the helix 2-3 interface, resulting in reduced binding to vWF A1 (Fig. 4.14).

Binding of protein A to IgG or vWF *in vivo* is likely to be dependent on the environmental niche within the host. Spa binds vWF in the presence of physiological IgG concentrations *in vitro* and in whole blood. It is possible that binding of full-length Spa to IgG and vWF can occur simultaneously through separate Spa domains.

The binding site on vWF was also investigated by studying the ability of known ligands for vWF A1 to block binding to Spa and testing the ability of Spa to bind vWF A1 variants with active or inactive conformations for platelet binding. The vWF ligands included the vWF A1 modulators botrocetin, ristocetin and collagen and a number of anti-vWF A1 mAb Fab fragments. Inhibition studies using these ligands revealed that ristocetin blocked vWF A1 binding to Spa in a dose-dependent and saturable manner (Fig. 4.18). Dose-dependent inhibition of the interaction was also observed by the addition of collagen, although saturation was not achieved (Fig. 4.18). None of the anti-vWF A1 mAbs inhibited binding to Spa, suggesting that the vWF A1 regions Ser 523-Gly588, Ser593-Ser678 do not contain the protein A binding site. Indeed, an increase in Spa-vWF A1 binding was observed when mAbs 700 and 724 were employed. There is no data on the nature of the mAb 700 binding site on vWF A1 whereas mAb 724 promotes vWF-induced shear-dependent platelet aggregation, presumably through conformational changes induced in vWF A1. It is possible that binding to vWF A1 by mAb 724 induces a more favourable conformation for the interaction with Spa. This is made more plausible by the fact that binding by *S. aureus* to vWF in solution is dependent on high shear. It is also possible that the inhibition of Spa-vWF A1 binding by ristocetin and collagen occurs through structural changes in A1 upon ligand binding rather than shared binding sites.

To investigate this further, vWF A1 variants known to cause constitutively active or inactive conformations in vWF A1 were tested. These variants were identified from patients with type 2B and 2M VWD, respectively. Type 2B VWD is characterised by

increased binding to GpIb- $\alpha$  due to a conformationally active vWF A1 domain whereas vWF from patients with type 2M VWD has a lowered binding to GpIb- $\alpha$ . The vWF A1 variants used were S522F, G562S (type 2M VWD) and R578Q (type 2B VWD). The substitution G562S has been shown to impair the conformational change in vWF A1 induced by collagen binding. Each vWF A1 variant bound GST-SpaD dose-dependently and saturable with equal affinity when tested by solid-phase binding (Fig. 4.21). This suggests that inhibition of the Spa-vWF A1 interaction by collagen and ristocetin is due to competitive binding at a site on vWF A1.

The binding of Spa to vWF A1 in a region overlapping the site for ristocetin and collagen opens the possibility that Spa may influence the conformation of vWF A1. The interaction between protein A and vWF has been shown to promote adherence to vWF- or collagen-coated surfaces to platelets (Hartleib *et al.*, 2000; Mascari and Ross, 2003). Protein A also binds to platelets directly through the gC1qR/p33 receptor (Nguyen *et al.*, 2000). gC1qR/p33 is only expressed on the surface of platelets that have been activated for example by adhesion to immobilised fibrinogen or fibronectin. For this reason, the Spa-gC1qR/p33 interaction is believed to contribute to bacterial colonisation at sites of vascular injury where a thrombus has formed rather than initiating bacterial tethering to resting platelets. The binding of *S. aureus* to platelets in suspension occurs under conditions of high shear predominantly through Spa-vWF bridging (Pawar *et al.*, 2004).

It has been clearly demonstrated that bacterial attachment to platelets via fibrinogen or fibronectin bridges involving ClfA or FnBPs causes rapid platelet activation and subsequent aggregation (Fitzgerald *et al.*, 2006; Loughman *et al.*, 2005). Spa-deficient mutants of *S. aureus* have an increased lag time of platelet aggregation (O'Brien *et al.*, 2002). However heterologous expression of protein A on the surface of *L. lactis* does not activate platelets.

Figure 4.26 confirms previous data by O'Brien *et al.* that expression of protein A on the surface of *L. lactis* is not sufficient for bacterial-induced platelet aggregation in the conditions of low shear. The low shear rates present in a standard aggregometer ( $300 \text{ s}^{-1}$ ) do not support vWF-platelet binding unless a modulator such as ristocetin is added. It is possible that Spa plays a role in *S. aureus*-induced platelet aggregation in conditions where vWF-platelet interactions occur. To investigate this, the effect of pre-incubation of PRP with recombinant Spa on ristocetin-induced platelet aggregation (RIPA) was tested. The aggregation trace in Figure 4.27 shows inhibition of RIPA by soluble Spa. Platelet aggregation promoted by botrocetin, ADP, thrombin-receptor activating peptide (TRAP), collagen and *S. aureus* Newman were each blocked by Spa (Fig. 4.28). Botrocetin binds



vWF A1 on a site distinct from Spa (Fig. 4.19) and ADP, TRAP and collagen induce platelet agglutination independent of vWF. Stationary phase *S. aureus* Newman cells activate and agglutinate platelets through ClfA and fibrinogen along with IgG (Loughman *et al.*, 2005). Taken together, these data suggest a direct interaction between Spa and platelets.

Platelet adherence assays showed that protein A bound directly to gel-filtered platelets which lack any plasma proteins. Inhibition of platelet aggregation by Spa pointed towards the receptor for Spa being involved in the aggregation process. When tirofiban, which specifically blocks the platelet membrane glycoprotein  $\alpha_{IIb}\beta_3$ , was added to platelets prior to incubation with immobilised *L. lactis* expressing Spa, platelet adherence was also blocked. These data implicate  $\alpha_{IIb}\beta_3$  in Spa binding. If protein A on the surface of *S. aureus* can interact directly with platelets *in vivo* it is most likely to help promote adherence of *S. aureus* to infectious vegetations in the vascular endothelium as *S. aureus* Newman which expresses an array of surface proteins including Spa, is a potent aggregator of platelets.

The GST-Spa variants generated in this study were also used to identify the region on Spa involved in binding TNFR1 in collaboration with Alice Prince's research group in Columbia University, New York. In addition to Fc $\gamma$ , V<sub>H</sub>3-Fab and now vWF, all individual Spa domains were demonstrated to bind epithelial cell expressing tumour necrosis factor receptor-1 (TNFR1) (Fig. 4.30) and the epidermal growth factor receptor (EGFR). The binding site within Spa localised to the helix 1-2 face, the region also involved in binding vWF and Fc $\gamma$  (Fig. 4.31). Binding to TNFR1 and EGFR is through a distinct region, as the SpaD variants F5A and L17A bound TNFR1 but not EGFR. This indicates multifunctional roles for Spa in the pathogenesis of *S. aureus* in the airway epithelium.

In conclusion, the Spa-vWF binding region has been mapped to residues on helices 1 and 2 of a Spa domain and a region in close proximity to the collagen- and ristocetin-binding site on vWF A1, near helix  $\alpha_6$ . Binding of vWF by Spa does not enhance platelet aggregation in the presence of vWF modulators and soluble Spa can inhibit platelet aggregation through  $\alpha_{IIb}\beta_3$ -binding. The role of Spa in *S. aureus*-induced platelet aggregation is most likely through adherence either directly via  $\alpha_{IIb}\beta_3$  on the platelet surface or through a vWF bridge in conditions of high shear. Binding of protein A to TNFR1 on airway epithelial cells through the same region as Fc $\gamma$  and vWF is compelling evidence that Spa is a multifunctional virulence factor in different environmental niches within the host.



## **Chapter 5**

### **Studies on Sbi, a Second Immunoglobulin-binding Protein of *Staphylococcus aureus***

## 5.1 Introduction

Phage display studies of *S. aureus* strain 8325-4 revealed a novel Ig-binding peptide that was later characterised as part of the Second Binding protein of Immunoglobulin (Sbi) (Zhang *et al.*, 1998). Sbi comprises 436 residues, including a 29 aa N-terminal signal sequence. A proline-rich repeat region beginning at position 267 may represent a potential cell-wall spanning domain. However, unlike the surface anchored MSCRAMM proteins, the putative wall-spanning region is not followed by an LPXTG motif and hydrophobic domain in Sbi. A schematic diagram of the Sbi protein is shown in Figure 5.1. Characterisation of Sbi has been hindered by both its similar reactivity to various mammalian Igs and its similar apparent molecular mass (50.07 Da) to Spa (~ 47 Da). The *sbi* gene is present in all sequenced strains in *S. aureus* (Zhang *et al.*, 1998). The putative promoter sequence is different from that of *spa*, suggesting a different mechanism of transcriptional regulation. Taken together, this indicates that most strains of *S. aureus* express at least one Ig-binding protein.

The exact cellular location of Sbi has not yet been elucidated although it appears to be present on the *S. aureus* cell surface (Zhang *et al.*, 2000). The pKa of Sbi is 9.8, indicating the protein is basic, and it has been suggested that electrostatic interactions play a role in its anchoring to the cell surface via acidic residues in teichoic acid, like Internalin B of *Listeria monocytogenes* (Braun *et al.*, 1997). The secreted Sbi protein comprises four domains. A protein A-like Ig-binding region of about 60 residues is located at the N-terminus of Sbi, followed by a second putative Ig-binding domain (Figure 5.2). These domains are followed by a  $\beta_2$ -glycoprotein I binding region located between residues 204 and 261. Recently domains 3 and 4 have been shown to form separately folded elements that contain a binding domain for complement factor C3 (Dr. Jean van den Elsen, ISSSI symposium, 2006). The remainder of Sbi is made up of the proline-rich repeat domain and a C-terminal region rich in tyrosine and threonine (Fig. 5.1). Apart from the protein A-like Ig-binding domains the Sbi amino acid sequence bears little homology to any other proteins in the NCBI database. Therefore, *in silico* analysis on the primary sequence was performed to predict the likely structure and localisation of Sbi. While a great number of powerful programs now exist online for the prediction of a range of protein characteristics, results should be interpreted with caution. In parallel with *in silico* analysis, fractionation studies of the *S. aureus* cell envelope were performed to localise Sbi.

## 5.2 Results

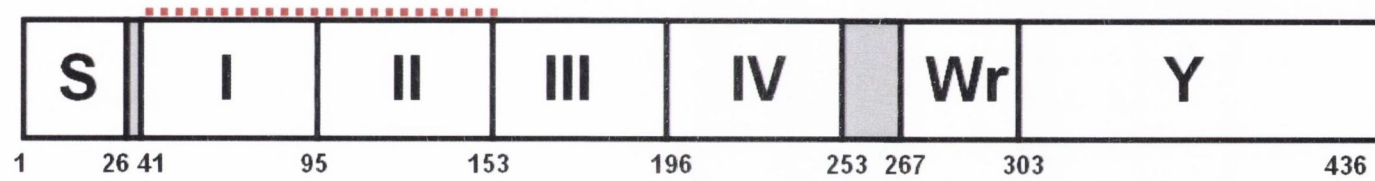
### 5.2.1 Cellular location of Sbi

Fractionation studies using three *S. aureus* strains were performed to investigate both the levels of Sbi expression and to determine its cellular location. Spa-deficient strains of *S. aureus* were used because of the immunoglobulin-binding activity and similar molecular mass of Spa. Washed cells from the stationary phase of growth were fractionated into cell wall and protoplast fractions by digestion of the cell wall with lysostaphin in the presence of 30% (w/v) raffinose and MgCl<sub>2</sub> followed by centrifugation. Digestion with lysostaphin has previously been shown to solubilise cell wall-associated proteins that are covalently bound by cleavage of the pentaglycine bridge of cell wall peptidoglycan. The supernatant contained the products of the lysostaphin digestion including peptidoglycan and solubilised cell wall-associated proteins. The pellet contained protoplasts, which were gently washed and resuspended in the osmotically stabilising raffinose-MgCl<sub>2</sub> buffer. Fractions were boiled in sample buffer for analysis by SDS-PAGE and Western blotting.

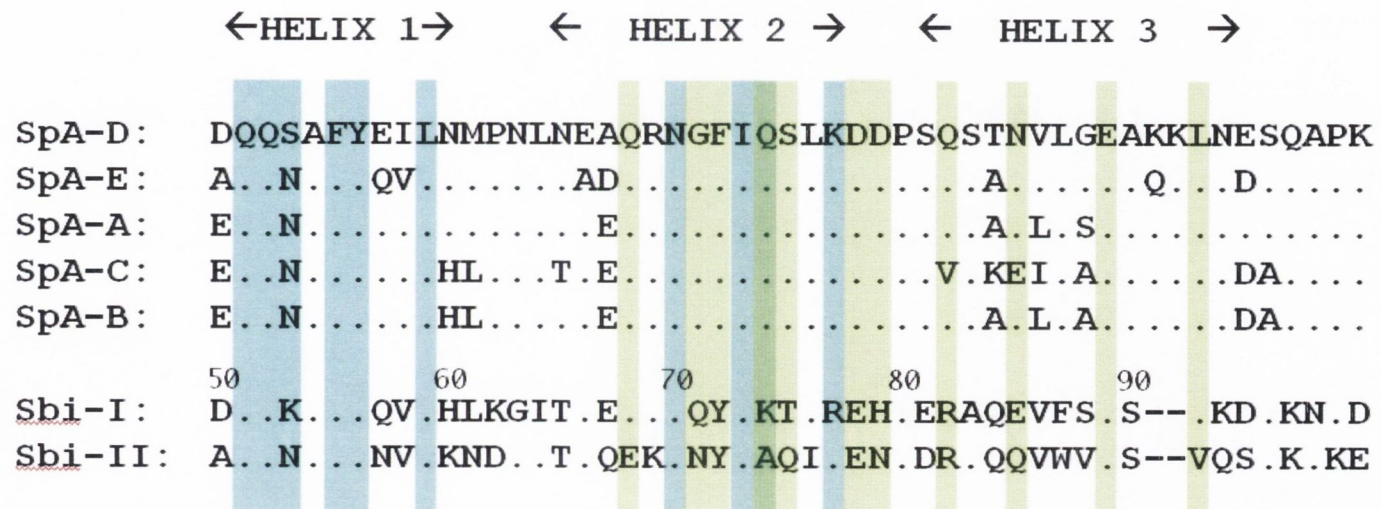
Protoplasts were also further separated into protoplast membrane and cytoplasmic fractions by gentle lysis of the protoplasts in the absence of the osmoprotectant raffinose, followed by centrifugation. The supernatant containing the cytoplasmic fraction was retained and the protoplast membrane pellet washed and resuspended in a 50 mM Tris buffer. Samples were boiled in sample buffer for analysis by SDS-PAGE and Western blotting. Whole-cell lysates were also prepared by prolonged lysostaphin digestion of bacterial cells, followed by boiling samples in SDS. In addition, the culture medium from the stationary phase cultures was concentrated for analysis of secreted proteins. A summary of the fractionation procedures described is illustrated in Fig. 5.3. Samples were analysed by SDS-PAGE and stained using Coomassie Blue or transferred onto PVDF membranes for Western blotting using an anti-Sbi antibody (a gift from Dr. Jean van den Elsen). Western blots using anti-ClfA and anti-EbpS antibodies were also performed in the case of 8325-4. ClfA is cell wall anchored via a C-terminal LPXTG motif and EbpS an integral membrane protein with three transmembrane domains (Downer *et al.*, 2002). Proteins detected in cell wall, protoplast or cytoplasmic fractions should be present in whole cell lysates.

Figures 5.4 A, 5.5 A and 5.6 A show profiles of proteins from fractions of the *S. aureus* cells stained using Coomassie Blue. A 50 kDa protein presumably corresponding to Sbi (50.07 kDa) was detected in the protoplast fraction in all strains tested when Western

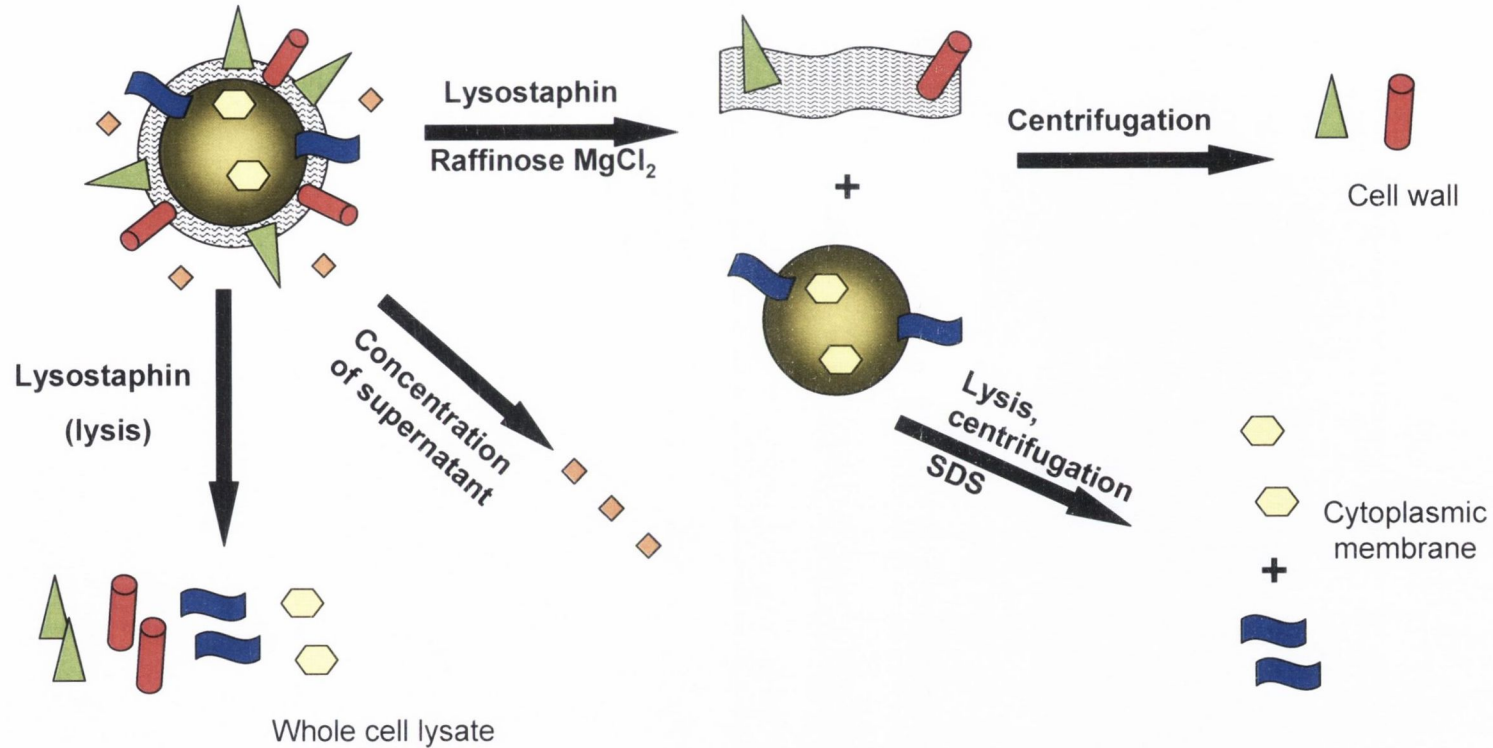




**Fig. 5.1 Schematic diagram of the structural organization of Sbi.** 'S' represents the signal sequence and proposed extracellular domains are represented by roman numerals. Domains I and II have homology to Spa and are proposed to bind IgG (red dashed line). Domain IV contains a  $\beta$ -2 glycoprotein-binding region. Wr denotes a possible wall-spanning region and the C-terminal tyrosine-rich region is indicated by 'Y'

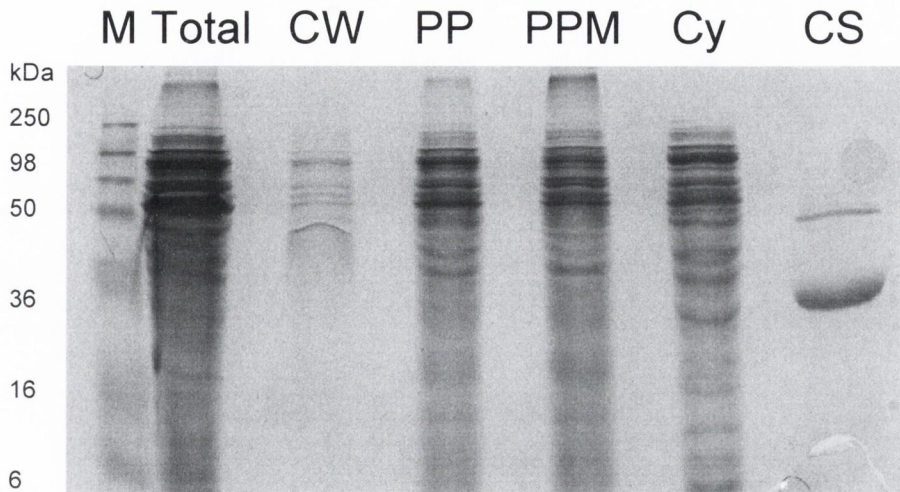
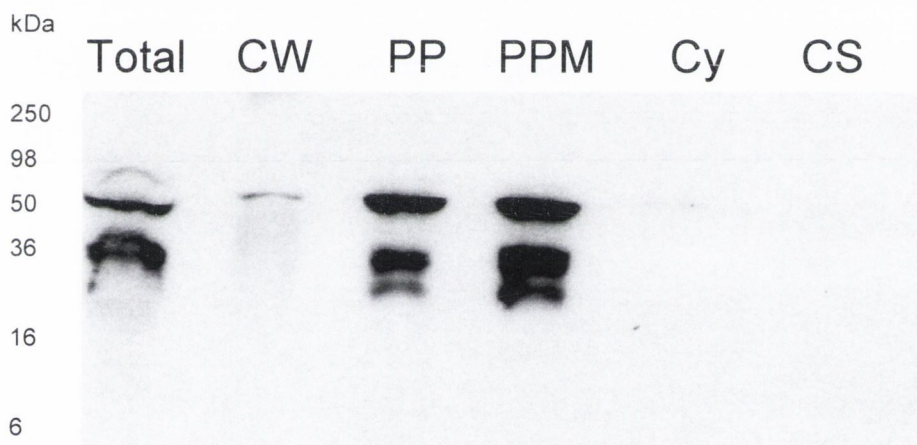


**Fig. 5.2. Alignment of Spa and Sbi IgG-binding domains.** Domains are aligned with SpaD. Residues on Spa involved in binding Fc $\gamma$  and V<sub>H</sub>3-Fab are highlighted blue and green, respectively. The corresponding residues in Sbi are also highlighted.



**Fig. 5.3 Fractionation of the *S. aureus* cell envelope.** Stationary phase cultures *S. aureus* cells were harvested and the culture supernatant was concentrated for analysis of secreted proteins (orange). Cells were resuspended in a Tris buffer containing the osmotic stabiliser raffinose, MgCl<sub>2</sub> and protease inhibitors. The cell wall was digested in this buffer by addition of lysostaphin and the solubilised cell wall associated proteins (green and red) were isolated from protoplasts by centrifugation. Alternatively, whole cell lysates were produced by prolonged incubation of cells in lysostaphin. Proteins associated with the cytoplasmic membrane (blue) or the cytoplasm (yellow) were isolated by lysis of protoplasts and separation by centrifugation.



**A****B**

**Fig. 5.4. Analysis of cell envelope fractions of *S. aureus* 8325-4 *spa* for Sbi.** *S. aureus* 8325-4 cells were separated into cell wall (CW), protoplasts (PP) protoplast membrane (PPM) and cytoplasm fractions (Cy) and analysed by SDS-PAGE. A whole cell lysate (Total) and a concentrated supernatant representing secreted proteins (CS) were also included. Gels were stained for proteins with Coomassie Blue (A) or analysed by Western blotting with anti-Sbi antibody (B). Approximate molecular weights estimated from a standard marker (M) are indicated.

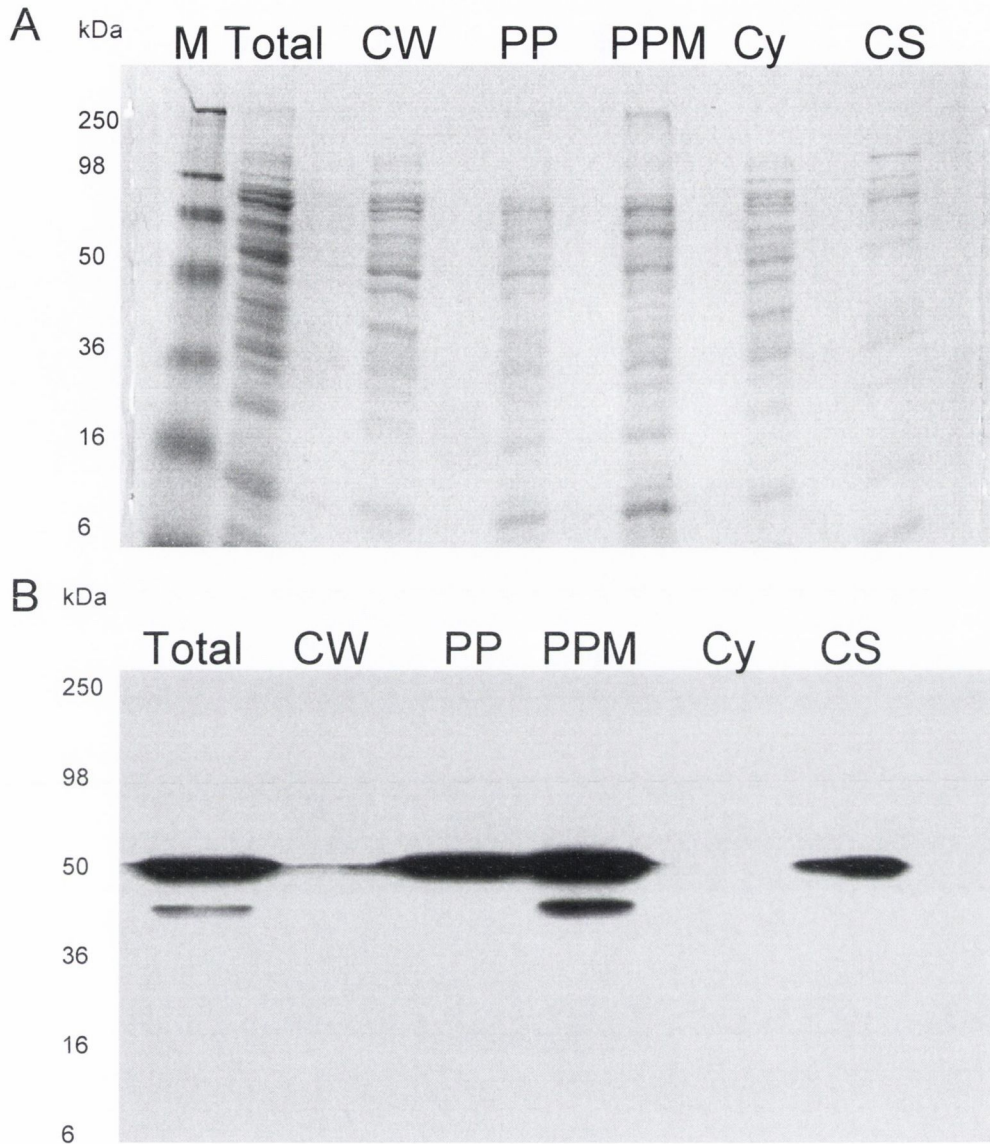


**Fig. 5.5. Analysis of cell envelope fractions of *S. aureus* Newman *spa* for Sbi.** *S. aureus* Newman cells were separated into cell wall (CW), protoplasts (PP) protoplast membrane (PPM) and cytoplasm fractions (Cy) and analysed by SDS-PAGE. A whole cell lysate (Total) and a concentrated supernatant representing secreted proteins (CS) were also included. Gels were stained for proteins with Coomassie Blue (A) or analysed by Western blotting with anti-Sbi antibody (B). Approximate molecular weights estimated from a standard marker (M) are indicated.



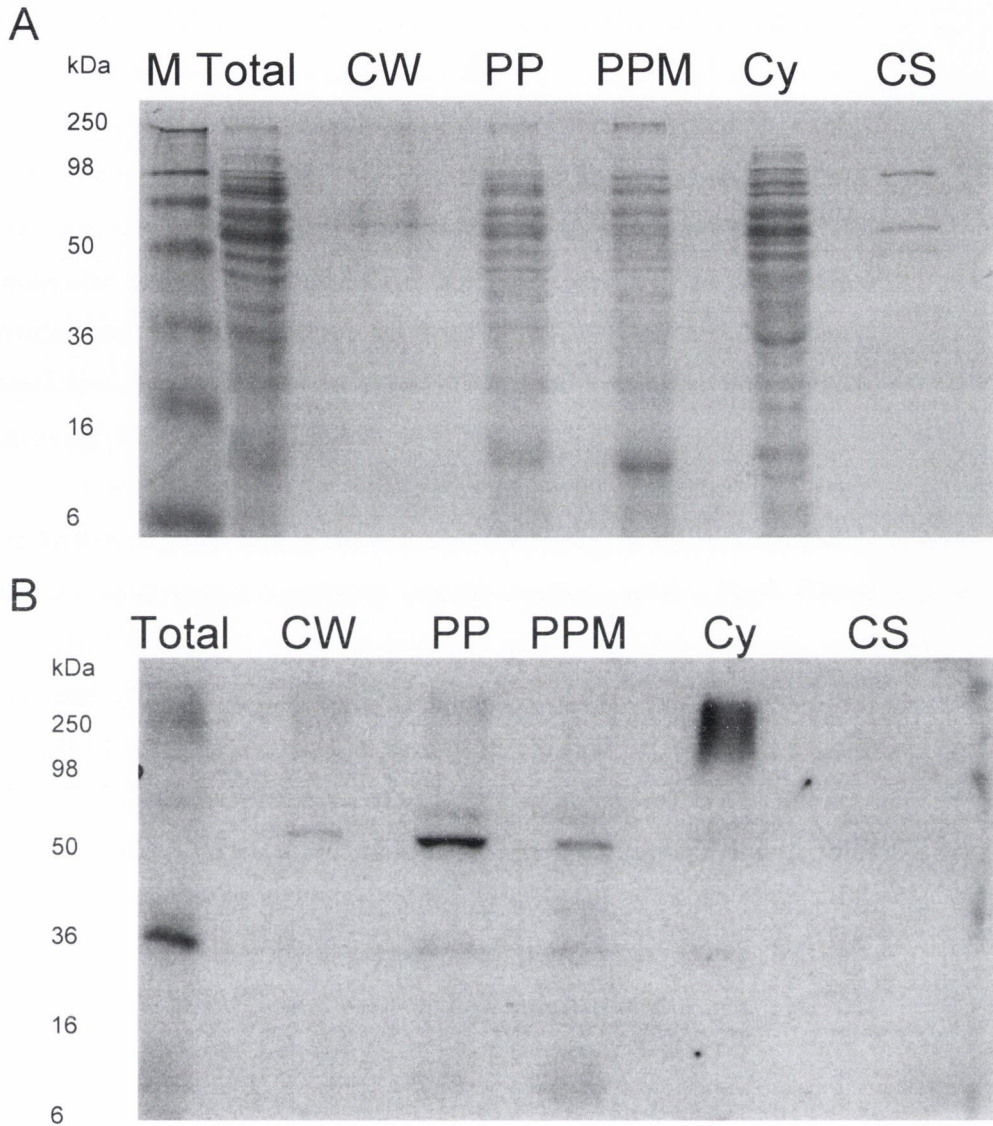


**Fig. 5.6. Analysis of cell envelope fractions of *S. aureus* SH1000 *spa* for Sbi.** *S. aureus* SH1000 cells were separated into cell wall (CW), protoplasts (PP) protoplast membrane (PPM) and cytoplasm fractions (Cy) and analysed by SDS-PAGE. A whole cell lysate (Total) and a concentrated supernatant representing secreted proteins (CS) were also included. Gels were stained for proteins with Coomassie Blue (A) or analysed by Western blotting with anti-Sbi antibody (B). Approximate molecular weights estimated from a standard marker (M) are indicated.



blots were probed with anti-Sbi antibody. Trace amounts of protein were detected in the cell wall fraction (Figs. 5.4 B, 5.5 B and 5.6 B). This is consistent with Sbi not containing signals for sortase-mediated anchoring to peptidoglycan. Strain Newman *spa* expressed significantly higher levels of Sbi than the other strains tested and samples were diluted 10-fold prior to Western blotting with anti-Sbi antibody (Fig. 5.6 A). Expression levels between strains correlated with data from previous studies of Sbi expression (Zhang *et al.*, 1998; Zhang *et al.*, 2000). Sbi was detected in the extracellular medium of *S. aureus* Newman *spa* indicating that this protein may also be secreted (Fig. 5.5). Bands of lower molecular weight than full-length Sbi (approximately 32 kDa) detected in whole cell lysates and in the protoplast fractions of 8325-4 *spa* and Newman *spa* may represent breakdown products of Sbi or a staphylococcal protein that cross-reacted with the anti-Sbi antibody (Figs. 5.4 B, 5.5 B and 5.6 B).

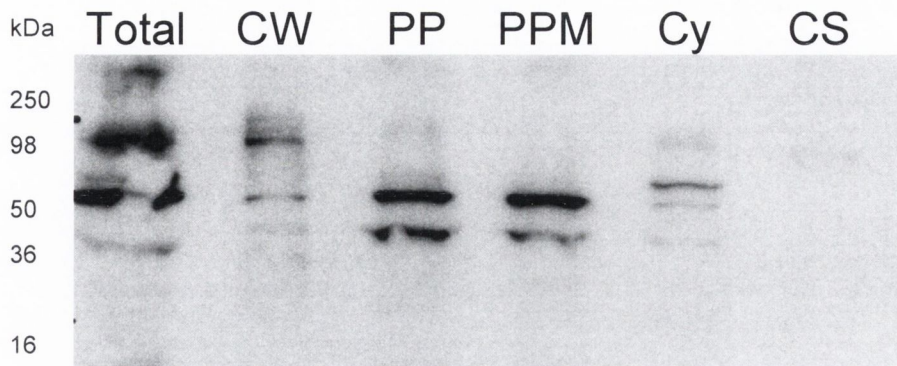
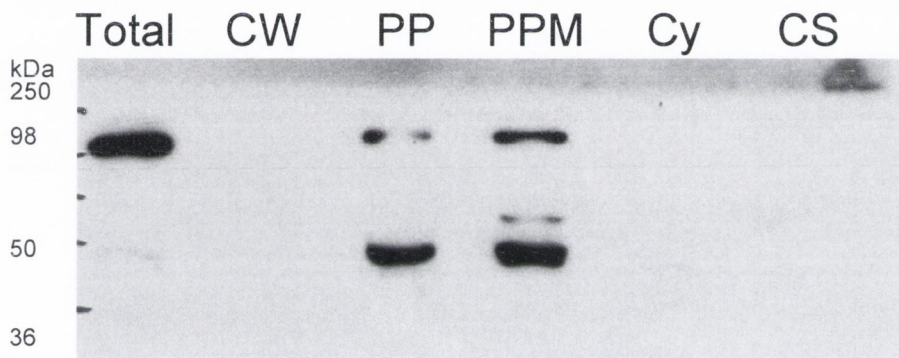
Control experiments were performed with antibodies that react with proteins that are known to be present in the cell wall (clumping factor A, ClfA (McDevitt *et al.*, 1995)) and the cytoplasmic membrane (elastin-binding protein, EbpS (Downer *et al.*, 2002)). Western blots of cell envelope fractions using anti-ClfA antibody revealed bands of 140 kDa and 110 kDa in the whole cell lysate and cell wall fractions of 8325-4 *spa*. This is consistent with the covalent anchoring of ClfA to the cell wall peptidoglycan by sortase (Fig. 5.7 A). Immunoreactive bands (50 kDa and 32 kDa) detected in the protoplast may represent truncated ClfA protein or more likely the IgG binding to Sbi. EbpS is associated with the cytoplasmic membrane and was detected as an 83 kDa protein in the protoplast fractions, in agreement with previous reports (Downer *et al.*, 2002). A 50 kDa band was also detected in the protoplast fractions, most likely due to IgG reacting with Sbi as occurred when probing with anti-ClfA antibodies (Fig. 5.7 B). To investigate this, cell envelope fractions of *S. aureus* Newman or Newman *spa* were resolved by SDS-PAGE and probed with peroxidase-conjugated rabbit IgG1. A 50 kDa band was observed in all fractions in wild-type *S. aureus* Newman (Fig. 5.8 A). Reactive bands were absent in the cell wall and cytoplasmic fractions in Newman *spa* (Fig. 5.8 B). This is explained by the absence of its cell wall-anchored Spa and perhaps unprocessed Spa in the cytoplasm. These data confirm the presence of a 50 kDa IgG-binding protein in the protoplast fraction of *S. aureus*, presumably Sbi.

## 5.2.2 *In silico* analysis of Sbi

It has been determined by fractionation studies that Sbi is present in the extracellular milieu and the protoplast membrane of *S. aureus*. Therefore, Sbi could be an integral membrane protein, spanning the cytoplasmic membrane. However, the sequence does not possess the necessary stretch of 15-30 hydrophobic residues to traverse the prokaryotic membrane lipid bilayer. The Sbi sequence was analysed by Kyte-Doolittle hydrophathy plotting for putative transmembrane regions. The elastin-binding protein (EbpS) of *S. aureus*, which is expressed as an integral membrane protein, was also analysed by this method. Kyte-Doolittle plots provide information about the putative structure of a protein based on hydrophobic residues in the amino acid sequence. Residues are given a hydrophobicity score between -4.5 (very hydrophilic) and 4.5 (very hydrophobic). After input of a protein sequence, a window size is set to for displaying the data. A window size of 19 residues gives the best results when searching for a potential transmembrane sequence. The hydrophobicity score for this sequence is averaged and the mean score assigned to the middle residue in the window. Then the computer program calculates the average of all the hydrophobicity scores in the next window, which is one amino acid down from the previous window. The pattern continues to the end of the sequence, computing the average score for each window and assigning it to the middle amino acid in the sequence. The averages are then plotted on a graph. The y axis represents the hydrophobicity scores and the x axis represents the position in the protein sequence. For example, the hydrophathy score at position 10 on the graph represents the average hydrophathy of the 19 residues from position 1 to 19 in the protein sequence. Analysis of the Sbi sequence from *S. aureus* NCTC 8325 using the algorithm of Kyte and Dolittle to identify regions of hydrophobicity did not reveal any significant regions in the entire protein other than the N-terminal signal sequence (Fig. 5.9 A). EbpS produced three peaks of which one of which is predicted to membrane-spanning. These correspond to the reported hydrophobic domains H1 (205-224), H2 (265-280) and H3 (315-342) of EbpS (Fig. 5.9 B).

Transmembrane prediction using Hidden Markov Models (TMHMM) predicts transmembrane  $\alpha$ -helices utilising both the hydrophathy index of the protein sequence and current knowledge of membrane insertion mechanisms. This method combines the hydrophobic signal and the charge bias signal, in which an abundance of positively charged residues are usually located in the protein sequence at the cytoplasmic side of a cell membrane (the 'positive-inside' rule) into one integrated algorithm. The Hidden



**A****B**

**Fig. 5.7. Analysis of cell envelope fractions of *S. aureus* 8325-4 *spa* for ClfA and EbpS.** Cell envelopes of *S. aureus* 8325-4 *spa* were separated into cell wall (CW), protoplasts (PP) protoplast membrane (PPM) and cytoplasm fractions (Cy) and analysed by SDS-PAGE. A whole cell lysate (Total) and a concentrated supernatant representing secreted proteins (CS) were also included. Gels were analysed by Western blotting with anti-ClfA antibody (A) or anti-EbpS antibody (B). ClfA resolves at 175 kDa and EbpS at 83 kDa. Approximate molecular weights are indicated.



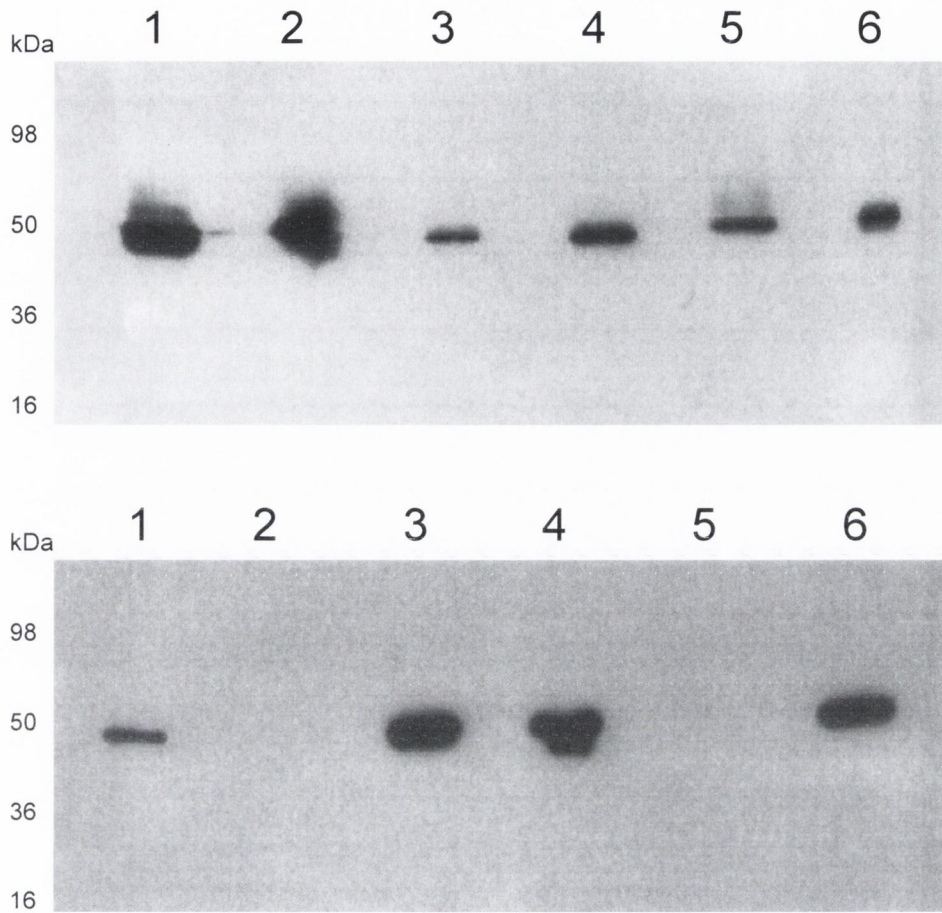


**Fig. 5.8. Analysis of cell envelope fractions of *S. aureus* Newman and Newman *spa* for IgG binding.** Cell envelopes of *S. aureus* Newman (A) or Newman *spa* (B) were separated into cell wall (lane 2), protoplasts (lane 3) protoplast membranes (lane 4) and cytoplasm fractions (lane 5) and analysed by SDS-PAGE. A whole cell lysate (lane 1) and a concentrated supernatant representing secreted proteins (lane 6) were also included. Gels were analysed by Western blotting with peroxidase-conjugated rabbit IgG. Approximate molecular weights are indicated.

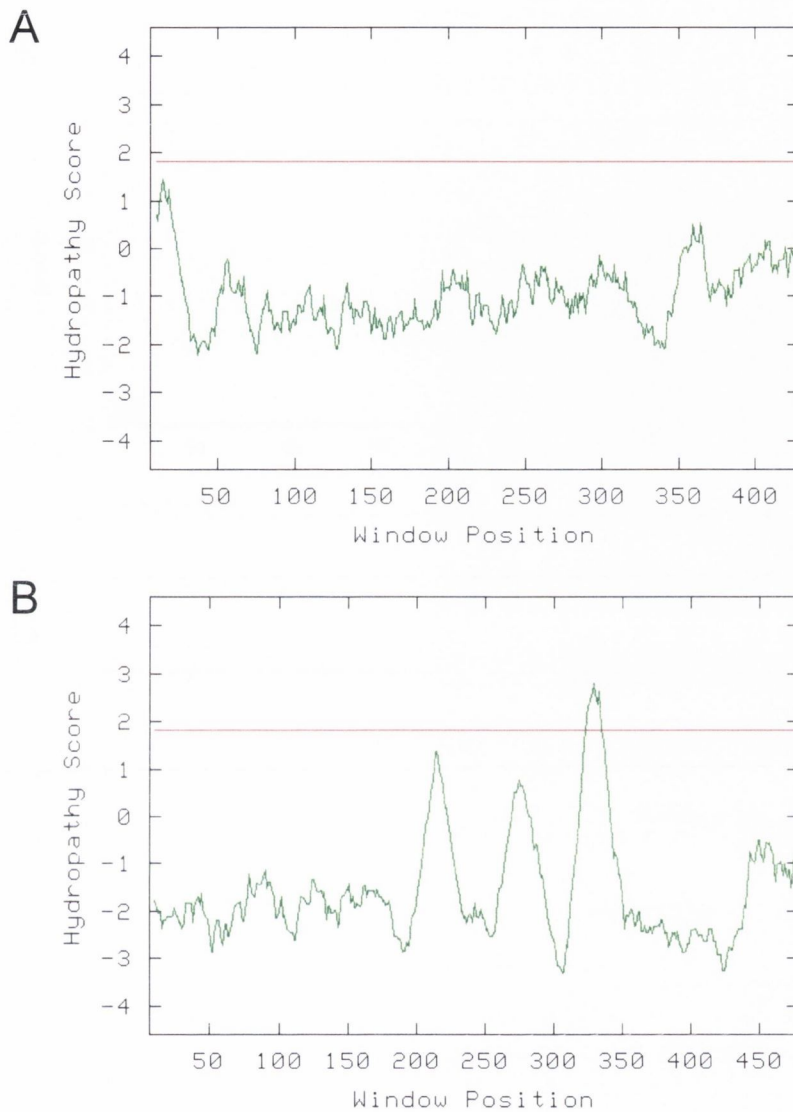


**Fig. 5.9. Kyte-Doolittle hydropathy plotting for putative transmembrane regions of Sbi.** The amino acid sequence of Sbi from *S. aureus* NCTC 8325 was analysed by Kyte-Doolittle hydropathy plotting (A). Kyte-Doolittle hydropathy plotting is based on assigned hydropathy scores for each residue as outlined in section 5.2.2. Putative transmembrane regions in the protein sequence exceed a score of 1.8 (red line). The *S. aureus* cytoplasmic membrane-associated protein EbpS was also analysed (B).

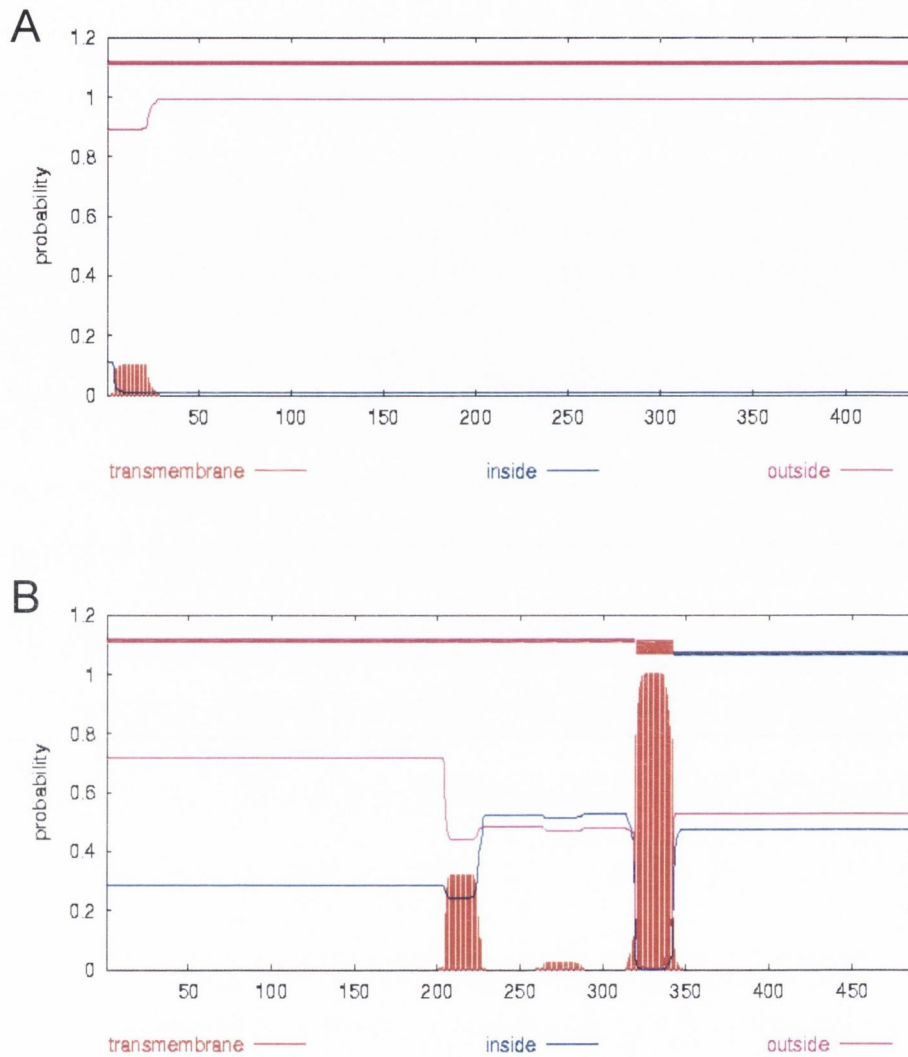


**Fig. 5.10. Prediction of transmembrane  $\alpha$ -helices on Sbi using the TMHMM program.** The amino acid sequence of Sbi from *S. aureus* NCTC 8325 was analysed for potential transmembrane  $\alpha$ -helices using the TMHMM program (A). TMHMM utilises both the hydropathy index of the protein sequence and current knowledge of membrane insertion mechanisms. This program was successfully used to predict two membrane spanning domains (H1 and H3) in EbpS (B).



Markov Model (a pattern recognition algorithm) is well suited for prediction of transmembrane helices because it can incorporate hydrophobicity, charge bias, helix lengths, and biological 'rules' (e.g. that loops of transmembrane proteins must alternate between cytoplasmic and non-cytoplasmic) into one model for which algorithms for parameter estimation and prediction already exist. This program was successfully used to predict two membrane spanning domains (H1 and H3) in EbpS (Fig. 5.10 B). However it failed to identify any putative membrane-spanning regions in Sbi (Fig. 5.10 A). Another web-based program for the prediction of possible transmembrane regions of a given peptide sequence is the dense alignment surface (DAS) method. A scoring matrix previously derived from a collection of non-homologous membrane proteins is used to generate low-stringency dot-plots of the query sequence. In this way, the DAS method improves the prediction abilities of protein sequences that have no known homologues. When analysed in this way, the Sbi sequence yields a potential 9-residue membrane-associated region, at position 354 (Fig. 5.11 A). The DAS method predicts three transmembrane regions in the EbpS sequence, corresponding to H1, H2 and H3 of the protein (Fig. 5.11 B).

### 5.2.3 Construction of recombinant Sbi-II

To perform binding studies with the Sbi protein A-like repeats for ligands of Spa, the region encoding two putative Ig-binding domains of Sbi were used. Recombinant Sbi-E, corresponding to residues 28-266 and Sbi-I, the first protein A-like repeat of Sbi (residues 42-94), produced as N-terminal 6xhistidine fusion proteins were generous gifts from Dr. Jean van den Elsen. Recombinant Sbi-II (residues 92-156) was constructed here. For this, DNA encoding this region was amplified and directionally cloned into the expression vector pGEX-KG. The GST-fusion protein was expressed in *E. coli* BL21. Passing the bacterial lysate over immobilised glutathione purified the GST-tagged protein. The GST tag was removed by on-column thrombin cleavage and the highly purified, untagged protein eluted directly into a benzamidine column to remove thrombin from the preparation. Analysis by SDS-PAGE revealed bands of expected size for recombinant Sbi-E (31 kDa), Sbi-I (6.7 kDa) and Sbi-II (7.4 kDa). Bands of the same size were detected by Western immunoblotting using anti-Sbi antibodies (Fig. 5.12).

Sbi shows high homology to the Spa Ig-binding domains, specifically to residues involved in the Fc $\gamma$  interaction (in helices 1 and 2). The binding site on Spa for vWF is also located on helices 1 and 2. There is no homology in Sbi to the V<sub>H3</sub>-binding domain of helices 2 and 3 of Spa (Fig. 5.2). The ability of Sbi to bind ligands of protein A was investigated. Sbi proteins were tested for their ability to interact with rabbit IgG1, recombinant human V<sub>H3</sub>-Fab and the vWF A1 domain compared to GST-SpaEDABC and GST-SpaD. Sbi has been previously demonstrated by phage display to bind most mammalian IgG via Sbi-I (Zhang *et al.*, 1998). To investigate whether Sbi-II could also interact with IgG, microtitre plates were coated with equal concentrations of recombinant Sbi and Spa truncates (10  $\mu$ g/ml) and assayed for solid-phase binding to soluble peroxidase-conjugated rabbit IgG ranging in concentration from 140 nM to 2 nM. GST-SpaEDABC and GST-SpaD bound specifically and with high affinity. Both Sbi-E and Sbi-I bound in a dose-dependent manner but binding was not saturable at the IgG concentrations tested (Fig. 5.13). Binding was weaker than that observed for GST-SpaEDABC and GST-SpaD (half-maximal binding for both proteins  $\sim$  30 nM). No significant interaction was observed for Sbi-II (Fig. 5.13).

Protein A binds V<sub>H3</sub>-Fab through residues in helices 2 and 3 that do not share homology with Sbi. Solid phase binding assays were employed to investigate if Sbi could bind V<sub>H3</sub>-Fab. Immobilised Spa or Sbi truncates (10  $\mu$ g/ml) were incubated with recombinant V<sub>H3</sub>-Fab ranging from 1  $\mu$ M to 15.625 nM and bound ligand was detected using a peroxidase-conjugated chicken anti-human IgG antibody followed by incubation in a chromogenic substrate (see section 2.14.1). Dose-dependent and saturable binding was observed for both GST-SpaEDABC and GST-SpaD, but no interaction occurred between V<sub>H3</sub>-Fab and the Sbi constructs (Fig. 5.14).

A similar assay was performed to measure solid-phase binding of the Spa and Sbi truncates to soluble vWF A1. The binding site of vWF A1 shares a number of residues also involved in Fc-binding on the helix 1-2 face of the Spa repeat. It is therefore conceivable that Sbi could also bind vWF through this region. Solid-phase binding assays were employed to investigate this. 96-well plates were coated with Spa or Sbi constructs (10  $\mu$ g/ml) followed by incubation with serial dilutions of recombinant vWF A1 (1.2  $\mu$ M to 18.75 nM). Bound vWF A1 was detected using peroxidase-conjugated anti-vWF (Fab)<sub>2</sub> fragments followed by incubation in chromogenic substrate. Anti-6xHis antibody could not be used in this assay as both soluble vWF A1 and the immobilised Sbi harboured a His-tag.

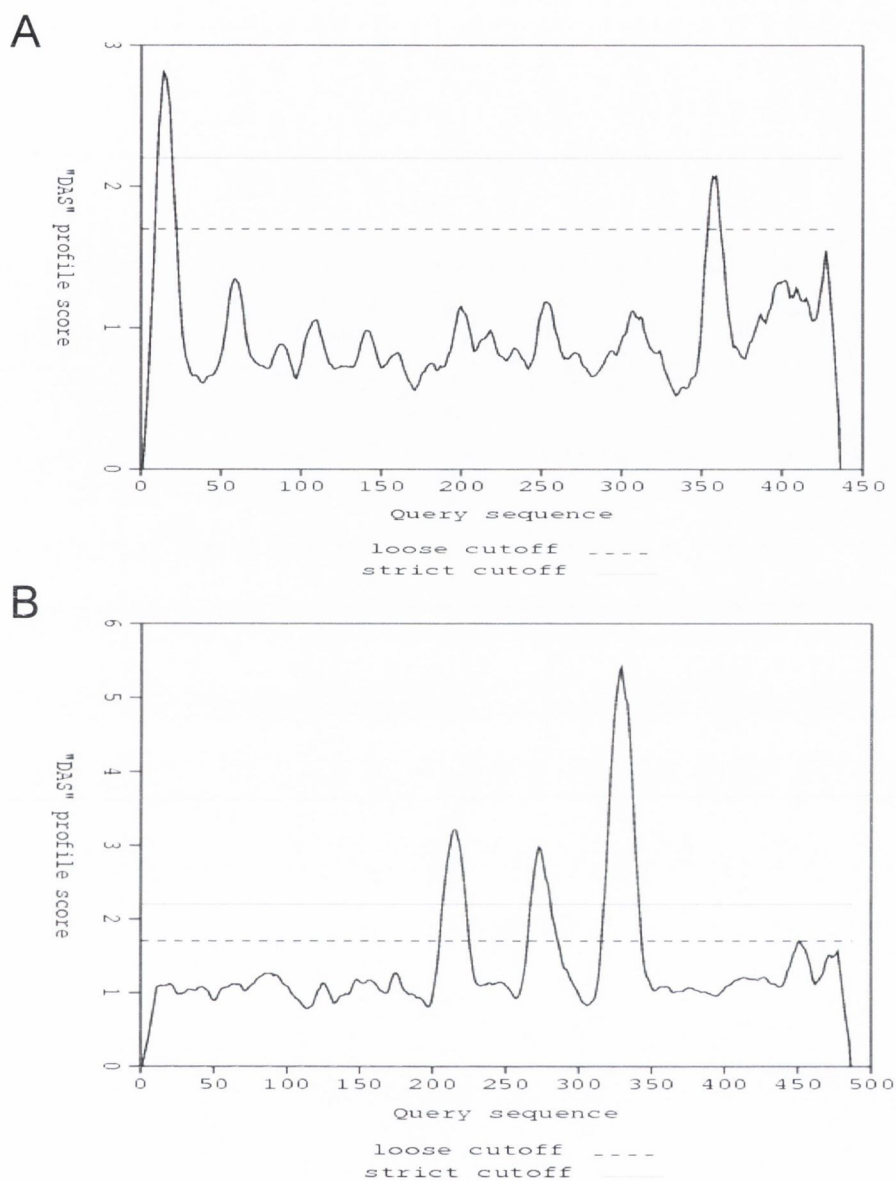


**Fig. 5.11. Prediction of possible transmembrane regions of a given peptide sequence is the dense alignment surface (DAS) method.** The amino acid sequence of Sbi from *S. aureus* NCTC 8325 was analysed for potential transmembrane regions by DAS (A). A scoring matrix previously derived from a collection of non-homologous membrane proteins is used to generate low-stringency dot-plots of the query sequence. EbpS was also analysed by DAS (B).



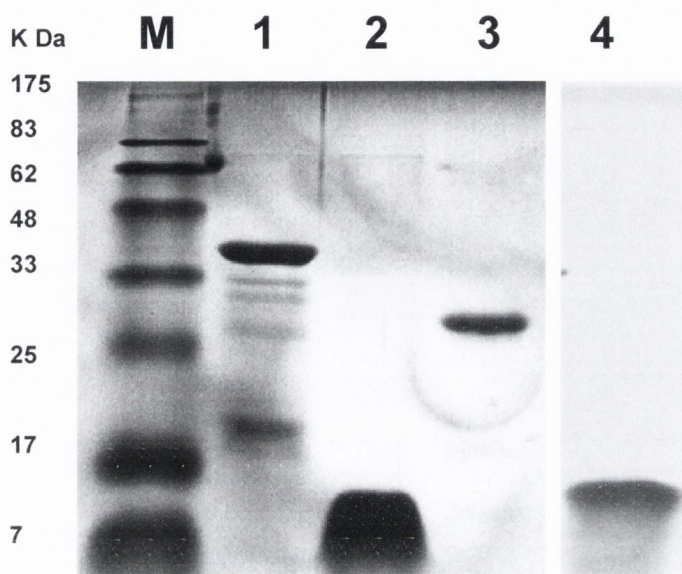


**Fig. 5.12 Recombinant Sbi proteins used in this study.** Recombinant hexahistidine-tagged Sbi proteins were resolved by SDS-PAGE and stained using Coomassie Blue. Samples were loaded in the following order M, molecular weight marker. 1, Sbi-E (31 kDa). 2, Sbi-1 (6.7 kDa). 3, GST (26 kDa). 4, Sbi-2 (7.4 kDa).

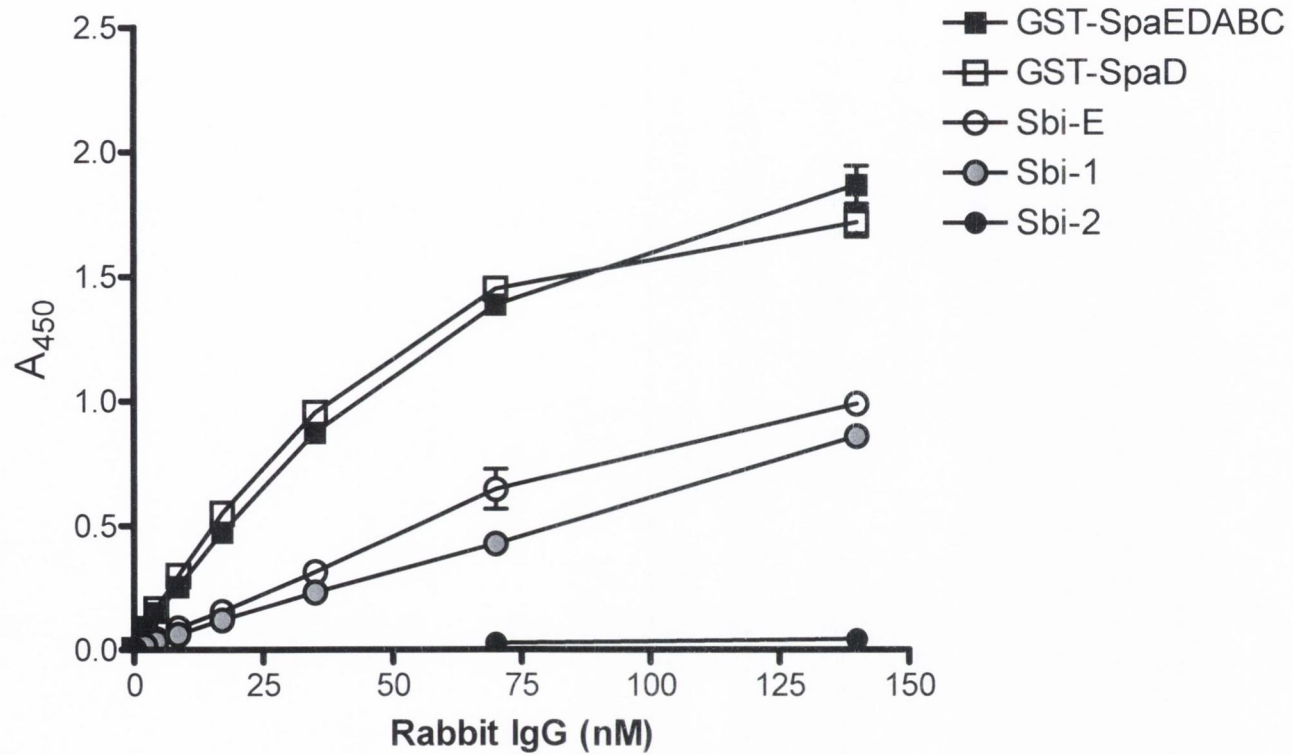


**Fig. 5.13 Interaction of Sbi and Spa truncates with rabbit immunoglobulin.** 96-well plates coated with Sbi or GST-Spa (10  $\mu\text{g}/\text{ml}$ ) were incubated with increasing concentrations of peroxidase-conjugated rabbit IgG I ranging from 140 nM to 2 nM. Bound antibody was detected directly by incubation with a chromogenic substrate. Experiments were performed in triplicate, data represents the mean  $\pm$  standard deviation of three independent experiments.

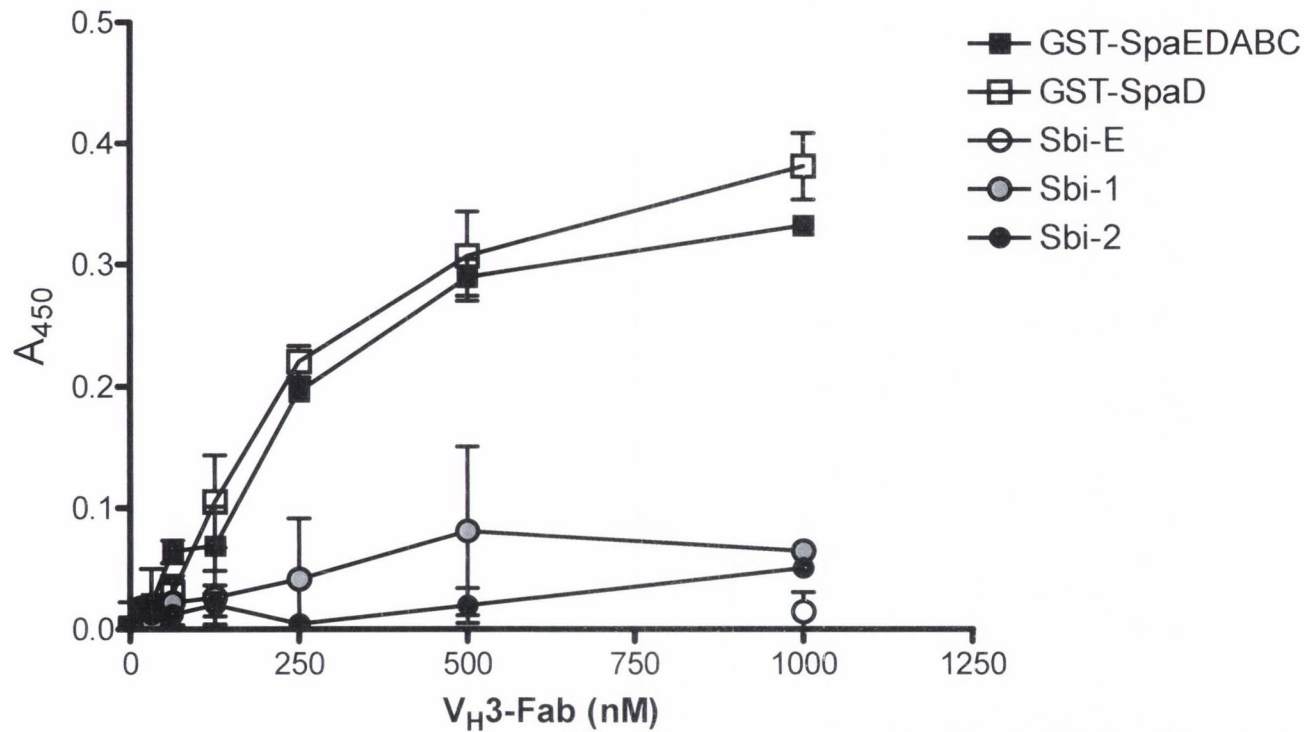


**Fig. 5.14 Interaction of Sbi and Spa truncates with V<sub>H</sub>3-Fab.** 96-well plates coated with Sbi or GST-Spa (10 µg/ml) were incubated with increasing concentrations of recombinant V<sub>H</sub>3-Fab ranging from 1 µM to 15.625 nM. Bound ligand was detected using peroxidase-conjugated chicken anti-human IgG followed by incubation with a chromogenic substrate. Experiments were performed in triplicate, data represents the mean ± standard deviation of three independent experiments.



Dose-dependent and saturable binding to GST-SpaEDABC and GST-SpaD was detected. Binding did not occur with Sbi (Fig. 5.15).

The ability of *S. aureus* to bind IgG was thought to be entirely attributable to the expression of cell wall-anchored protein A. However, a second Ig-binding protein with two putative protein A-like Ig-binding domains has been recently identified (Zhang *et al.*, 1998). Protein A contains binding sites for V<sub>H3</sub>-Fab, vWF and TNFR1. The binding site for V<sub>H3</sub>-Fab is distinct from that of Fc $\gamma$  but binding sites for vWF and TNFR1 share numerous residues on Spa with the Fc $\gamma$ -binding region. The putative IgG-binding domains of Sbi are highly homologous to Spa in the Fc $\gamma$ -binding region but no similarity exists in the site for V<sub>H3</sub>-Fab-binding (Fig. 5.1). Therefore, while it is unlikely Sbi can bind V<sub>H3</sub>-Fab, there may be reactivity to IgG, vWF and other ligands.

In this study the cellular location of Sbi was investigated and the ability of Sbi domains I and II to bind IgG, V<sub>H3</sub>-Fab and vWF was tested. Sbi has previously been detected on the surface of *S. aureus spa* mutants. Fractionation of the *S. aureus* envelope was performed with *spa* mutants of strains 8325-4, Newman and SH1000. When strains were analysed by Western blotting with anti-Sbi antibody, reactive bands of 50 kDa, the predicted molecular weight of Sbi, were detected in all cases (Figs. 5.4-5.6). These reactive bands were also detected when cell envelope fractions were analysed by Western blotting for the presence of the cell-wall protein ClfA and the cytoplasmic membrane anchored protein EbpS, indicating the presence of an IgG-binding protein of the same size as Sbi detected with anti-Sbi antibodies. (Fig. 5.7) This was confirmed by Western analysis using a peroxidase-conjugated rabbit IgG. The Sbi protein co-migrates with Spa in wild-type *S. aureus* samples.

Fractionation studies indicate that Sbi is present in the protoplast and culture supernatant fractions. However, analysis of the amino acid sequence does not reveal a putative membrane-spanning stretch of 15-30 hydrophobic residues. Comparative *in silico* analysis of Sbi with the cytoplasmic membrane-anchored protein EbpS by Kyte-Doolittle hydropathy plotting or the TMHMM program did not shed any light on the mechanism by which Sbi is membrane-anchored (Figs. 5.9 and 5.10). A possible and perhaps novel anchoring mechanism was identified when the Sbi sequence was analysed by dense alignment scattering (DAS), which highlighted a 9 residue stretch as potentially being membrane-associated (Fig. 5.11). This region is too short to traverse the membrane, however it is possible that Sbi is peripherally associated with the cytoplasmic membrane, but does not traverse it, like the LppC protein of *Streptococcus equisimilis* (Gase *et al.*, 1997). Another possibility is that Sbi is indirectly associated with the cell membrane

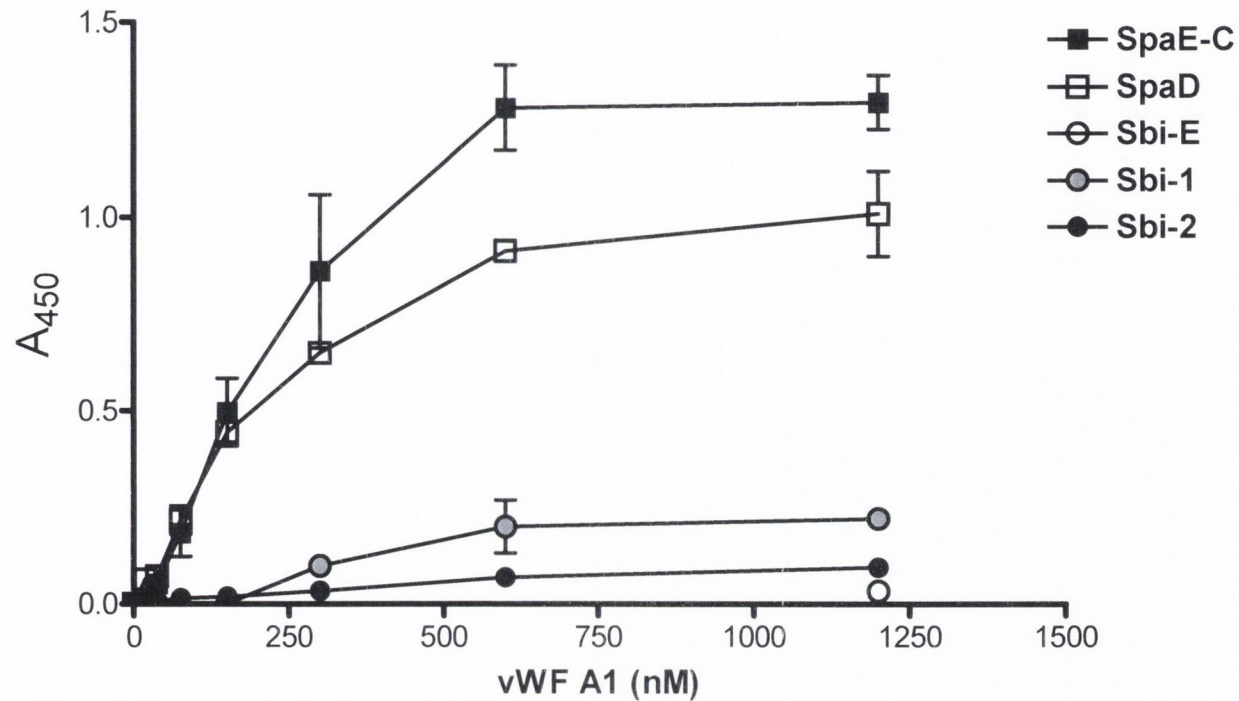


**Fig. 5.15 Interaction of Sbi and Spa truncates with vWF A1.** Microtitre plates were coated with Sbi or GST-Spa (10  $\mu\text{g/ml}$ ) and incubated with increasing concentrations of recombinant vWF A1 ranging from 1.2  $\mu\text{M}$  to 18.75 nM. Bound vWF was detected using peroxidase-conjugated anti-vWF F(ab)<sub>2</sub> fragments followed by incubation with a chromogenic substrate. Experiments were performed in triplicate, data represents the mean  $\pm$  standard deviation of three independent experiments.



lipoteichoic acid, as reported for internalin B of *Listeria monocytogenes* (Braun *et al.*, 1997). This could be via electrostatic interactions with the basic residues associated with the C-terminal domain of Sbi.

Recombinant Sbi truncates were produced to examine the ability of Sbi Spa-like domains I and II to bind the range of ligands recognised by Spa. This could be of importance in interpretation of virulence studies using animal models of Spa-deficient strains of *S. aureus*. Recombinant Sbi-E which contains domains I and II, Sbi-I and Sbi-II were tested for ligand binding by solid-phase assays. Sbi-E and Sbi-I bound IgG. However, no interaction was observed when Sbi-II was tested (Fig. 5.13). Binding was lower than that of Spa. The lack of any interaction between Sbi-II and IgG may be due to structural changes in Sbi-II due to residues not directly involved in IgG binding. None of the Sbi constructs bound V<sub>H3</sub>-Fab, consistent with the lack of homology between Sbi and the V<sub>H3</sub>-binding site on Spa (Fig. 5.14). In addition, no significant interaction was recorded when Sbi constructs were analysed for vWF A1 binding (Fig. 5.15). Phe-30 on Spa is replaced by Tyr in Sbi. This residue is important in the interaction of Spa with vWF A1 and this substitution may contribute to lack of binding by Sbi. A more thorough investigation is necessary using GST-fusions to the Sbi truncates, as GST-Spa bound to its ligands more strongly than untagged protein. Binding should also be examined for both soluble and immobilised forms of ligand.

In conclusion, the mature Sbi protein appears to be anchored to the cytoplasmic membrane but the mechanism is unclear when the Sbi sequence is analysed *in silico*. Significant IgG binding is detectable in Spa-deficient mutants of *S. aureus* and there is clearly a need for a null mutant of both *spa* and *sbi* to accurately address the importance of Ig-binding in pathogenesis of staphylococci at sites of infection. Binding of Sbi to the other ligands of protein A, V<sub>H3</sub>-Fab and vWF A1 was not detected in this study, but a more thorough analysis needs to be performed.

## **Chapter 6**

### **Discussion**

Several *S. aureus* surface proteins interact with plasma proteins that form bridges between the bacterium and circulating platelets. This is thought to be an important step in the development of vascular infections and infective endocarditis. Fibrinogen forms a bridge between ClfA on the surface of *S. aureus* to the platelet integrin  $\alpha_{IIb}\beta_3$  and this triggers platelet activation and aggregation provided antibody bound to ClfA also binds platelets through the Fc $\gamma$ R<sub>IIa</sub> receptor. This is the dominant mechanism of *S. aureus*-induced platelet aggregation on cells in the stationary phase of growth (Loughman *et al.*, 2005). In exponential growth phase, the fibronectin binding proteins (FnBPs) mediate platelet aggregation through fibrinogen or fibronectin bridges to  $\alpha_{IIb}\beta_3$ . Specific antibody is also involved (Fitzgerald *et al.*, 2006). Several other *S. aureus* surface proteins (SraP, SdrE, and ClfB) and secreted proteins ( $\alpha$ -toxin, Efb) can also promote binding or trigger activation by other mechanisms (reviewed in section 1.9.2.1). Protein A is postulated to induce platelet binding and activation by using vWF as a bridge to GpIb- $\alpha$  on resting platelets (George *et al.*, 2006; Mascari and Ross, 2003; Pawar *et al.*, 2004). Immobilised vWF can adhere to and activate platelets, as can soluble vWF (but only at high shear rates). Studies in solution at low shear rates (excluding the influence of vWF) identified the FnBPs and ClfA to be the major mechanisms of platelet aggregation by staphylococci in exponential and stationary growth phase, respectively (Fitzgerald *et al.*, 2006; Loughman *et al.*, 2005). This opens up the possibility that protein A may trigger platelet activation and aggregation at higher shear rates regardless of the phase of growth of the bacterial cells.

Recent fluid-shear experiments have shown that Spa is the dominant factor in promoting adherence of *S. aureus* to platelets in whole blood under high shear rates (5000 s<sup>-1</sup>), such as those found in stenotic blood vessels (George *et al.*, 2006; Pawar *et al.*, 2004). Mutants defective in protein A did not exhibit platelet adherence in high shear. The hypothesis that vWF bridges the bacterial cells to the platelet surface was supported by the fact that platelet binding by staphylococci was inhibited by blocking the primary vWF receptor on the platelet surface (GpIb- $\alpha$ ) or removing vWF from plasma. ClfA was of importance only in low shear (100 s<sup>-1</sup>). A second role for the Spa-vWF interaction in initiating infectious vegetations in blood vessels may be when vWF binds to sub-endothelial collagen that becomes exposed upon damage to the vascular endothelium. This setting was mimicked by perfusion studies with *S. aureus* using vWF immobilised to a collagen surface. It was shown that Spa-expressing *S. aureus* were captured by the immobilised vWF, while isogenic *spa* mutants were not (Mascari and Ross, 2003). This



was performed at low shear ( $100 \text{ s}^{-1}$ ). However, the requirement of Spa to be present on the *S. aureus* surface for bacterial adherence to vWF and platelets did not rule out a role for other surface proteins. The study described in this thesis addressed this by demonstrating that expression of protein A on the surface of *L. lactis* in the absence of other surface proteins of *S. aureus* is sufficient to support bacterial adherence to immobilized vWF under low shear conditions ( $50 \text{ s}^{-1}$ ) representing normal venous shear rates (Fig. 3.1). It is plausible that Spa promotes bacterial binding to immobilized vWF *in vivo*, either bound directly to exposed sub-endothelial tissue or to platelets that had been previously captured. This raises the possibility that vWF contributes to the recruitment of Spa-expressing bacteria into vWF-rich platelet thrombi.

The nature of the interaction between Spa and vWF has not been investigated to date. This study set out to determine the region(s) on vWF involved in Spa-binding and the site on Spa that interacts with vWF. To identify the region within vWF responsible for binding Spa, a number of recombinant vWF truncates and domain deletions were employed in solid-phase binding studies with a GST-fusion to the extracellular portion of Spa that encodes the Ig-binding domains, GST-SpaEDABC. vWF truncates and deletions representative of the major ligand-binding domains of vWF were screened for binding to GST-SpaEDABC. Two binding regions on vWF for Spa were identified, domains D'-D3 and A1 (Fig. 3.14). Single Spa domains bound vWF A1 and D'-D3 with estimated half-maximal binding values of 100 nM and 250 nM, comparable to the affinity seen for the five-domain Spa construct, GST-SpaEDABC.

The binding site on Spa for vWF was mapped by mutagenesis of a Spa domain and by inhibition studies with  $\text{Fc}\gamma$  and  $\text{V}_{\text{H}3}$ -Fab. There was agreement between the data from both studies that the binding site on Spa for vWF A1 and D'-D3 resides on the helix 1-2 face of Spa. This is the same region as the site for  $\text{Fc}\gamma$  binding, although mutagenesis studies indicated that the site is not identical. Binding of protein A to IgG or vWF *in vivo* is likely to be dependent on the environmental niche within the host. Spa binds vWF in the presence of physiological IgG concentrations *in vitro* and in whole blood. It is possible that binding of full-length Spa to IgG and vWF can occur simultaneously through separate Spa domains. The binding site on vWF was also investigated by studying the ability of known ligands for vWF A1 to block binding to Spa and testing the ability of Spa to bind vWF A1 variants with active or inactive conformations for platelet binding. The vWF ligands included the vWF A1 modulators botrocetin, ristocetin and collagen and a number of anti-vWF A1 mAb Fab fragments. Inhibition studies using these ligands revealed that ristocetin and collagen blocked vWF A1 binding to Spa in a dose-dependent and saturable manner

(Fig. 4.18). Inhibition was shown to be due to competitive binding at a site on vWF A1 and not due to conformational changes in vWF upon binding ristocetin or collagen. The structure of Spa in complex with vWF A1 (and other ligands) would provide more information on how protein A has evolved to interact with important host factors and could enable the design of inhibitory compounds for therapeutic use. This study failed to produce a crystal structure of a Spa domain in complex with the vWF A1 domain. This may be due to the fact that the untagged Spa domains formed multimers. Graille *et al.* showed that the D domain of Spa dimerised through the helix 1-2 face, the region involved in binding to vWF A1. Recombinant monomeric Spa domains have been produced containing an STII signal sequence (Starovasnik *et al.*, 1996), an N-terminal 6xHis-tag (Lendel *et al.*, 2002) and a TrpLE leader peptide (Cedergren *et al.*, 1993). It may be that these N-terminal extensions prevent multimerisation of Spa domains through the helix 1-2 region. Alternatively, single domain variants of Spa that minimise the formation of multimers but retain binding to vWF A1 could allow the Spa-vWF A1 complex to be solved.

A direct interaction between *S. aureus* and platelets can occur through Spa binding the platelet receptor gC1qR/p33 which is only expressed on the surface of platelets that have been activated (Nguyen *et al.*, 2000). For this reason, the importance of the Spa-gC1qR/p33 interaction *in vivo* may be confined to sites of vascular injury where a thrombus has formed rather than in initiating bacterial tethering to resting platelets. Indeed, Spa binding to gC1qR was shown to enhance *S. aureus* colonization of endovascular lesions by supporting bacterial interactions with activated platelets and platelet-associated fibrinogen/fibrin interactions in an experimental rat model of endocarditis (Peerschke *et al.*, 2006). This study also identified another ligand for Spa, the platelet membrane glycoprotein,  $\alpha_{IIb}\beta_3$ . However, the nature and affinity of binding requires further investigation. Since *S. aureus* expresses an array of surface proteins (including Spa) that can bind to and activate resting platelets, Spa binding to gC1qR/p33 and  $\alpha_{IIb}\beta_3$  most likely contributes further to the adherence of *S. aureus* to infectious vegetations in the vascular endothelium. A model for protein A-mediated interactions with platelets and the sub-endothelial matrix is summarised in Figure 6.1.

A recently identified second Ig-binding protein of *S. aureus* (named Sbi) has two putative protein A-like Ig-binding domains (Zhang *et al.*, 1998). The putative IgG-binding domains of Sbi are highly homologous to Spa in the Fc $\gamma$ -binding region but not at the site for V<sub>H</sub>3-Fab binding (Fig. 5.1). Binding of recombinant Sbi to the other ligands bound by protein A (V<sub>H</sub>3-Fab and vWF A1) was not detected in this study, but a more thorough analysis needs to be performed. However, significant IgG binding is detectable in Spa-



deficient mutants of *S. aureus* and there is clearly a need for a null mutant of both *spa* and *sbi* to address accurately the importance of expression of Ig-binding domains in pathogenesis of *S. aureus* infections. Fractionation studies indicated that Sbi is present in the protoplast and culture supernatant. However, analysis of the amino acid sequence did not reveal a membrane-spanning stretch of 15-30 hydrophobic residues. It is possible that Sbi is peripherally associated with the cytoplasmic membrane, but does not traverse it, like the LppC protein of *Streptococcus equisimilis*. Another possibility is that Sbi indirectly binds lipoteichoic acid, as reported for internalin B of *Listeria monocytogenes*. This could be through electrostatic interactions with the basic residues associated with the C-terminal domain of Sbi.

The GST-Spa variants generated in this study were also used to identify the region on Spa involved in binding tumour necrosis factor receptor-1 (TNFR1) in collaboration with Alice Prince's research group in Columbia University, New York. In addition to Fc $\gamma$ , V<sub>H</sub>3-Fab and now vWF, all individual Spa domains were shown to bind epithelial cells expressing TNFR1 (Fig. 4.30) and the epidermal growth factor receptor (EGFR). The binding site in Spa for TNFR1 was localised to the helix 1-2 face, the region on Spa also involved in binding vWF and Fc $\gamma$  (Fig. 4.31). Binding to TNFR1 and EGFR may be through a distinct site on Spa, as the SpaD variants F5A and L17A (on helix 1) bound TNFR1 but not EGFR. However, TNFR1 binding by these Spa variants was reduced when compared to wild-type Spa and the EGFR binding site most likely overlaps that of TNFR1. It may be that the binding site for EGFR is also located on the helix 1-2 face of Spa (with different residues involved to those of TNFR1) or perhaps through a binding site created by helices 1 and 3. This has yet to be investigated. This indicates multifunctional roles for Spa in the pathogenesis of *S. aureus* in the airway epithelium. *S. aureus* expressing protein A recognises the ectodomain of TNFR1 expressed on the surface of airway epithelial cells through residues on the helix 1-2 face of each Spa repeat and induces signalling events of the pro-inflammatory cascade. Spa also recognises EGFR and induces phosphorylation of EGFR and an anti-inflammatory cascade with subsequent phosphorylation of the TNF- $\alpha$  converting enzyme (TACE). TACE is mobilised to the apical surface and causes shedding of TNFR1. This anti-inflammatory effect may be a way for *S. aureus* to regulate the level of surface-located TNFR1 and modulate the host immune response. A model for pathogenesis of the airway epithelium through staphylococcal protein A is proposed in Figure 6.2.

Taken together, this work has identified the binding site on Spa for vWF and TNFR-1. This region of Spa also contains the binding site for Fc $\gamma$  and important residues



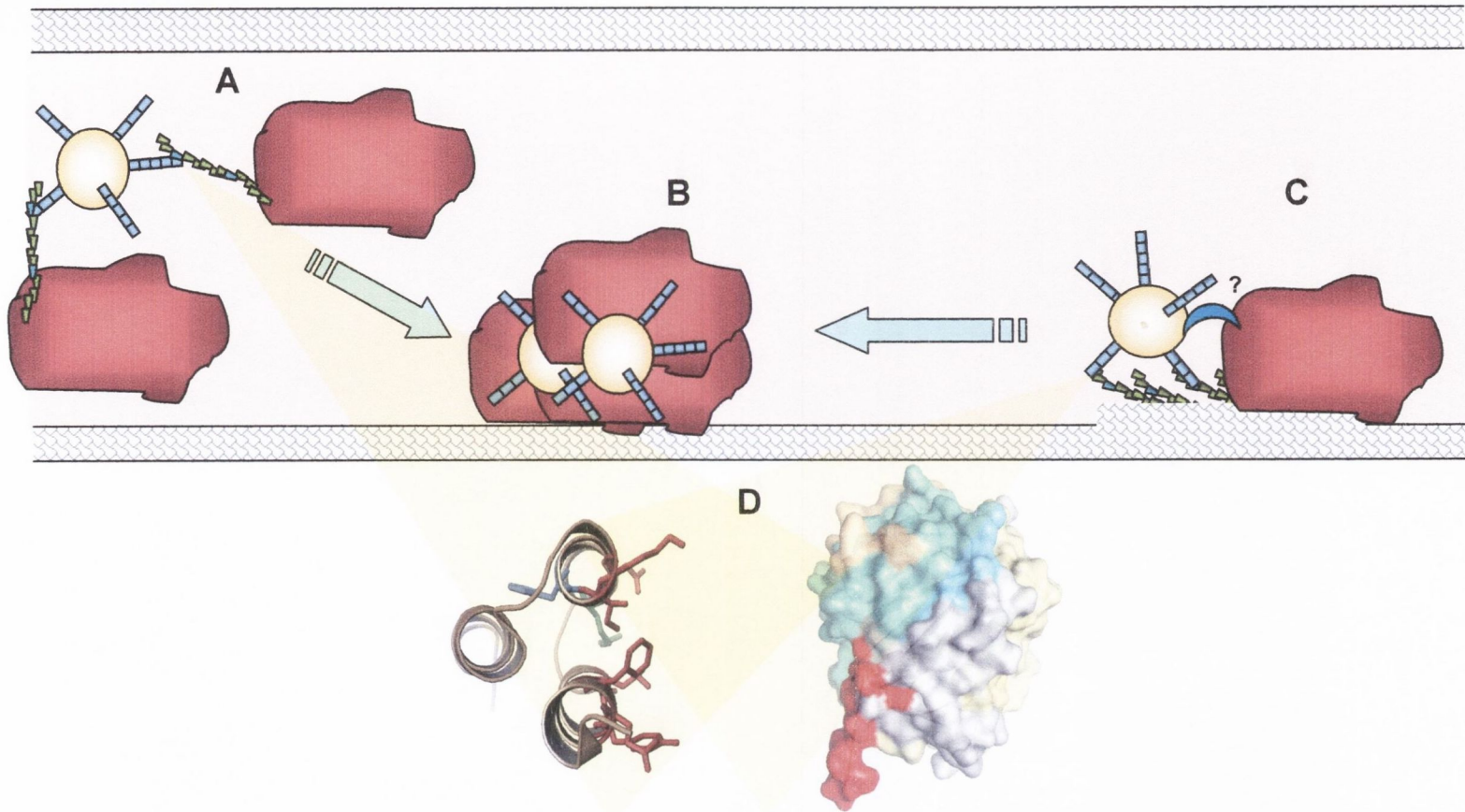


**Fig. 6.1 Model for the role of protein A binding vWF in the vascular endothelium.** (A) In conditions of high shear, vWF (green) adopts an active conformation and is bound by protein A (blue) expressed on the *S. aureus* surface. Other *S. aureus* surface proteins are not effective in platelet interactions at high shear (B). This bridges *S. aureus* to the platelet surface to allow platelet activation and aggregation and subsequent infected vegetative thrombi. (C) In damaged blood vessels, exposed subendothelial collagen is bound by circulating vWF, which becomes conformationally active for platelet binding. Bacteria bind to the activated vWF allowing *S. aureus* interactions with the vascular endothelium or platelets through other surface proteins (cyan) or perhaps a direct interaction between Spa and  $\alpha_{IIb}\beta_3$  and the formation of infectious thrombi. (D) Residues on helices 1 and 2 of Spa (left) are responsible for binding to vWF, predominantly through the A1 domain (right). The region on vWF A1 may reside close to the collagen and ristocetin binding site(s) (in red).

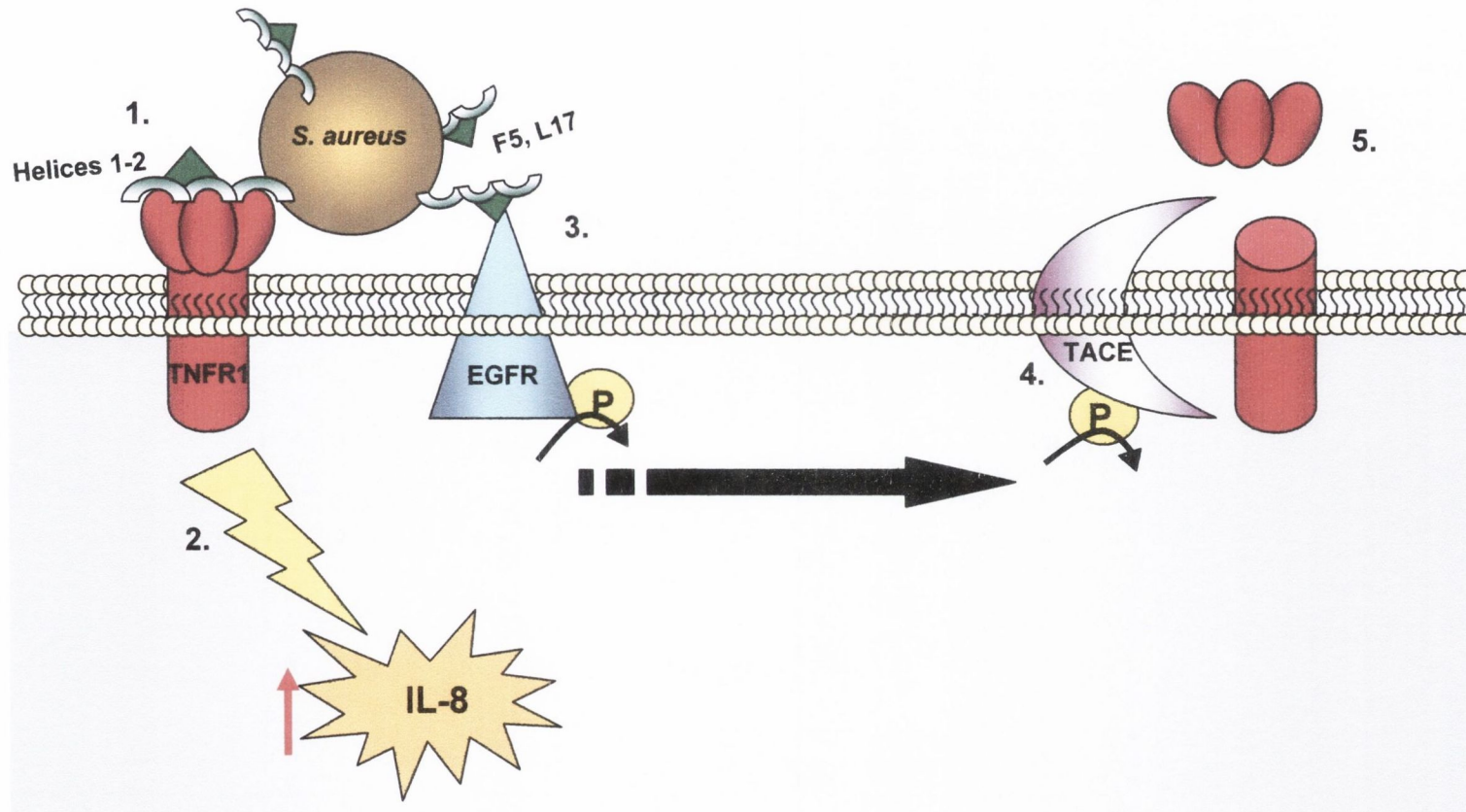


**Fig. 6.2 Model for inflammation of the airway epithelium caused by protein A.** (1) *S. aureus* expressing protein A (green) recognises the ectodomain of TNFR1 expressed on the surface of airway epithelial cells through residues on the helix1-2 face of each Spa repeats. (2) Binding induces signalling events of the pro-inflammatory cascade including induction of IL-8. (3) Spa also recognises EGFR with residues F5 and L17 on helix 1 essential for binding. (4) Binding induces phosphorylation of EGFR and an anti-inflammatory cascade with subsequent phosphorylation of TACE. TACE mobilises to the apical surface and causes shedding of TNFR1. This latter anti-inflammatory effect may be a way for *S. aureus* to regulate the level of surface TNFR1 and the host immune response.



for EGFR binding. This reveals protein A to be a multifunctional virulence factor. The presence of ligand binding sites on each repeat domain allows Spa to bind multiple ligands simultaneously. This feature is not unique to Spa and other proteins that bind multiple ligands have been shown through structural studies to use virtually the same set of contact residues for binding. An example of this is the Fc portion of IgG which can bind four distinctly folded proteins; protein A (Deisenhofer, 1981), protein G (Sauer-Eriksson *et al.*, 1995), rheumatoid factor (Corper *et al.*, 1997), and neonatal Fc-receptor (Burmeister *et al.*, 1994) within a small region on the protein. This opens up the possibility for the design of peptides or humanised monoclonal antibodies that could provide passive immunization by blocking binding by Spa to many of its ligands. This could be particularly important with the rise of community-associated methicillin-resistant *S. aureus* (CA-MRSA) strains (Chambers, 2005). There is a strong association between CA-MRSA strains and the Panton Valentine leukocidin (PVL) (Chambers, 2005; Gillet *et al.*, 2002; Vandenesch *et al.*, 2003). Recently PVL has been shown to be an important virulence factor in the pathogenesis of pneumonia in mice (Labandeira-Rey *et al.*, 2007). Interestingly, the up-regulated production of PVL in CA-MRSA strains was responsible for increased Spa expression. Increased expression of Spa was also reported in *S. aureus* isolated from patients with Kawasaki disease, an acute vasculitis in children (Wann *et al.*, 1999). Spa and PVL were shown to act co-operatively to cause severe necrotising pneumonia (Labandeira-Rey *et al.*, 2007). The increased expression of Spa in CA-MRSA strains could play a key role in their increased virulence.



## References

- Ajzenberg, N., Ribba, A.S., Rastegar-Lari, G., Meyer, D., and Baruch, D. (2000) Effect of recombinant von Willebrand factor reproducing type 2B or type 2M mutations on shear-induced platelet aggregation. *Blood* **95**: 3796-3803.
- Akerstrom, B., and Bjorck, L. (1989) Protein L: an immunoglobulin light chain-binding bacterial protein. Characterization of binding and physicochemical properties. *J Biol Chem* **264**: 19740-19746.
- Andrade, M.A., Ciccarelli, F.D., Perez-Iratxeta, C., and Bork, P. (2002) NEAT: a domain duplicated in genes near the components of a putative Fe<sup>3+</sup> siderophore transporter from Gram-positive pathogenic bacteria. *Genome Biol* **3**: RESEARCH0047.
- Ansorge, W. (1985) Fast and sensitive detection of protein and DNA bands by treatment with potassium permanganate. *J Biochem Biophys Methods* **11**: 13-20.
- Arciola, C.R., Campoccia, D., Gamberini, S., Baldassarri, L., and Montanaro, L. (2005) Prevalence of *cna*, *fnbA* and *fnbB* adhesin genes among *Staphylococcus aureus* isolates from orthopedic infections associated to different types of implant. *FEMS Microbiol Lett* **246**: 81-86.
- Azuma, H., Hayashi, T., Dent, J.A., Ruggeri, Z.M., and Ware, J. (1993) Disulfide bond requirements for assembly of the platelet glycoprotein Ib-binding domain of von Willebrand factor. *J Biol Chem* **268**: 2821-2827.
- Baddour, L.M., Lowrance, C., Albus, A., Lowrance, J.H., Anderson, S.K., and Lee, J.C. (1992) *Staphylococcus aureus* microcapsule expression attenuates bacterial virulence in a rat model of experimental endocarditis. *J Infect Dis* **165**: 749-753.
- Bayer, M.G., Heinrichs, J.H., and Cheung, A.L. (1996) The molecular architecture of the *sar* locus in *Staphylococcus aureus*. *J Bacteriol* **178**: 4563-4570.

Benito, Y., Kolb, F.A., Romby, P., Lina, G., Etienne, J., and Vandenesch, F. (2000) Probing the structure of RNAIII, the *Staphylococcus aureus agr* regulatory RNA, and identification of the RNA domain involved in repression of protein A expression. *Rna* **6**: 668-679.

Bennett, J.S., and Kolodziej, M.A. (1992) Disorders of platelet function. *Dis Mon* **38**: 577-631.

Berndt, M.C., Ward, C.M., Booth, W.J., Castaldi, P.A., Mazurov, A.V., and Andrews, R.K. (1992) Identification of aspartic acid 514 through glutamic acid 542 as a glycoprotein Ib-IX complex receptor recognition sequence in von Willebrand factor. Mechanism of modulation of von Willebrand factor by ristocetin and botrocetin. *Biochemistry* **31**: 11144-11151.

Bhasin, N., Albus, A., Michon, F., Livolsi, P.J., Park, J.S., and Lee, J.C. (1998) Identification of a gene essential for O-acetylation of the *Staphylococcus aureus* type 5 capsular polysaccharide. *Mol Microbiol* **27**: 9-21.

Bienkowska, J., Cruz, M., Atiemo, A., Handin, R., and Liddington, R. (1997) The von willebrand factor A3 domain does not contain a metal ion-dependent adhesion site motif. *J Biol Chem* **272**: 25162-25167.

Bischoff, M., Dunman, P., Kormanec, J., Macapagal, D., Murphy, E., Mounts, W., Berger-Bachi, B., and Projan, S. (2004) Microarray-based analysis of the *Staphylococcus aureus* sigmaB regulon. *J Bacteriol* **186**: 4085-4099.

Bjorck, L. (1988) Protein L. A novel bacterial cell wall protein with affinity for Ig L chains. *J Immunol* **140**: 1194-1197.

Boden, M.K., and Flock, J.I. (1994) Cloning and characterization of a gene for a 19 kDa fibrinogen-binding protein from *Staphylococcus aureus*. *Mol Microbiol* **12**: 599-606.

Bozzini, S., Visai, L., Pignatti, P., Petersen, T.E., and Speziale, P. (1992) Multiple binding sites in fibronectin and the staphylococcal fibronectin receptor. *Eur J Biochem* **207**: 327-333.

Braun, L., Dramsi, S., Dehoux, P., Bierne, H., Lindahl, G., and Cossart, P. (1997) InlB: an invasion protein of *Listeria monocytogenes* with a novel type of surface association. *Mol Microbiol* **25**: 285-294.

Brogden, K.A. (2005) Antimicrobial peptides: pore formers or metabolic inhibitors in bacteria? *Nat Rev Microbiol* **3**: 238-250.

Bronner, S., Monteil, H., and Prevost, G. (2004) Regulation of virulence determinants in *Staphylococcus aureus*: complexity and applications. *FEMS Microbiol Rev* **28**: 183-200.

Burmeister, W.P., Huber, A.H., and Bjorkman, P.J. (1994) Crystal structure of the complex of rat neonatal Fc receptor with Fc. *Nature* **372**: 379-383.

Byrne, M.F., Kerrigan, S.W., Corcoran, P.A., Atherton, J.C., Murray, F.E., Fitzgerald, D.J., and Cox, D.M. (2003) *Helicobacter pylori* binds von Willebrand factor and interacts with GPIIb to induce platelet aggregation. *Gastroenterology* **124**: 1846-1854.

Carew, J.A., Quinn, S.M., Stoddart, J.H., and Lynch, D.C. (1992) O-linked carbohydrate of recombinant von Willebrand factor influences ristocetin-induced binding to platelet glycoprotein 1b. *J Clin Invest* **90**: 2258-2267.

Cauwenberghs, N., Vanhoorelbeke, K., Vauterin, S., and Deckmyn, H. (2000) Structural determinants within platelet glycoprotein Ibalpha involved in its binding to von Willebrand factor. *Platelets* **11**: 373-378.

Cauwenberghs, N., Vanhoorelbeke, K., Vauterin, S., Westra, D.F., Romo, G., Huizinga, E.G., Lopez, J.A., Berndt, M.C., Harsfalvi, J., and Deckmyn, H. (2001) Epitope mapping of inhibitory antibodies against platelet glycoprotein Ibalpha reveals interaction between the leucine-rich repeat N-terminal and C-terminal flanking domains of glycoprotein Ibalpha. *Blood* **98**: 652-660.

Cedergren, L., Andersson, R., Jansson, B., Uhlen, M., and Nilsson, B. (1993) Mutational analysis of the interaction between staphylococcal protein A and human IgG1. *Protein Eng* **6**: 441-448.



Celikel, R., Varughese, K.I., Madhusudan, Yoshioka, A., Ware, J., and Ruggeri, Z.M. (1998) Crystal structure of the von Willebrand factor A1 domain in complex with the function blocking NMC-4 Fab. *Nat Struct Biol* **5**: 189-194.

Celli, J., and Finlay, B.B. (2002) Bacterial avoidance of phagocytosis. *Trends Microbiol* **10**: 232-237.

Chambers, H.F. (2005) Community-associated MRSA--resistance and virulence converge. *N Engl J Med* **352**: 1485-1487.

Chan, P.F., Foster, S.J., Ingham, E., and Clements, M.O. (1998) The *Staphylococcus aureus* alternative sigma factor sigmaB controls the environmental stress response but not starvation survival or pathogenicity in a mouse abscess model. *J Bacteriol* **180**: 6082-6089.

Chavakis, T., Hussain, M., Kanse, S.M., Peters, G., Bretzel, R.G., Flock, J.I., Herrmann, M., and Preissner, K.T. (2002) *Staphylococcus aureus* extracellular adherence protein serves as anti-inflammatory factor by inhibiting the recruitment of host leukocytes. *Nat Med* **8**: 687-693.

Cheung, A.L., Eberhardt, K., and Heinrichs, J.H. (1997) Regulation of protein A synthesis by the *sar* and *agr* loci of *Staphylococcus aureus*. *Infect Immun* **65**: 2243-2249.

Cheung, A.L., Chien, Y.T., and Bayer, A.S. (1999) Hyperproduction of alpha-hemolysin in a sigB mutant is associated with elevated SarA expression in *Staphylococcus aureus*. *Infect Immun* **67**: 1331-1337.

Cheung, A.L., Schmidt, K., Bateman, B., and Manna, A.C. (2001) SarS, a SarA homolog repressible by *agr*, is an activator of protein A synthesis in *Staphylococcus aureus*. *Infect Immun* **69**: 2448-2455.

Cheung, A.L., Bayer, A.S., Zhang, G., Gresham, H., and Xiong, Y.Q. (2004) Regulation of virulence determinants in vitro and in vivo in *Staphylococcus aureus*. *FEMS Immunol Med Microbiol* **40**: 1-9.

Chien, Y., and Cheung, A.L. (1998) Molecular interactions between two global regulators, *sar* and *agr*, in *Staphylococcus aureus*. *J Biol Chem* **273**: 2645-2652.

Chien, Y., Manna, A.C., Projan, S.J., and Cheung, A.L. (1999) SarA, a global regulator of virulence determinants in *Staphylococcus aureus*, binds to a conserved motif essential for *sar*-dependent gene regulation. *J Biol Chem* **274**: 37169-37176.

Christophe, O., Obert, B., Meyer, D., and Girma, J.P. (1991) The binding domain of von Willebrand factor to sulfatides is distinct from those interacting with glycoprotein Ib, heparin, and collagen and resides between amino acid residues Leu 512 and Lys 673. *Blood* **78**: 2310-2317.

Christophe, T., Karlsson, A., Dugave, C., Rabiet, M.J., Boulay, F., and Dahlgren, C. (2001) The synthetic peptide Trp-Lys-Tyr-Met-Val-Met-NH<sub>2</sub> specifically activates neutrophils through FPRL1/lipoxin A4 receptors and is an agonist for the orphan monocyte-expressed chemoattractant receptor FPRL2. *J Biol Chem* **276**: 21585-21593.

Clarke, S.R., Wiltshire, M.D., and Foster, S.J. (2004) IsdA of *Staphylococcus aureus* is a broad spectrum, iron-regulated adhesin. *Mol Microbiol* **51**: 1509-1519.

Clawson, C.C. (1973) Platelet interaction with bacteria. 3. Ultrastructure. *Am J Pathol* **70**: 449-471.

Corper, A.L., Sohi, M.K., Bonagura, V.R., Steinitz, M., Jefferis, R., Feinstein, A., Beale, D., Taussig, M.J., and Sutton, B.J. (1997) Structure of human IgM rheumatoid factor Fab bound to its autoantigen IgG Fc reveals a novel topology of antibody-antigen interaction. *Nat Struct Biol* **4**: 374-381.

Cosgrove, S.E., Carroll, K.C., and Perl, T.M. (2004) *Staphylococcus aureus* with reduced susceptibility to vancomycin. *Clin Infect Dis* **39**: 539-545.

Cregg, K.M., Wilding, I., and Black, M.T. (1996) Molecular cloning and expression of the *spsB* gene encoding an essential type I signal peptidase from *Staphylococcus aureus*. *J Bacteriol* **178**: 5712-5718.

Cruz, M.A., Handin, R.I., and Wise, R.J. (1993) The interaction of the von Willebrand factor-A1 domain with platelet glycoprotein Ib/IX. The role of glycosylation and disulfide bonding in a monomeric recombinant A1 domain protein. *J Biol Chem* **268**: 21238-21245.

Cruz, M.A., Diacovo, T.G., Emsley, J., Liddington, R., and Handin, R.I. (2000) Mapping the glycoprotein Ib-binding site in the von willebrand factor A1 domain. *J Biol Chem* **275**: 19098-19105.

Cunnion, K.M., Zhang, H.M., and Frank, M.M. (2003) Availability of complement bound to *Staphylococcus aureus* to interact with membrane complement receptors influences efficiency of phagocytosis. *Infect Immun* **71**: 656-662.

Davis, S.L., Gurusiddappa, S., McCrea, K.W., Perkins, S., and Hook, M. (2001) SdrG, a fibrinogen-binding bacterial adhesin of the microbial surface components recognizing adhesive matrix molecules subfamily from *Staphylococcus epidermidis*, targets the thrombin cleavage site in the Bbeta chain. *J Biol Chem* **276**: 27799-27805.

de Haas, C.J., Veldkamp, K.E., Peschel, A., Weerkamp, F., Van Wamel, W.J., Heezius, E.C., Poppelier, M.J., Van Kessel, K.P., and van Strijp, J.A. (2004) Chemotaxis inhibitory protein of *Staphylococcus aureus*, a bacterial antiinflammatory agent. *J Exp Med* **199**: 687-695.

De Luca, M., Facey, D.A., Favalaro, E.J., Hertzberg, M.S., Whisstock, J.C., McNally, T., Andrews, R.K., and Berndt, M.C. (2000) Structure and function of the von Willebrand factor A1 domain: analysis with monoclonal antibodies reveals distinct binding sites involved in recognition of the platelet membrane glycoprotein Ib-IX-V complex and ristocetin-dependent activation. *Blood* **95**: 164-172.

De Marco, L., Girolami, A., Russell, S., and Ruggeri, Z.M. (1985) Interaction of asialo von Willebrand factor with glycoprotein Ib induces fibrinogen binding to the glycoprotein IIb/IIIa complex and mediates platelet aggregation. *J Clin Invest* **75**: 1198-1203.

Deisenhofer, J. (1981) Crystallographic refinement and atomic models of a human Fc fragment and its complex with fragment B of protein A from *Staphylococcus aureus* at 2.9- and 2.8-Å resolution. *Biochemistry* **20**: 2361-2370.



Deivanayagam, C.C., Rich, R.L., Carson, M., Owens, R.T., Danthuluri, S., Bice, T., Hook, M., and Narayana, S.V. (2000) Novel fold and assembly of the repetitive B region of the *Staphylococcus aureus* collagen-binding surface protein. *Structure* **8**: 67-78.

Deivanayagam, C.C., Wann, E.R., Chen, W., Carson, M., Rajashankar, K.R., Hook, M., and Narayana, S.V. (2002) A novel variant of the immunoglobulin fold in surface adhesins of *Staphylococcus aureus*: crystal structure of the fibrinogen-binding MSCRAMM, clumping factor A. *Embo J* **21**: 6660-6672.

Dong, J.F., Berndt, M.C., Schade, A., McIntire, L.V., Andrews, R.K., and Lopez, J.A. (2001) Ristocetin-dependent, but not botrocetin-dependent, binding of von Willebrand factor to the platelet glycoprotein Ib-IX-V complex correlates with shear-dependent interactions. *Blood* **97**: 162-168.

Dong, Z., Thoma, R.S., Crimmins, D.L., McCourt, D.W., Tuley, E.A., and Sadler, J.E. (1994) Disulfide bonds required to assemble functional von Willebrand factor multimers. *J Biol Chem* **269**: 6753-6758.

Downer, R., Roche, F., Park, P.W., Mecham, R.P., and Foster, T.J. (2002) The elastin-binding protein of *Staphylococcus aureus* (EbpS) is expressed at the cell surface as an integral membrane protein and not as a cell wall-associated protein. *J Biol Chem* **277**: 243-250.

Dryla, A., Gelbmann, D., von Gabain, A., and Nagy, E. (2003) Identification of a novel iron regulated staphylococcal surface protein with haptoglobin-haemoglobin binding activity. *Mol Microbiol* **49**: 37-53.

Dryla, A., Prustomersky, S., Gelbmann, D., Hanner, M., Bettinger, E., Kocsis, B., Kustos, T., Henics, T., Meinke, A., and Nagy, E. (2005) Comparison of antibody repertoires against *Staphylococcus aureus* in healthy individuals and in acutely infected patients. *Clin Diagn Lab Immunol* **12**: 387-398.

Dumas, J.J., Kumar, R., McDonagh, T., Sullivan, F., Stahl, M.L., Somers, W.S., and Mosyak, L. (2004) Crystal structure of the wild-type von Willebrand factor A1-glycoprotein Ibalpha complex reveals conformation differences with a complex bearing von Willebrand disease mutations. *J Biol Chem* **279**: 23327-23334.

Dunman, P.M., Murphy, E., Haney, S., Palacios, D., Tucker-Kellogg, G., Wu, S., Brown, E.L., Zagursky, R.J., Shlaes, D., and Projan, S.J. (2001) Transcription profiling-based identification of *Staphylococcus aureus* genes regulated by the *agr* and/or *sarA* loci. *J Bacteriol* **183**: 7341-7353.

Duthie, E.S., and Lorenz, L.L. (1952) Staphylococcal coagulase; mode of action and antigenicity. *J Gen Microbiol* **6**: 95-107.

Elasri, M.O., Thomas, J.R., Skinner, R.A., Blevins, J.S., Beenken, K.E., Nelson, C.L., and Smeltzer, M.S. (2002) *Staphylococcus aureus* collagen adhesin contributes to the pathogenesis of osteomyelitis. *Bone* **30**: 275-280.

Emsley, J., King, S.L., Bergelson, J.M., and Liddington, R.C. (1997) Crystal structure of the I domain from integrin alpha2beta1. *J Biol Chem* **272**: 28512-28517.

Emsley, J., Cruz, M., Handin, R., and Liddington, R. (1998) Crystal structure of the von Willebrand Factor A1 domain and implications for the binding of platelet glycoprotein Ib. *J Biol Chem* **273**: 10396-10401.

Fedtke, I., Gotz, F., and Peschel, A. (2004) Bacterial evasion of innate host defenses--the *Staphylococcus aureus* lesson. *Int J Med Microbiol* **294**: 189-194.

Fischer, B.E., Kramer, G., Mitterer, A., Grillberger, L., Reiter, M., Mundt, W., Dorner, F., and Eibl, J. (1996) Effect of multimerization of human and recombinant von Willebrand factor on platelet aggregation, binding to collagen and binding of coagulation factor VIII. *Thromb Res* **84**: 55-66.

Fitzgerald, J.R., Foster, T.J., and Cox, D. (2006a) The interaction of bacterial pathogens with platelets. *Nat Rev Microbiol* **4**: 445-457.

Fitzgerald, J.R., Loughman, A., Keane, F., Brennan, M., Knobel, M., Higgins, J., Visai, L., Speziale, P., Cox, D., and Foster, T.J. (2006b) Fibronectin-binding proteins of *Staphylococcus aureus* mediate activation of human platelets via fibrinogen and fibronectin bridges to integrin GPIIb/IIIa and IgG binding to the Fcγ3R1a receptor. *Mol Microbiol* **59**: 212-230.

Forsgren, A., and Nordstrom, K. (1974) Protein A from *Staphylococcus aureus*: the biological significance of its reaction with IgG. *Ann N Y Acad Sci* **236**: 252-266.

Foster, P.A., Fulcher, C.A., Marti, T., Titani, K., and Zimmerman, T.S. (1987) A major factor VIII binding domain resides within the amino-terminal 272 amino acid residues of von Willebrand factor. *J Biol Chem* **262**: 8443-8446.

Fournier, B., Klier, A., and Rapoport, G. (2001) The two-component system ArlS-ArlR is a regulator of virulence gene expression in *Staphylococcus aureus*. *Mol Microbiol* **41**: 247-261.

Fowler, V.G., Jr., Miro, J.M., Hoen, B., Cabell, C.H., Abrutyn, E., Rubinstein, E., Corey, G.R., Spelman, D., Bradley, S.F., Barsic, B., Pappas, P.A., Anstrom, K.J., Wray, D., Fortes, C.Q., Anguera, I., Athan, E., Jones, P., van der Meer, J.T., Elliott, T.S., Levine, D.P., and Bayer, A.S. (2005) *Staphylococcus aureus* endocarditis: a consequence of medical progress. *Jama* **293**: 3012-3021.

Fowler, W.E., Fretto, L.J., Hamilton, K.K., Erickson, H.P., and McKee, P.A. (1985) Substructure of human von Willebrand factor. *J Clin Invest* **76**: 1491-1500.

Fraser, J., Arcus, V., Kong, P., Baker, E., and Proft, T. (2000) Superantigens - powerful modifiers of the immune system. *Mol Med Today* **6**: 125-132.

Fujimura, Y., Titani, K., Holland, L.Z., Russell, S.R., Roberts, J.R., Elder, J.H., Ruggeri, Z.M., and Zimmerman, T.S. (1986) von Willebrand factor. A reduced and alkylated 52/48-kDa fragment beginning at amino acid residue 449 contains the domain interacting with platelet glycoprotein Ib. *J Biol Chem* **261**: 381-385.



Fujimura, Y., Titani, K., Holland, L.Z., Roberts, J.R., Kostel, P., Ruggeri, Z.M., and Zimmerman, T.S. (1987) A heparin-binding domain of human von Willebrand factor. Characterization and localization to a tryptic fragment extending from amino acid residue Val-449 to Lys-728. *J Biol Chem* **262**: 1734-1739.

Fukuda, K., Doggett, T., Laurenzi, I.J., Liddington, R.C., and Diacovo, T.G. (2005) The snake venom protein botrocetin acts as a biological brace to promote dysfunctional platelet aggregation. *Nat Struct Mol Biol* **12**: 152-159.

Gao, J., and Stewart, G.C. (2004) Regulatory elements of the *Staphylococcus aureus* protein A (Spa) promoter. *J Bacteriol* **186**: 3738-3748.

Gase, K., Liu, G., Bruckmann, A., Steiner, K., Ozegowski, J., and Malke, H. (1997) The lppC gene of *Streptococcus equisimilis* encodes a lipoprotein that is homologous to the e (P4) outer membrane protein from *Haemophilus influenzae*. *Med Microbiol Immunol (Berl)* **186**: 63-73.

Gemmell, C., Tree, R. , Patel, A. , O'Reilly, M. , Foster, T. J. (1991) Susceptibility to opsonophagocytosis of protein A, alpha-haemolysin and beta-toxin deficient mutants of *Staphylococcus aureus* isolated by allele-replacement. . *Zentralbl. Bakteriol.* **21 (Suppl.)**: 273-277.

George, N.P., Wei, Q., Shin, P.K., Konstantopoulos, K., and Ross, J.M. (2006) *Staphylococcus aureus* adhesion via Spa, ClfA, and SdrCDE to immobilized platelets demonstrates shear-dependent behavior. *Arterioscler Thromb Vasc Biol* **26**: 2394-2400.

Gibbins, J.M. (2004) Platelet adhesion signalling and the regulation of thrombus formation. *J Cell Sci* **117**: 3415-3425.

Gillet, Y., Issartel, B., Vanhems, P., Fournet, J.C., Lina, G., Bes, M., Vandenesch, F., Piemont, Y., Brousse, N., Floret, D., and Etienne, J. (2002) Association between *Staphylococcus aureus* strains carrying gene for Panton-Valentine leukocidin and highly lethal necrotising pneumonia in young immunocompetent patients. *Lancet* **359**: 753-759.

Ginsburg, D., and Sadler, J.E. (1993) von Willebrand disease: a database of point mutations, insertions, and deletions. For the Consortium on von Willebrand Factor Mutations and Polymorphisms, and the Subcommittee on von Willebrand Factor of the Scientific and Standardization Committee of the International Society on Thrombosis and Haemostasis. *Thromb Haemost* **69**: 177-184.

Goerke, C., Campana, S., Bayer, M.G., Doring, G., Botzenhart, K., and Wolz, C. (2000) Direct quantitative transcript analysis of the *agr* regulon of *Staphylococcus aureus* during human infection in comparison to the expression profile in vitro. *Infect Immun* **68**: 1304-1311.

Gomez, M.I., Lee, A., Reddy, B., Muir, A., Soong, G., Pitt, A., Cheung, A., and Prince, A. (2004) *Staphylococcus aureus* protein A induces airway epithelial inflammatory responses by activating TNFR1. *Nat Med* **10**: 842-848.

Goodyear, C.S., and Silverman, G.J. (2003) Death by a B cell superantigen: In vivo VH-targeted apoptotic supraclonal B cell deletion by a Staphylococcal Toxin. *J Exp Med* **197**: 1125-1139.

Goodyear, C.S., Narita, M., and Silverman, G.J. (2004) In vivo VL-targeted activation-induced apoptotic supraclonal deletion by a microbial B cell toxin. *J Immunol* **172**: 2870-2877.

Goodyear, C.S., and Silverman, G.J. (2004) Staphylococcal toxin induced preferential and prolonged in vivo deletion of innate-like B lymphocytes. *Proc Natl Acad Sci U S A* **101**: 11392-11397.

Gouda, H., Torigoe, H., Saito, A., Sato, M., Arata, Y., and Shimada, I. (1992) Three-dimensional solution structure of the B domain of staphylococcal protein A: comparisons of the solution and crystal structures. *Biochemistry* **31**: 9665-9672.

Graille, M., Stura, E.A., Corper, A.L., Sutton, B.J., Taussig, M.J., Charbonnier, J.B., and Silverman, G.J. (2000) Crystal structure of a *Staphylococcus aureus* protein A domain complexed with the Fab fragment of a human IgM antibody: structural basis for recognition of B-cell receptors and superantigen activity. *Proc Natl Acad Sci U S A* **97**: 5399-5404.

Graille, M., Stura, E.A., Housden, N.G., Beckingham, J.A., Bottomley, S.P., Beale, D., Taussig, M.J., Sutton, B.J., Gore, M.G., and Charbonnier, J.B. (2001) Complex between *Peptostreptococcus magnus* protein L and a human antibody reveals structural convergence in the interaction modes of Fab binding proteins. *Structure* **9**: 679-687.

Greene, C., McDevitt, D., Francois, P., Vaudaux, P.E., Lew, D.P., and Foster, T.J. (1995) Adhesion properties of mutants of *Staphylococcus aureus* defective in fibronectin-binding proteins and studies on the expression of *fnb* genes. *Mol Microbiol* **17**: 1143-1152.

Haas, P.J., de Haas, C.J., Poppelier, M.J., van Kessel, K.P., van Strijp, J.A., Dijkstra, K., Scheek, R.M., Fan, H., Kruijtzter, J.A., Liskamp, R.M., and Kemmink, J. (2005) The structure of the C5a receptor-blocking domain of chemotaxis inhibitory protein of *Staphylococcus aureus* is related to a group of immune evasive molecules. *J Mol Biol* **353**: 859-872.

Handin, R.I. (2003) A hitchhiker's guide to the galaxy--an *H.pylori* travel guide. *Gastroenterology* **124**: 1983-1985.

Harraghy, N., Hussain, M., Hagggar, A., Chavakis, T., Sinha, B., Herrmann, M., and Flock, J.I. (2003) The adhesive and immunomodulating properties of the multifunctional *Staphylococcus aureus* protein Eap. *Microbiology* **149**: 2701-2707.

Hartford, O., O'Brien, L., Schofield, K., Wells, J., and Foster, T.J. (2001a) The Fbe (SdrG) protein of *Staphylococcus epidermidis* HB promotes bacterial adherence to fibrinogen. *Microbiology* **147**: 2545-2552.

Hartford, O.M., Wann, E.R., Hook, M., and Foster, T.J. (2001b) Identification of residues in the *Staphylococcus aureus* fibrinogen-binding MSCRAMM clumping factor A (ClfA) that are important for ligand binding. *J Biol Chem* **276**: 2466-2473.

Hartleib, J., Kohler, N., Dickinson, R.B., Chhatwal, G.S., Sixma, J.J., Hartford, O.M., Foster, T.J., Peters, G., Kehrel, B.E., and Herrmann, M. (2000) Protein A is the von Willebrand factor binding protein on *Staphylococcus aureus*. *Blood* **96**: 2149-2156.



Hawiger, J., Marney, S.R., Jr., Colley, D.G., and Des Prez, R.M. (1972) Complement-dependent platelet injury by staphylococcal protein A. *J Exp Med* **136**: 68-80.

Hawiger, J., Steckley, S., Hammond, D., Cheng, C., Timmons, S., Glick, A.D., and Des Prez, R.M. (1979) Staphylococci-induced human platelet injury mediated by protein A and immunoglobulin G Fc fragment receptor. *J Clin Invest* **64**: 931-937.

Herrmann, M., Lai, Q.J., Albrecht, R.M., Mosher, D.F., and Proctor, R.A. (1993) Adhesion of *Staphylococcus aureus* to surface-bound platelets: role of fibrinogen/fibrin and platelet integrins. *J Infect Dis* **167**: 312-322.

Hienz, S.A., Schennings, T., Heimdahl, A., and Flock, J.I. (1996) Collagen binding of *Staphylococcus aureus* is a virulence factor in experimental endocarditis. *J Infect Dis* **174**: 83-88.

Higgins, J., Loughman, A., van Kessel, K.P., van Strijp, J.A., and Foster, T.J. (2006) Clumping factor A of *Staphylococcus aureus* inhibits phagocytosis by human polymorphonuclear leucocytes. *FEMS Microbiol Lett* **258**: 290-296.

Hiramatsu, K., Cui, L., Kuroda, M., and Ito, T. (2001) The emergence and evolution of methicillin-resistant *Staphylococcus aureus*. *Trends Microbiol* **9**: 486-493.

Horsburgh, M.J., Ingham, E., and Foster, S.J. (2001) In *Staphylococcus aureus*, fur is an interactive regulator with PerR, contributes to virulence, and is necessary for oxidative stress resistance through positive regulation of catalase and iron homeostasis. *J Bacteriol* **183**: 468-475.

House-Pompeo, K., Xu, Y., Joh, D., Speziale, P., and Hook, M. (1996) Conformational changes in the fibronectin binding MSCRAMMs are induced by ligand binding. *J Biol Chem* **271**: 1379-1384.

Hoylaerts, M.F., Nuyts, K., Peerlinck, K., Deckmyn, H., and Vermeylen, J. (1995) Promotion of binding of von Willebrand factor to platelet glycoprotein Ib by dimers of ristocetin. *Biochem J* **306 ( Pt 2)**: 453-463.

Hoylaerts, M.F., Yamamoto, H., Nuyts, K., Vreys, I., Deckmyn, H., and Vermeylen, J. (1997) von Willebrand factor binds to native collagen VI primarily via its A1 domain. *Biochem J* **324** ( Pt 1): 185-191.

Huizinga, E.G., Martijn van der Plas, R., Kroon, J., Sixma, J.J., and Gros, P. (1997) Crystal structure of the A3 domain of human von Willebrand factor: implications for collagen binding. *Structure* **5**: 1147-1156.

Huizinga, E.G., Tsuji, S., Romijn, R.A., Schiphorst, M.E., de Groot, P.G., Sixma, J.J., and Gros, P. (2002) Structures of glycoprotein Ibalpha and its complex with von Willebrand factor A1 domain. *Science* **297**: 1176-1179.

Huntzinger, E., Boisset, S., Saveanu, C., Benito, Y., Geissmann, T., Namane, A., Lina, G., Etienne, J., Ehresmann, B., Ehresmann, C., Jacquier, A., Vandenesch, F., and Romby, P. (2005) *Staphylococcus aureus* RNAIII and the endoribonuclease III coordinately regulate *spa* gene expression. *Embo J* **24**: 824-835.

Hussain, M., Hagggar, A., Heilmann, C., Peters, G., Flock, J.I., and Herrmann, M. (2002) Insertional inactivation of Eap in *Staphylococcus aureus* strain Newman confers reduced staphylococcal binding to fibroblasts. *Infect Immun* **70**: 2933-2940.

Inganas, M., Johansson, S.G., and Sjoquist, J. (1981) Further characterization of the alternative protein-A interaction of immunoglobulins: demonstration of an Fc-binding fragment of protein A expressing the alternative reactivity. *Scand J Immunol* **14**: 379-388.

Jackson, S.P., Nesbitt, W.S., and Kulkarni, S. (2003) Signaling events underlying thrombus formation. *J Thromb Haemost* **1**: 1602-1612.

Jansson, B., Uhlen, M., and Nygren, P.A. (1998) All individual domains of staphylococcal protein A show Fab binding. *FEMS Immunol Med Microbiol* **20**: 69-78.

Janzon, L., and Arvidson, S. (1990) The role of the delta-lysin gene (*hld*) in the regulation of virulence genes by the accessory gene regulator (*agr*) in *Staphylococcus aureus*. *Embo J* **9**: 1391-1399.

Jendeberg, L., Persson, B., Andersson, R., Karlsson, R., Uhlen, M., and Nilsson, B. (1995) Kinetic analysis of the interaction between protein A domain variants and human Fc using plasmon resonance detection. *J Mol Recognit* **8**: 270-278.

Jendeberg, L., Tashiro, M., Tejero, R., Lyons, B.A., Uhlen, M., Montelione, G.T., and Nilsson, B. (1996) The mechanism of binding staphylococcal protein A to immunoglobulin G does not involve helix unwinding. *Biochemistry* **35**: 22-31.

Jendeberg, L., Nilsson, P., Larsson, A., Denker, P., Uhlen, M., Nilsson, B., and Nygren, P.A. (1997) Engineering of Fc(1) and Fc(3) from human immunoglobulin G to analyse subclass specificity for staphylococcal protein A. *J Immunol Methods* **201**: 25-34.

Ji, G., Beavis, R.C., and Novick, R.P. (1995) Cell density control of staphylococcal virulence mediated by an octapeptide pheromone. *Proc Natl Acad Sci U S A* **92**: 12055-12059.

Jin, T., Bokarewa, M., Foster, T., Mitchell, J., Higgins, J., and Tarkowski, A. (2004) *Staphylococcus aureus* resists human defensins by production of staphylokinase, a novel bacterial evasion mechanism. *J Immunol* **172**: 1169-1176.

Jonsson, I.M., Mazmanian, S.K., Schneewind, O., Verdrengh, M., Bremell, T., and Tarkowski, A. (2002) On the role of *Staphylococcus aureus* sortase and sortase-catalyzed surface protein anchoring in murine septic arthritis. *J Infect Dis* **185**: 1417-1424.

Jonsson, I.M., Mazmanian, S.K., Schneewind, O., Bremell, T., and Tarkowski, A. (2003) The role of *Staphylococcus aureus* sortase A and sortase B in murine arthritis. *Microbes Infect* **5**: 775-780.

Jonsson, I.M., Arvidson, S., Foster, S., and Tarkowski, A. (2004) Sigma factor B and RsbU are required for virulence in *Staphylococcus aureus*-induced arthritis and sepsis. *Infect Immun* **72**: 6106-6111.

Jonsson, K., Signas, C., Muller, H.P., and Lindberg, M. (1991) Two different genes encode fibronectin binding proteins in *Staphylococcus aureus*. The complete nucleotide sequence and characterization of the second gene. *Eur J Biochem* **202**: 1041-1048.



Jonsson, K., McDevitt, D., McGavin, M.H., Patti, J.M., and Hook, M. (1995) *Staphylococcus aureus* expresses a major histocompatibility complex class II analog. *J Biol Chem* **270**: 21457-21460.

Josefsson, E., McCrea, K.W., Ni Eidhin, D., O'Connell, D., Cox, J., Hook, M., and Foster, T.J. (1998) Three new members of the serine-aspartate repeat protein multigene family of *Staphylococcus aureus*. *Microbiology* **144 ( Pt 12)**: 3387-3395.

Josefsson, E., Hartford, O., O'Brien, L., Patti, J.M., and Foster, T. (2001) Protection against experimental *Staphylococcus aureus* arthritis by vaccination with clumping factor A, a novel virulence determinant. *J Infect Dis* **184**: 1572-1580.

Katsumi, A., Tuley, E.A., Bodo, I., and Sadler, J.E. (2000) Localization of disulfide bonds in the cystine knot domain of human von Willebrand factor. *J Biol Chem* **275**: 25585-25594.

Kaufman, R.J., Dorner, A.J., and Fass, D.N. (1999) von Willebrand factor elevates plasma factor VIII without induction of factor VIII messenger RNA in the liver. *Blood* **93**: 193-197.

Kerrigan, S.W., Douglas, I., Wray, A., Heath, J., Byrne, M.F., Fitzgerald, D., and Cox, D. (2002) A role for glycoprotein Ib in Streptococcus sanguis-induced platelet aggregation. *Blood* **100**: 509-516.

Kessler, C.M., Nussbaum, E., and Tuazon, C.U. (1991) Disseminated intravascular coagulation associated with *Staphylococcus aureus* septicemia is mediated by peptidoglycan-induced platelet aggregation. *J Infect Dis* **164**: 101-107.

Koedam, J.A., Hamer, R.J., Beeser-Visser, N.H., Bouma, B.N., and Sixma, J.J. (1990) The effect of von Willebrand factor on activation of factor VIII by factor Xa. *Eur J Biochem* **189**: 229-234.

Kruger, R.G., Otvos, B., Frankel, B.A., Bentley, M., Dostal, P., and McCafferty, D.G. (2004) Analysis of the substrate specificity of the *Staphylococcus aureus* sortase transpeptidase SrtA. *Biochemistry* **43**: 1541-1551.

Kullik, I., Giachino, P., and Fuchs, T. (1998) Deletion of the alternative sigma factor sigmaB in *Staphylococcus aureus* reveals its function as a global regulator of virulence genes. *J Bacteriol* **180**: 4814-4820.

Kupferwasser, L.I., Yeaman, M.R., Shapiro, S.M., Nast, C.C., Sullam, P.M., Filler, S.G., and Bayer, A.S. (1999) Acetylsalicylic acid reduces vegetation bacterial density, hematogenous bacterial dissemination, and frequency of embolic events in experimental *Staphylococcus aureus* endocarditis through antiplatelet and antibacterial effects. *Circulation* **99**: 2791-2797.

Kuroda, M., Ohta, T., Uchiyama, I., Baba, T., Yuzawa, H., Kobayashi, I., Cui, L., Oguchi, A., Aoki, K., Nagai, Y., Lian, J., Ito, T., Kanamori, M., Matsumaru, H., Maruyama, A., Murakami, H., Hosoyama, A., Mizutani-Ui, Y., Takahashi, N.K., Sawano, T., Inoue, R., Kaito, C., Sekimizu, K., Hirakawa, H., Kuhara, S., Goto, S., Yabuzaki, J., Kanehisa, M., Yamashita, A., Oshima, K., Furuya, K., Yoshino, C., Shiba, T., Hattori, M., Ogasawara, N., Hayashi, H., and Hiramatsu, K. (2001) Whole genome sequencing of methicillin-resistant *Staphylococcus aureus*. *Lancet* **357**: 1225-1240.

Labandeira-Rey, M., Couzon, F., Boisset, S., Brown, E.L., Bes, M., Benito, Y., Barbu, E.M., Vazquez, V., Hook, M., Etienne, J., Vandenesch, F., and Bowden, M.G. (2007) *Staphylococcus aureus* Panton Valentine Leukocidin Causes Necrotizing Pneumonia. *Science*.

Laemmli, U.K. (1970) Cleavage of structural proteins during the assembly of the head of bacteriophage T4. *Nature* **227**: 680-685.

Langley, R., Wines, B., Willoughby, N., Basu, I., Proft, T., and Fraser, J.D. (2005) The staphylococcal superantigen-like protein 7 binds IgA and complement C5 and inhibits IgA-Fc alpha RI binding and serum killing of bacteria. *J Immunol* **174**: 2926-2933.

Lankhof, H., van Hoeij, M., Schiphorst, M.E., Bracke, M., Wu, Y.P., Ijsseldijk, M.J., Vink, T., de Groot, P.G., and Sixma, J.J. (1996) A3 domain is essential for interaction of von Willebrand factor with collagen type III. *Thromb Haemost* **75**: 950-958.

Le, Y., Oppenheim, J.J., and Wang, J.M. (2001) Pleiotropic roles of formyl peptide receptors. *Cytokine Growth Factor Rev* **12**: 91-105.

- Le, Y., Murphy, P.M., and Wang, J.M. (2002) Formyl-peptide receptors revisited. *Trends Immunol* **23**: 541-548.
- Lee, J.C., Takeda, S., Livolsi, P.J., and Paoletti, L.C. (1993) Effects of in vitro and in vivo growth conditions on expression of type 8 capsular polysaccharide by *Staphylococcus aureus*. *Infect Immun* **61**: 1853-1858.
- Lee, J.C., Park, J.S., Shepherd, S.E., Carey, V., and Fattom, A. (1997) Protective efficacy of antibodies to the *Staphylococcus aureus* type 5 capsular polysaccharide in a modified model of endocarditis in rats. *Infect Immun* **65**: 4146-4151.
- Lee, J.O., Rieu, P., Arnaout, M.A., and Liddington, R. (1995) Crystal structure of the A domain from the alpha subunit of integrin CR3 (CD11b/CD18). *Cell* **80**: 631-638.
- Lee, L.Y., Miyamoto, Y.J., McIntyre, B.W., Hook, M., McCrea, K.W., McDevitt, D., and Brown, E.L. (2002) The *Staphylococcus aureus* Map protein is an immunomodulator that interferes with T cell-mediated responses. *J Clin Invest* **110**: 1461-1471.
- Lee, L.Y., Hook, M., Haviland, D., Wetsel, R.A., Yonter, E.O., Syribeys, P., Vernachio, J., and Brown, E.L. (2004a) Inhibition of complement activation by a secreted *Staphylococcus aureus* protein. *J Infect Dis* **190**: 571-579.
- Lee, L.Y., Liang, X., Hook, M., and Brown, E.L. (2004b) Identification and characterization of the C3 binding domain of the *Staphylococcus aureus* extracellular fibrinogen-binding protein (Efb). *J Biol Chem* **279**: 50710-50716.
- Lendel, C., Wahlberg, E., Berglund, H., Eklund, M., Nygren, P.A., and Hard, T. (2002) <sup>1</sup>H, <sup>13</sup>C and <sup>15</sup>N resonance assignments of an affibody-target complex. *J Biomol NMR* **24**: 271-272.
- Liew, C.K., Smith, B.T., Pilpa, R., Suree, N., Ilangovan, U., Connolly, K.M., Jung, M.E., and Clubb, R.T. (2004) Localization and mutagenesis of the sorting signal binding site on sortase A from *Staphylococcus aureus*. *FEBS Lett* **571**: 221-226.



Lina, G., Jarraud, S., Ji, G., Greenland, T., Pedraza, A., Etienne, J., Novick, R.P., and Vandenesch, F. (1998) Transmembrane topology and histidine protein kinase activity of AgrC, the *agr* signal receptor in *Staphylococcus aureus*. *Mol Microbiol* **28**: 655-662.

Longenecker, G.L., Swift, I.A., Bowen, R.J., Beyers, B.J., and Shah, A.K. (1985) Kinetics of ibuprofen effect on platelet and endothelial prostanoid release. *Clin Pharmacol Ther* **37**: 343-348.

Loughman, A., Fitzgerald, J.R., Brennan, M.P., Higgins, J., Downer, R., Cox, D., and Foster, T.J. (2005) Roles for fibrinogen, immunoglobulin and complement in platelet activation promoted by *Staphylococcus aureus* clumping factor A. *Mol Microbiol* **57**: 804-818.

Lowy, F.D. (1998) *Staphylococcus aureus* infections. *N Engl J Med* **339**: 520-532.

Ludwig, W., Seewaldt, E., Kilpper-Balz, R., Schleifer, K.H., Magrum, L., Woese, C.R., Fox, G.E., and Stackebrandt, E. (1985) The phylogenetic position of Streptococcus and Enterococcus. *J Gen Microbiol* **131**: 543-551.

Luong, T.T., and Lee, C.Y. (2002) Overproduction of type 8 capsular polysaccharide augments *Staphylococcus aureus* virulence. *Infect Immun* **70**: 3389-3395.

Luong, T.T., Newell, S.W., and Lee, C.Y. (2003) Mgr, a novel global regulator in *Staphylococcus aureus*. *J Bacteriol* **185**: 3703-3710.

Maita, N., Nishio, K., Nishimoto, E., Matsui, T., Shikamoto, Y., Morita, T., Sadler, J.E., and Mizuno, H. (2003) Crystal structure of von Willebrand factor A1 domain complexed with snake venom, bitiscetin: insight into glycoprotein I $\alpha$  binding mechanism induced by snake venom proteins. *J Biol Chem* **278**: 37777-37781.

Marcus, A.J. (1999) *Platelets: their role in hemostasis, thrombosis and inflammation* In: *Inflammation: basic principles and clinical correlates*. Gallin, J.I., Snyderman, R. eds. Philadelphia: Lippincott Williams & Wilkins.

Marrack, P., and Kappler, J. (1990) The staphylococcal enterotoxins and their relatives. *Science* **248**: 1066.

Marti, T., Rosselet, S.J., Titani, K., and Walsh, K.A. (1987) Identification of disulfide-bridged substructures within human von Willebrand factor. *Biochemistry* **26**: 8099-8109.

Mascari, L.M., and Ross, J.M. (2003) Quantification of staphylococcal-collagen binding interactions in whole blood by use of a confocal microscopy shear-adhesion assay. *J Infect Dis* **188**: 98-107.

Massey, R.C., Kantzanou, M.N., Fowler, T., Day, N.P., Schofield, K., Wann, E.R., Berendt, A.R., Hook, M., and Peacock, S.J. (2001) Fibronectin-binding protein A of *Staphylococcus aureus* has multiple, substituting, binding regions that mediate adherence to fibronectin and invasion of endothelial cells. *Cell Microbiol* **3**: 839-851.

Massey, R.C., Dissanayeke, S.R., Cameron, B., Ferguson, D., Foster, T.J., and Peacock, S.J. (2002) Functional blocking of *Staphylococcus aureus* adhesins following growth in ex vivo media. *Infect Immun* **70**: 5339-5345.

Matsuka, Y.V., Anderson, E.T., Milner-Fish, T., Ooi, P., and Baker, S. (2003) *Staphylococcus aureus* fibronectin-binding protein serves as a substrate for coagulation factor XIIIa: evidence for factor XIIIa-catalyzed covalent cross-linking to fibronectin and fibrin. *Biochemistry* **42**: 14643-14652.

Matsushita, T., and Sadler, J.E. (1995) Identification of amino acid residues essential for von Willebrand factor binding to platelet glycoprotein Ib. Charged-to-alanine scanning mutagenesis of the A1 domain of human von Willebrand factor. *J Biol Chem* **270**: 13406-13414.

Mazmanian, S.K., Ton-That, H., and Schneewind, O. (2001) Sortase-catalysed anchoring of surface proteins to the cell wall of *Staphylococcus aureus*. *Mol Microbiol* **40**: 1049-1057.

Mazmanian, S.K., Ton-That, H., Su, K., and Schneewind, O. (2002) An iron-regulated sortase anchors a class of surface protein during *Staphylococcus aureus* pathogenesis. *Proc Natl Acad Sci U S A* **99**: 2293-2298.

Mazmanian, S.K., Skaar, E.P., Gaspar, A.H., Humayun, M., Gornicki, P., Jelenska, J., Joachmiak, A., Missiakas, D.M., and Schneewind, O. (2003) Passage of heme-iron across the envelope of *Staphylococcus aureus*. *Science* **299**: 906-909.

Mazzucato, M., Spessotto, P., Masotti, A., De Appollonia, L., Cozzi, M.R., Yoshioka, A., Perris, R., Colombatti, A., and De Marco, L. (1999) Identification of domains responsible for von Willebrand factor type VI collagen interaction mediating platelet adhesion under high flow. *J Biol Chem* **274**: 3033-3041.

McAleese, F.M., Walsh, E.J., Sieprawska, M., Potempa, J., and Foster, T.J. (2001) Loss of clumping factor B fibrinogen binding activity by *Staphylococcus aureus* involves cessation of transcription, shedding and cleavage by metalloprotease. *J Biol Chem* **276**: 29969-29978.

McCrea, K.W., Hartford, O., Davis, S., Eidhin, D.N., Lina, G., Speziale, P., Foster, T.J., and Hook, M. (2000) The serine-aspartate repeat (Sdr) protein family in *Staphylococcus epidermidis*. *Microbiology* **146 ( Pt 7)**: 1535-1546.

McDevitt, D., Francois, P., Vaudaux, P., and Foster, T.J. (1995) Identification of the ligand-binding domain of the surface-located fibrinogen receptor (clumping factor) of *Staphylococcus aureus*. *Mol Microbiol* **16**: 895-907.

McDevitt, D., Nanavaty, T., House-Pompeo, K., Bell, E., Turner, N., McIntire, L., Foster, T., and Hook, M. (1997) Characterization of the interaction between the *Staphylococcus aureus* clumping factor (ClfA) and fibrinogen. *Eur J Biochem* **247**: 416-424.

McGavin, M.J., Zahradka, C., Rice, K., and Scott, J.E. (1997) Modification of the *Staphylococcus aureus* fibronectin binding phenotype by V8 protease. *Infect Immun* **65**: 2621-2628.



Michie, C.A., and Cohen, J. (1998) The clinical significance of T-cell superantigens. *Trends Microbiol* **6**: 61-65.

Miura, S., Fujimura, Y., Sugimoto, M., Kawasaki, T., Ikeda, Y., Titani, K., and Yoshioka, A. (1994) Structural elements influencing von Willebrand factor (vWF) binding affinity for platelet glycoprotein Ib within a dispase-digested vWF fragment. *Blood* **84**: 1553-1558.

Miyata, S., and Ruggeri, Z.M. (1999) Distinct structural attributes regulating von Willebrand factor A1 domain interaction with platelet glycoprotein Ib $\alpha$  under flow. *J Biol Chem* **274**: 6586-6593.

Moks, T., Abrahmsen, L., Nilsson, B., Hellman, U., Sjoquist, J., and Uhlen, M. (1986) Staphylococcal protein A consists of five IgG-binding domains. *Eur J Biochem* **156**: 637-643.

Mongkolrattanothai, K., Boyle, S., Kahana, M.D., and Daum, R.S. (2003) Severe *Staphylococcus aureus* infections caused by clonally related community-acquired methicillin-susceptible and methicillin-resistant isolates. *Clin Infect Dis* **37**: 1050-1058.

Morales, L.D., Martin, C., and Cruz, M.A. (2006) The interaction of von Willebrand factor-A1 domain with collagen: mutation G1324S (type 2M von Willebrand disease) impairs the conformational change in A1 domain induced by collagen. *J Thromb Haemost* **4**: 417-425.

Moreillon, P., Entenza, J.M., Francioli, P., McDevitt, D., Foster, T.J., Francois, P., and Vaudaux, P. (1995) Role of *Staphylococcus aureus* coagulase and clumping factor in pathogenesis of experimental endocarditis. *Infect Immun* **63**: 4738-4743.

Moreillon, P., and Que, Y.A. (2004) Infective endocarditis. *Lancet* **363**: 139-149.

Mylonakis, E., and Calderwood, S.B. (2001) Infective endocarditis in adults. *N Engl J Med* **345**: 1318-1330.

Nagaoka, M., and Akaike, T. (2003) Single amino acid substitution in the mouse IgG1 Fc region induces drastic enhancement of the affinity to protein A. *Protein Eng* **16**: 243-245.

Nguyen, T., Ghebrehiwet, B., and Peerschke, E.I. (2000) *Staphylococcus aureus* protein A recognizes platelet gC1qR/p33: a novel mechanism for staphylococcal interactions with platelets. *Infect Immun* **68**: 2061-2068.

Ni, H., and Freedman, J. (2003) Platelets in hemostasis and thrombosis: role of integrins and their ligands. *Transfus Apher Sci* **28**: 257-264.

Nicolau, D.P., Freeman, C.D., Nightingale, C.H., Quintiliani, R., Coe, C.J., Maderazo, E.G., and Cooper, B.W. (1993) Reduction of bacterial titers by low-dose aspirin in experimental aortic valve endocarditis. *Infect Immun* **61**: 1593-1595.

Niemann, S., Spehr, N., Van Aken, H., Morgenstern, E., Peters, G., Herrmann, M., and Kehrel, B.E. (2004) Soluble fibrin is the main mediator of *Staphylococcus aureus* adhesion to platelets. *Circulation* **110**: 193-200.

Nilsson, B., Moks, T., Jansson, B., Abrahmsen, L., Elmblad, A., Holmgren, E., Henrichson, C., Jones, T.A., and Uhlen, M. (1987) A synthetic IgG-binding domain based on staphylococcal protein A. *Protein Eng* **1**: 107-113.

Nilsson, I.M., Lee, J.C., Bremell, T., Ryden, C., and Tarkowski, A. (1997) The role of staphylococcal polysaccharide microcapsule expression in septicemia and septic arthritis. *Infect Immun* **65**: 4216-4221.

Nilsson, I.M., Patti, J.M., Bremell, T., Hook, M., and Tarkowski, A. (1998) Vaccination with a recombinant fragment of collagen adhesin provides protection against *Staphylococcus aureus*-mediated septic death. *J Clin Invest* **101**: 2640-2649.

Nishio, K., Fujimura, Y., Niinomi, K., Takahashi, Y., Yoshioka, A., Fukui, H., Usami, Y., Titani, K., Ruggeri, Z.M., and Zimmerman, T.S. (1990) Enhanced botrocetin-induced type IIB von Willebrand factor binding to platelet glycoprotein Ib initiates hyperagglutination of normal platelets. *Am J Hematol* **33**: 261-266.

Normark, B.H., Normark, S., and Norrby-Teglund, A. (2004) Staphylococcal protein A inflames the lungs. *Nat Med* **10**: 780-781.

Novak, L., Deckmyn, H., Damjanovich, S., and Harsfalvi, J. (2002) Shear-dependent morphology of von Willebrand factor bound to immobilized collagen. *Blood* **99**: 2070-2076.

Novick, R.P., Ross, H.F., Projan, S.J., Kornblum, J., Kreiswirth, B., and Moghazeh, S. (1993) Synthesis of staphylococcal virulence factors is controlled by a regulatory RNA molecule. *Embo J* **12**: 3967-3975.

Novick, R.P. (2003) Autoinduction and signal transduction in the regulation of staphylococcal virulence. *Mol Microbiol* **48**: 1429-1449.

O'Brien, L., Kerrigan, S.W., Kaw, G., Hogan, M., Penades, J., Litt, D., Fitzgerald, D.J., Foster, T.J., and Cox, D. (2002) Multiple mechanisms for the activation of human platelet aggregation by *Staphylococcus aureus*: roles for the clumping factors ClfA and ClfB, the serine-aspartate repeat protein SdrE and protein A. *Mol Microbiol* **44**: 1033-1044.

O'Riordan, K., and Lee, J.C. (2004) *Staphylococcus aureus* capsular polysaccharides. *Clin Microbiol Rev* **17**: 218-234.

Pallen, M.J. (2002) The ESAT-6/WXG100 superfamily -- and a new Gram-positive secretion system? *Trends Microbiol* **10**: 209-212.

Palma, M., Nozohoor, S., Schennings, T., Heimdahl, A., and Flock, J.I. (1996) Lack of the extracellular 19-kilodalton fibrinogen-binding protein from *Staphylococcus aureus* decreases virulence in experimental wound infection. *Infect Immun* **64**: 5284-5289.

Palma, M., Shannon, O., Quezada, H.C., Berg, A., and Flock, J.I. (2001) Extracellular fibrinogen-binding protein, Efb, from *Staphylococcus aureus* blocks platelet aggregation due to its binding to the alpha-chain. *J Biol Chem* **276**: 31691-31697.

Palmqvist, N., Foster, T., Tarkowski, A., and Josefsson, E. (2002) Protein A is a virulence factor in *Staphylococcus aureus* arthritis and septic death. *Microb Pathog* **33**: 239-249.



- Palmqvist, N., Patti, J.M., Tarkowski, A., and Josefsson, E. (2004) Expression of staphylococcal clumping factor A impedes macrophage phagocytosis. *Microbes Infect* **6**: 188-195.
- Patel, A.H., Nowlan, P., Weavers, E.D., and Foster, T. (1987) Virulence of protein A-deficient and alpha-toxin-deficient mutants of *Staphylococcus aureus* isolated by allele replacement. *Infect Immun* **55**: 3103-3110.
- Patel, A.H., Kornblum, J., Kreiswirth, B., Novick, R., and Foster, T.J. (1992) Regulation of the protein A-encoding gene in *Staphylococcus aureus*. *Gene* **114**: 25-34.
- Patti, J.M., Jonsson, H., Guss, B., Switalski, L.M., Wiberg, K., Lindberg, M., and Hook, M. (1992) Molecular characterization and expression of a gene encoding a *Staphylococcus aureus* collagen adhesin. *J Biol Chem* **267**: 4766-4772.
- Patti, J.M., Boles, J.O., and Hook, M. (1993) Identification and biochemical characterization of the ligand binding domain of the collagen adhesin from *Staphylococcus aureus*. *Biochemistry* **32**: 11428-11435.
- Patti, J.M., Allen, B.L., McGavin, M.J., and Hook, M. (1994) MSCRAMM-mediated adherence of microorganisms to host tissues. *Annu Rev Microbiol* **48**: 585-617.
- Patti, J.M., House-Pompeo, K., Boles, J.O., Garza, N., Gurusiddappa, S., and Hook, M. (1995) Critical residues in the ligand-binding site of the *Staphylococcus aureus* collagen-binding adhesin (MSCRAMM). *J Biol Chem* **270**: 12005-12011.
- Pawar, P., Shin, P.K., Mousa, S.A., Ross, J.M., and Konstantopoulos, K. (2004) Fluid shear regulates the kinetics and receptor specificity of *Staphylococcus aureus* binding to activated platelets. *J Immunol* **173**: 1258-1265.
- Peacock, S.J., Day, N.P., Thomas, M.G., Berendt, A.R., and Foster, T.J. (2000) Clinical isolates of *Staphylococcus aureus* exhibit diversity in *fnb* genes and adhesion to human fibronectin. *J Infect* **41**: 23-31.

Peacock, S.J., de Silva, I., and Lowy, F.D. (2001) What determines nasal carriage of *Staphylococcus aureus*? *Trends Microbiol* **9**: 605-610.

Peacock, S.J., Moore, C.E., Justice, A., Kantzanou, M., Story, L., Mackie, K., O'Neill, G., and Day, N.P. (2002) Virulent combinations of adhesin and toxin genes in natural populations of *Staphylococcus aureus*. *Infect Immun* **70**: 4987-4996.

Peerschke, E.I., and Ghebrehiwet, B. (2001) Human blood platelet gC1qR/p33. *Immunol Rev* **180**: 56-64.

Peerschke, E.I., Murphy, T.K., and Ghebrehiwet, B. (2003) Activation-dependent surface expression of gC1qR/p33 on human blood platelets. *Thromb Haemost* **89**: 331-339.

Peerschke, E.I., Bayer, A.S., Ghebrehiwet, B., and Xiong, Y.Q. (2006) gC1qR/p33 blockade reduces *Staphylococcus aureus* colonization of target tissues in an animal model of infective endocarditis. *Infect Immun* **74**: 4418-4423.

Peschel, A., Otto, M., Jack, R.W., Kalbacher, H., Jung, G., and Gotz, F. (1999) Inactivation of the *dlt* operon in *Staphylococcus aureus* confers sensitivity to defensins, protegrins, and other antimicrobial peptides. *J Biol Chem* **274**: 8405-8410.

Peschel, A., Jack, R.W., Otto, M., Collins, L.V., Staubitz, P., Nicholson, G., Kalbacher, H., Nieuwenhuizen, W.F., Jung, G., Tarkowski, A., van Kessel, K.P., and van Strijp, J.A. (2001) *Staphylococcus aureus* resistance to human defensins and evasion of neutrophil killing via the novel virulence factor MprF is based on modification of membrane lipids with l-lysine. *J Exp Med* **193**: 1067-1076.

Peschel, A. (2002) How do bacteria resist human antimicrobial peptides? *Trends Microbiol* **10**: 179-186.

Phonimdaeng, P., O'Reilly, M., Nowlan, P., Bramley, A.J., and Foster, T.J. (1990) The coagulase of *Staphylococcus aureus* 8325-4. Sequence analysis and virulence of site-specific coagulase-deficient mutants. *Mol Microbiol* **4**: 393-404.

Pilpa, R.M., Fadeev, E.A., Villareal, V.A., Wong, M.L., Phillips, M., and Clubb, R.T. (2006) Solution structure of the NEAT (NEAr Transporter) domain from IsdH/HarA: the human hemoglobin receptor in *Staphylococcus aureus*. *J Mol Biol* **360**: 435-447.

Plow, E.F., Haas, T.A., Zhang, L., Loftus, J., and Smith, J.W. (2000) Ligand binding to integrins. *J Biol Chem* **275**: 21785-21788.

Polanowska-Grabowska, R., Simon, C.G., Jr., and Gear, A.R. (1999) Platelet adhesion to collagen type I, collagen type IV, von Willebrand factor, fibronectin, laminin and fibrinogen: rapid kinetics under shear. *Thromb Haemost* **81**: 118-123.

Ponnuraj, K., Bowden, M.G., Davis, S., Gurusiddappa, S., Moore, D., Choe, D., Xu, Y., Hook, M., and Narayana, S.V. (2003) A "dock, lock, and latch" structural model for a staphylococcal adhesin binding to fibrinogen. *Cell* **115**: 217-228.

Prat, C., Bestebroer, J., de Haas, C.J., van Strijp, J.A., and van Kessel, K.P. (2006) A new staphylococcal anti-inflammatory protein that antagonizes the formyl peptide receptor-like 1. *J Immunol* **177**: 8017-8026.

Qu, A., and Leahy, D.J. (1995) Crystal structure of the I-domain from the CD11a/CD18 (LFA-1, alpha L beta 2) integrin. *Proc Natl Acad Sci U S A* **92**: 10277-10281.

Que, Y.A., Haefliger, J.A., Piroth, L., Francois, P., Widmer, E., Entenza, J.M., Sinha, B., Herrmann, M., Francioli, P., Vaudaux, P., and Moreillon, P. (2005) Fibrinogen and fibronectin binding cooperate for valve infection and invasion in *Staphylococcus aureus* experimental endocarditis. *J Exp Med* **201**: 1627-1635.

Raghavachari, M., Tsai, H., Kottke-Marchant, K., and Marchant, R.E. (2000) Surface dependent structures of von Willebrand factor observed by AFM under aqueous conditions. *Colloids Surf B Biointerfaces* **19**: 315-324.



Randi, A.M., Rabinowitz, I., Mancuso, D.J., Mannucci, P.M., and Sadler, J.E. (1991) Molecular basis of von Willebrand disease type IIB. Candidate mutations cluster in one disulfide loop between proposed platelet glycoprotein Ib binding sequences. *J Clin Invest* **87**: 1220-1226.

Randi, A.M., Jorieux, S., Tuley, E.A., Mazurier, C., and Sadler, J.E. (1992) Recombinant von Willebrand factor Arg578-->Gln. A type IIB von Willebrand disease mutation affects binding to glycoprotein Ib but not to collagen or heparin. *J Biol Chem* **267**: 21187-21192.

Roben, P.W., Salem, A.N., and Silverman, G.J. (1995) VH3 family antibodies bind domain D of staphylococcal protein A. *J Immunol* **154**: 6437-6445.

Roche, F.M., Massey, R., Peacock, S.J., Day, N.P., Visai, L., Speziale, P., Lam, A., Pallen, M., and Foster, T.J. (2003) Characterization of novel LPXTG-containing proteins of *Staphylococcus aureus* identified from genome sequences. *Microbiology* **149**: 643-654.

Roghmann, M., Taylor, K.L., Gupte, A., Zhan, M., Johnson, J.A., Cross, A., Edelman, R., and Fattom, A.I. (2005) Epidemiology of capsular and surface polysaccharide in *Staphylococcus aureus* infections complicated by bacteraemia. *J Hosp Infect* **59**: 27-32.

Rooijackers, S.H., Ruyken, M., Roos, A., Daha, M.R., Presanis, J.S., Sim, R.B., van Wamel, W.J., van Kessel, K.P., and van Strijp, J.A. (2005a) Immune evasion by a staphylococcal complement inhibitor that acts on C3 convertases. *Nat Immunol* **6**: 920-927.

Rooijackers, S.H., van Wamel, W.J., Ruyken, M., van Kessel, K.P., and van Strijp, J.A. (2005b) Anti-opsonic properties of staphylokinase. *Microbes Infect* **7**: 476-484.

Roth, G.J., Titani, K., Hoyer, L.W., and Hickey, M.J. (1986) Localization of binding sites within human von Willebrand factor for monomeric type III collagen. *Biochemistry* **25**: 8357-8361.

Ruggeri, Z.M., Pareti, F.I., Mannucci, P.M., Ciavarella, N., and Zimmerman, T.S. (1980) Heightened interaction between platelets and factor VIII/von Willebrand factor in a new subtype of von Willebrand's disease. *N Engl J Med* **302**: 1047-1051.

Rus, H., Cudrici, C., and Niculescu, F. (2005) The role of the complement system in innate immunity. *Immunol Res* **33**: 103-112.

Sadler, J.E. (1991) von Willebrand factor. *J Biol Chem* **266**: 22777-22780.

Sadler, J.E. (1998) Biochemistry and genetics of von Willebrand factor. *Annu Rev Biochem* **67**: 395-424.

Said-Salim, B., Dunman, P.M., McAleese, F.M., Macapagal, D., Murphy, E., McNamara, P.J., Arvidson, S., Foster, T.J., Projan, S.J., and Kreiswirth, B.N. (2003) Global regulation of *Staphylococcus aureus* genes by Rot. *J Bacteriol* **185**: 610-619.

Sambrook, J., E.F.F., and T. Maniatis. (1989) *Molecular cloning: a laboratory manual*. NY: Cold Spring Harbor Laboratory.

Sasano, M., Burton, D.R., and Silverman, G.J. (1993) Molecular selection of human antibodies with an unconventional bacterial B cell antigen. *J Immunol* **151**: 5822-5839.

Sasso, E.H., Silverman, G.J., and Mannik, M. (1989) Human IgM molecules that bind staphylococcal protein A contain VHIII H chains. *J Immunol* **142**: 2778-2783.

Sasso, E.H., Silverman, G.J., and Mannik, M. (1991) Human IgA and IgG F(ab')<sub>2</sub> that bind to staphylococcal protein A belong to the VHIII subgroup. *J Immunol* **147**: 1877-1883.

Sauer-Eriksson, A.E., Kleywegt, G.J., Uhlen, M., and Jones, T.A. (1995) Crystal structure of the C2 fragment of streptococcal protein G in complex with the Fc domain of human IgG. *Structure* **3**: 265-278.

Savolainen, K., Paulin, L., Westerlund-Wikstrom, B., Foster, T.J., Korhonen, T.K., and Kuusela, P. (2001) Expression of pls, a gene closely associated with the mecA gene of methicillin-resistant *Staphylococcus aureus*, prevents bacterial adhesion in vitro. *Infect Immun* **69**: 3013-3020.

Schiffmann, E., Corcoran, B.A., and Wahl, S.M. (1975) N-formylmethionyl peptides as chemoattractants for leucocytes. *Proc Natl Acad Sci U S A* **72**: 1059-1062.

Schmidt, K.A., Manna, A.C., and Cheung, A.L. (2003) SarT influences *sarS* expression in *Staphylococcus aureus*. *Infect Immun* **71**: 5139-5148.

Schwarz-Linek, U., Werner, J.M., Pickford, A.R., Gurusiddappa, S., Kim, J.H., Pilka, E.S., Briggs, J.A., Gough, T.S., Hook, M., Campbell, I.D., and Potts, J.R. (2003) Pathogenic bacteria attach to human fibronectin through a tandem beta-zipper. *Nature* **423**: 177-181.

Shannon, O., and Flock, J.I. (2004) Extracellular fibrinogen binding protein, Efb, from *Staphylococcus aureus* binds to platelets and inhibits platelet aggregation. *Thromb Haemost* **91**: 779-789.

Shannon, O., Uekotter, A., and Flock, J.I. (2005) Extracellular fibrinogen binding protein, Efb, from *Staphylococcus aureus* as an antiplatelet agent in vivo. *Thromb Haemost* **93**: 927-931.

Shattil, S.J., and Newman, P.J. (2004) Integrins: dynamic scaffolds for adhesion and signaling in platelets. *Blood* **104**: 1606-1615.

Shelton-Inloes, B.B., Titani, K., and Sadler, J.E. (1986) cDNA sequences for human von Willebrand factor reveal five types of repeated domains and five possible protein sequence polymorphisms. *Biochemistry* **25**: 3164-3171.

Shiba, E., Lindon, J.N., Kushner, L., Matsueda, G.R., Hawiger, J., Kloczewiak, M., Kudryk, B., and Salzman, E.W. (1991) Antibody-detectable changes in fibrinogen adsorption affecting platelet activation on polymer surfaces. *Am J Physiol* **260**: C965-974.

Siboo, I.R., Cheung, A.L., Bayer, A.S., and Sullam, P.M. (2001) Clumping factor A mediates binding of *Staphylococcus aureus* to human platelets. *Infect Immun* **69**: 3120-3127.

Siboo, I.R., Chambers, H.F., and Sullam, P.M. (2005) Role of SraP, a Serine-Rich Surface Protein of *Staphylococcus aureus*, in binding to human platelets. *Infect Immun* **73**: 2273-2280.



Siedlecki, C.A., Lestini, B.J., Kottke-Marchant, K.K., Eppell, S.J., Wilson, D.L., and Marchant, R.E. (1996) Shear-dependent changes in the three-dimensional structure of human von Willebrand factor. *Blood* **88**: 2939-2950.

Sieprawska-Lupa, M., Mydel, P., Krawczyk, K., Wojcik, K., Puklo, M., Lupa, B., Suder, P., Silberring, J., Reed, M., Pohl, J., Shafer, W., McAleese, F., Foster, T., Travis, J., and Potempa, J. (2004) Degradation of human antimicrobial peptide LL-37 by *Staphylococcus aureus*-derived proteinases. *Antimicrob Agents Chemother* **48**: 4673-4679.

Sieradzki, K., and Tomasz, A. (1998) Suppression of glycopeptide resistance in a highly teicoplanin-resistant mutant of *Staphylococcus aureus* by transposon inactivation of genes involved in cell wall synthesis. *Microb Drug Resist* **4**: 159-168.

Signas, C., Raucci, G., Jonsson, K., Lindgren, P.E., Anantharamaiah, G.M., Hook, M., and Lindberg, M. (1989) Nucleotide sequence of the gene for a fibronectin-binding protein from *Staphylococcus aureus*: use of this peptide sequence in the synthesis of biologically active peptides. *Proc Natl Acad Sci USA* **86**: 699-703.

Silverman, G.J., Sasano, M., and Wormsley, S.B. (1993) Age-associated changes in binding of human B lymphocytes to a VH3-restricted unconventional bacterial antigen. *J Immunol* **151**: 5840-5855.

Silverman, G.J., Cary, S.P., Dwyer, D.C., Luo, L., Wagenknecht, R., and Curtiss, V.E. (2000) A B cell superantigen-induced persistent "Hole" in the B-1 repertoire. *J Exp Med* **192**: 87-98.

Singh, V.K., Schmidt, J.L., Jayaswal, R.K., and Wilkinson, B.J. (2003) Impact of sigB mutation on *Staphylococcus aureus* oxacillin and vancomycin resistance varies with parental background and method of assessment. *Int J Antimicrob Agents* **21**: 256-261.

Sixma, J.J., Schiphorst, M.E., Verweij, C.L., and Pannekoek, H. (1991) Effect of deletion of the A1 domain of von Willebrand factor on its binding to heparin, collagen and platelets in the presence of ristocetin. *Eur J Biochem* **196**: 369-375.

Sjoberg, U., Ringdahl, U., and Ruggeri, Z.M. (2002) Induction of platelet thrombi by bacteria and antibodies. *Blood* **100**: 4470-4477.

Skaar, E.P., Humayun, M., Bae, T., DeBord, K.L., and Schneewind, O. (2004) Iron-source preference of *Staphylococcus aureus* infections. *Science* **305**: 1626-1628.

Skaar, E.P., and Schneewind, O. (2004) Iron-regulated surface determinants (Isd) of *Staphylococcus aureus*: stealing iron from heme. *Microbes Infect* **6**: 390-397.

Smeltzer, M.S., Gillaspay, A.F., Pratt, F.L., and Thames, M.D. (1997) Comparative evaluation of use of *cna*, *fnbA*, *fnbB*, and *hly* for genomic fingerprinting in the epidemiological typing of *Staphylococcus aureus*. *J Clin Microbiol* **35**: 2444-2449.

Sobel, M., Soler, D.F., Kermode, J.C., and Harris, R.B. (1992) Localization and characterization of a heparin binding domain peptide of human von Willebrand factor. *J Biol Chem* **267**: 8857-8862.

Sottile, J., Schwarzbauer, J., Selegue, J., and Mosher, D.F. (1991) Five type I modules of fibronectin form a functional unit that binds to fibroblasts and *Staphylococcus aureus*. *J Biol Chem* **266**: 12840-12843.

Sporn, L.A., Marder, V.J., and Wagner, D.D. (1986) Inducible secretion of large, biologically potent von Willebrand factor multimers. *Cell* **46**: 185-190.

Sporn, L.A., Marder, V.J., and Wagner, D.D. (1987) von Willebrand factor released from Weibel-Palade bodies binds more avidly to extracellular matrix than that secreted constitutively. *Blood* **69**: 1531-1534.

Stackebrandt, E., and Teuber, M. (1988) Molecular taxonomy and phylogenetic position of lactic acid bacteria. *Biochimie* **70**: 317-324.

Starovasnik, M.A., Skelton, N.J., O'Connell, M.P., Kelley, R.F., Reilly, D., and Fairbrother, W.J. (1996) Solution structure of the E-domain of staphylococcal protein A. *Biochemistry* **35**: 15558-15569.

Starovasnik, M.A., Braisted, A.C., and Wells, J.A. (1997) Structural mimicry of a native protein by a minimized binding domain. *Proc Natl Acad Sci USA* **94**: 10080-10085.

Starovasnik, M.A., O'Connell, M.P., Fairbrother, W.J., and Kelley, R.F. (1999) Antibody variable region binding by Staphylococcal protein A: thermodynamic analysis and location of the Fv binding site on E-domain. *Protein Sci* **8**: 1423-1431.

Stepanian, A., Ribba, A.S., Lavergne, J.M., Fressinaud, E., Juhan-Vague, I., Mazurier, C., Girma, J.P., and Meyer, D. (2003) A new mutation, S1285F, within the A1 loop of von Willebrand factor induces a conformational change in A1 loop with abnormal binding to platelet GPIb and botrocetin causing type 2M von Willebrand disease. *Br J Haematol* **120**: 643-651.

Stranger-Jones, Y.K., Bae, T., and Schneewind, O. (2006) Vaccine assembly from surface proteins of *Staphylococcus aureus*. *Proc Natl Acad Sci USA* **103**: 16942-16947.

Stutzmann Meier, P., Entenza, J.M., Vaudaux, P., Francioli, P., Glauser, M.P., and Moreillon, P. (2001) Study of *Staphylococcus aureus* pathogenic genes by transfer and expression in the less virulent organism *Streptococcus gordonii*. *Infect Immun* **69**: 657-664.

Sullam, P.M., Bayer, A.S., Foss, W.M., and Cheung, A.L. (1996) Diminished platelet binding in vitro by *Staphylococcus aureus* is associated with reduced virulence in a rabbit model of infective endocarditis. *Infect Immun* **64**: 4915-4921.

Symersky, J., Patti, J.M., Carson, M., House-Pompeo, K., Teale, M., Moore, D., Jin, L., Schneider, A., DeLucas, L.J., Hook, M., and Narayana, S.V. (1997) Structure of the collagen-binding domain from a *Staphylococcus aureus* adhesin. *Nat Struct Biol* **4**: 833-838.

Takahashi, Y., Kalafatis, M., Girma, J.P., Sewerin, K., Andersson, L.O., and Meyer, D. (1987) Localization of a factor VIII binding domain on a 34 kilodalton fragment of the N-terminal portion of von Willebrand factor. *Blood* **70**: 1679-1682.



Tashiro, M., Tejero, R., Zimmerman, D.E., Celda, B., Nilsson, B., and Montelione, G.T. (1997) High-resolution solution NMR structure of the Z domain of staphylococcal protein A. *J Mol Biol* **272**: 573-590.

Taylor, J.M., and Heinrichs, D.E. (2002) Transferrin binding in *Staphylococcus aureus*: involvement of a cell wall-anchored protein. *Mol Microbiol* **43**: 1603-1614.

Tegmark, K., Karlsson, A., and Arvidson, S. (2000) Identification and characterization of SarH1, a new global regulator of virulence gene expression in *Staphylococcus aureus*. *Mol Microbiol* **37**: 398-409.

Thakker, M., Park, J.S., Carey, V., and Lee, J.C. (1998) *Staphylococcus aureus* serotype 5 capsular polysaccharide is antiphagocytic and enhances bacterial virulence in a murine bacteremia model. *Infect Immun* **66**: 5183-5189.

Titani, K., Kumar, S., Takio, K., Ericsson, L.H., Wade, R.D., Ashida, K., Walsh, K.A., Chopek, M.W., Sadler, J.E., and Fujikawa, K. (1986) Amino acid sequence of human von Willebrand factor. *Biochemistry* **25**: 3171-3184.

Ton-That, H., Mazmanian, S.K., Faull, K.F., and Schneewind, O. (2000) Anchoring of surface proteins to the cell wall of *Staphylococcus aureus*. Sortase catalyzed in vitro transpeptidation reaction using LPXTG peptide and NH(2)-Gly(3) substrates. *J Biol Chem* **275**: 9876-9881.

Torigoe, H., Shimada, I., Saito, A., Sato, M., and Arata, Y. (1990a) Sequential <sup>1</sup>H NMR assignments and secondary structure of the B domain of staphylococcal protein A: structural changes between the free B domain in solution and the Fc-bound B domain in crystal. *Biochemistry* **29**: 8787-8793.

Torigoe, H., Shimada, I., Waelchli, M., Saito, A., Sato, M., and Arata, Y. (1990b) <sup>15</sup>N nuclear magnetic resonance studies of the B domain of staphylococcal protein A: sequence specific assignments of the imide <sup>15</sup>N resonances of the proline residues and the interaction with human immunoglobulin G. *FEBS Lett* **269**: 174-176.

Torres, V.J., Pishchany, G., Humayun, M., Schneewind, O., and Skaar, E.P. (2006) *Staphylococcus aureus* IsdB is a hemoglobin receptor required for heme iron utilization. *J Bacteriol* **188**: 8421-8429.

Townsend, D.E., and Wilkinson, B.J. (1992) Proline transport in *Staphylococcus aureus*: a high-affinity system and a low-affinity system involved in osmoregulation. *J Bacteriol* **174**: 2702-2710.

Vandenesch, F., Naimi, T., Enright, M.C., Lina, G., Nimmo, G.R., Heffernan, H., Liassine, N., Bes, M., Greenland, T., Reverdy, M.E., and Etienne, J. (2003) Community-acquired methicillin-resistant *Staphylococcus aureus* carrying Panton-Valentine leukocidin genes: worldwide emergence. *Emerg Infect Dis* **9**: 978-984.

Veldkamp, K.E., Heezius, H.C., Verhoef, J., van Strijp, J.A., and van Kessel, K.P. (2000) Modulation of neutrophil chemokine receptors by *Staphylococcus aureus* supernate. *Infect Immun* **68**: 5908-5913.

Vermeiren, C.L., Pluym, M., Mack, J., Heinrichs, D.E., and Stillman, M.J. (2006) Characterization of the heme binding properties of *Staphylococcus aureus* IsdA. *Biochemistry* **45**: 12867-12875.

Vijaranakul, U., Nadakavukaren, M.J., de Jonge, B.L., Wilkinson, B.J., and Jayaswal, R.K. (1995) Increased cell size and shortened peptidoglycan interpeptide bridge of NaCl-stressed *Staphylococcus aureus* and their reversal by glycine betaine. *J Bacteriol* **177**: 5116-5121.

Vlot, A.J., Koppelman, S.J., van den Berg, M.H., Bouma, B.N., and Sixma, J.J. (1995) The affinity and stoichiometry of binding of human factor VIII to von Willebrand factor. *Blood* **85**: 3150-3157.

Vlot, A.J., Koppelman, S.J., Meijers, J.C., Dama, C., van den Berg, H.M., Bouma, B.N., Sixma, J.J., and Willems, G.M. (1996) Kinetics of factor VIII-von Willebrand factor association. *Blood* **87**: 1809-1816.

- Voorberg, J., Fontijn, R., van Mourik, J.A., and Pannekoek, H. (1990) Domains involved in multimer assembly of von willebrand factor (vWF): multimerization is independent of dimerization. *Embo J* **9**: 797-803.
- Wagner, D.D., Fay, P.J., Sporn, L.A., Sinha, S., Lawrence, S.O., and Marder, V.J. (1987a) Divergent fates of von Willebrand factor and its propolypeptide (von Willebrand antigen II) after secretion from endothelial cells. *Proc Natl Acad Sci U S A* **84**: 1955-1959.
- Wagner, D.D., Lawrence, S.O., Ohlsson-Wilhelm, B.M., Fay, P.J., and Marder, V.J. (1987b) Topology and order of formation of interchain disulfide bonds in von Willebrand factor. *Blood* **69**: 27-32.
- Wann, E.R., Fehring, A.P., Ezechuk, Y.V., Schlievert, P.M., Bina, P., Reiser, R.F., Hook, M.M., and Leung, D.Y. (1999) *Staphylococcus aureus* isolates from patients with Kawasaki disease express high levels of protein A. *Infect Immun* **67**: 4737-4743.
- Watson, S.P., Clements, M.O., and Foster, S.J. (1998) Characterization of the starvation-survival response of *Staphylococcus aureus*. *J Bacteriol* **180**: 1750-1758.
- Weiss, W.J., Lenoy, E., Murphy, T., Tardio, L., Burgio, P., Projan, S.J., Schneewind, O., and Alksne, L. (2004) Effect of *srtA* and *srtB* gene expression on the virulence of *Staphylococcus aureus* in animal models of infection. *J Antimicrob Chemother* **53**: 480-486.
- Xiao, T., Takagi, J., Coller, B.S., Wang, J.H., and Springer, T.A. (2004) Structural basis for allostery in integrins and binding to fibrinogen-mimetic therapeutics. *Nature* **432**: 59-67.
- Xu, Y., Rivas, J.M., Brown, E.L., Liang, X., and Hook, M. (2004) Virulence potential of the staphylococcal adhesin CNA in experimental arthritis is determined by its affinity for collagen. *J Infect Dis* **189**: 2323-2333.
- Yang, D., Chen, Q., Le, Y., Wang, J.M., and Oppenheim, J.J. (2001) Differential regulation of formyl peptide receptor-like 1 expression during the differentiation of monocytes to dendritic cells and macrophages. *J Immunol* **166**: 4092-4098.



- Yang, L., Biswas, M.E., and Chen, P. (2003) Study of binding between protein A and immunoglobulin G using a surface tension probe. *Biophys J* **84**: 509-522.
- Yeaman, M.R., Sullam, P.M., Dazin, P.F., Norman, D.C., and Bayer, A.S. (1992) Characterization of *Staphylococcus aureus*-platelet binding by quantitative flow cytometric analysis. *J Infect Dis* **166**: 65-73.
- Zhang, L., Jacobsson, K., Vasi, J., Lindberg, M., and Frykberg, L. (1998) A second IgG-binding protein in *Staphylococcus aureus*. *Microbiology* **144** ( Pt 4): 985-991.
- Zhang, L., Rosander, A., Jacobsson, K., Lindberg, M., and Frykberg, L. (2000) Expression of staphylococcal protein Sbi is induced by human IgG. *FEMS Immunol Med Microbiol* **28**: 211-218.
- Zhang, L., Gray, L., Novick, R.P., and Ji, G. (2002) Transmembrane topology of AgrB, the protein involved in the post-translational modification of AgrD in *Staphylococcus aureus*. *J Biol Chem* **277**: 34736-34742.
- Zheng, X., Chung, D., Takayama, T.K., Majerus, E.M., Sadler, J.E., and Fujikawa, K. (2001) Structure of von Willebrand factor-cleaving protease (ADAMTS13), a metalloprotease involved in thrombotic thrombocytopenic purpura. *J Biol Chem* **276**: 41059-41063.
- Zong, Y., Bice, T.W., Ton-That, H., Schneewind, O., and Narayana, S.V. (2004) Crystal structures of *Staphylococcus aureus* sortase A and its substrate complex. *J Biol Chem* **279**: 31383-31389.
- Zong, Y., Xu, Y., Liang, X., Keene, D.R., Hook, A., Gurusiddappa, S., Hook, M., and Narayana, S.V. (2005) A 'Collagen Hug' model for *Staphylococcus aureus* CNA binding to collagen. *Embo J* **24**: 4224-4236.